Technische Universität München
Fakultät für Chemie
Lehrstuhl für Biochemie

Investigations of carbon fixation in model organisms and in cell-free prebiotic transition metal-catalyzed reactions

Jessica Sobotta

Vollständiger Abdruck der von der Fakultät für Chemie der Technischen Universität München zur Erlangung des akademischen Grades eines

Doktors der Naturwissenschaften (Dr. rer. nat.)

genehmigten Dissertation.

Vorsitzender: Prof. Dr. Tobias Gulder

Prüfer der Dissertation:

1. Apl. Prof. Dr. Wolfgang Eisenreich
2. Prof. Dr. Dieter Braun (LMU)

Diese Dissertation wurde am 13.06.2018 bei der Technischen Universität München eingereicht und durch die Fakultät für Chemie am 16.07.2018 angenommen.

Die vorliegende Arbeit entstand im Zeitraum von September 2014 bis August 2018 unter der Anleitung von Herrn Prof. Dr. Wolfgang Eisenreich am Lehrstuhl für Biochemie der Technischen Universität München.

Für Stefan

Danksagung

Ohne das Mitwirken der folgenden Personen wäre diese Arbeit nicht dieselbe bzw. unmöglich gewesen und deshalb möchte ich mich an dieser Stelle bei euch herzlich bedanken:

Meinem Doktorvater Herrn **Prof. Dr. Eisenreich** möchte ich besonders für die freundliche Aufnahme, die Überlassung dieses spannenden Themas, für die Betreuung und fachlichen Anregungen sowie sein Vertrauen in mich enorm bedanken.

Meinem Zweitprüfer Herrn **Prof. Dr. Braun** danke ich für die tolle Organisation des OLIM-Netzwerks und dem resultierenden SFB. Dies ermöglichte mir, tiefere Einblicke auf diesem Forschungsgebiet zu gewinne und Kooperationen mit anderen Gruppen zu schließen.

Ebenfalls möchte ich mich bei **Dr. Wächtershäuser** für die zahlreichen Gespräche und der mannigfachen Ideengebung bedanken, die maßgeblich zu dieser Arbeit beigetragen haben.

Des Weiteren bedanke ich mich herzlich bei Frau **Dr. Huber**, die stets ein offenes Ohr für mich hatte und mich immer unterstützt und mich hervorragend betreut hat.

Mein außerordentlicher Dank gilt Herrn **Prof. Dr. Groll** und dem ganzen **Lehrstuhl** sowie den **Ehemaligen** vor allem **Ina** & **Fan** und meinen **Studenten**. Ich bedanke mich für euer Interesse, Anregungen und den konstruktiven Austausch. Besonders werden mir **Lena**, **Tine** & die **Thomasse** wegen der persönlichen Bindung aber auch wegen ihrer enormen Hilfsbereitschaft in Erinnerung bleiben. Besonderes möchte ich mich nochmal für das Korrekturlesen bei den **Thomassen** sowie bei meiner Freundin **Birgit** bedanken.

Mein ganz besonderer Dank gilt meiner ganzen Familie, meinen Eltern **Marianne** & **Detlef**, meinen Großeltern **Inge** & **Manfred** sowie meinen verstorbenen Großeltern **Hans** & **Giesela**, meinem Bruder und seiner Frau **Thorsten** & **Myriam**, die mir meinen bisherigen Lebensweg ermöglichten und immer für mich da waren. Danke für all das, was ihr mir beigebracht habt und dass ihr mich stark gemacht habt für jedes Problem eine Lösung zu finden.

Meinem Freund **Stefan** danke ich besonders für den starken emotionalen Rückhalt über die Dauer meines gesamten Studiums und Doktorarbeit, der mich immer motiviert hat höhere Zielen anzustreben, sowie seinen Eltern **Renate** & **Josef** für das endlose Vertrauen und ihre herzliche Unterstützung.

Ich möchte an dieser Stelle auch der Stiftung „**Hans-Fischer-Gesellschaft“** danken, die mich durch ein Stipendium für die Forschungsprojekte meiner Doktorarbeit hindurch finanziell unterstützt hat.

Zusammenfassung

Methoden der Systembiologie und Chemie zeigen, dass selbst einfachste Zellen ein hochkomplexes Netzwerk an niedermolekularen Soffen besitzen. Dennoch befindet sich in dieser Komplexität eine erstaunliche Konvergenz in der zugrundeliegenden molekularen Biochemie unabhängig von der Art und Größe des Organismus. Diese gemeinsame biochemische Basis erlaubt es, Rückschlüsse auf den Ursprung des Lebens vor mehr als 4 Milliarden Jahren zu ziehen. Die biochemisch wichtigsten Grundbausteine aller Lebensformen bestehen aus einfachen Kohlenstoffgerüsten. In einer gängigen Hypothese des Lebensursprungs wird die Bildung dieser organischen Verbindungen durch Kohlenstofffixierungs-Reaktionen aus kleinen anorganischen Vorstufen wie zum Beispiel CO_2, CO und C_2H_2 postuliert. Demnach spielen autokatalytische Kohlenstofffixierungs-Zyklen wie zum Beispiel der reduktive Zitronensäure Zyklus (rTCA) eine wichtige Rolle im Stoffwechsel von phylogenetisch tief verankerten Organismen. Ein weiterer wichtiger Schritt auf dem Weg zur ersten zellulären Einheit ist die Bildung von abgetrennten Kompartimenten. Grundlage dafür sind bipolare Moleküle wie z. B. Fettsäuren.

In der vorliegenden Arbeit wird die bis heute für unmöglich geglaubte Reversibilität der Citrat-Synthase (CS) im Modelorganismus *Desulfurella acetivorans* demonstriert. Unter autotrophen Bedingungen katalysiert in diesem thermophilen Bakterium die CS die Citratspaltung in die reduktive Richtung des Zitronensäurezyklus. Somit könnte in der frühen Evolution ein reversibler Citratzyklus unter Beteiligung der CS entstanden sein. Auch aufgrund des einfacheren molekularen Aufbaus der CS im Vergleich zur klassischen Citratlyase im rTCA ist diese Hypothese attraktiv.

Zusätzlich beschäftigt sich diese Arbeit mit zellfreien „präbiotischen“ Übergangsmetall-katalysierten Reaktionen ausgehend von Kohlenstoffmonoxid und Acetylen, die zur Synthese längerer Kohlenstoffketten, im speziellen Fettsäuren, führen. In einer heißen wässrigen Lösung in Gegenwart von Nickel Katalysatoren konnten aus CO und C_2H_2 beispielsweise $C_{3,5,7,9}$-Monocarbonsäuren gebildet werden. Dieser Weg hin zu primitiven Fettsäuren könnte zu einer ersten primordialen Kompartimentierung geführt haben.

Um die entstanden kurzkettigen präbiotischen Fettsäuren erfolgreich zu identifizieren, wurde im Rahmen dieser Arbeit ebenfalls ein neuer Syntheseweg für 2,4-Diolefin- und 2,4,6-Triolefinmonocarbonsäuren etabliert. Dazu bedienten wir uns einer Kondensationsreaktion von α- bzw. α,β-ungesättigten Aldehyden mit Glutaconsäure, welche zu einer Decarboxylierung führte.

Abstract

Advances in the modern techniques of biochemistry revealed a great insight into highly complex metabolic networks, which are even present in the simplest cells. Nonetheless, independent of the size and type of a specific organism, there is a notable convergence in each of their molecular biochemistry. This biochemical relationship allows a backward projection to the origin of life that dates back more than 4 billion years. In all living organisms, the biochemical building blocks are based on simple carbon skeletons. In one of the common hypotheses for the origin of life, it is postulated that organic compounds are formed by carbon fixation reactions of small inorganic carbon sources such as CO_2, CO and C_2H_2. In line with hypothesis, autocatalytic carbon fixation cycles like the reductive citric acid cycle (rTCA) play an important role in phylogenetically deep-branching organisms. A further step towards a pre-cellular organism is the compartmentalization of the surrounding environment. Therefore, bipolar molecules such as fatty acids are necessary.

In this work, reversibility of the citrate synthase (CS) in the model organism *Desulfurella acetivorans* is demonstrated, which was considered as impossible until now. Under autotrophic conditions in this thermophilic bacterium, the CS catalyzes the cleavage of citrate in the reductive direction of the TCA. Thus, in evolutionary terms, these results suggest the early occurrence of a reductive citric acid cycle involving CS or a CS-like predator catalyst. An additional indication for such an early rTCA cycle can be found in the simpler molecular structure of CS in comparison to classical citrate lyase.

On the other hand, this work demonstrates a possible pathway to create carbon chains or in more detail, primordial fatty acids by transition metal catalysis of carbon monoxide and acetylene. This one-pot reaction of CO and C_2H_2 in the presence of nickel sulfide in hot aqueous medium, revealed the synthesis of $C_{3,5,7,9}$-monocarboxylic acids. This synthetic pathway to primitive fatty acids is maybe a starting point of a proto-cellular compartmentalization.

To successfully identify these short prebiotic fatty acids, a novel synthetic approach to form 2,4-diolefinic and 2,4,6-triolefinic monocarboxylic acids by one-pot decarboxylative condensation of an optionally α,β-unsaturated aldehyde with glutaconic acid could also be established in the course of this thesis.

List of Abbreviations

3-GAP	glyceraldehyde 3-phosphate
3-HPB cycle	3-hydroxypropionate–bicycle
3-HP/4-HB cycle	3-hydroxypropionate–4-hydroxybutyrate cycle
ACL	ATP-citrate lyase
Ala	alanine
ATP	adenosine triphosphate
CBB cycle	Calvin-Benson-Bassham-cycle
CODH	carbon monoxide dehydrogenase
CoA	coenzyme A
CCL	citryl-CoA lyase
CCS	citryl-CoA synthetase
COSY	correlation spectroscopy
CS	citrate synthase
DC/4-HB cycle	dicarboxylate–4-hydroxybutyrate cycle
DNA	deoxyribonucleic acid
FT-ICR-MS	Fourier-transform ion cyclotron resonance mass spectrometry
GC/MS	gas chromatography–mass spectrometry
GNA	glycol nucleic acid
HMBC	heteronuclear multiple bond correlation
HSQC	heteronuclear single quantum coherence
LUCA	last universal common ancestor
mRNA	messenger ribonucleic acid
NAD(P)H	nicotinamide adenine dinucleotide phosphate
NMR	nuclear magnetic resonance
PEP	phosphoenolpyruvate
PNA	peptide nucleic acid
RNA	ribonucleic acid
roTCA cycle	reversed oxidative citric acid cycle
rRNA	ribosomal ribonucleic acid
rTCA	reductive citric acid cycle
RuBisCO	ribulose-1,5-bisphosphate carboxylase/oxygenase
RuP	ribulose-5-phosphate
TEM	transmission electron microscopy
TNA	threofuranosyl nucleic acid
WL-pathway	Wood-Ljungdahl-pathway

Table of Contents

CHAPTER 1
INTRODUCTION

1.1 Chemical Evolution and the Origin of Life

One of the still unresolved basic but yet major scientific question is how life originated on early Earth and where do we come from? Although multiple attempts have been made to solve this riddle, this question is still obscure since almost all traces of earlier life on earth are lost. This lack of evidence gave rise to a plethora of theories. There are two directions to investigate the transition from abiotic to a biotic Earth, the “Top-Down” or “Bottom-Up” approach (Peters and Williams 2012). The latter method relies on considerations that life on the primeval earth may have arisen in the Hadean eon by coalescence of inanimate matter also known as chemical evolution or abiogenesis. The advocators of this chemical evolution suggest a stepwise evolution from nonliving to living systems, through biomolecules formed in the atmosphere, lithosphere or hydrosphere. Precursors such as reactive gases were provided by early Earth or even by outer space, which were brought to earth by meteorites or comets. Conversely, the “Top Down” approach focuses on biochemistry and phylogeny of extant organisms, to infer fundamental processes, pathways or assemblies reflecting links back to ancient life and its origin. The differences in theories do not only lie in the suggested potential prebiotic habitats, they are also based on the assumed source of energy. The earth offers a vast amount of different environments including impact craters (Cockell 2006), volcanoes (Miller 1953, Bada 2013), ice (Hao *et al*. 2018), submarine vents (Wächtershäuser 1992, Nitschke and Russell 2009) and several energy sources such as e.g. ultraviolet light (Khare and Sagan 1971), lightning (Miller 1953) and other scenarios. The first fundamental work to investigate on the origin of life in such a scenario was performed by Miller (Miller 1953).

1.1.2 Pioneer Experiments

Miller’s amino acids - In regard to Oparin’s theory (Oparin 1924) of a prebiotic broth, Miller envisaged experiments in a “volcanic” apparatus (Bada 2013) with a reducing gas atmosphere consisting of a mixture of CH_4, NH_3, H_2O, and H_2 (Miller 1953). These gases reacted with each other after induced electrical discharges, which simulated lightning. In the obtained aqueous solution, Miller found amino acids, which constituted important building blocks for biological polymers such as peptides and proteins (Miller 1953). It is supposed that the amino acids found in Miller’s experiment were formed *via* the Strecker synthesis (Bada 2013, Strecker 1850). The Strecker synthesis is one of the earliest examples of today’s well-known multicomponent reactions (Eckert 2017) in the chemical evolution research area. This condensation reaction is performed with ammonia in the presence of aldehydes and hydrogen cyanide (HCN) (Strecker 1850), both produced as secondary products in Miller’s experiment. Miller’s synthesis of

biomolecules under simulated conditions of early Earth carried out is based on the primordial soup theory. Briefly, this theory suggests that molecules were formed on early Earth from gases, which later on accumulated in the ocean (McNichol 2008).

Oró's nucleobases - Oró progressed the experiments of Miller by the prebiotic synthesis of adenine (Oró 1960), one of the nucleobases in deoxyribonucleic acid (DNA) and ribonucleic acid (RNA) and important key factor in the energy metabolism of extant life in the form of adenosine triphosphate (ATP). To achieve this, Oró heated an aqueous solution of ammonium hydroxide saturated with hydrogen cyanide to around 90°C for one day (Oró 1960). Considering the molecular formula of adenine, $C_5H_5N_5$, Oró concluded that the purine must be prepared from a pentamer of HCN, which is a cometary molecule (Oró 1961, Oró and Kimball 1961). Oró pointed out that three of the major constituents of comets, as are hydrogen cyanide, ammonia and water (Oró and Kimball 1961). It was suggested that cometary bombardment on primitive Earth may have provided the molecular precursors for the emergence of life (Oró and Kimball 1961).

Anyhow, in the early Earth's vast oceans, the dilution of the organic compounds lowered the chance of chemical reaction or interaction between the originated molecules (Hagmann 2002, Mojzsis *et al*. 2005). Therefore, main criticism of the both, soup theory and cometary collisions theory, is the lack of high local molecule concentration required to form more complex biomolecules. Plausible concentration processes or interactions for example on mineral surfaces must therefore enhance this theory.

1.1.3 Hydrothermal Systems

After the discovery of hydrothermal vents in the late 1970s, these hot springs got into the focus of the origin of life debate (Lonsdale 1977, Corliss *et al*. 1979). Within such hot springs, one found out that submarine hydrothermal vents occur along the mid ocean ridges, where cold seawater is heated by hot basaltic magma chambers and circulates back into the vent afterwards (Colín-García *et al*. 2016). In this process, a high thermal gradient is induced and water can reach temperatures above 400°C. The hot seawater is rich in dissolved minerals and chemicals, which are responsible for the chimney structure and the precipitated plume. Pressures up to several hundred bars can be reached by hydrostatic pressure in a depth of 2000-3000m below NN (Colín-García *et al*. 2016). Hydrothermal vents are found in places of volcanic activity caused by plate tectonics. Their life span reaches from several decades up to several hundreds of years. Hydothermal vents can be categorised into two basic types. The so-called "black smokers" are a subclass of hydrothermal vents and spit out hot magmatic

water containing iron and other metal sulphides resulting in a turbid black cloud with low pH (Figure 1A). The other type is named “white smoker” and spits out seawater, which is saturated with calcium ions and forms sulphate rich carbonate deposits (Figure 1B).

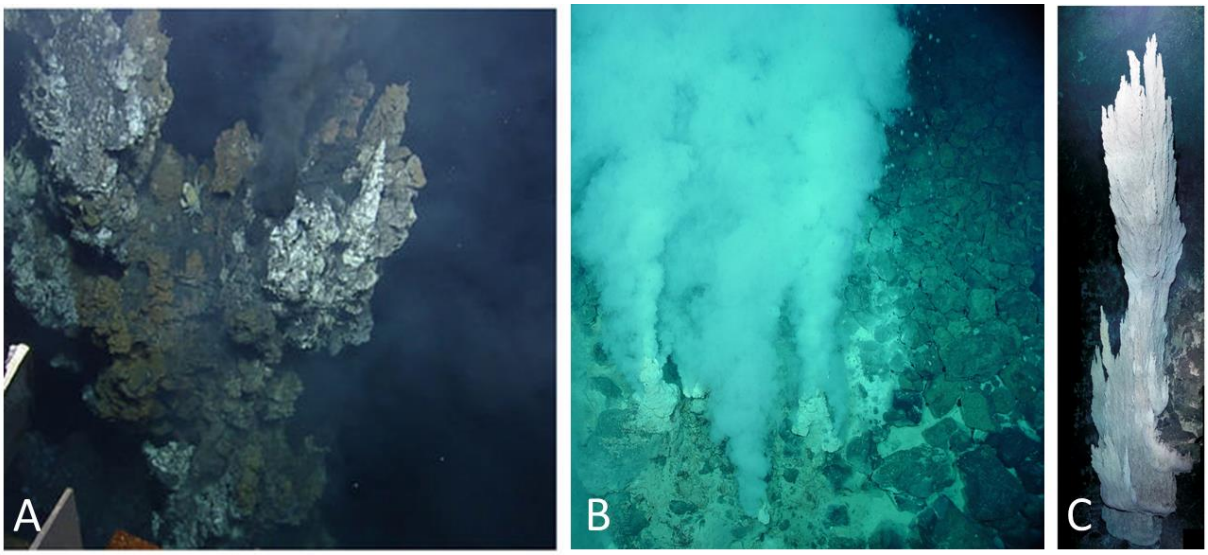

Figure 1: Hydrothermal systems; (A) black smoker (Salinas-de-León *et al*. 2018) (B) white smoker (Eifuka Japan 2004 photo: public domain) (C) “Lost City” vent (Kelley *et al*. 2005).

The temperature range inside this hydrothermal vent is smaller and lays between 40 to 75°C with an alkaline pH (Colín-García *et al*. 2016). Corliss *et al*. indicated a possible connection between the submarine systems and abiotic origin of life (Corliss *et al*. 1981). In 1988, Wächtershäuser revisited the problem of substance dilution by the ocean and the source of energy and postulated a thermophilic and chemoautotrophic origin of life by pyrite-pulled surface metabolism (Wächtershäuser 1988a, 1988b, 1992). In this origin of life theory hydrothermal vents would not derived by plate tectonic. Rather, primeval volcanic hydrothermal vents might have played a major role. These vents may have been formed by a high volcanic activity on early Earth when the crust was still much thinner. Russell focused on engineering the emergence of life through serpentinization and methanotrophy (Russell *et al*. 2014). These conditions that can be found at hydrothermal fields in the mid-Atlantic differ significantly from volcanic hydrothermal vents (Kelley *et al*. 2001). The so-called “Lost City” was discovered in 2000 and is characterized by tall carbonate chimneys with alkaline pH ranges from 9-11, temperatures of 40° to 90°C and low magnesium concentration (Kelley *et al*. 2001) (Figure 1C). Although these chimneys seem similar to hydrothermal vent systems, their formation underlie a circulation process *via* serpentinization, which in consequence leads to the formation of H_2, CH_4 and heat (Boetius 2005). The variations of gases, catalysts, pH and

supplied energy of all these hydrothermal systems lead to several theories and offer a wide field of potential experimental setups.

1.1.4 Iron Sulphur World by Günter Wächtershäuser

Further developing his theory, Wächtershäuser coined the term of the “iron sulphur world”, which postulates a chemoautotrophic origin of life (Wächtershäuser 1988b, 1990a, 1992). He suggests a pioneer organism is developed at sites of volcanic hydrothermal vents that is formed by surface catalysis.

Definition Pioneer organism - The term “pioneer organism” describes an organized being at the starting point of evolution and can be considered as the transition from the abiotic to the biotic world. It stands in sharp contrast to the idea of a primeval soup as revealed in Figure 2 (Wächtershäuser 2014). In Figure 2a, a backward projection of extant genetic features (F_1-F_n) is directed straight towards several precursor features (P_1-P_n) and leads to primordial broth.

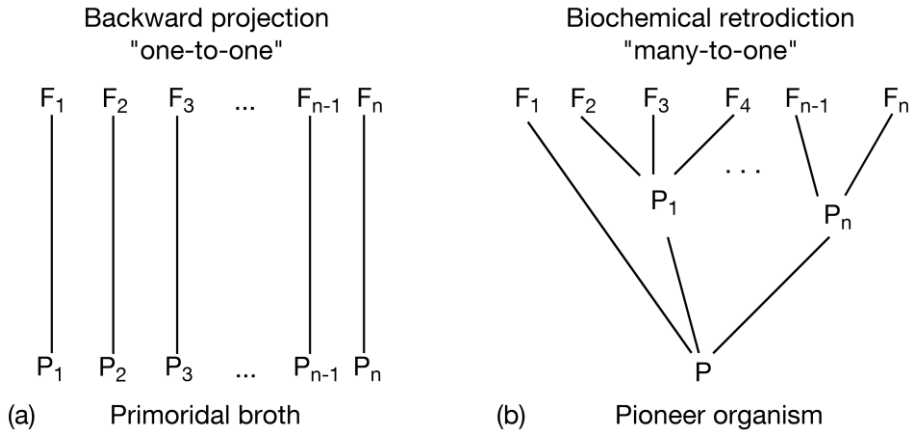

Figure 2: Methodologies of (a) backward projection and (b) biochemical retrodiction. The left part (a) leads to a community of primitive cells with different genomes and (b) to a single ancestor here the pioneer organism “P”. F stand for extant biochemical feature and P for precursor feature (adapted from Wächtershäuser 2014).

This “one-to-one” projection is not derived from one single pioneer organism. Instead, this projection is more likely originating from a community of primeval cells and is termed “primordial broth”. In Figure 2b, a biochemical retrodiction is suggested with tree-like structures leading to one pioneer organism. Moreover, in this “many-to-one” network he also involved the principle of horizontal gene transfer between the precursor features. His idea of the iron sulphur world is not only bio-inspired by retrodiction of features of extant life, it also focuses on a

plausible geochemical scenario for the emergence of pioneer organism. He postulates, that the pioneer organism is based at the one hand on non-metal elements H, C, N, O, Se, S and on the other hand on catalytically active transition metals Fe, Co, Ni, W (Wächtershäuser 2014).

Energy source for pioneer organism - Both molecules, iron sulfid (FeS) and nickel sulfid (NiS), were present on early Earth (Allègre *et al*. 1995) and can be found in volcanic hydrothermal fluid flows through the precipitation of soluble Ni^{2+}- and Fe^{2+}-ions with hydrogen sulphide (H_2S). Wächtershäuser recognized that methanogens acquire their energy by the reduction of CO_2 with H_2 to form CH_4, but an endergonic barrier must be overcome by an additional energy source (Wächtershäuser 1988a). Wächtershäuser concluded that the oxidative formation of pyrite (FeS_2) from FeS/H_2S under H_2-formation is exergonic and could serve as a continuous energy source for carbon fixation (Wächtershäuser 1990a, Drobner *et al*. 1990). The equation 1 shows the calculated exergonic pyrite formation, which provides reducing power to the pioneer metabolism with a Gibbs energy of -38.4 kJ/mol (pH=0 and T=25°C) (Wächtershäuser 1990a).

$$FeS + H_2S \rightarrow FeS_2 + 2H^+ + 2e^- \qquad \Delta G° = -38.4\ kJ/mol \qquad (1)$$

Reducing reactions driven by FeS and H_2S were also proven to occur, e.g. by the conversion of NO_3^- to NH_3 or alkynes to alkanes under primordial conditions (Blöchl *et al*. 1992). The Fe-S theory mainly gets approval by researchers in the field of enzyme activity (Span *et al*. 2012, Berg *et al*. 2010a) due to the fact that the in nature existing metallo-enzymes contain metal-sulfur clusters. And it is among others these enzymes that catalyse gas-based redox reactions involving H_2, N_2, CO, CO_2 and CH_4 (Fontecilla-Camps *et al*. 2009; Volbeda and Fontecilla-Camps 2006). Enzymes with this important function are for example carbon monoxide dehydrogenase (CODH), which interconverts CO_2 and CO, (Ragsdale 2009), acetyl coenzyme A synthase (Darnault *et al*. 2003) which utilizes CO, as well as hydrogenases that catalyse the oxidation of H_2 (Rauchfuss 2010; Bürstel *et al*. 2012) and nitrogenases important for nitrogen fixation (Yilin and Ribbe 2016). This analogy between the activity of Fe-S minerals and enzymatic Fe-S clusters supports the theory of a primordial surface metabolism on transition-metal sulfides. According to Wächtershäuser's FeS theory the elements H, O, C, N, Mg, Fe, S, Ca, Na, Ni, and P make up the bulk of biomass, originate from the Earth mantle and form volcanic gases such as H_2O, CO_2, CO, COS, H_2S, N_2, NH_3, H_2, HCN, and P_4O_{10} (Figure 3). These volcanic exhalations reacting with crustal minerals such as FeS_2 in a hot flow channel of hydrothermal vents by autocatalytic C-fixation (Wächtershäuser 2014). Low-molecular

organic compounds are formed on the catalytic surface, and represent the origin of the pioneer organism. With evolving chemoautotrophic reactions, and thus “metabolism first”, polymers can be created, fundamentally for genetic evolution.

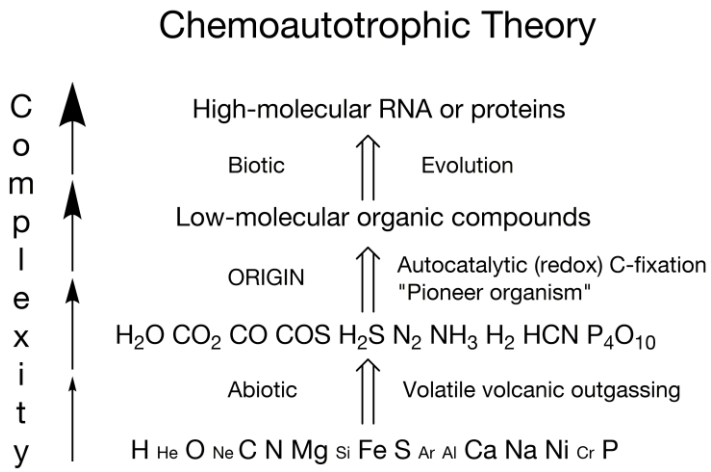

Figure 3: Schematic representation the chemoautotrophic theory by Wächtershäuser. Volcanic gases containing the elements necessary for the abiotic origin of the “Pioneer organism” *via* C-fixation. The Formation of low-molecular organic compounds leads to the transition to biotic evolution and further to polymerization reactions (photo: personal communication with Wächtershäuser).

Setting of the Pioneer organism - The pioneer organism exists at a nearly neutral pH range. Orthosilicates (<45% SiO_2) are dominantly present in Hadean eon and generate alkaline conditions (pH 9–12) but neutralisation is caused by acidic volcanic gases (Wächtershäuser 2014, Wächtershäuser 1992). Also the highly reducing magmatic exhalations offer a high molar ratio of CO/CO_2 (Wächtershäuser 2007). HCN is formed by the condensation reaction of NH_3 and CO (Elsner *et al*. 2002) and the omnipresent transition metals form highly stable ligand complexes with cyanides. COS, formed from CO and H_2S and converted into methanethiol (CH_3SH) by hydrogenation steps under volcanic hydrothermal vent conditions, is considered as a further reactive carbon source for the pioneer organism (Barrault *et al*. 1987, Wächtershäuser 2007). These conversion processes of nutrients (gases) to organic compounds are surface catalysed by the positively charged pyrite surface (transition metal ligand complex catalysis) and the strong interaction with the resulting anions such as $–COO^-$, $–PO_3^{2-}$ or $–S^-$ (Wächtershäuser 1992). These functionalised organic compounds further grew and developed into a pioneer organism. A hypothetic mechanism for example of acetic acid, thioacetic acid, or methyl thioacetate formation on a catalytic surface of (Ni/Fe)S is shown in Figure 4. These products can have occurred by carbonylation of methylthiol as proposed by

Huber and Wächtershäuser on the metallo-sulfidic surfaces (Huber and Wächtershäuser 1997).

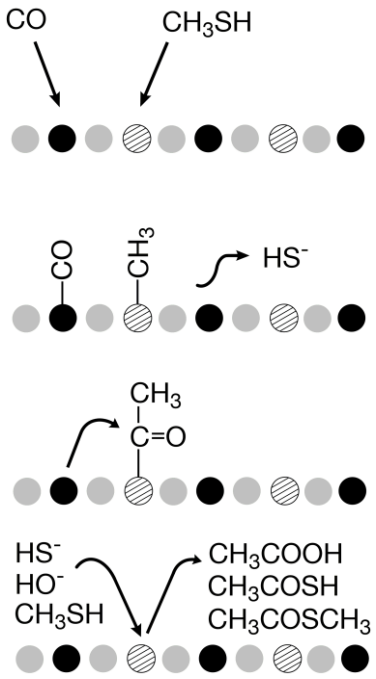

Figure 4: A hypothetic mechanism of a (Ni/Fe)S surface catalysed reaction between CH_3SH and CO as proposed by Huber and Wächtershäuser (Huber and Wächtershäuser 1997). A methyl group derived from methyl mercaptan is transferred to a nickel atom and carbon monoxide to an adjacent iron atom. Nickel-bounded acetyl group is formed by carbonyl insertion. Nucleophilic attack by either hydoxyl, bisulfide, or methane thiol yields acetic acid, thioacetic acid, or methyl thioacetate, respectively (Figure adapted from Cody 2004).

This surface interaction plays a central role in the Fe-S theory as this could overcome the dilution problem of the “soup” theory. This important factor attracted also other scientists in the field. They evidenced concentration dependent processes with the help of a thermal gradient in hydrothermal pores (Mast *et al*. 2013, Kreysing *et al*. 2015) as well as in alternative scenarios including drying lagoons (Patel *et al*. 2015) or ice inclusions (Hao *et al*. 2018).

Superstructure of Pioneer organism – In Figure 5 a cross-sectional representation of the pioneer organism is shown. Carbon fixation of volcanic gases leads to an organic superstructure on a mineral surface containing (Ni/Fe)S (Wächtershäuser 2006).

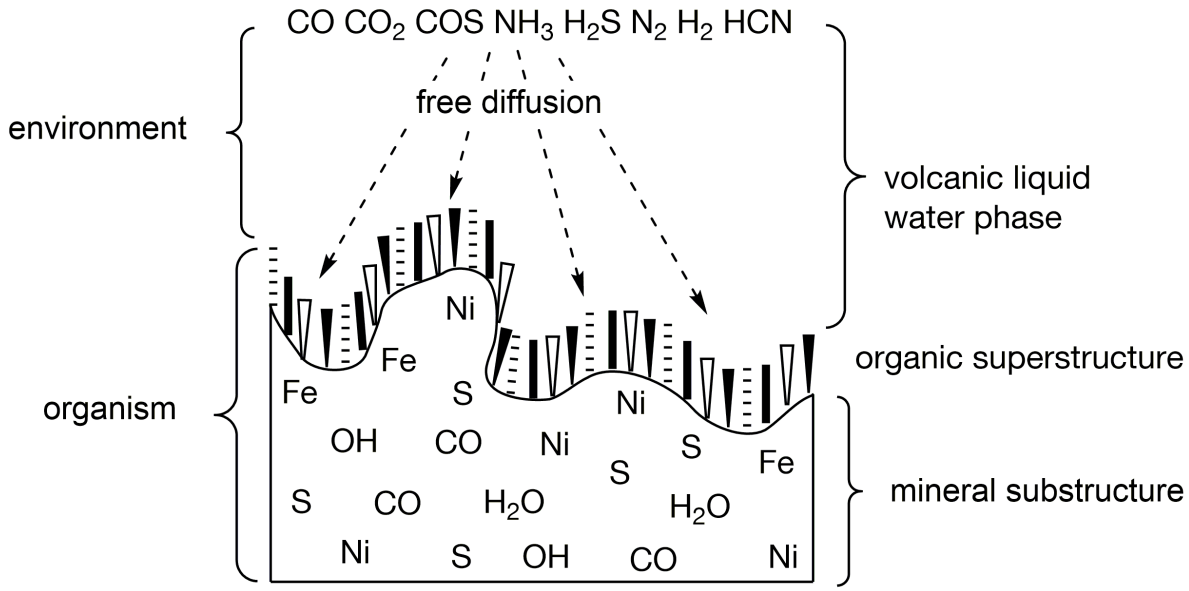

Figure 5: Cross-sectional representation of the pioneer organism. An organic superstructure yielded by C-fixation is formed on mineral surface. Both together represent the organism, which is separated from its environment. Permanent supply of solved volcanic gases ensure growth of the pioneer organism by free diffusion through the lipophilisated surface (adapted from Wächtershäuser 2006).

Both together, mineral surface and organic superstructure represent the pioneer organism, which is separated from its environment. Permanent supply of solved volcanic gases ensure growth of the pioneer organism by free diffusion through the lipophilisated surface (Wächtershäuser 2006). The pyrite-pulled surface mechanism offers a stepwise conversion from a surface metabolism to a cellular organism as shown in Figure 6a-c. The stepwise autocatalytic process begins with the self-lipophilisation of the pyrite surface by formed lipids (Wächtershäuser 1992). Thereafter, surface membranisation to a semi-cell takes place. During the same time, lipids are extended by autocatalysis. The formation of a pre-cellular structure ends with the inclusion of volcanic liquid water and a subsequent separation process of longer lipids leading to a prototypic membrane. A two-dimensional phase separation can be obtained by three different types of lipids, just like any other lipids characterised by a hydrophilic head and a hydrophobic tail (Figure 6i-iii). Lipid-Typ (i) consists of membrane-spanning lipids with a carbohydrate chain and hydrophilic groups at each end. Typ (ii) and (iii) are describing hydrophobic chain with a mono hydrophilic head whereby (iii) exhibit additional polar groups, for example hydroxyl groups, leading to an interdigitated bilayer membrane (Wächtershäuser 1992).

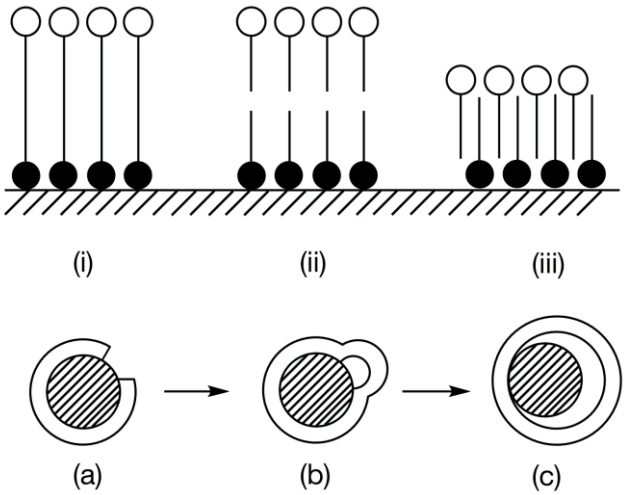

Figure 6: Upper part: schematic representation of different prebiotic lipids types: membrane-spanning lipids (i); hydrophobic chain with a mono hydrophilic head (ii) and (iii) whereby (iii) exhibit additional polar groups. Lower part: self-lipophilisation process of the pioneer organism on a pyrite surface (black core): semi-cell formation (a), complete cellularization and growth process (b), pioneer organism (c) (adapted from Wächtershäuser 1992).

Autocatalysis in the Pioneer organism - A further central piece in the puzzle of understanding the origin of life besides the membranisation of the pioneer organism is the evolution of an autocatalytic metabolism in the form of a self-replicating cycle. Wächtershäuser argued against a heterotrophic origin of life and proposed instead a modified autotrophic carbon fixation pathway of extant life for metabolic reproduction. Based on the aerobic and reducing environment of the early Earth, he focused on the reductive citric acid cycle (rTCA) (Wächtershäuser 1990b). The rTCA cycle can be simplified as followed (see Figure 7): the cycle starts with oxaloacetate, a four-carbon unit whereby two CO_2 are introduced in the cyclic process to give the six-carbon unit of citrate. The cycle ends with the cleavage of citrate to form acetate and oxaloacetate.

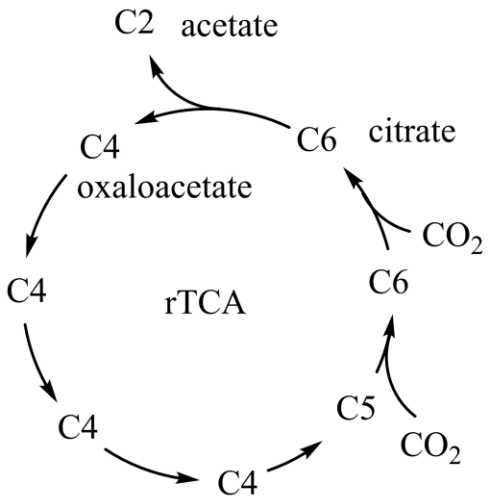

Figure 7: Simplified reductive citric acid cycle. The cycle starts with oxaloacetate, a four-carbon followed by two CO_2 incorporations to the six-carbon, citrate. Citrate cleavage yields in oxaloacetate and acetate.

Wächtershäuser proposed that the CO_2 fixation can be achieved through the reduction potential of the FeS/H_2S-system. Further, he suggested that the cycle should continue autocatalytically if small primer such as succinate or acetate are available. It was calculated that the pyrite-pulled formation of succinic acid is extremely exergonic with a rounded Gibbs energy of -420.0 kJ/mol (pH=0) as shown in equation 2 (Wächtershäuser 1990b).

$$4CO_2 + 7FeS + 7H_2S \rightarrow HOOC\text{-}CH_2\text{-}CH_2\text{-}COOH + 7FeS_2 + 4H_2O \quad \Delta G°=-420\ kJ/mol \quad (2)$$

It is to mention that the evolutionary origin of the rTCA cycle is currently not clear and thus the subject of discussions (Keller *et al*. 2017, Orgel 2008, Smith and Morowitz 2004, Ross 2007, Zhang and Martin 2006, Berg *et al*. 2010a).

Amination of α-keto acids - The rTCA provides precursors for the biosynthesis of amino acids by enzymatic catalysed amination of the α-keto acids intermediates of the rTCA. In early experiments, reductive amination under pyrite formation was tested (Hafenbrandl *et al*. 1995). To this aim, ammonium carbonate was dissolved in water (pH 8.5) at 100°C in the presence of 2-oxo compounds. The prosperous amination for example of phenylpyruvate to phenylalanine under pyrite pulled prebiotic conditions was seen as a further piece of evidence for the iron sulphur world theory. The reductive amination was revisited by Huber *et al*. as they found out that a slightly alkaline pH ~9 and freshly precipitated FeS is more efficient than the dried FeS used in the earlier experiments in 1995 (Huber and Wächtershäuser 2003).

Activated acetic acid - Experimental investigations on “metabolism first” theory by Wächtershäuser were performed in 1997 in cooperation with C. Huber. Indeed, acetic acid could be obtained in experiments with methylthiol and carbon monoxide in the presence of co-precipitated NiS and FeS at 100°C and a neutral pH under atmospheric pressure (Huber and Wächtershäuser 1997). Furthermore, the methyl thioester of acetic acid was successfully isolated from that aqueous reaction mixture indicating the formation of “activated” acetic acid under these conditions. This great found can be seen as a piece of evidence for the “metabolism first” theory.

Pyruvate - In 2000, experiments were carried out using the Wächtershäuser system FeS/H_2S and CO as carbon source, which provided experimental support for the formation of pyruvic acid, one of the most crucial constituents of metabolism (Cody *et al*. 2000). More specifically FeS, formic acid and nonylthiol in addition to elevated pressure of 2000 bar and 250°C were required to form pyruvate. Through the thermal decomposition of formic acid to CO and H_2O a reactive C1-source was given. Still, though from a geological point of view, it remains to be clarified whether such conditions can be found at hydrothermal vents in Hadean times (Wächtershäuser 2000).

α-Amino and α-hydroxy acids – Besides the investigation on activated acetic acid, also the formation of amino acids and further metabolic intermediates was further looking into. A series of α-hydroxy and α-amino was found as main products in a hydrothermal setting containing Ni and/or Fe and carbon sources such as CO, KCN, CH_3SH (Huber and Wächtershäuser 2006). Therefore, the carbon fixation was carried out between 80°C and 120°C and a pressure up to 75 bar. To prevent acidification, $Ca(OH)_2$ or $Mg(OH)_2$ were used as a buffer. This set-up lead to products consisting of up to C4 chain length such as, 2-hydroxy butanoic acid as well as pyruvate, glycolate, lactate and glycerate. With the addition of a nitrogen source, glycine, alanine, serine and amino-butanoic acid were obtained for the first time under this conditions (Huber and Wächtershäuser 2006). However, the experimental conditions led to a controversial debate by some competitors (Bada *et al*. 2007). They criticized the high concentration of cyanide in volcanic solutions which would rapidly hydrolyze at 100°C. As a response, Wächtershäuser and Huber pointed out that they did not perform reactions with dissolved free cyanide ions, which were not detectable in the solutions, but with stable transition metal complexes with cyano ligands (author reply Bada *et al*. 2007). Further, Bada *et al*. criticized the high CO pressure of 75 bar used in the experiments (Bada *et al*. 2007). Anyhow, Huber and Wächtershäuser pointed out that in one experiment with 1 bar CO the products were also detected, albeit at lower concentrations. They also explained that their intension was to shorten reaction times by increasing one parameter such as pressure (10 or 75 bar CO) (author reply Bada *et al*. 2007).

They further demonstrated, in modelled volcanic hydrothermal vent experiments, that an increased reaction temperature between 145°C to 280°C is more efficient in formation of α-amino and α-keto acids (Huber *et al*. 2010). In this context they supposed that the synthesis of these molecules must be localised in flow zones with temperatures as high as 280°C. In addition, they also detected an extended product range of amides like glycolamide, glycine amide, lactamide, alanine amide and glyceramide as reaction intermediates. Using experiments with stable isotope labeled precursors, they were also able to identify KCN as the major carbon and nitrogen source and CO as the reductant and a minor carbon source (Huber *et al*. 2010).

Based on these results, Huber *et al*. suggested an organo-metal-catalysed mechanism for the formation of the obtained α-amino and α-hydroxy acids in a further publication (Huber *et al*. 2012). They proposed a hypothetical mechanistic scheme leading to alanine and lactate by multiple cyanide insertion *via* a nickel complex, which is shown in Figure 8. They assumed the first stage of the mechanism to be a stable tetracyanonickelate ion $[Ni(CN)_4]^{2-}$ in the presence of H_2 or CO.

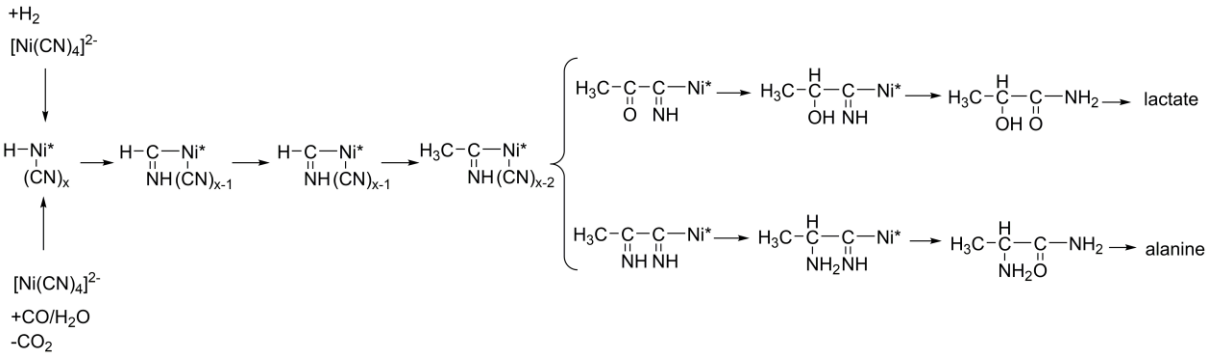

Figure 8: Hypothetical mechanism of the reduction reaction leading to alanine or lactate by multiple cyanide insertion in an unknown Ni-complex (adapted from Huber 2013, Huber *et al*. 2012).

Reductive addition of a hydride-ligand leads to a complex in which the nuclearity, oxidation state, geometry and ligand sphere of nickel is unknown. It is therefore noted as [Ni*] in Figure 8. The next step is the rearrangement and insertion of a cyano ligand into the H-Ni* bond which is followed by several reduction steps yielding a methyl ligand. According to the products, the steps can be repeated to get an elongation of the C-skeleton. Their hypothetical mechanism involves an optional hydrolysis in α-position and ends with subsequent reduction and release of the free amides to finally produce alanine or lactate, respectively (Huber *et al*. 2012).

Peptides - Consequently, the next main interest after having a theoretical explanation of the formation of amino acid was to look into the emergence of peptides, as they are crucial molecules for the evolution of life as it is today. The pioneers in this field, Huber and Wächtershäuser were thus able to activate α-amino acids with CO and showed a condensation reaction yielding mainly dipeptides, as well as tripeptides (Huber and Wächtershäuser 1998). The formation of peptide bonds was demonstrated with phenylalanine (Phe), tyrosine (Tyr) and glycine (Gly) in the presence of co-precipitated (Ni,Fe)S in a favoured pH range between 8 to 9.5. In separate experiments, the authors also observed hydrolysis of small peptides under the same hot aqueous conditions (Huber and Wächtershäuser 1998). They compared this balance between synthesis and hydrolysis to anabolic and catabolic reactions, which are typical for extant metabolism. In an ensuing paper, Huber *et al.* propose a possible peptide cycle (Huber *et al*. 2003).

In Figure 9, a CO-driven cyclic reaction starting from alanine to the desired dipeptide alanylalanine is shown (Huber 2013). A ring closure of Ala-Ala to the conforming hydantoin derivative by CO insertion is also observed. *Via* a hydrolysis step of one amide bond, the heterocyclic by-product is converted into an urea-type intermediate.

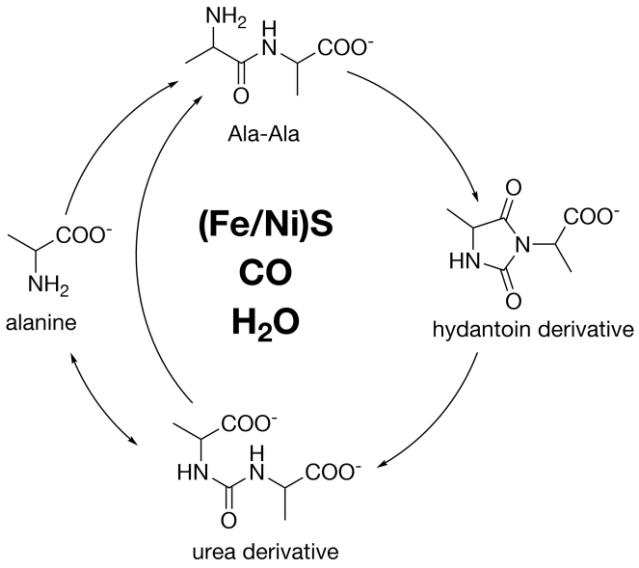

Figure 9: Schematic CO-driven peptide cycle with alanine in aqueous (Ni/Fe)S system. Dipeptide formation of Ala-Ala *via* hydantoin derivate and urea derivate (adapted from Huber *et al*. 2003, Huber 2013).

Alternatively, linking two alanines in the presence of CO can also form such intermediate. After cleaving off a carboxyl-group, a rearrangement of the urea derivate leads again to the dipeptide. Huber *et al*. also referred to the analogy between the occurring urea derivatives and their hydrolysis under prebiotic conditions to the today's nickel enzyme, urease. In addition,

they suggested that the continuously formed hydantoin could be considered a simple heterocyclic precursor for purines. Finally, through increased pressure they also successfully synthesised tetrapeptides (Huber 2013, Huber *et al*. 2003). In total, these results of several important classes of biomolecules under the conditions of volcanic hydrothermal vents, gave an insight of the amazing potential of the iron sulphur world.

1.2 Evolution of Life

Up to now (see chapter 1.1) the evolution of small molecules to build biomolecules was theorized out of the "Bottom-Up" point of view. To fully understand this process of the emergence of life, another powerful tool is found in the retrodiction of the biochemistry back to simpler forms, the so-called "Top-Down" approach (Peters and Williams 2012). But the consideration of living organism or systems leads inevitable to a further fundamental debate, the problem of defining "life" (Trifonov 2011). There is no unequivocal definition but the following criteria have been found so far in all living systems (Eigen 1995):

I. *Metabolism* - external energy and material supply is necessary; without this, an equilibrium state would be reached.
II. *Self-reproduction* - implies the information transfer; without it, information gets lost after every generation.
III. *Mutation* - implies the development of a living system; without it, information would be invariant.

Darwinian evolution - A pioneer of the "Top-Down" convergence was Charles Darwin. His groundbreaking observations and ideas are culminated in his work "On the origin of species" (Darwin 1859). He revealed numerous evidences that all living beings change properties by natural selection over a longer period of time. As a direct consequence, Darwin reasoned in the same publication that there was one progenitor for all life forms:

"*Therefore I should infer from analogy that probably all the organic beings which have ever lived on this earth have descended from some one primordial form, into which life was first breathed.*"

Central dogma of molecular biology - However, Darwin was not able to explain how heritable information is passed from generation to generation. It took almost one century to find out that the heritable information is genetically encoded by of four nucleobases (Gamow 1954; Nirenberg and Matthaei 1961, Woese *et al*. 1966), and is passed on by the replication of deoxyribonucleic acid (DNA) (Watson and Crick 1953). Furthermore, it was Crick, who

stated first an explanation about the flow of genetic information in biological systems, the so-called “central dogma of molecular biology” as shown in Figure 10 (Crick 1970).

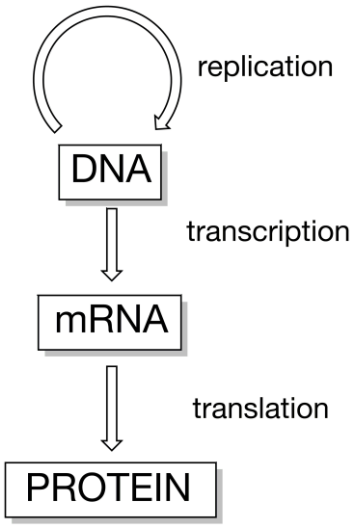

Figure 10: Cricks’s “Central Dogma of Molecular Biology” (adapted from Crick 1970).

Information flow starts with the replication of DNA, carried out by a DNA polymerase. Afterwards, the information is transcribed into other types of nucleic acids, known as messenger ribonucleic acid (mRNA), by a RNA polymerase and then translated into proteins by ribosomes.

1.2.1 The RNA World Theory

Assuming, that self-replicating systems in general and translation in particular are significant for the emergence of life, a “genetic first” theory became more and more popular. In Crick´s central dogma (Crick 1970), it was pointed out that both, DNA and proteins depend on each other. The sole function of DNA is to store information without any catalytically properties, while proteins that are encoded by the DNA fold into complex structures that give them strong catalytic activities. Both functions are central features of living systems but it seemed improbable to the researchers that both types of molecules occurred simultaneously and thus a hen-egg dilemma between DNA and proteins occurred. RNA offers a possible resolution of this problem. As a polynucleotide, RNA is able to store genetic information similar to DNA. Furthermore, since the discovery of ribozymes it is also known that RNA shows enzymatic activities (Kruger *et al*. 1982, Guerrier-Takada *et al*. 1983). Their finding argues for RNA as

candidate for a first replicator and forms the foundation of “The RNA world” hypothesis (Gilbert 1986). The RNA world hypothesis belongs to the heterotrophic origin of life based on a replicating system of organic macromolecules and stands in contrary to an autotrophic metabolism first hypothesis. The size of a ribozymes with the ability to replicate RNA sequences should have had a length of at least 200 nucleotides, which is an enormous macromolecule as origin of life (Wochner *et al*. 2011, Mast *et al*. 2013). On the one hand, exploration in the RNA world could focus on prebiotic scenarios that may enhance the polymerization of monomers or oligomers without the help of enzymes (Morasch *et al*. 2016, Mast *et al*. 2013). Further, even if RNA single strands can be built up further issues such as non-enzymatic copying reaction and later on replication processes of RNA still needs to be proven. On the other hand, perhaps the first challenge in the RNA World is the prebiotic synthesis of RNA. It is a great challenge to the prebiotic chemist, and is the focus of many investigations (Becker *et al*. 2016, Powner *et al*. 2009). Alternatively and based on the consideration of the chemical complexity of RNA, other possible polymeric substances are suggested as potential precursor of RNA. Efforts were mainly put on the existence explanation of the sugar-phosphate backbone of RNA, which can additionally be replaced for example by peptides (PNA) (Nelson *et al*. 2000), threofuranosyl (TNA) (Schöning *et al*. 2000), or glycol (GNA) (Zhang *et al*. 2005). Numerous studies on the RNA world carried out in the recent years and lead to a further open question: What was first: genetics or metabolism?

1.3 Approaching Origin of Life from the “Top-Down”

1.3.1 Phylogenetic Tree of Life

Phylogenetic tree - Due to the enormous diversity of species on earth today, the understanding of Darwinian evolution is essential for the reconstruction of a family tree for all living organisms to try to solve the question of a common beginning. Woese was able to construct such a diagram by comparing the differences between ribosomal RNA (rRNA) sequences from many species (Woese 1981). In 1981, he discovered unusual bacteria, the archaea, and revisioned the order of life. Together with Kandler, Woese implemented a three-domain model divided into two kingdoms, shared in prokaryotes including bacteria and archaea with a branched symbiogenetic eukaryote partnership (Figure 11) (Woese *et al*. 1990).

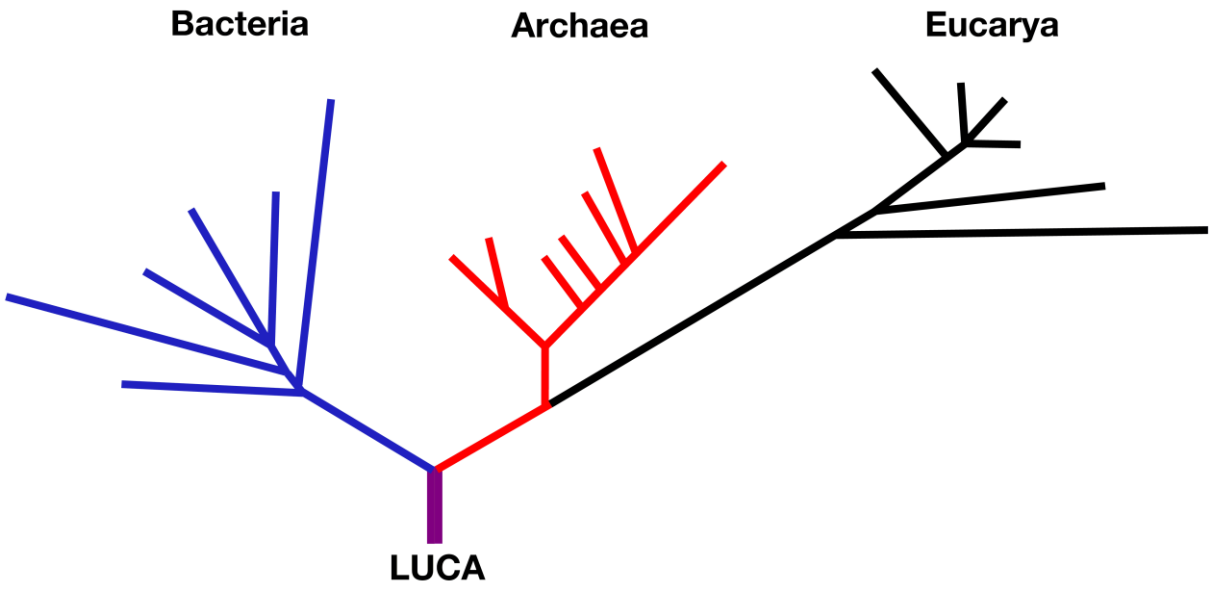

Figure 11: Phylogenetic tree of life for rRNA sequences, showing three domains bacteria (blue), archaea (red) and eucarya (black) (adapted from Woese *et al*. 1990).

Modified tree of life - The traditional tree of life is vertical and thus shows a lateral gene transfer from ancestor to successor. However, there are discrepancies in this traditional tree as it was discovered that secondary processes are involved in some microorganisms, which are called horizontal gene transfers. It is the transfer of genetic material between two organisms that are not parent and offspring. Thus, vertical and horizontal gene transfer can modify the tree of life (Doolittle 2000). This tree originates of a community of primitive cells, as already discussed in Figure 2. However, many scientists considered that the change in genes

of that 16S rRNA, used for the monophylogenetic tree of life by Woese, is so little that the old representation is still valid.

Differences archaea vs bacteria - For unraveling the course of cellular evolution backwards in time a detailed analysis of the phylogenetic tree is necessary. Archaea resemble bacteria in their structural organization because of their lack of a nucleus. Anyhow, there are nonetheless clear differences. Archaea differ from bacteria not only in RNA sequence but also for example in their cell membrane and lipid structure as shown in Figure 12 (De Rosa *et al*. 1986). Two ether linkages with methyl-branched prenyl group tails mainly characterize archaea lipids. Bacteria-type membrane lipids typically consist of two monopolar linear fatty acid chains joined to a glycerol moiety *via* ester linkages. These glycerol phosphate head groups are mirror images of each other and therefore differ in chirality (De Rosa *et al*. 1986).

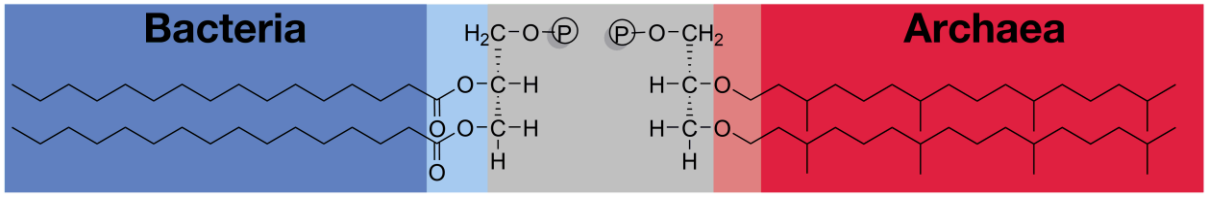

Figure 12: The different membranes of archaea and bacteria in comparison. On the left hand: Archaeal glycerol phosphate head group are linked to isoprene chains (dark red) *via* ether linkages (light red). On the right hand: Bacterial glycerol phosphate head group are linked to straight chains (dark blue) *via* ester linkages (light blue) (adapted from De Rosa *et al*. 1986).

Bacterial cell walls additionally have mesh like structures of peptidoglycans, also known as murein, formed by *N*-acetylglucosamine, *N*-acetylmuramic acid and amino acids (Schleifer and Kandler 1972). Furthermore, bacteria distinguish from archaea by their RNA polymerases (Hirata and Murakami 2009, Jun *et al*. 2012). The archael basal transcription apparatus resembles more to those of eukaryotes in construction and translation processes. Bacteria have only one ribosomal RNA (rRNA) polymerase while archaea have three rRNA polymerases. These differences lead to a Y-type phylogenetic tree, ending with a vertical monophylic line, which can be seen as the trunk of the tree. It represents a hypothesis of a common beginning with an unknown “Last Universal Common Ancestor” (LUCA).

Oldest microfossils - The geological studies of the oldest sedimentary rocks point towards an origin of LUCA under hydrothermal systems. Analysis of isotopic compositions of methane fluid inclusions in ~3.5 billion years old rocks in Australia indicate microbial methanogenesis in

the early *Archaean* era (Ueno *et al*. 2006). Additionally, carbonaceous inclusions in West Greenland and Akilia Island from the Isua supracrustal belt were found. The carbon-isotope composition analysis suggested carbon fixation and provided evidence for the emergence of life on earth at least 3.8 billion years ago (Mojzsis *et al*. 1996). In the same belt region, as mentioned before, stromatolites with microbial structures were found indicating the establishment of biotic CO_2 fixation about 3.7 billion years ago (Nutman *et al*. 2016). Further, stable isotope evidence of carbon fixation was found in ca. 4.1 billion years old zircons from the Jack Hills in Western Australia (Bell *et al*. 2015). In addition to that, microbial structures within a fossilized hydrothermal vent (~3.8 billion years old) were found in sedimentary rocks from the Nuvvuagittuq belt in Canada (Dodd *et al*. 2017). These geological findings reinforce the hypothesis of a chemical evolution at hydrothermal systems and a chemoautotrophic origin by reductive carbon fixation (Wächtershäuser 1992). Indeed, many microorganisms such as archaea still live close to hot volcanic flow environments and are capable of autotrophic metabolism (Berg *et al*. 2010a).

1.3.2 Autotrophic Origin of Life

Autotrophic CO_2 fixation pathways.- There are currently six different pathways for reductive carbon fixation operating in bacteria and archaea (Hügler and Sievert 2011): the Calvin-Benson-Bassham (CBB) cycle (Bassham *et al*. 1954); the reductive tricarboxylic acid (rTCA) cycle (Buchanan and Arnon 1990); the reductive acetyl-CoA or Wood-Ljungdahl (WL) pathway (Ljungdahl 1986); the 3-hydroxypropionate bicycle (3-HPB) (Zarzycki *et al*. 2009); the 3-hydroxypropionate/4-hydroxybutyrate (3-HP/4-HB) (Berg *et al*. 2007), and the dicarboxylate/4-hydroxybutyrate (DC/4-HB) cycle (Huber et al. 2008). In the following each of the cycles will be discussed.

Calvin-Benson-Bassham-cycle - The reductive pentose phosphate cycle is the predominant carbon fixation pathway on our planet (Erb and Zarzycki 2017). The CBB cycle can be split into three important steps. In the first step three CO_2 molecules are fixated *via* electrophilic addition to three molecules of ribulose 1,5-bisphosphate catalysed by the key enzyme ribulose-1,5-bisphosphate carboxylase/oxygenase (RuBisCO). This carboxylation leads to three unstable C6-intermediates that quickly hydrolyse into six molecules of 3-phosphoglycerate (see Figure 13). The next step is the reduction to glyceraldehyde 3-phosphate (3-GAP). In the last step, ribulose-1,5-bisphosphate is regenerated out of five molecules of 3-GAP. Altogether, three CO_2 molecules are incorporated in one cycle to produce one molecule of 3-GAP, which then can be used for the synthesis of sugars or other metabolites. For a functional cycle,

RuBisCO and phosphoribulokinase, a transferase, which catalyses the phosphorylation of ribulose-5-phosphate (RuP), are necessary.

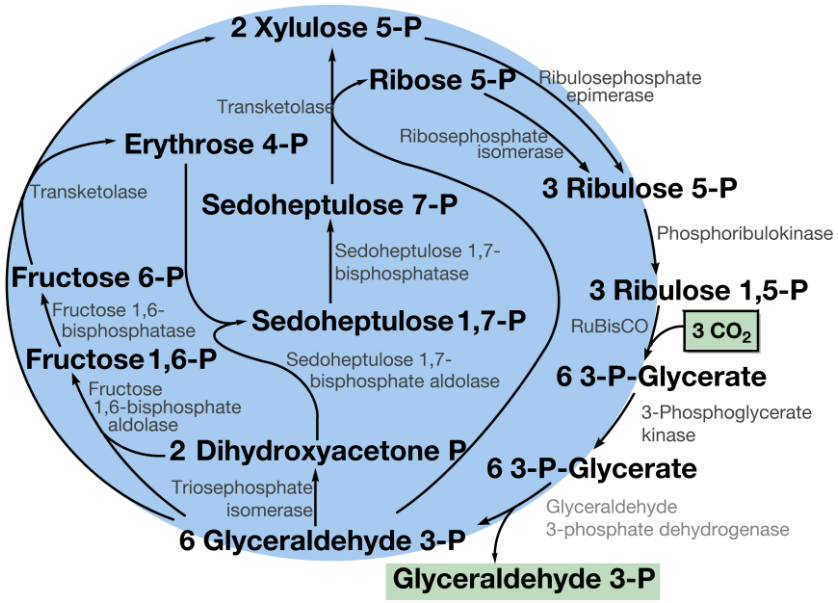

Figure 13: The CBB cycle. The biochemical reactions involved, as well as the enzymes catalysing the reactions, are depicted (adapted from Berg 2011).

The CBB cycle can be found in plants, algae and many different bacterial species but apparently not in archaea, because they only encode one of both key enzymes, the RuBisCO (Berg 2011). Presently, four different forms are known I, II, III and IV whereby type IV doesn't catalyse the carboxylation and seems to be only a RuBisCo like protein without function (Tabita *et al*. 2007). However, phylogenetic analysis supports a common origin of all forms whereby it is suggested that the archaeal RuBisCo III was the predecessor to all eukaryotic and bacterial lineages (Tabita *et al*. 2008). Among the autotrophic pathways, the CBB cycle is considered less ancient. CBB is adapted to less extreme habitants as suggested for the origin of life. This autotrophic CO_2 fixation pathway tolerates oxygen and heat-labile intermediates are included (Berg 2011). Additionally, the energy cost of an organism using the CBB cycle is enormous and devours seven ATP per molecule of pyruvate synthesized.

Reverse tricarboxylic acid cycle - The rTCA cycle reverses the reaction steps of the oxidative citric acid cycle, also known as Krebs cycle as shown in Figure 14. To operate the cycle in the reductive direction, several enzymes considered to be irreversible must be exchanged: succinate dehydrogenase is replaced by fumarate reductase, α-ketoglutarate dehydrogenase by a synthase and the citrate synthase by the ATP-citrate lyase (Ivanovsky *et al*. 1980, Evans *et al*. 1966, Fuchs 2011). The two latter enzymes can be considered as the

key enzymes for the complete CO_2 fixation cycle. However, most enzymes of the pathway catalyze also reactions in both directions such as malate dehydrogenase, fumarate hydratase, succinyl-CoA synthase, isocitrate dehydrogenase and aconitate hydratase. The rTCA cycle generates acetyl-CoA from two molecules of CO_2 by reductive carboxylation steps catalyzed by α-ketoglutarate synthase and isocitrate dehydrogenase (Fuchs 2011, Hügler and Sievert 2011).

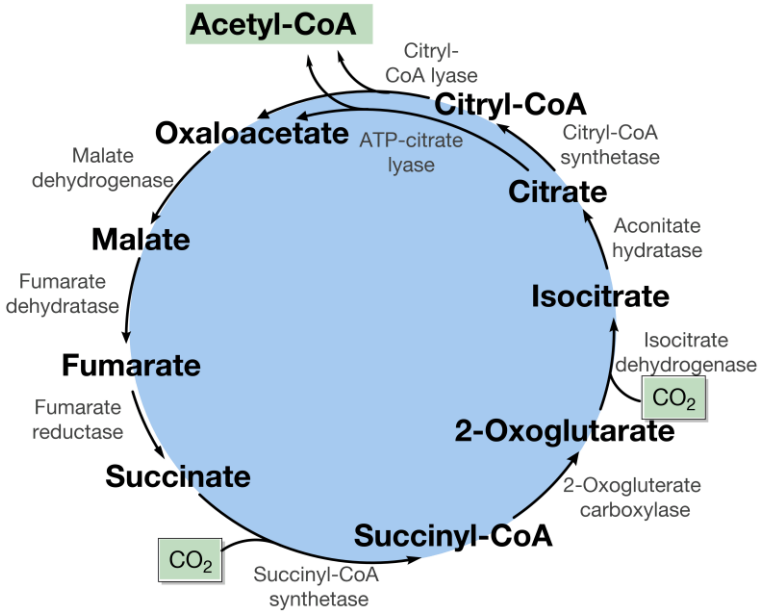

Figure 14: The reverse tricarboxylic acid cycle. The biochemical reactions involved, as well as the enzymes catalysing the reactions, are depicted (adapted from Hügler and Sievert 2011).

The cycle requires both reduced ferredoxin and nicotinamide adenine dinucleotide phosphate NAD(P)H as electron donors and only two ATP equivalents to form pyruvate. Thus it is much less energy-consuming than the Calvin-Bensson cycle that requires seven ATP equivalents (Berg 2011). The rTCA cycle is used by green sulfur bacteria including *Chlorobi* from a deep-sea hydrothermal vent, which possess a FeS photosynthetic reaction center that is capable of direct reduction of ferredoxin at extremely low light intensities (Beatty *et al*. 2005, Bryant and Frigaard 2006). Furthermore besides CO_2, green sulfur bacteria also make use of acetate and pyruvate to grow as mixotrophs (Feng *et al*. 2010). This ability of a co-assimilation of organic compounds might pay off in the evolution and is probably a bio-signature of primordial microorganism (Fuchs 2011, Berg *et al*. 2010a). Nonetheless, in regard of the phylogenetic distribution, the rTCA cycle is present in quite diverse anaerobic bacteria but until now it has not been found in the archaeal domain (Berg *et al*. 2010a, Ramos-Vera 2011). The evolutionary origin of the rTCA cycle is not certain, but the widespread occurrence of at least

its oxidative reactions indicates a possible succession of the primordial cycle (Wächtershäuser 1990b, Smith and Morowitz 2004, Keller *et al*. 2017).

Wood-Ljungdahl-pathway - Of the autotrophic pathways known today, the Wood-Ljungdahl pathway is the only pathway that has been found to operate in both, bacteria *via* acetogenesis, and archaea *via* methanogenesis (see Figure 15 blue and red). This pathway is a candidate thought to have evolved first (Fuchs 2011, Berg 2011). Furthermore, this is the only autotrophic pathway that generates energy by noncyclic exergonic carbon assimilation (Fuchs 2011, Berg 2011).

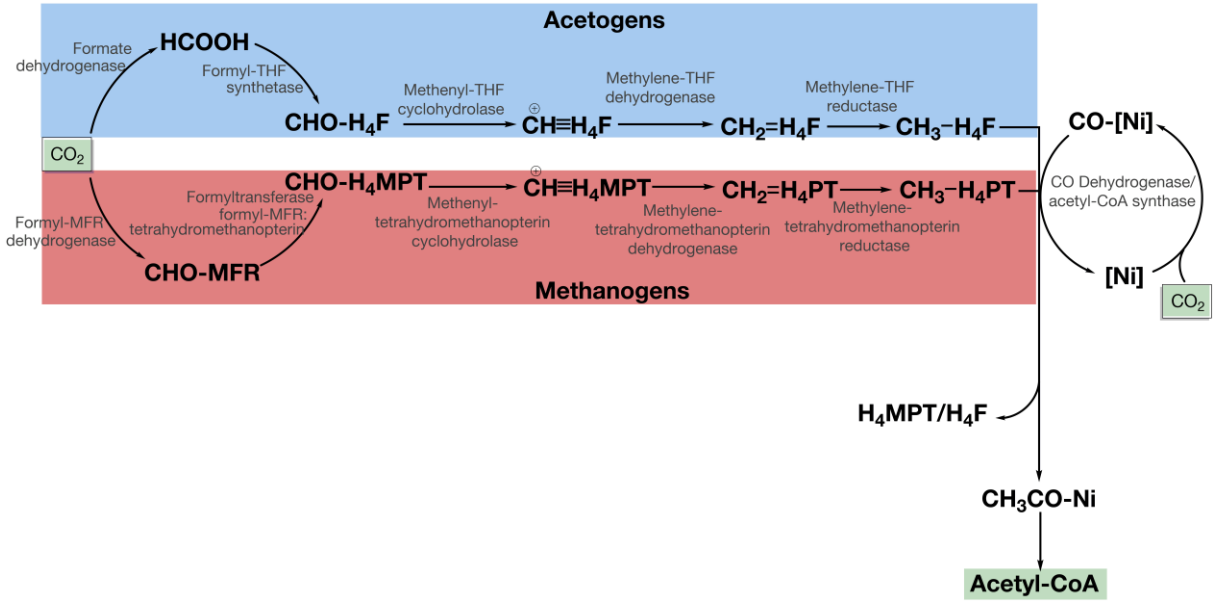

Figure 15: The Wood-Ljungdahl pathway. The biochemical reactions involved, as well as the enzymes catalysing the reactions, are depicted. The upper part shows the variant of the pathway functioning in acetogens (blue), and the lower part depicts the pathway in methanogens (red). It has to be noted that the reductive acetyl-CoA pathway is so far the only known CO_2 fixation pathway used by bacteria as well as archaea (adapted from Berg 2011, Fuchs 2011).

In Figure 15, the variant of methanogenesis is depicted, whereby two molecules of CO_2 are simultaneously fixed and reduced by hydrogen. One CO_2 is reduced to a methyl group bound to the carrier tetrahydropterin followed by a methyl transfer. In Figure 15, the upper part shows the variant of acetogens, which mainly differs in the reduction of CO_2 by formate dehydrogenase to the free intermediate formate. This intermediate is activated by formyl-tetrahydrofolate synthase and is subsequently converted to an activated methyl group. The key characteristics of the reductive acetyl-CoA pathway fit well with a presumed emergence of life at hydrothermal scenarios and can be summarized in low demands of one ATP per

molecule of acetyl-CoA, high oxygen sensitivity, enormous heat stability and high requirement of many different transition metals (Mo or W, Co, Ni, and Fe) (Berg 2011).

The 3-hydroxypropionate–bicycle - This autotrophic CO_2 fixation pathway was discovered by Holo and originally proposed as a monocycle but several years later it turned out to be a bicycle (Holo 1989, Strauss and Fuchs 1993, Herter *et al*. 2002, Zarzycki et al. 2009). As shown in Figure 16, two cycles are involved in this autotrophic CO_2 fixation pathway and lead consequently to its name, 3-hydroxypropionate bicycle. One of the cycles starts with the carboxylation of acetyl-CoA *via* bicarbonate to malonyl-CoA, which is further reduced to 3-hydroxypropionate and subsequently to propionyl-CoA (Hügler and Sievert 2011). A second carboxylation step of propionyl-CoA yields the C4 unit methylmalonyl-CoA, which is converted to (S)-malyl-CoA *via* succinyl-CoA, succinate, fumarate and malate. Finally, the starting molecule of the cycle, acetyl-CoA is regenerated by the cleavage of (S)-malyl-CoA and releases glyoxylate as a first carbon fixation product (Strauss and Fuchs 1993).

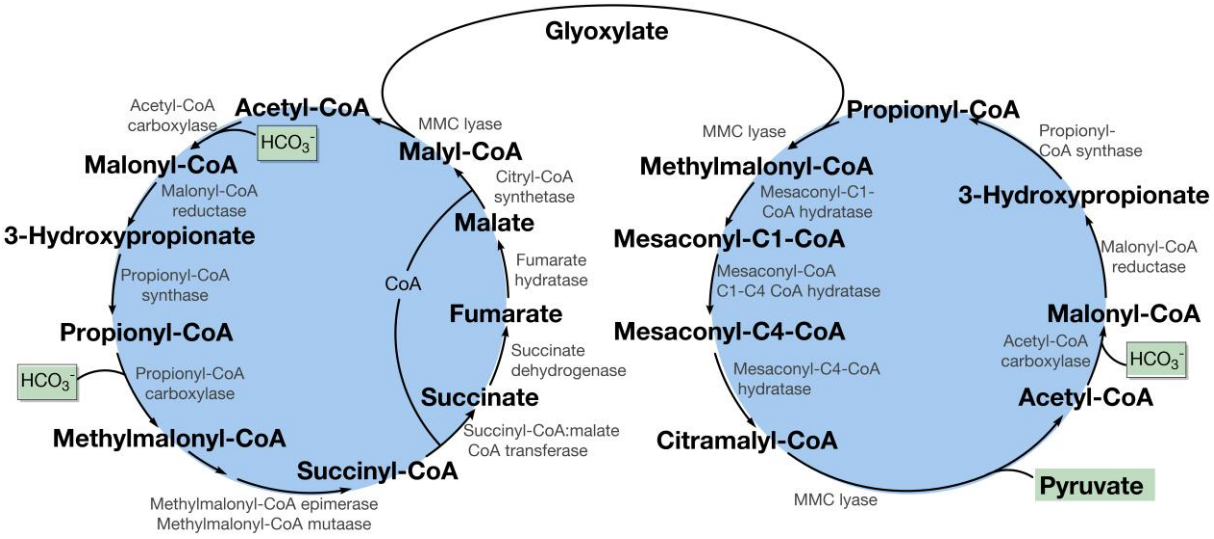

Figure 16: The 3-hydroxy propionate bicycle. The biochemical reactions involved, as well as the enzymes catalysing the reactions, are depicted (adapted from Hügler and Sievert 2011).

Glyoxylate induces a second assimilation cycle by addition to propionyl-CoA, leading to methylmalyl-CoA, which is converted *via* mesaconyl-CoA to citramalyl-CoA. At this point, the second cycle is closed by the cleavage of citramalyl-CoA to pyruvate and acetyl-CoA. In total, under the requirement of seven ATP and three molecules of bicarbonate, one molecule of pyruvate is formed (Berg 2011). Interestingly, the bicycle involving 19 reaction steps is catalysed by only 13 non oxygen sensitive multifunctional enzymes including the key enzymes malonyl-CoA reductase, propionyl-CoA synthase and malyl-CoA lyase (Hügler and Sievert 2011, Berg 2011). This autotrophic pathway appears to be restricted to bacteria, which

can be found in species from hot spring microbial mats (van der Meer 2000). Probably *Chloroflexaceae* may profit from using bicarbonate as inorganic precursor, for the reason that the concentration is much higher in its favoured habitant of slightly alkaline water. The 3-HPB cycle allows co-assimilation of numerous compounds such as acetate, propionate, succinate and the corresponding alcohols (Zarzycki *et al*. 2009).

The 3-hydroxypropionate–4-hydroxybutyrate cycle - The 3-HP/4-HB cycle functions in extreme thermoacidoophilic archaea, namely *Crenarchaeota* and *Sulfolobales* that prefer volcanic areas with a pH of around 2 and a temperature of 60–90 °C (Ishii *et al*. 1997, Menendez *et al*. 1999, Berg *et al*. 2007, Berg *et al*. 2010b). The discovery of the acetyl-CoA carboxylase in these archaea was surprising due to the lack of fatty acids in archaeal membranes (Norris *et al*. 1989, Burton *et al*. 1999, Hügler *et al*. 2003, Chuakrut *et al*. 2003).

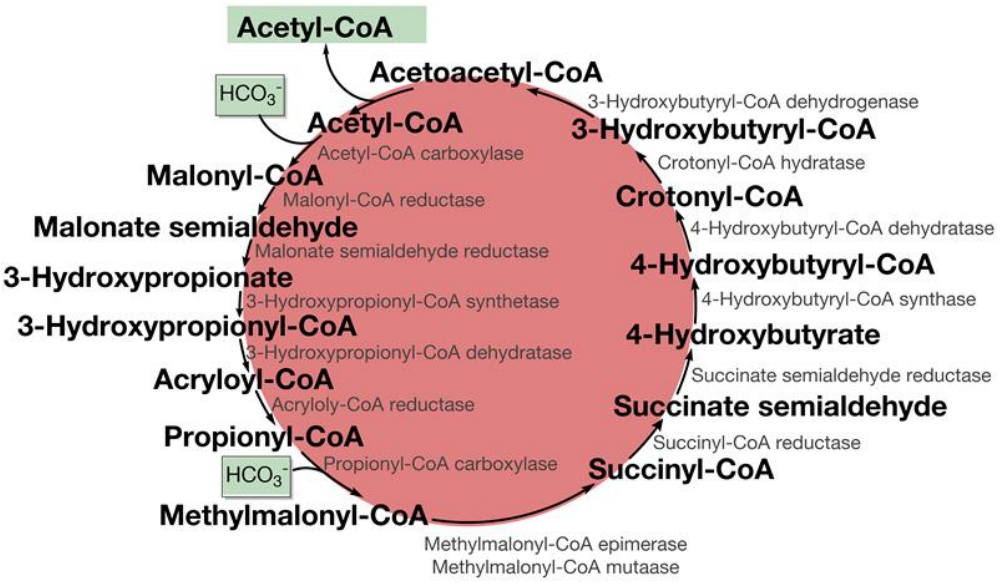

Figure 17: The 3-hydroxypropionate/ 4-hydroxybutyrate cycle. The biochemical reactions involved, as well as the enzymes catalysing the reactions, are depicted (adapted from Hügler and Sievert 2011).

In bacteria and eukarya, this enzyme is typically used to catalyse the first step in fatty acid biosynthesis and, thus, this enzyme obviously has a different role in archaea as they do not show such lipids. Hence, this acetyl-CoA carboxylase is found to be active in carbon fixation similar to the 3-HPB (see Figure 17). The first part of the 3-HP/4-HB bicycle from acetyl-CoA to succinyl-CoA has the same intermediates as the first turn of the bacterial 3-HPB. But the enzymes used, differ and are not homologues so that they might have evolved independently (Berg *et al*. 2010a). Additionally the archaic 3-HP cycle is modified by further intermediates such as malonate-semialdehyde, 3-hydroxypropionyl-CoA and acryloyl-CoA. The second part of the bicycle is completely different in comparison to the C4 units, which are used in the 3-HPB. Succinyl-CoA is transformed to acetoacetyl-CoA *via* succinate-semialdehyde, 4-

hydroxbutyrate, 4-hydroxybutyryl-CoA, crotonyl-CoA and 3-hydroxybutyryl-CoA. The cycle is closed by the cleavage of acetoacetyl-CoA into two molecules of acetyl-CoA. The archaic species used in the 3-HP/4-HB cycle, require nine ATPs and might have returned to an anaerobic lifestyle while retaining oxygen tolerant enzymes (Berg *et al*. 2010a). Interestingly in context of the origin of life most of these *Sulfolobales* can grow chemo-autotrophically on sulphur or pyrite or H_2 (Auernik *et al*. 2008, Berg *et al*. 2010a).

The dicarboxylate–4-hydroxybutyrate cycle - The differentiation of this DC/4-HB cycle from the others is difficult because no enzyme is unique for this pathway. One part involves the conversion of oxaloacetate to succinyl-CoA similar to the rTCA, while the second part corresponds to the reaction sequence of succinyl-CoA to acetyl-CoA matching the 4-HB of the 3-HP/4-HB cycle (see Figure 18).

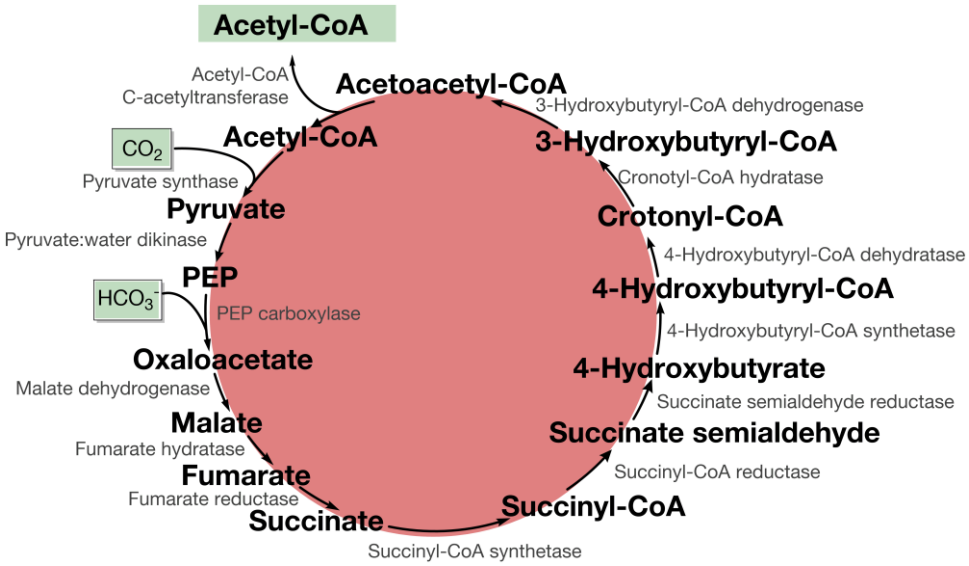

Figure 18: The dicarboxylate/4-hydroxy butyrate cycle. The biochemical reactions involved, as well as the enzymes catalysing the reactions, are depicted (adapted from Hügler and Sievert 2011).

To convert acetyl-CoA to oxaloacetate three additional enzymes are necessary: Pyruvate synthase, pyruvate:water dikinase and phosphoenolpyruvate (PEP) carboxylase (Hügler and Sievert 2011). It seems that the DC/4-HB cycle is present in almost all anaerobic autotrophic members of both order *Desulfurococcales* and *Thermoproteales* of archaea (Fuchs 2011). In terms of ATP costs, the synthesis of one molecule of pyruvate requires five units of ATP within the use of oxygen sensitive enzymes (Berg *et al*. 2010a).

Summary - In Table 1 the six different autotrophic pathways are summarized concerning their ATP cost *versus* pyruvate production, heat stability and oxygen tolerance and the distribution in the phylogenetic tree of bacteria and archaea. These data of extant microorganisms could

retain some characteristics of LUCA and may give some insights into the evolution of carbon fixation.

Table 1: The six autotrophic CO_2 fixation pathways and their properties related to the origin of life in microorganisms (adapted from Berg et al. 2010a, Berg 2011, Hügler and Sievert 2011).

Pathway	ATP cost/ pyruvate	Heat stability	O_2-tolerance	Distribution in phylogenetic tree
CBB-cycle	7	thermophilic	yes	bacteria
rTCA cycle	2	hyperthermophilic	no	bacteria
WL-pathway	~1	hyperthermophilic	no	bacteria/archaea
3-HP bicycle	7	mesophilic	yes	bacteria
3-HP/4-HB cycle	9	hyperthermophilic	yes	archaea
DC/4-HB cycle	5	hyperthermophilic	no	archaea

CHAPTER 2
MOTIVATION

The question of the emergence of life is an extremely exciting topic, but also highly complex. To solve this conundrum, the collaboration of astronomers, geoscientists, chemists, theorists, physicists and biologists is necessary. This work covers multiple disciplines, belonging to chemistry, biology and geoscience. The aim of this work is to find and to establish ties between the abiotic chemoautotrophic carbon fixation of the pioneer organism according to the iron sulfur world and extant chemoautotrophic CO_2-fixation pathways, still used by ancient microorganisms at hydrothermal vents.

2.1 Experiments based on the Iron Sulphur World

In the last 20 years, the study of surface-catalyzed reactions under volcanic hydrothermal vent conditions resulted in the production of a plenty of biomolecules such as amino acids, small peptides, α-hydroxy and α-keto acids as well as activated acetic acid. To validate the hypothesis of a pioneer organism in terms of the iron sulphur world, further experiments were projected to form lipids or lipid like molecules under the conditions proposed by Wächtershäuser. The still not examined source for primordial lipids in the FeS-world took a prominent role among the major open problems for the origin of life. It is not clear when and how they arose, however, cellular encapsulation, meaning isolation from the surrounding environment, is necessary for a primordial organism. It is often assumed that a protocellular compartment was defined by much “simpler” fatty acids than the phospholipids used by extant organisms to form bilayer structures (Chen and Walde 2010). This work was therefore aimed to focus on the terrestrial formation of fatty acids under suboceanic volcanic hydrothermal vent conditions by using reactive volatiles, surface-catalyzed by redox active minerals such FeS or NiS according to the iron sulphur world.

Interestingly, a high relative gas, acetylene, was found in fumarolic gases (Oremland and Voytek 2008, Igari *et al*. 2000) archean quartz (Schreiber *et al*. 2017) and as a product of volcanic simulation experiments (Mukhin 1976). Bearing these exiting findings in our mind, we suggested that the hydrolysis of carbide (Wiberg 2007) on early Earth would have caused the outgassing of acetylene. The question arises if acetylene, a C2-body, acts similar to the key substrate, acetyl-CoA used in archaeal and bacterial lipid biosynthesis (see Figure 19) as chain elongation precursor. Thus, it slipped in our focus as an adequate candidate for an experimental setup to form lipids according to the iron sulphur world.

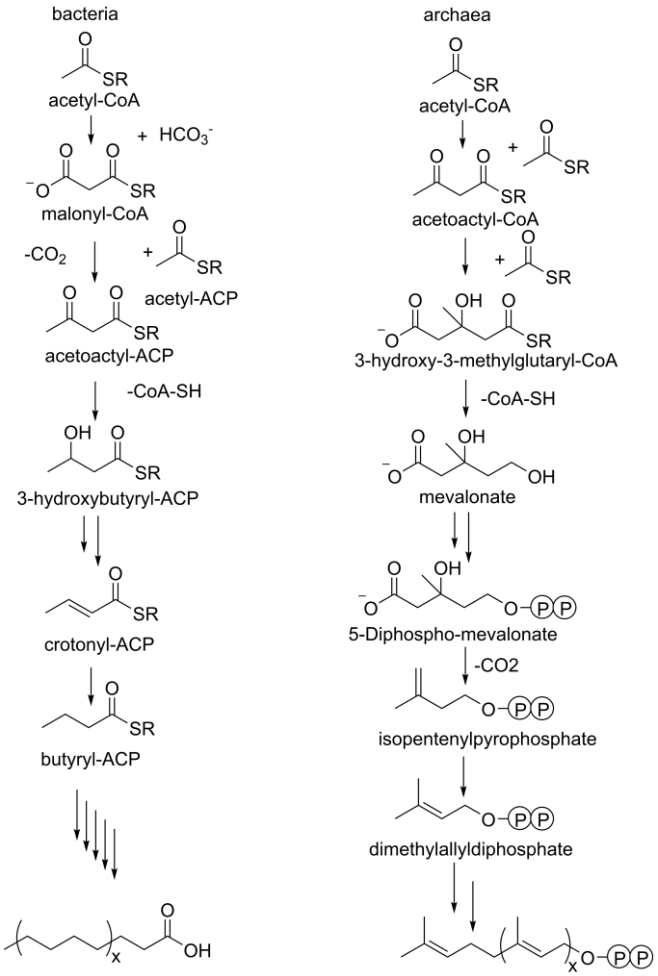

Figure 19: On the right hand, the archaic lipid/isoprenoid biosynthesis *via* the mevalonate pathway, which leads to dimethylallyldiphosphate and isopentenyldiphosphate by using three molecules acetatyl-CoA. On the left hand, the well-known bacterial fatty acid biosynthesis leads to also starts from acetyl-CoA.

2.2 Isotoplogue Analysis of extant Microbes using autocatalytic Carbon-Fixation

The emergence of life is hypothesized to be linked to autocatalytic carbon fixation pathways under hydrothermal conditions as discussed above (see chapter 1.3.2). Autotrophic pathways are still present in extant hydrothermal microbes and thought to be derived from the “Ur-metabolism”. Within the sequence of *Desulfurella acetivorans*, a thermophilic sulfur reducing deltaproteobacterium, neither ACL nor homologous enzymes such CCS and CCL are present, although the organism can grow autotrophically by means of the rTCA cycle (Figure 20). The current consensus is that a novel type of enzyme may be active. Therefore this is a highly interesting study organism. In this work, experimental proof for the citrate cleavage activity of *Desulfurella acetivorans* shall be provided in the context of origin of life.

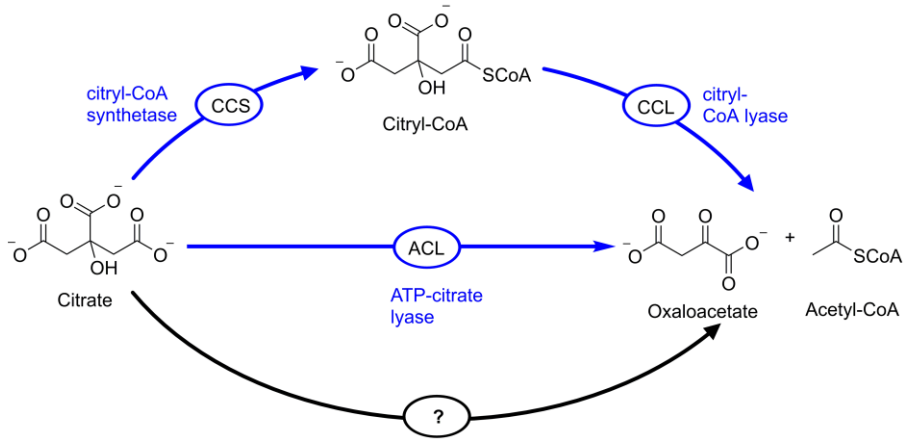

Figure 20: Different known variants of citrate cleavage in the rTCA cycle. The blue arrows represent ATP-citrate lyase (ACL) reaction, citryl-CoA synthetase/citryl-CoA lyase (CSS/CCL) reactions. The black arrow stands for the unknown citrate cleavage (adapted from Mall *et al*. 2018).

CHAPTER 3
RESULTS

3.1 Summary & Article: Unsaturated $C_{3,5,7,9}$-Monocarboxylic Acids by aqueous, One-pot Carbon Fixation: Possible Relevance for the Origin of Life

In the iron sulphur world, the pioneer organism became cellular and thus a chemical path of amphiphilic compound synthesis would be necessary. In this article, our group has shown a surface catalysed fatty acid formation using acetylene as C2 precursor in analogy to acetyl-CoA. For the primordial synthesis of short fatty acids under volcanic hydrothermal vent conditions, a batch reactor was charged with an aqueous suspension of NiS and/or $Ni(OH)_2$ (see table 2 experiments a-f) with a gas ratio of C_2H_2 to CO of 1:1 at a combined pressure of 1 bar at room temperature, followed by heating to 105ºC under autogenous pressure for 7 days. GC/MS analysis of the supernatant revealed the presence of more than 150 products, including a set of $C_{3,5,7,9}$-monocarboxylic acids with an combined fatty acid concentration of up to 20mM (Table 2). It was denoted that a more realistic high pressure would increase yields and chain lengths of the primordial fatty acids. The primary products were polyunsaturated monocarboxylic acids and their hydrogenated analogues. In this publication we present for the first time the formation of short fatty acids according to the iron sulphur world.

Table 2: A list of the unsaturated and saturated monocarboxylic acid products and their concentration [µM] of run a-f, sorted by ascending order of chain length (adapted from Scheidler *et al*. 2016).

run	a	b	c	d	e	f
mmol NiS	1	1	0.5	0.5	0	0
mmol $Ni(OH)_2$ (α or β)	0	0	0.5(α)	0.5(β)	1(α)	1(β)
end-pH	8.8	6.7	8.3	8.9	8.0	9.8
C_3-acids (µM)						
C_2H_3-COOH	3884	5822	3318	6675	250	243
C_2H_5-COOH	7132	1069	461	7391	510	171
C_5-acids (µM)						
ΣC_4H_5-COOH	466	1597	970	1463	53	0
ΣC_4H_7-COOH	7498	2641	1390	7269	11	0
C_4H_9-COOH	309	32	11	363	0	0
C_7-acids (µM)						
Σ$C_6H_{5,7}$-COOH	63	30	31	61	0	0
ΣC_6H_9-COOH	320	148	69	246	0	0
ΣC_6H_{11}-COOH	52	42	6	96	0	0
C_9-acids (µM)						
ΣC_6H_5-$C_2H_{2,4}$-COOH	1.8	4.4	3.1	1.5	0	0
C_8H_{11}-COOH	0.6	0.8	0.1	0	0	0
ΣC_8H_{13}-COOH	4.6	1.3	3.6	5.9	0	0
C_8H_{15}-COOH	3.9	0.4	0.4	3.7	0	0
ΣC_3-C_9	**19735**	**11388**	**6263**	**23575**	**824**	**414**

My individual contribution of this work included the design and performance of the experiments with analytics and interpretation of the data. Additionally I was involved in the preparation of the published manuscript.

SCIENTIFIC REPORTS

OPEN

Unsaturated $C_{3,5,7,9}$-Monocarboxylic Acids by Aqueous, One-Pot Carbon Fixation: Possible Relevance for the Origin of Life

Received: 09 March 2016
Accepted: 20 May 2016
Published: 10 June 2016

Christopher Scheidler[1,*], Jessica Sobotta[1,*], Wolfgang Eisenreich[1], Günter Wächtershäuser[2] & Claudia Huber[1]

All scientific approaches to the origin of life share a common problem: a chemical path to lipids as main constituents of extant cellular enclosures. Here we show by isotope-controlled experiments that unsaturated $C_{3,5,7,9}$-monocarboxylic acids form by one-pot reaction of acetylene (C_2H_2) and carbon monoxide (CO) in contact with nickel sulfide (NiS) in hot aqueous medium. The primary products are *toto*-olefinic monocarboxylic acids with CO-derived COOH groups undergoing subsequent stepwise hydrogenation with CO as reductant. In the resulting unsaturated monocarboxylic acids the double bonds are mainly centrally located with mainly trans-configuration. The reaction conditions are compatible with an origin of life in volcanic-hydrothermal sub-seafloor flow ducts.

Carbonaceous meteorites have been found to contain saturated, aliphatic C_{2-12}-monocarboxylic acids with an excess of branched structures and with abundancies that decrease with increasing carbon atom numbers[1–3]. The relevance of these findings for the origin of life came into its own when hydrophobic residues of chloroform extracts of carbonaceous meteorites were shown to form membranous structures in aqueous media[4]. Meteoritic sources would, however, have been slow at releasing their lipids into the primitive ocean with the result of a highly diluted lipid solution, and possible concentration processes would have been countermanded by massive sedimentation, notably of adsorptive volcanic ashes[5]. A promising alternative emerged with the finding that monocarboxylic acids are formed at 400 °C by contacting metallic iron from certain meteorites with CO and H_2 (1:1)[6]. The characteristics, however, of an absence of water (except for reaction water) and of a presence of anhydrous (hygroscopic) K_2CO_3[6] speak against hydrothermal vent scenarios for these Fischer-Tropsch reactions. Subsequent reports of a Fischer-Tropsch formation of monocarboxylic acids under water-saturated hydrothermal vent conditions turned out to be problematic because the monocarboxylic acids appear to be formed by gas-solid reactions at catalytic steel surfaces of the reactor wall[7,8]. Bearing in mind that the biosynthesis of fatty acids from acetyl-CoA proceeds in C2-increments we probed acetylene as simple, yet highly reactive primordial C2-precursor.

Results and Discussion

Synthetic reactions. We reacted an aqueous suspension of freshly precipitated NiS with C_2H_2 and CO as gas phase at a combined gas pressure of ~1 bar at room temperature, followed by heating to 105 °C under an autogenous gas/steam pressure of ~2.5 bar for 7 days. A glass reactor was used in order to avoid artifacts by catalytic reactor walls. The aqueous medium was not buffered and its pH developed autogenously to an end-pH that was measured. After freeze-drying of the supernatant organic products in the residue were silylated and analyzed by gas chromatography-mass spectrometry (GC-MS). The analysis revealed the presence of a suite of $C_{3,5,7,9}$-monocarboxylic acids, their chain length increasing by increments of two C-atoms (see Table 1 and for more detailed information Suppl. Tables S1 and S2, Fig. S4). All detected $C_{3,5,7,9}$-monocarboxylic acids sum up to a concentration of up to about 20 mM, (for detailed conversion rates see Suppl. Table S3). Runs with ^{13}CO and D_2O ascertained that these products are genuine reaction products. In the absence of C_2H_2 and/or CO they are not formed. The yields of the monocarboxylic acids show a decrease with increasing chain length (Fig. 1).

[1]Lehrstuhl für Biochemie, Technische Universität München, Lichtenbergstraße 4, D-85747 Garching Germany. [2]2209 Mill Race Drive, Chapel Hill, NC 27514, USA. *These authors contributed equally to this work. Correspondence and requests for materials should be addressed to C.H. (email: claudia.huber@mytum.de)

run	a	b	c	d	e	f
mmol NiS	1	1	0.5	0.5	0	0
mmol $Ni(OH)_2$ (α or β)	0	0	0.5(α)	0.5(β)	1(α)	1(β)
end-pH	8.8	6.7	8.3	8.9	8.0	9.8
C_3-acids (μM)						
C_2H_3-COOH	3884	5822	3318	6675	250	243
C_2H_5-COOH	7132	1069	461	7391	510	171
ΣC_3	11016	6891	3779	14066	760	414
C_5-acids (μM)						
ΣC_4H_5-COOH	466	1597	970	1463	53	0
ΣC_4H_7-COOH	7498	2641	1390	7269	11	0
C_4H_9-COOH	309	32	11	363	0	0
ΣC_5	8273	4270	2371	9095	64	0
C_7-acids (μM)						
$\Sigma C_6H_{5,7}$-COOH	63	30	31	61	0	0
ΣC_6H_9-COOH	320	148	69	246	0	0
ΣC_6H_{11}-COOH	52	42	6	96	0	0
ΣC_7	435	220	106	403	0	0
C_9-acids (μM)						
ΣC_6H_5-$C_2H_{2,4}$-COOH	1.8	4.4	3.1	1.5	0	0
C_8H_{11}-COOH	0.6	0.8	0.1	0	0	0
ΣC_8H_{13}-COOH	4.6	1.3	3.6	5.9	0	0
C_8H_{15}-COOH	3.9	0.4	0.4	3.7	0	0
ΣC_9	10.9	6.9	7.2	11.1	0	0
ΣC_3–C_9	**19735**	**11388**	**6263**	**23575**	**824**	**414**

Table 1. Monocarboxylic acid products of the NiS-catalyzed reaction of acetylene with carbon monoxide. Reactions were carried out in 125 ml serum bottles with 5 ml aqueous liquid phase for 7 days at 105 °C; Products were identified by GC-MS as *tert*-butyldimethylsilyl derivatives.

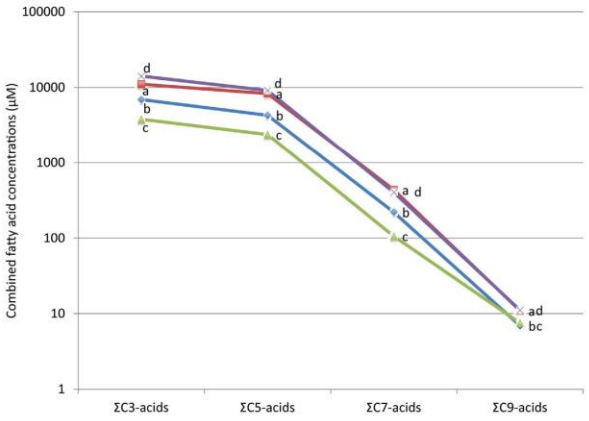

Figure 1. Combined fatty acid concentrations. Total yields of $C_{3,5,7,9}$-monocarboxylic acids of runs a to d are plotted on a logarithmic scale: a: NiS, pH8.8; b: NiS, pH6.7; c: coprecipitated NiS and α-$Ni(OH)_2$, pH8.3; d: NiS, precipitated onto β-$Ni(OH)_2$, pH8.9; for detailed information see Suppl. Table S1.

Ancillary investigations. For safety reasons (danger of explosion) and for technical reasons the reactions had to be carried out at low partial pressure (<1 bar) of C_2H_2. At a high sub-seafloor pressure (>1000 bar) yields and chain lengths would be increased, because of negative volumes of reaction and activation[9,10]. Productivity of the reaction is pH-sensitive with highest yields in the near neutral pH range of about 6.5 to 9, increasing from pH 6.7 (run b) to pH 8.8 (run a). Much stronger alkaline conditions disfavor reaction yields as well as chain elongation. With freshly precipitated α-$Ni(OH)_2$ (run e) only $C_{3,5}$-acids were formed, and in lower yields than with freshly precipitated NiS. With coprecipitated NiS and α-$Ni(OH)_2$ in a molar ratio of 1:1 (run c) yields were diminished compared to NiS alone. Apparently, α-$Ni(OH)_2$ acts as antagonist. With aged β-$Ni(OH)_2$ alone (run f) only C_3-acids were formed, and in lower yields than with α-$Ni(OH)_2$. However, with β-$Ni(OH)_2$ as carrier for freshly precipitated NiS the yields were slightly increased (run d compared to run a). These comparisons point

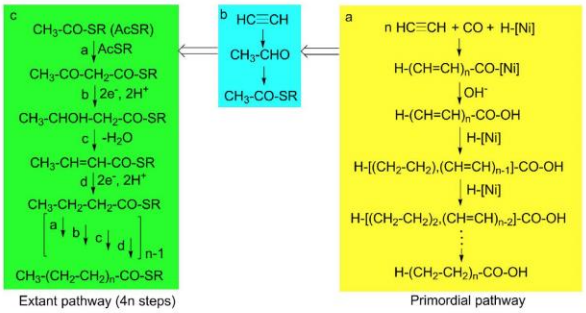

Figure 2. Evolution of monocarboxylic acid biosynthesis. (**a**) Primordial one-pot pathway; (**b**) Conversion of acetylene to acetyl-thioester; (**c**) Extant biosynthesis dependent on acetyl-thioester condensation. [Ni] signifies a catalytic nickel complex (unknown nuclearity, ligand sphere, oxidation state and relationship to mineral surfaces) that converts to H-[Ni] (with hydride ligand) by oxidation of CO to CO_2; ⇒ signifies an evolutionary transformation.

to a wide range of compositions for the exploration of more effective catalysts. Against the backdrop of previous production of organics by reaction of $C_2H_2/H_2O/CO$ with non-sulfidic Ni-catalysts in organic reaction media[11,12], it is surprising that heterogeneous catalysis by NiS in hot water generates elongated, unsaturated monocarboxlic acids, which undergo *in situ* hydrogenation with the same catalyst and with CO as reductant.

Proposed mechanism. We suggest an organo-metal reaction mechanism (Fig. 2a), wherein CO acts as carbon source for the carboxyl group and also as reducing agent via hydride transfer. When run a was repeated with the addition of H-$(CH{=}CH)_2$-COOH, but without C_2H_2, the same suite of C_5-monocarboxylic acids was formed with the same quantitative relationships as in run a with C_2H_2 ($\Delta^3 > \Delta^4 > \Delta^2$). Therefore, we suggest *toto*-olefinic H-$(CH{=}CH)_n$-CO-[Ni] as early intermediate, which is hydrolyzed to the corresponding free acid. Subsequently, the free *toto*-olefinic monocarboxylic acids undergo stepwise hydrogenation. The *toto*-olefinic monocarboxylic acids are highly reactive and have a propensity to undergo self-condensation and resinification as established for 2,4,6-heptatrienoic acid and its derivatives[13,14]. Therefore, the yield of long-chain monocarboxylic acids is expected to increase with increasing rates of hydrogenation. For $n = 1–3$ the free *toto*-olefinic mono-carboxylic acids have been detected. A mechanism of electrocyclization and aromatization of *toto*-olefinic monocarboxylic acids with the penultimate double bond in cis-configuration explains the formation of benzoic acid ($n = 3$)[13] as well as cinnamic acid and hydrocinnamic acid ($n = 4$).

The mechanism explains the results with the additional proposition that hydrogenation rates follow three rules. *Rule 1:* The rate is higher if hydrogenation involves the α-carbon atom rather than only more distal carbon atoms. *Rule 2:* Hydrogenation of conjugated double bonds is favored over hydrogenation of isolated double bonds. *Rule 3:* Conjugated double bonds undergo preferably end-to-end hydrogenation. These rules jointly explain why the yields of the mono-unsaturated C_5-acids (Suppl. Table S1) follow the order $\Delta^3 > \Delta^4 > \Delta^2$. Moreover, they show that with increasing chain length the proportion of saturated fatty acids decreases sharply and that regioisomers with double bonds in the middle of the carbon chain are favored. Remarkably, double bonds with trans-configuration are also favored. Finally, these rules mean also that multiple double bonds are mainly conjugated.

Primordial Sources of Starting Materials. We now turn to the possible sources for reactants and catalysts. In the extant atmosphere of the Earth acetylene occurs only in trace amounts close to the detection limit, but much higher levels of atmospheric acetylene have been suggested as contained in a presumptive methane-rich primordial atmosphere due to photolysis of methane[15]. Acetylene has also been detected in extant fumarolic gases[16], in volcanic glasses[17], and as products of volcanic simulation experiments[18]. Acetylene has been suggested as product of hydrolysis of calcium carbide (CaC_2) in the context of the Archaean eon[15] and in the context of the Hadean eon[19,20]. CaC_2 may be formed by the following transformations in the hot Hadean mantle[21]:

$$CaCO_3 \rightarrow CaO + CO_2 (T > 900^{\circ}C);$$

$$CaO + 3C \rightarrow CaC_2 + CO (T > 1600^{\circ}C;\ at\, p_{CO} = 1\, bar),$$

CaC_2 would have become subsequently emplaced in the Hadean crust to later come in contact with the aqueous vent fluid. The stoichiometrically formed CO would have been continuously removed from the sites of CaC_2 formation by diffusion and volcanic exhalation. CaC_2 is a member of the class of acetylenic carbides, i.e. the calcium salt of acetylene, consisting of a lattice of Ca^{2+} cations and C_2^{2-} anions. It undergoes facile hydrolysis with cold neutral water to form exclusively acetylene[21]. CaC_2 is distinguished from iron carbides. The latter have been hydrolyzed with concentrated DCl in D_2O and fully deuterated, saturated C_{3-7}-hydrocarbons have been reported as products[22].

In the presence of graphite the molar ratio of $CO:CO_2$ increases with increasing temperature and decreasing pressure. It assumes for example a value of 1:1 at 1200 °C and 2 kbar, or at 900 °C and 0.1 kbar[23]. The Hadean volcanic exhalations containing a high ratio of $CO:CO_2$ would eventually have been mixed with relatively cold cycling water in volcanic-hydrothermal flow ducts. The resulting quenching effect would have prevented equilibration of the $CO:CO_2$ ratio to low-temperature values[24].

Nickel is the second-most abundant transition metal (after iron) in the Solar System[25] and in the crust of the Earth[26]. Iron-nickel sulfides are among the earliest stages of mineral evolution[27]. Therefore, nickel sulfides would have been abundant in the Hadean crust to come in contact with volcanic-hydrothermal vent fluids. Nickel ions have been found to leach out of crustal minerals into hydrothermal vent fluids[28] and it has been proposed that under the very hot conditions of the Hadean Earth nickel transport in hydrothermal fluids was much more intense than today[29]. Upon contact with H_2S nanoparticulate nickel sulfide precipitates[30].

Evolutionary Considerations. Acetylene utilization has been detected in extant microbial phyla (for review see ref. 15). It shows a characteristic kinetic isotope effect[31]. *Pelobacter acetylenicus* utilizes acetylene as sole carbon and energy source by means of a tungstopterin enzyme that hydrates acetylene to acetaldehyde, which in turn converts to acetic acid plus ethanol. This enzyme still bears the mark of an original redox function[32]. A possibly related relic is provided by the [FeS]-enzyme IspH for the last step in the non-mevalonate pathway to isoprenoid lipids[33]. While it is today clearly a redox enzyme catalyzing the conversion of 1-hydroxy-2-methyl-2(*E*)-butenyl 4-phosphate into a mixture of isopentenyl diphosphate and dimethylallyl diphosphate, it also has an ability to hydrate acetylene[34]. These two enzymes may reflect a deep history of enzyme recruitments and functional recruitments.

Based on the above considerations we project that acetylene utilization may have been a prominent feature of the early metabolism. Hadean volcanic-hydrothermal vent fluids, laden with CO and C_2H_2, would have passed through myriads of flow zones. Thereby they would have come in contact with NiS under conditions suitable for the formation of the type of monocarboxylic acids here reported, but perhaps of greater lengths due to high reaction pressure (>1000 bar). These then would have been carried along by the fluid flow in the style of reaction chromatography, the short ones travelling faster than the longer ones[35].

Let us consider now the possible function of the here reported monocarboxylic acids in the course of the cellularization of life. At the outset we note that the experimentally detected monocarboxylic acids are short (C_{3-9}) and that under the chosen experimental conditions of a low partial pressure of acetylene (~0.6 bar at 105 °C) the productivity for the C_9-monocarboxylic acids is low. It is not unrealistic, however, to expect that future explorations for more effective NiS catalysts may be successful and that higher productivities and greater chain lengths may result at a higher partial pressure of C_2H_2 and at a high total pressure (>1000 bar). With these provisos in mind we distinguish here two alternative scenarios for the origin of life.

Heterotrophic origin in a prebiotic broth. In this scenario it is assumed that lipid membrane vesicles form *ab initio*. Therefore, the concentration of dissolved monocarboxylic acids in the prebiotic broth must be high enough and their chain length great enough to be able to exceed the critical vesicle concentration (CVC). It has been found that decanoic acid has a CVC at pH 7.2 of ~20 mM[36], while the CVCs are still higher for nonanoic acid and octanoic acid[37]. The CVC has been shown to be lowered by the inclusion of hydrocarbons[4], which are known to form by Fischer-Tropsch reactions under hydrothermal conditions[7] or of the alcohol equivalent of the monocarboxylic acid[37]. Further, the CVC is lowered by the presence of short monocarboxylic acids (e.g. those with 3 to 7 carbon atoms that are reported here) in the solution[36], which may contribute to reach the saturation level of the disturbance of the structure of liquid water that is required for vesicle formation. With the concentrations of monocarboxylic acids as reported here *ab initio* vesicle formation from solution is questionable.

Aside from the above physico-chemical restriction of heterotrophic *ab initio* vesicle formation from the kind of short monocarboxylic acids here reported, we should note a more principle topological shortcoming of this approach. By the logic of this approach lipid production and supply is located external to the vesicles in question. Growth and reproduction of early vesicles would therefore require lipid nutrients to enter the membrane from the outside with the need for a flipping of lipid molecules from the outer leaflet to the inner leaflet. This outside-in process is the topological opposite of extant cell membrane growth of non-parasitic microbes, which occurs exlusively inside-out, i.e. by the internal synthesis of the lipid molecules followed by their entry into the inner leaflet with subsequent flipping from the inner leaflet to the outer leaflet. This topological difference correlates immediately with a thermodynamic difference. Membrane growth by lipid molecule insertion requires a driving force, which can only be provided by a sufficient lipid concentration. Given the restricted vesicle volume the inside-out process will easily satisfy the concentration requirement, ultimately driven by the synthetic chemical potential of the metabolism. In case of outside-in growth the outside volume is in principle an unrestricted diffusion space with the consequence of unending dilution.

Autotrophic origin in a volcanic-hydrothermal fluid flow. In this scenario it is assumed that cellularization is preceded by a surface metabolism with a cascade of intervening functional steps as precursors of the eventual lipid function. The first step in this hypothetical cascade consists of a lipophilization of the catalytic mineral surface by the accumulation of surface-bonded monocarboxylic acids that operate like a two-dimensional hydrophobic solvent[38]. All here reported monocarboxylic acids, even the short ones, are capable of contributing to such surface lipophilization. As a consequence the activity of H_2O (and of H_3O^+ or OH^-) is lower at the mineral-water interface than in bulk water, thereby protecting hydrolytically sensitive constituents, notably organo-metal intermediates and condensation products. By this collectively autocatalytic effect ever-longer monocarboxylic acids would form in ever-greater proportions. Eventually, a state would be reached, wherein monocarboxylic acids with lipid function form surface-bonded bilayer membranes[38]. At this stage the above-mentioned saturation effects[36]

may come into play. Eventually, semi-cellular structures would form, with a cytosol bounded partly by a lipid membrane and partly by a mineral surface. Still later, evolutionary precursors of true cellular entities with internal catalytic NiS would emerge[38]. Throughout this evolutionary cascade the principle of continuity (topological, structural, nutritional, catalytic and biochemical) would be maintained. Monocarboxylic acids would form first on the open NiS surfaces, later on the NiS surfaces inside the semi-cellular structures, still later on NiS particles inside membrane vesicles, and finally by intracellular enzyme catalysis. Throughout this cascade membrane growth would have proceeded as today — inside-out.

With the cooling of the Earth the acetylene nutrient would have vanished in most habitats of life and the biosynthesis of lipids by organo-metal C2-incremental acetylene fixation would have been replaced by enzymatic C2-incremental acetyl-CoA condensation (Fig. 2c). This gradual transformation would have been mediated by hydration of acetylene to acetaldehyde, followed by oxidative reaction with a mercaptan to form an acetyl-thioester (Fig. 2b). Moreover, we note that extant membranes of the domains Bacteria and Archaea typically comprise a mixture of fatty acid lipids and that a mixture of an even-numbered monocarboxylic acid and an uneven-numbered monocarboxylic acid shows a lowered CVC compared to the single even-numbered case[36]. Therefore, a gradual transition from uneven-numbered to even-numbered carbon chains would not have violated the principle of evolutionary continuity.

Monocarboxylic acids previously invoked in the context of the cellularization of life have been exclusively saturated. By contrast, the here reported synthetic pathways begin by the formation of *toto*-olefinic monocarboxylic acids that undergo subsequent incremental hydrogenation of their double bonds. With the $C_{3,5}$-monocarboxylic acids the fully hydrogenated, saturated state was reached. But with the higher C_{7-9}-monocarboxylic acids the saturated states are not reached and the products consist of mixtures of unsaturated monocarboxylic acids with one, two or three double bonds. The double bonds have mainly trans-configuration and multiple double bonds are mainly conjugated. These insights open hitherto unexplored avenues of research into cellularization.

Extant cell membranes of the domains Bacteria and Eukarya are characterized by the presence of natural unsaturated fatty-acyl lipids within membranes of saturated lipids. The unsaturated monocarboxylic acids reported here agree with natural unsaturated lipids with regard to the location of the double bonds in the middle of the hydrophobic tail. While in the here reported synthetic pathway the unsaturated $C_{>3}$-monocarboxylic acids are the exclusive reaction products, the natural unsaturated fatty acids are produced in anaerobic bacteria as minor components by special variants of the fatty acid synthesis machinery.

The natural unsaturated fatty acids have mainly cis-configuration that causes a kinked structure with the effect of a decrease of the membrane packing density. This means an increase of membrane fluidity, as it is required by a mesophilic lifestyle. The trans-unsaturated monocarboxylic acids are actually more similar to their saturated monocarboxylic acid counterparts in terms of their molecular structure and in terms of their effect on membrane properties[39]. With the presence of multiple trans-unsaturations, in their carbon chain the molecules become overall more rigid and less bulky. Now, when the multiple trans-unsaturations are conjugated, as projected for the type of reactions here reported, the carbon chains are even more rigid and rather flat with the result of greater membrane compactness. This provides an outlook to primordial membranes of monocarboxylic acids with conjugated polyunsaturations that may well have properties that are more in tune with the requirements of a (hyper) thermophilic lifestyle. These considerations are speculative, but suitable for empirical verification or falsification.

The chemical reaction here reported is by itself not restricted to any particular scenario as long as the required materials and conditions are present. When viewed, however, in the Iron-Sulfur World context of a volcanic-hydrothermal flow scenario for a chemo-autotrophic origin of life[24,35,38,40], the here presented reactions show a considerable coherence with previously reported synthetic reactions (nutrients in volcanic-hydrothermal fluid flows and catalytic minerals from crustal flow ducts): Lower alkyl mercaptans form from CO_2 and H_2S with FeS[41]; NH_3 forms from N_2 with FeS/H_2S[42]; CH_3-CO-SCH_3 forms from CO/CH_3SH with (Fe,Ni)S[43]; amino acids form from HCN with NiS[44]; amino acids are activated by CO/H_2S/NiS to form peptides that engage in a peptide cycle by undergoing N-terminal degradation by CO/H_2S/NiS[45]. This degree coherence may be viewed as a road sign to the origin of life in an open flow system: chemically singular and chemically predetermined.

Methods

In a typical run a 125 ml glass serum bottle was charged with 0.5 or 1.0 mmol $NiSO_4 \cdot 6H_2O$ and closed with a silicon stopper. Additionally or alternatively, β-$Ni(OH)_2$ was charged in runs d and f, respectively. For achieving a constant ion strength run d and f were supplemented with 0.5 mmol and 1 mmol Na_2SO_4, respectively. Three times the bottle was evacuated and filled with argon, finally ending in a deaerated state. Subsequently the bottle was charged with argon-saturated water (calculated for the end volume of 5 ml), with 0.5 or 1.0 mL argon-saturated 1M Na_2S solution, with 0.5 (run a und b), 1.0 (run c) or 2.0 ml (run e) 1M NaOH solution and finally with 60 ml CO and 60 ml acetylene, using for the injections gas-tight syringes. To confirm the authenticity of the products, ^{13}CO or D_2O were used in representative experiments. Variations in the initial pH of the reaction batches were induced through the addition of 1M NaOH or 1M H_2SO_4. Reactions were carried out at 105 °C.

After 7 days the reaction mixture was allowed to cool down and was centrifuged at 10,000 rpm for 5 minutes. The pH was measured by a glass electrode and 1 ml of the supernatant was freeze-dried. For analysis by GC-MS, the residue was dissolved in 250 µl anhydrous acetonitrile and derivatized with 250 µl N-tert-butyldimethylsilyl-N-methyltrifluoroacetamide for 30 minutes at 70 °C.

Analysis was performed with GC-MS, using GC-2010 coupled with MS-QP2010 Plus (Shimadzu GmbH, D-Duisburg) with a 30 m × 0.25 mm × 0.25 µm fused silica capillary column (Equity TM5, Supelco, Bellefonte, PA, USA) and AOC-20i auto injector. Temperature program and settings:

Program 1: 0–6 min at 60 °C; 6–25 min at 60–280 °C, 10 °C/min; 25–28 min at 280 °C; injector temperature: 260 °C; detector temperature: 260 °C; column flow rate: 1 mL/min; scan interval: 0.5 sec; injection volume 0.2 µl.

Program 2 (used for analysis of C9 acids): 0–6 min at 90 °C; 6–25 min at 90–280 °C, 10 °C/min; 25–28 min at 280 °C;

Otherwise identical to program 1; injection volume 1 µl.

Peak assignment was achieved by comparison of retention times and mass spectra of purchased reference compounds, synthesized products and data from NIST spectra library; for details see Footnotes of Supplemental Table S1.

Quantification was performed by external calibration using known concentrations of commercially available reference compounds (for details see Footnotes of Supplemental Table S1).

All chemicals were purchased from Sigma Aldrich GmbH (D-Steinheim) in the highest purity available. Acetylene was purchased from Linde AG (D-Pullach). Carbon monoxide, Argon 4.6 from Westfalen AG (D-Münster) and ^{13}CO from Cambridge Isotopes Laboratories Inc. (USA-MA-Tewksbury).

Heptatrienoic acid was not commercially available and was synthesized by reacting 2 mmol trans-glutaconic acid with 2.2 mmol acrolein in tetrahydrofuran (THF) in the presence of 8 mmol 4-dimethylaminopyridine (DMAP) at 70 °C for 24 h. The product was isolated from the reaction mixture and confirmed by NMR-spectroscopy (AV500 Bruker, Rheinstetten) and GC-MS.

References

1. Lawless, J. G. & Yuen, G. U. Quantification of monocarboxylic acids in the Murchison carbonaceous meteorite. *Nature* **282,** 396–398 (1979).
2. Yuen, G., Blair, N., Des Marais, D. J. & Chang, S. Carbon isotope composition of low molecular weight hydrocarbons and monocarboxylic acids from Murchison meteorite. *Nature* **307,** 252–254 (1984).
3. Shimoyama, A., Naraoka, H., Yamamoto, H. & Harada, K. Carboxylic acids in the Yamato-791198 carbonaceous chondrites from Antarctica. *Chem. Lett.* 1561–1564 (1986).
4. Deamer, D. Boundary structures are formed by organic components of the Murchison carbonaceous meteorite. *Nature* **317,** 792–794 (1985).
5. Brooks, J. & Shaw, G. *Origin and development of living systems.* (Academic Press, London 1973), p. 359.
6. Nooner, D. W. & Oro, J. Synthesis of fatty acids by a closed system Fischer-Tropsch process In Hydrocarbon synthesis from carbon monoxide and hydrogen *Advances in Chemistry* (eds Kugler, E. F. & Steffgen, F. W.). **178,** 159–171, (1979).
7. McCollom, T. M. & Seewald, J. S. Abiotic Synthesis of organic compounds in deep-sea hydrothermal environments. *Chem. Rev.* **107,** 382–401 (2007).
8. McCollom, T. M. Miller-Urey and beyond: What we have learned about prebiotic organic synthesis reactions in the past 60 years? *Annu. Rev. Earth Planet. Sci.* **41,** 207–229 (2013).
9. Matsumoto, K., Sera, A. & Uchida, T. Organic Synthesis under high pressure. *Synthesis* 1–26 (1985).
10. Klärner, F.-G. & Wurche, F. The effect of pressure on organic reactions. *J. Prakt. Chem.* **342,** 609–636 (2000).
11. Trotus, I.-T., Zimmermann, T. & Schüth, F. Catalytic reactions of acetylene: A feedstock for the chemical industry revisited. *Chem. Rev.* **114,** 1761–1782 (2014).
12. Lin, T. J., Meng, X. & Shi, L. Catalytic hydrocarboxylation of acetylene to acrylic acid using Ni_2O_3 and cupric bromide as combined catalysts. *J. Mol. Cat. A.* **396,** 77–83 (2015).
13. Cairns, T. L., Engelhardt, V. A., Jackson, H. L., Kalb, G. H. & Sauer, J. C. The reaction of acetylene with acrylic compounds. *J. Am. Chem. Soc.* **74,** 5636–5640 (1952).
14. Acker, D. S. & Anderson, B. C. Some reactions of methyl 2,4,6-heptatrienooate *J. Org. Chem.* **24,** 1162–1163 (1959).
15. Oremland, R. S. & Voytek, M. A. Acetylene as fast food: Implications for development of life on anoxic primordial Earth and in the outer Solar System. *Astrobiology* **8,** 45–58 (2008).
16. Igari, S., Maekawa, T. & Sakata, S. Light hydrocarbons in fumarolic gases: A case study in the Kakkonda geothermal area. *Chikyukagau* **34,** 103–109 (2000).
17. Muenow, D. W. High temperature mass spectrometric gas-release studies of Hawaiian volcanic glass: Pele's tears. *Geochim. Cosmochim. Acta* **37,** 1551–1561 (1973).
18. Mukhin, L. M. Volcanic processes and synthesis of simple organic compounds on primitive Earth. *Orig. Life* **7,** 355–368 (1976).
19. Wächtershäuser, G. The place of RNA in the origin and early evolution of the genetic machinery. *Life* **4,** 1050–1091 (2014).
20. Patel, B. H., Percivalle, C., Ritson D. J., Duffy C. D. & Sutherland, J. D. Common origins of RNA protein and lipid precursors in a cyanosulfidic protometabolism. *Nature Chem.* **7,** 301–307 (2015).
21. Wiberg, N. *Hollemann-Wiberg, Lehrbuch der anorganischen Chemie* 1243–1247 (Walter de Gruyter, 2007).
22. Marquez, C., Lazcano, A., Miller, S. L. & Oro, J. Fully deuterated aliphatic hydrocarbons obtained from iron carbide treated with DCl and D_2O. *Orig. Life Evol. Biosph.* **26,** 3–5.
23. Holloway, J. R. & Blank, J. G. Applications of experimental results to C-O-H species in natural melts. *Reviews in Mineralogy.* **30,** 187–230 (1994).
24. Wächtershäuser, G. On the chemistry and evolution of the pioneer organism. *Chem. Biodivers.* **4,** 584–602 (2007).
25. Lodders K. Solar System abundances and condensation temperatures of the elements. *The astrophysical Journal.* **591,** 1220–1247 (2003).
26. Cox P. A. *The elements: Their origin, abundance and distribution.* (Oxford University Press, 1989).
27. Hazen, R. Evolution of minerals. *Sci. Am.* **302,** 58–65 (2010).
28. Douville, E. *et al.* The rainbow vent fluids (36°14′N, MAR): the influence of ultramafic rocks and phase separation on trace metal content in Mid-Atlantic Ridge hydrothermal fluids. *Chem. Geol.* **184,** 37–48 (2002).
29. Kornhauser, K. O. *et al.* Oceanic nickel depletion and a methanogen famine before the Great Oxidation Event. *Nature* **458,** 750–753 (2009).
30. Huang *et al.*, The composition of nanoparticulate nickel sulfide. *Chem. Geol.* **277,** 207–213 (2010).
31. Miller, L. G., Baesman, S. M. & Oremland, R. S. Stable carbon isotope fractionation during bacterial acetylene fermentation: Potential for life detection in hydrocarbon-rich volatiles of icy planet(oid)s. *Astrobiology* **15,** 977–986 (2015).
32. Seiffert, G. B. *et al.* Structure of the non-redox-active tungsten/[4Fe:4S] enzyme acetylene hydratase. *Proc. Natl. Acad. Sci. USA* **104,** 3073–3077 (2007).
33. Rohdich, F. *et al.* Studies on the nonmevalonate terpene biosynthetic pathway: Metabolic role of IspH (LytB) protein. *Proc. Natl. Acad. Sci. USA* **99,** 1158–1163 (2002).
34. Span, I. *et al.* Discovery of acetylene hydratase activity of the iron-sulphur protein IspH. *Nat. Commun.* **3,** 1042, doi: 10.1038/ncomms2052 (2012).
35. Wächtershäuser, G. From volcanic origins of chemoautotrophic origin of life to bacteria, archaea aeukarya. *Phil. Trans. R. Soc. B* **361,** 1787–1808 (2006).
36. Cape, J. L., Monnard P.-A. & Boncella, J. M. Prebiotically relevant mixed fatty acid vesicles support anionic solute encapsulation and photochemically catalyzed trans-membrane charge transport. *Chem. Sci.* **2,** 661–671 (2011).

37. Apel, C. L., Deamer, D. W. & Mautner, M. N. Self-assembled vesicles of monocarboxylic acids and alcohols: conditions for stability and for the encapsulation of biopolymers. *Biochim. Biophys. Acta* **1559,** 1–9 (2002).
38. Wächtershäuser, G. Before enzymes and templates: theory of surface metabolism. *Microbiol. Rev.* **52,** 452–484 (1988).
39. Roach, C. *et al.* Comparison of cis and trans fatty acid containing phosphatidylcholines on membrane properties. *Biochem.* **43,** 6344–6351 (2004).
40. Wächtershäuser, G. Groundworks for an evolutionary biochemistry:The iron-sulphur world. *Prog. Biophys. molec. Biol.* **58,** 85–201 (1992).
41. Heinen, W. & Lauwers, A. M. Organic sulfur compounds resulting from the interaction of iron sulfide, hydrogen sulfide and carbon dioxide in an anaerobic aqueous environment. *Orig. Life Evol. Biosph.* **26,** 131–150 (1996).
42. Dörr M. *et al.*, A possible prebiotic formation of ammonia from dinitrogen on iron-sulfide surfaces. *Angew. Chem. Int. Ed.* **42,** 1540–1543 (2003).
43. Huber, C. & Wächtershäuser, G. Activated acetic acid by carbon fixation on (Fe,Ni)S under primordial conditions. *Science* **276,** 245–247 (1997).
44. Huber, C. & Wächtershäuser, G. α-Hydroxy and α-amino acids under possible hadean, volcanic origin-of-life conditions. *Science* **324,** 630–632 (2006).
45. Huber, C., Eisenreich, W., Hecht, S. & Wächtershäuser, G. A possible primordial peptide cycle. *Science* **301,** 938–940 (2003).

Acknowledgements

This work was funded by Hans-Fischer Gesellschaft. Development of the experimental techniques was funded by Deutsche Forschungsgemeinschaft (EI-384 3-1). We thank A. Bacher and M. Groll for encouragement and support and German Research Foundation (DFG) and Technical University of Munich (TUM) in the framework of the Open Access Publishing Program. This work is dedicated to the memory of Prof. Dr. Helmut Simon.

Author Contributions

C.S. and J.S. jointly performed the experiments; W.E. and G.W. designed this study; C.H. developed the methodology, supervised and coordinated the experiments. All authors read, commented on and jointly approved submission of this article.

Additional Information

Supplementary information accompanies this paper at http://www.nature.com/srep

Competing financial interests: The authors declare no competing financial interests.

How to cite this article: Scheidler, C. *et al.* Unsaturated $C_{3,5,7,9}$-Monocarboxylic Acids by Aqueous, One-Pot Carbon Fixation: Possible Relevance for the Origin of Life. *Sci. Rep.* **6**, 27595; doi: 10.1038/srep27595 (2016).

3.2 Summary & Article: One-pot Formation of 2,4-di- or 2,4,6-tri-olefinic Monocarboxylic Acids by straight Chain C4-Extension

The identification of the saturated monocarboxylic acids reported in chapter 3.1 “Unsaturated $C_{3,5,7,9}$-Monocarboxylic Acids by Aqueous, One-Pot Carbon Fixation: Possible Relevance for the Origin of Life” was achieved by GC/MS analysis of references. Today, some of these compounds are commercially available, but not the unsaturated monocaboxylic acid, 2*E*,4*E*-heptatrienoic acid **3a**. Within this paper, a novel synthetic approach to the formation of targeted olefin product **3a** was investigated and successfully introduced to the scientific community. Encouraged by the principle of vinylogy (Fuson 1935, Krishnamurthy 1982), a one-pot decarboxylative condensation analog to Knoevenagel reaction (Jones 1967) was performed as shown in Figure 21. Instead of a C2-extension of aldehydes, into their α-unsaturated monocarboxylic acids achieved by using malonic acid, C4-extension was done by the aid of trans-glutaconic acid **1** (Figure 21). The formation of the set of 2,4,6-triolefinic monocarboxylic acid **3a** was achieved at a temperature range of 65-70°C and 4-dimethylamino-pyridine as catalyst. In this setup, tetrahydrofuran was used as solvent. NMR spectroscopic investigations (^{1}H, ^{13}C, COSY, HSQC, HMBC) revealed a high stereo-selectivity of 93 %. Under the favored reaction conditions, a set of 2,4-di or 2,4,6-triolefinic monocarboxylic acids **3a-f** was successfully synthesized.

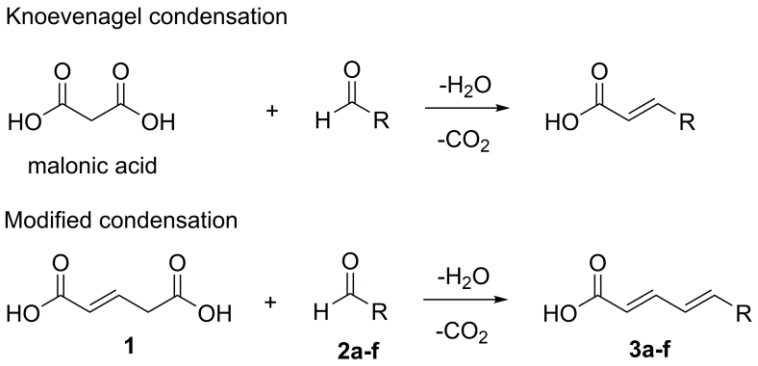

Figure 21: Representation of the vinylogy between the Knoevenagel reaction using malonic acid and the newly published decarboxylative condensation reaction and formation of α,β-unsaturated monocarboxylic acids **3a-f** by C4 extension using glutaconic acid **1** and aldehydes **2a-f** (Sobotta *et al*. 2017).

My individual contribution of this work included conception, design and performance of the experiments including analytics and interpretation of the data as well as the preparation of the published article.

Heliyon

Received:
15 February 2017
Revised:
19 July 2017
Accepted:
19 July 2017

Cite as: Jessica Sobotta, Maximilian Schmalhofer, Thomas M. Steiner, Wolfgang Eisenreich, Günter Wächtershäuser, Claudia Huber. One-pot formation of 2,4-di- or 2,4,6-tri-olefinic monocarboxylic acids by straight chain C4-extension.
Heliyon 3 (2017) e00368.
doi: 10.1016/j.heliyon.2017.e00368

One-pot formation of 2,4-di- or 2,4,6-tri-olefinic monocarboxylic acids by straight chain C4-extension

Jessica Sobotta [a], **Maximilian Schmalhofer** [a], **Thomas M. Steiner** [a], **Wolfgang Eisenreich** [a], **Günter Wächtershäuser** [b], **Claudia Huber** [a,*]

[a] *Lehrstuhl für Biochemie, Technische Universität München, Lichtenbergstraße 4, Garching D-85747, Germany*

[b] *2209 Mill Race Drive, Chapel Hill, NC 27514, USA*

* Corresponding author.

E-mail address: claudia.huber@mytum.de (C. Huber).

Abstract

We report a one-pot formation of 2,4-diolefinic or 2,4,6-triolefinic monocarboxylic acids, R-(CH=CH)$_{2or3}$-COOH, by decarboxylative condensation of an optionally α,β-unsaturated aldehyde with glutaconic acid, HOOC-CH$_2$-CH=CH-COOH as straight chain C4-extender. The reaction is broadly applicable to saturated and unsaturated aldehydes and opens up a simple gateway to valuable organic products and reactive intermediates.

Keyword: Organic chemistry

1. Introduction

We are here concerned with the direct formation of α,β-unsaturated carboxylic acids by carbon chain extension of aldehydes. Previous reactions of this kind are limited to C2-extension: Peterson olefination [1], Wittig-Horner type reaction [2, 3], extension by (trimethylsilyl)ketene [4] or its acetal [5] and Knoevenagel extension with malonic acid [6, 7]. We now report a reaction which extends the carbon skeleton by a straight chain unit of four carbon atoms, thereby simultaneously introducing two conjugated olefinic bonds and a free carboxylic acid group. Specifically, we performed a one-pot decarboxylative condensation of

http://dx.doi.org/10.1016/j.heliyon.2017.e00368

aldehydes **2a-f** with trans-glutaconic acid **1** in the presence of a nitrogen base. Our reaction is related to the Knoevenagel reaction [6], encouraged by the principle of vinylogy [8, 9] (Fig. 1).

2. Results and discussion

The reaction is favored by tetrahydrofuran (THF) as solvent, by an elevated reaction temperature of preferably 65 to 70 °C, and by 4-dimethylamino-pyridine (DMAP) as a catalytic nitrogen base. The reaction also proceeds with pyridine alone, or with pyridine in combination with pyrrolidine, piperidine or diethylamine, albeit with reduced yields.

The two conjugated double bonds that are introduced by the C4-extender have mainly *E*-configuration as shown by NMR analysis. If an α,β-unsaturated aldehyde is used, the product, a 2,4,6-triolefinic monocarboxylic acid, acquires an additional conjugated double bond with retention of its stereo configuration. Educt aldehydes **2a-f** and products **3a-f** are shown in Fig. 2. Reaction yields for all products determined after ethyl acetate extraction are about 20%. GC/MS yields and stereo selectivities are listed in Table 1. For example, 2*E*,4*E*,6-heptatrienoic acid **3a** was obtained with a stereo selectivity of 93%. The reaction appears to proceed by condensation, followed by decarboxylation as evidenced by non-decarboxylated byproducts. All mass data and NMR spectra (^{1}H, ^{13}C, COSY, HSQC, HMBC) including signal assignments for products **3a-f** are given in the Supplemental Information section.

Our reaction conditions are related to those previously employed in the Knoevenagel reaction with malonic acid [7]. Compared to the conventional C2-extension, the here reported C4-extension reshuffles the synthetic burden between aldehyde and extender. Because the extender adds four carbon atoms, the aldehyde can be correspondingly shortened. Moreover, because the extender introduces an extra double bond into the final molecule, the aldehyde structure is correspondingly unburdened. A simplified aldehyde structure means a correspondingly simplified aldehyde synthesis. In this manner, the overall synthesis is characterized by a favorable reaction step economy.

The now presented reaction yields unsaturated free carboxylic acids, without a saponification step, which would be necessary in a reaction with glutaconic diester

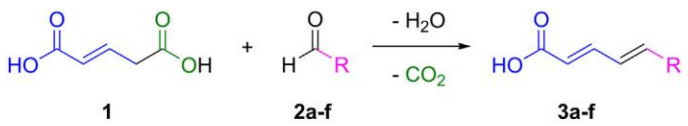

Fig. 1. Formation of α,β-unsaturated carboxylic acids **3a-f** by decarboxylative condensation of aldehydes **2a-f** with glutaconic acid **1**.

http://dx.doi.org/10.1016/j.heliyon.2017.e00368

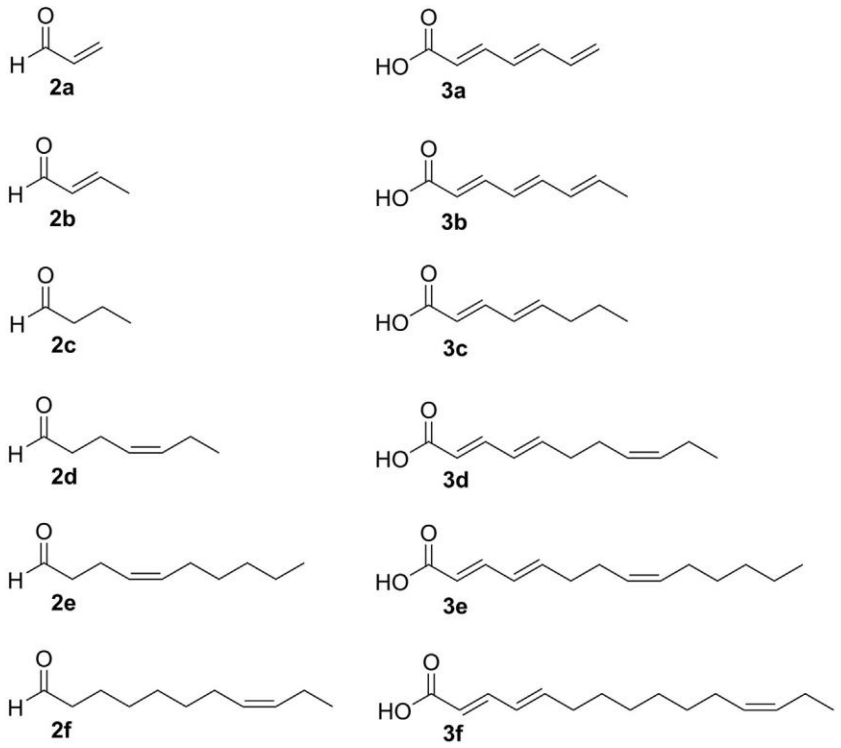

Fig. 2. Educt aldehydes **2a-f** and resulting unsaturated monocarboxylic acid **3a-f** by C4 extension.

[10, 11, 12]. Low yields are mainly caused by fast decarboxylation of glutaconic acid to butenoic acid at enhanced temperatures in the presence of DMAP. Aldol condensation of the aldehyde is also observed. As shown earlier for similar

Table 1. Conversion of aldehydes **2a-2f** to 2,4-diolefinic and 2,4,6-triolefinic monocarboxylic acids **3a-3f** by condensation with glutaconic acid and DMAP as catalyst in THF.

Aldehyde	Product	Stereo selectivity[#]	GC-MS Yield [%][*] of the *2E,4E* isomer
2a	**3a**	93:7	18.4
2b	**3b**	58:42	10.4
2c	**3c**	72:28	14.7
2d	**3d**	55:45	15.4
2e	**3e**	60:40	9.3
2f	**3f**	66:34	10.4

[*]Yields of 2*E*,4*E*-isomers, quantified by GC-MS with the following standards: 3-heptenoic acid for **3a**; 3-octenoic acid for **3b**,**c**; 3-dodecanoic acid for **3d**; 3-pentadecanoic acid for **3e** and **f**.

[#] Stereo selectivity of the 2*E*,4*E* products.

http://dx.doi.org/10.1016/j.heliyon.2017.e00368

reactions [7], the yields might be improved by varying the reaction conditions. However, this was not the aim of our proof-of-principle study.

Pending further optimization in terms of productivity and selectivity, the here reported reaction opens an efficient gateway to classes of valuable polyunsaturated monocarboxylic acids and their derivatives with potential utility in commercial products. These would include a host of natural products with a wide range of biological effects as well as their chemically modified analogs. We mention here specifically 2,4,6-octatrienoic acid (**3b** in Table 1) that may be used as tanning promoter and antioxidant in skin care products [13]. Moreover, a large class of natural polyunsaturated monocarboxylic acid amides [14, 15, 16, 17, 18] of the formula R-CH=CH-CH=CH-CO-NH-isobutyl, wherein R signifies a saturated or an unsaturated aliphatic group may now come into facile synthesis. They exhibit a wide range of biological properties and a corresponding range of possible utilities, notably as modulators or enhancers for the immune system [14, 15, 16] or as insecticides [17, 18].

3. Material and methods

All chemicals were purchased from Sigma Aldrich GmbH (Steinheim, Germany) in the highest purity available. All organic solvents were purchased from VWR International GmbH (Darmstadt, Germany) in the highest purity available. Commercial aldehydes were used without purification.

In a typical experiment, 65.0 mg of trans-glutaconic acid (0.5 mmol, 1 eq.) was dissolved in a mixture of 244 mg of 4-dimethylaminopyridine (DMAP) (2.0 mmol, 4 eq.) and 1.60 ml of tetrahydrofuran (THF) and stirred at 40 °C for 15 min. The solution was cooled down to room temperature and the aldehyde (3 eq.) was added. The reaction mixture was warmed up to 65–70 °C and stirred for 12 h. The reaction was finished by the addition of 1 ml of ethylacetate and aqueous H_2SO_4 (until slightly acidic pH) at room temperature. After phase separation the aqueous phase was extracted two more times using 1 ml of ethylacetate. The organic phases were combined and dried over Na_2SO_4. For analysis by GC-MS, 25 µl of the organic phase was derivatized with 75 µl *N-tert*-butyldimethylsilyl-*N*-methyltrifluoroacetamide for 30 min at 70 °C.

GC-MS analysis was performed with the Shimadzu instrument GC-17A and QP-5000 (Duisburg, Germany) using a 30 m x 0.25 mm x 0.25 µm fused silica capillary column (Equity ^{TM}-5, Supelco, Bellefonte, PA, USA) and AOC-20i auto injector. Temperature program and settings: 0–6 min at 60 °C, 6–25 min at 60–280 °C, 10 °C/min; 25–28 min at 280 °C; injector temperature: 260 °C; detector temperature: 260 °C; column flow rate: 1 mL/min; scan interval: 0.5 sec; detector voltage 1.5 kV. Quantification was performed by external calibration using known concentrations of commercially available reference compounds (for details see footnotes of Table 1).

http://dx.doi.org/10.1016/j.heliyon.2017.e00368

The product structures were also confirmed by one and two-dimensional NMR-spectroscopy using a Bruker AV-HD 500 instrument (Rheinstetten, Germany).

Declarations

Author contribution statement

Jessica Sobotta: Conceived and designed the experiments; Performed the experiments; Analyzed and interpreted the data; Wrote the paper.

Maximilian Schmalhofer, Thomas M. Steiner: Performed the experiments.

Wolfgang Eisenreich: Contributed reagents, materials, analysis tools or data; Wrote the paper.

Günter Wächtershäuser: Conceived and designed the experiments; Wrote the paper.

Claudia Huber: Conceived and designed the experiments;Analyzed and interpreted the data; Wrote the paper.

Funding statement

This work was funded by the Hans-Fischer Gesellschaft, Munich. Development of the experimental techniques was funded by the Deutsche Forschungsgemeinschaft (EI-384/3-1). This work was also supported by the German Research Foundation (DFG) and Technical University of Munich (TUM) in the framework of the Open Access Publishing Program.

Competing interest statement

The authors declare no conflict of interest.

Additional information

Supplementary content related to this article has been published online at http://dx.doi.org/10.1016/j.heliyon.2017.e00368

Acknowledgements

This study is dedicated to Adelbert Bacher on the occasion of his 75th birthday. We thank Adelbert Bacher and Michael Groll for encouragement and support. For technical support, we thank Christoph Graßberger, Christine Schwarz and Annemarie Machacek.

References

[1] P.A. Grieco, C.-L.J. Wang, S.D. Burke, Trimethylsilylacetic Acid Dianion: Application to Organic Synthesis, J. Chem. Soc. Chem. Commun. (1975) 537.

[2] G.A. Koppel, M.D. Kinnick, Carboxyvinylation; A one-step synthesis of α,β-unsaturated acids, Tetrahedron Lett. (1974) 711.

[3] H.J. Bestmann, R. Dostalek, R. Zimmermann, Phosphanalkenyle, 52. Umsetzung von [1-(Trimethylsilyl)alkyliden]triphenylphosphoranen mit Kohlendioxid und Folgereaktionen, Chem. Ber. 125 (1992) 2081.

[4] A.B. Concepcion, K. Maruoka, H. Yamamoto, Organoaluminum-promoted cycloaddition of trialkylsilylketene with aldehydes: A new, stereoselective approach to *cis*-2-oxetanones and 2(Z)-alkenoic acids, Tetrahedron 51 (1995) 4011.

[5] M. Bellassoued, M. Gaudemar, Stereoselective synthesis of (E)-α,β-unsaturated acids from C,O, O-tri(trimethylsilyl) ketene acetal and aldehydes, Tetrahedron Lett. 29 (1988) 4551.

[6] G. Jones, The Knoevenagel Condensation, Org. React. 15 (1967) 204.

[7] S.T. Kemme, T. Šmejkal, B. Breit, *Catal.* Practical Synthesis of (E)-α,β-Unsaturated Carboxylic Acids Using a One-Pot Hydroformylation/ Decarboxylative Knoevenagel Reaction Sequence, Adv. Synth. 350 (2008) 989.

[8] R.C. Fuson, The Principle of Vinylogy, Chem. Rev. 16 (1935).

[9] S.J. Krishnamurthy, The Principle of Vinylogy, Chem. Edu. 59 (1982) 543.

[10] F. Henrich, Zur Kenntnis des Glutaconsäureesters, Chem. Ber. 35 (1902) 1663.

[11] P.R. Nandaluru, G.J. Bodwell, Multicomponent Synthesis of 6*H*-Dibenzo[*b, d*]pyran-6-ones and a Total Synthesis of Cannabinol, Org. Lett. 14 (2012) 310.

[12] B. Pezzati, M.F. Chellat, J.J. Murphy, C. Besnard, G. Reginato, J.C. Stephens, A. Alexakis, Organocatalytic Asymmetric Annulation of 1,3-Bis(alkoxycarbonyl)buta-1,3-dienes and Aldehydes, Org. Lett. 15 (2013) 2950.

[13] E. Flori, A. Mastrofrancesco, D. Kovacs, Y. Ramot, S. Briganti, B. Bellei, R. Paus, M. Picardo, 2,4,6-Octatrienoic acid is a novel promoter of melanogenesis and antioxidant defence in normal human melanocytes via PPAR-γ activation, Pigment Cell Melanoma Res. 24 (2011) 618.

http://dx.doi.org/10.1016/j.heliyon.2017.e00368

[14] Z. Qiang, C. Hauck, J.A. McCoy, M.P. Widrlechner, M.B. Reddy, P.A. Murphy, S. Hendrich, *Echinacea sanguinea* and *Echinacea pallida* extracts stimulate glucuronidation and basolateral transfer of Bauer alkamides 8 and 10 and ketone 24 and inhibit P-glycoprotein transporter in Caco-2 cells, Planta. Med. 79 (2013) 266.

[15] R. Bauer, P. Remiger, TLC and HPLC Analysis of Alkamides in *Echinacea* Drugs 1,2, Planta. Med. 55 (1989) 367.

[16] G.C.L. Ee, C.M. Lim, M. Rahmani, K. Shaari, C.F. Bong, Pellitorine, a potential anti-cancer lead compound against HL6 and MCT-7 cell lines and microbial transformation of piperine from Piper Nigrum, Molecules 15 (2010) 2398.

[17] H. Greger, Alkamides structural relationships, distribution and biological activity, Planta. Med. 50 (1984) 366.

[18] M. Miyakado, I. Nakayama, H. Yoshioka, N. Nakatani, The *Piperaceae* Amides I: Structure of Pipercide, A New Insecticidal Amide from Piper nigrum L, Agric. Biol. Chem. 43 (1979) 1609.

http://dx.doi.org/10.1016/j.heliyon.2017.e00368

3.3 Summary & Article: Reversibility of Citrate Synthase allows autotrophic Growth of a thermophilic Bacterium

The genome of *Desulfurella acetivorans*, a sulfur-reducing thermophilic deltaproteobacterium, was sequenced and analysed for specific key enzymes that are considered to be necessary for known autotrophic carbon fixation pathways. Anyhow, no pathway was complete. Interestingly, high activity of Krebs cycle enzymes was measured in extracts of cells grown under heterotrophic conditions with acetate/CO_2 as well as autotrophic on H_2/CO_2. The genes for ACL and CCS/CCL were missing in this sulfur-reducing anaerobic bacterium, apart from the presence of ACL pseudogenes. In this article, our group suggested that the enzyme citrate synthase cleaves citrate into acetyl-CoA and oxaloacetate, a reaction that has been regarded as impossible (Figure 22).

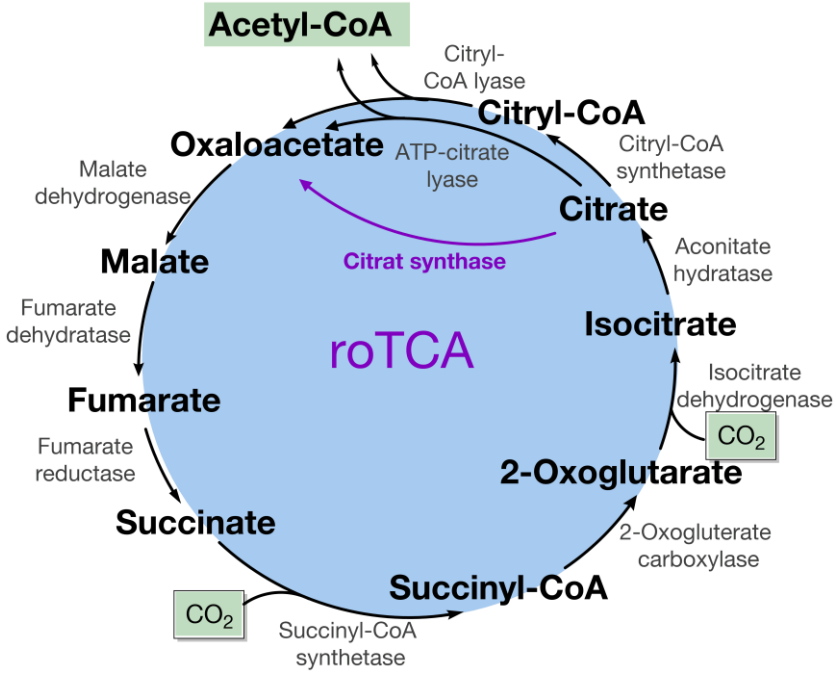

Figure 22: The roTCA: Citrate synthase (in blue) also catalyzes the cleavage of citrate to acetyl-CoA and oxaloacetate instead of ACL and CCS/CCL as always assumed.

To elucidate the reversibility of CS in *D. acetivorans*, enzyme activities under autotrophic conditions were proven and verified by liquid chromatography as well as NMR spectroscopy. Furthermore, the possible general concept behind this found reversibility among CS enzymes was demonstrated by NMR analysis by the aid of the porcine enzyme using ^{13}C tracer experiments as outlined in the publication. Apart from enzymatic evidence for an active reversible CS, *in vivo* evidence for its activity during autotrophic growth in the presence of stable isotope labelled precursor was obtained. As isotopologue profiling is a key technology

(Eisenreich *et al*. 2013, Eisenreich *et al*. 2010) to study bacterial metabolism, this was the technique of choice for this study. [1-^{13}C]pyruvate was used as the tracer. It´s uptake and the resulting modification of the isotopologue composition could be easily followed by spectrometry. In this course it was demonstrated that amino acids were labeled *via* rTCA. Especially alanine labeling was achieved, that demonstrated the amination of pyruvate under autotrophic conditions with H_2, CO_2 and S^0. All these results strongly support the new version of a reversed oTCA cycle (roTCA) in *D. acetivorans*. They provide an additional experimental evidence for the reductive carboxylation of pyruvate to 2-oxoglutarate under autotrophic growth only. In summary, our group's *in vivo* and *in vitro* experiments demonstrated for the first time that CS can catalyse citrate cleavage in the reductive direction of TCA cycle. In evolutionary terms, these results on the physiological reversibility of CS might predate the occurrence of roTCA cycle in wide range of ancient microorganism.

My individual contribution to this work included design and performance of the experiments especially the ^{13}C-incorperation experiments and their NMR and GC/MS analysis including interpretation and display of the data. Additionally I was involved in the preparation of the published manuscript.

Science

Reversibility of citrate synthase allows autotrophic growth of a thermophilic bacterium

Achim Mall[1,2], Jessica Sobotta[3], Claudia Huber[3], Carolin Tschirner[1], Stefanie Kowarschik[1], Katarina Bačnik[1], Mario Mergelsberg[1], Matthias Boll[1], Michael Hügler[4], Wolfgang Eisenreich[3]*, Ivan A. Berg[1,2]*

Science **359** (6375), 563-567.
DOI: 19.1126/science.aao2410.

[1]Mikrobiologie, Fakultät für Biologie, Albert-Ludwigs-Universität Freiburg, 79104 Freiburg, Germany.
[2]Institute for Molecular Microbiology and Biotechnology, University of Münster, 48149 Münster, Germany.
[3]Lehrstuhl für Biochemie, Technische Universität München, 85748 München, Germany.
[4]Department Microbiology and Molecular Biology, DVGW-Technologiezentrum Wasser (TZW), 76139 Karlsruhe, Germany.
*Correspondence to: ivan.berg@uni-muenster.de; wolfgang.eisenreich@mytum.de.

http://science.sciencemag.org/content/359/6375/563

Biological inorganic carbon fixation proceeds through a number of fundamentally different autotrophic pathways that are defined by specific key enzymatic reactions. Detection of the enzymatic genes in (meta)genomes is widely used to estimate the contribution of individual organisms or communities to primary production. Here we show that the sulfur-reducing anaerobic deltaproteobacterium *Desulfurella acetivorans* is capable of both acetate oxidation and autotrophic carbon fixation, with the tricarboxylic acid cycle operating either in the oxidative or reductive direction, respectively. Under autotrophic conditions, the enzyme citrate synthase cleaves citrate adenosine triphosphate independently into acetyl-coenzyme A and oxaloacetate, a reaction that has been regarded as impossible under physiological conditions. Because this overlooked, energetically efficient carbon fixation pathway lacks key enzymes, it may function unnoticed in many organisms, making bioinformatical predictions difficult, if not impossible.

Most organic carbon on Earth derives from biological CO_2 fixation. Six different autotrophic pathways responsible for this process are known today (*1-3*). Each of these pathways is characterized by certain

key enzymes, the genes for which can be confidently recognized in (meta)genomic databases, thus allowing an estimation of the autotrophic potential reaching from single species up to entire ecosystems. The reductive tricarboxylic acid cycle (rTCA cycle, or Arnon-Buchanan cycle) is among the most ancient metabolic processes (*4, 5*), probably emerged from a non-enzymatic precursor (*6*), and is present in bacteria belonging to various phylogenetic groups (*1*). It is a reversal of the oxidative tricarboxylic acid (oTCA) cycle, which provides redox equivalents and energy in organisms with a respiratory metabolism. The key step of the oTCA cycle is citrate synthesis from acetyl-coenzyme A (CoA) and oxaloacetate, catalyzed by citrate synthase (CS). This reaction is regarded as one of the irreversible steps in the oTCA cycle (*1, 2, 7*). The current consensus is that in organisms using the rTCA cycle, CS is substituted either by a reversible adenosine triphosphate (ATP)-dependent citrate lyase (ACL) (*8, 9*), or by homologous enzymes catalyzing the same reaction in two steps, citryl-CoA synthesis and cleavage (**Fig. S1**) (*10, 11*). The presence of ACL in a bacterium is therefore regarded as a key indication for autotrophic CO_2 fixation via the rTCA cycle (*12*). Our study challenges this concept by demonstrating through *in vivo* and *in vitro* experiments that citrate cleavage in the autotrophic rTCA cycle can be catalyzed by CS, which was thought to function only in the oxidative direction.

Desulfurella acetivorans is a sulfur-reducing thermophilic (growth optimum at 52-57 °C) deltaproteobacterium capable of growing either heterotrophically with acetate as electron donor and carbon source (*13*), or autotrophically with molecular hydrogen (*14*). In the heterotrophic route, acetate is oxidized via the oTCA cycle using CS and 2-oxoglutarate:ferredoxin oxidoreductase (*15*). Because the genome of *D. acetivorans* encodes neither ACL nor full sets of key enzymes for other known autotrophic pathways (**Table S1**), the pathway of CO_2 fixation could not be assigned yet. The genome contains pseudogenes for ACL with frame shifts in both the α- and β-subunits (region 484760-487933), which make it non-functional. Amplification of the *D. acetivorans* DNA fragment containing these pseudogenes and its sequencing (*16*) confirmed that *acl* was interrupted (**Fig. 1A**). Furthermore, the genome contains a gene for 4-hydroxybutyryl-CoA dehydratase, the characteristic enzyme of the archaeal 3-hydroxypropionate/4-hydroxybutyrate and dicarboxylate/4-hydroxybutyrate cycles (*17-19*), but genes for other specific enzymes of these cycles are missing (**Table S1**). Because the absence of key enzyme(s) of known CO_2 fixation pathways in an organism capable of autotrophic growth can be regarded as an indication of a novel pathway, we decided to study CO_2 fixation in *D. acetivorans* in more detail.

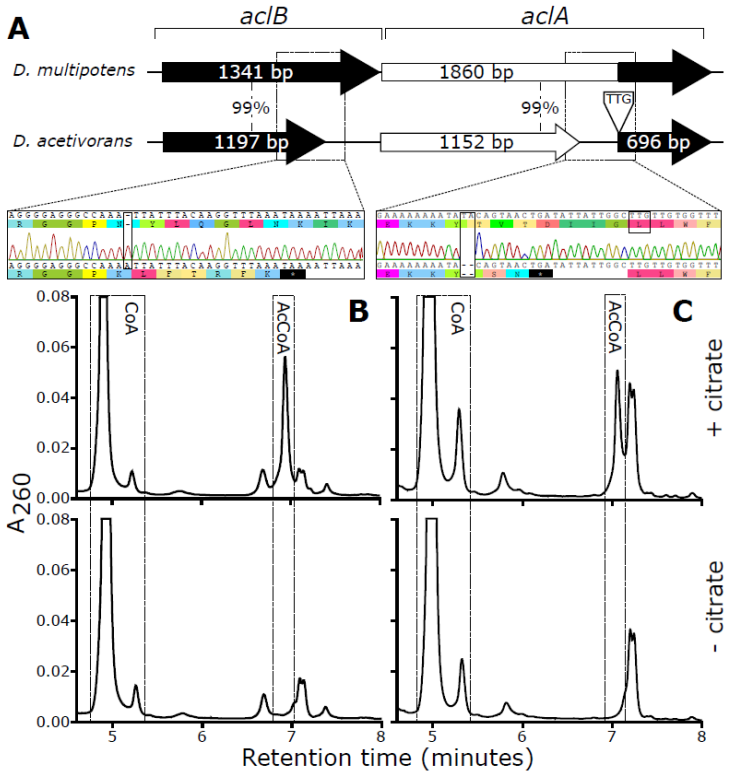

Fig. 1. ACL-independent citrate cleavage in *D. acetivorans*. (**A**) ACL pseudogene in *D. acetivorans* genome, as compared with the corresponding fragment of the genome of a closely related species *D. multipotens*, which possesses an intact *acl* gene. Numbers portray the pairwise nucleotides identity. bp, base pairs. (**B, C**) UPLC analysis of the CoA and CoA-esters formed from citrate in the reaction catalyzed by *D. acetivorans* cell extracts (**B**) and by CS and MDH from porcine heart (Sigma) (**C**). A_{260}, absorbance at 260 nm.

In accord with the published data, *D. acetivorans* grew both heterotrophically with acetate/CO_2 and autotrophically on H_2/CO_2 with minimal generation times of 5.7 and 4.9 hours to a density of 1.5×10^8 and 3.0×10^8 cells per ml, respectively. High activities of oTCA cycle enzymes were detected in extracts of cells grown under both conditions, with malate dehydrogenase (MDH) and CS activities being extremely high (**Table 1**). In contrast, no activities of key enzymes of known pathways of autotrophic CO_2 fixation were detected (**Table S1**). By ultra performance liquid chromatography (UPLC) analysis, we determined a citrate (20 mM)-, CoA (1 mM)-, and NADH (reduced form of nicotinamide adenine dinucleotide) (5 mM)-dependent formation of acetyl-CoA **(Figs. 1B, S2)**. Furthermore, a CoA- and citrate-dependent oxidation of NADH was observed that could be attributed to oxaloacetate formation followed by NADH-dependent reduction to malate by endogenous MDH (**Table 1**). However, none of these reactions were dependent on the presence of ATP, as would be expected if ACL or citryl-CoA synthetase/citryl-CoA lyase were operating.

Table 1. Enzymes of central carbon metabolism in *D. acetivorans*. Activities were measured at 55°C. The number of biological repetitions (n) is indicated. ND, not determined; ADP, adenosine diphosphate; acc., accession number.

Pathway / Enzyme	Specific activity [µmol min^{-1} mg^{-1} protein] ± standard deviation		Candidate gene(s), GenBank Acc.:
	$H_2 + CO_2$	Acetate + CO_2	
oTCA cycle			
Citrate synthase	42.1 ± 0.5 (n=8)	55.3 ± 20.4 (n=4)	AHF97305, AHF97477, AHF97591
Aconitase	0.74 ± 0.11 (n=3)	0.51 ± 0.01 (n=2)	AHF96494, AHF96888
Isocitrate dehydrogenase	18.4 ± 0.6 (n=3)	41.5 ± 4.7 (n=3)	AHF97114
Succinyl-CoA synthetase	0.58 ± 0.10 (n=2)	0.024 ± 0.014 (n=2)	AHF96923, AHF96924, AHF96945, AHF96946, AHF97285, AHF97286
Acetate:succinyl-CoA CoA-transferase	0.28 ± 0.15 (n=3)	0.37 ± 0.17 (n=3)	AHF 97575, AHF96498, AHF96963
Succinate dehydrogenase	0.26 ± 0.002 (n=2)	0.32 ± 0.13 (n=3)	AHF96724, AHF96725, AHF96726, AHF96727
Fumarase	6.4 ± 5.3 (n=3)	7.0± 2.7 (n=3)	AHF96722, AHF96723
Malate dehydrogenase (NADH)	70.4 ± 7.6 (n=6)	138.1 ± 11.6 (n=3)	AHF96721, AHF97578
Malate dehydrogenase (NADPH)	2.76 ± 1.36 (n=4)	7.6 ± 2.4 (n=3)	
rTCA cycle			
Citrate synthase, reverse (acetyl-CoA formation)	0.20 ± 0.05 (n=3)	0.39 ± 0.02 (n=2)	AHF97305, AHF97477, AHF97591
Citrate synthase, reverse (NADH oxidation)	0.35 ± 0.09 (n=10)	1.86 ± 0.48 (n=3)	
Fumarate reductase	0.009 ± 0.002 (n=2)	<0.001 (n=2)	AHF96724, AHF96725, AHF96726, AHF96727
2-Oxoglutarate synthase	0.44 ± 0.12 (n=3)	0.21 ± 0.06 (n=3)	AHF96882, AHF96883, AHF97110, AHF97111, AHF97112, AHF97113
Central carbon metabolism			
Acetyl-CoA synthetase / Acetate kinase + phosphate acetyltransferase	0.34 ± 0.05 (n=2)	0.06 ± 0.01 (n=2)	AHF97139, AHF97494, AHF97582, AHF97583
Pyruvate synthase	0.31 ± 0.08 (n=2)	0.017 ± 0.001 (n=2)	AHF96645, AHF96951, AHF97587, AHF96643, AHF96644
PEP carboxylase	< 0.005 (n=2)	< 0.005 (n=3)	-
PEP carboxykinase (ADP)	0.17 ± 0.05 (n=2)	0.12 ± 0.05 (n=2)	AHF96904
PEP synthase	0.03 ± 0.01 (n=2)	0.016 ± 0.004 (n=2)	AHF97619
Pyruvate carboxylase	0.14 ± 0.03 (n=4)	0.014 ± 0.005 (n=3)	AHF96546

To further elucidate the fate of citrate, we incubated cell extracts of *D. acetivorans* under anaerobic conditions in buffer containing [U-$^{13}C_6$]citrate in the presence of NADH and CoA. After 10 min of incubation, the reaction was stopped and subjected to ^{13}C nuclear magnetic resonance (NMR) analysis. Though the specific ^{13}C NMR signals for [U-$^{13}C_6$]citrate could still be detected, we also observed six ^{13}C NMR multiplets as a result of product formation (**Fig. 2, Table S2**). On the basis of the chemical shifts, the ^{13}C-^{13}C coupling constants and titration experiments, these signals were unequivocally attributed to [U-$^{13}C_4$]malate and [U-$^{13}C_2$]acetyl-CoA.

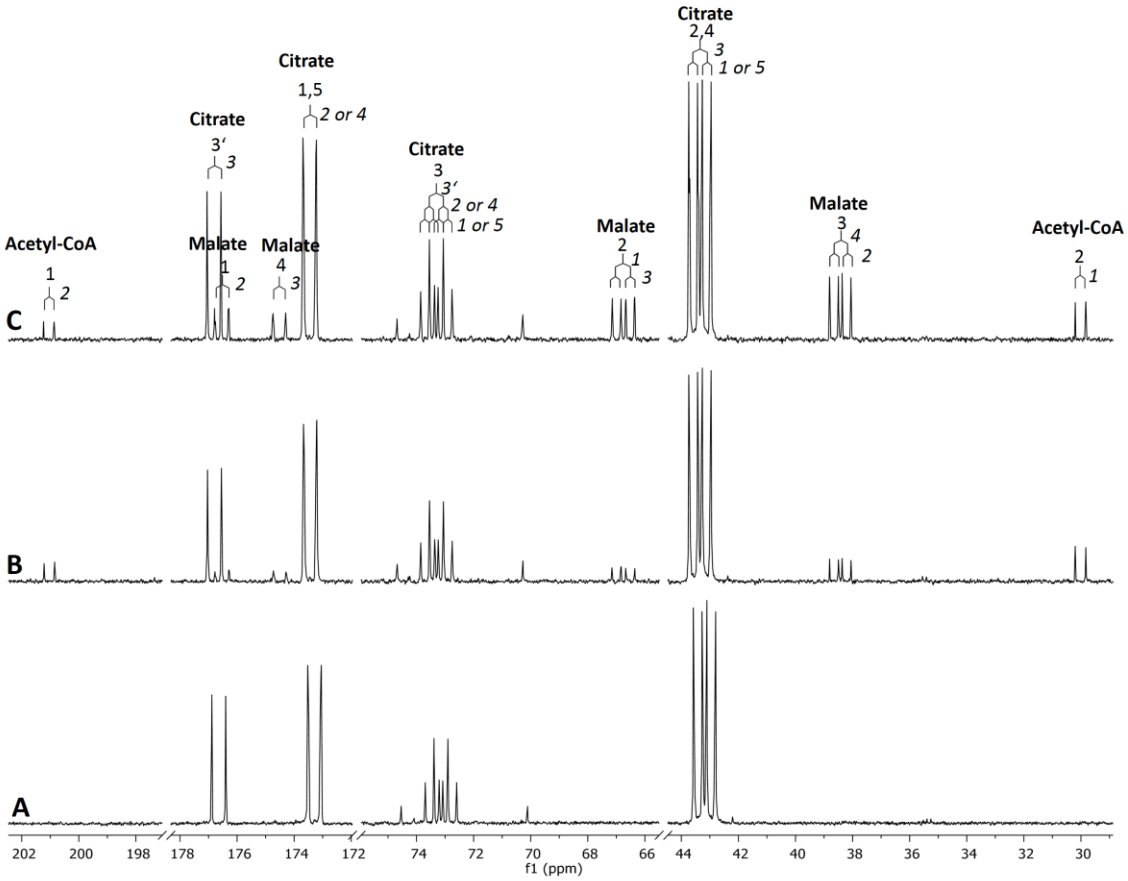

Fig. 2. ^{13}C-NMR analysis of [U-$^{13}C_6$]citrate cleavage catalyzed by cell extracts of autotrophically grown *D. acetivorans*. The reaction mixture contained 2 mM NADH, 2 mM CoA and 2 mM citrate. (**A**) Reaction after 0 min, (**B**) after 10 min of incubation, **(C)**: sample as in (**B**) plus 5 µg [U-$^{13}C_4$]malate reference. Signals and couplings of [U-$^{13}C_6$]citrate, [U-$^{13}C_4$]malate and [U-$^{13}C_2$]acetyl-CoA are indicated. For numerical values of chemical shifts and couplings, see **Table S2**. Note that citrate is a heat stable compound and did not degrade non-enzymatically. ppm, parts per million.

Together with the UPLC data, these results provide firm evidence for the cleavage of citrate to acetyl-CoA and oxaloacetate, with the latter being further reduced to malate by MDH, which was highly active in the cell extracts used (**Table 1**). The only possible enzyme in *D. acetivorans* that can catalyze an ATP-independent citrate cleavage to oxaloacetate and acetyl-CoA is CS. However, with a free-energy difference ΔG of −35.8 kJ mol^{-1} in the canonical direction of citrate formation (at pH 7, ionic strength 0.25 and 38 °C, *20*), the cleavage reaction has been regarded as impossible under physiological conditions. Even though the next reaction of the rTCA cycle- oxaloacetate reduction to malate (catalyzed by MDH)- is highly exergonic (ΔG of −27.1 kJ mol^{-1} at pH 7, ionic strength 0.25 and 38 °C, *20*), the reversal of the CS reaction would require high substrate and low product concentrations. Using liquid chromatography-mass spectrometry (LC-MS), we found that the CoA/acetyl-CoA ratio in autotrophically grown *D. acetivorans* cells (93, **Table S3**) was much higher than, for instance in glucose-grown *Escherichia coli* (2.3; *21*), whereas the citrate concentration in *D. acetivorans* was typical for

bacterial cells (1.4 mM; compared to 2 mM in *E. coli*, *21*). Using these concentrations of metabolites, we calculated an equilibrium oxaloacetate concentration of 0.13 µM. Although it is low, this concentration is still in a physiological range, similar to for example the mitochondrial oxaloacetate concentration that is in the low micromolar range (*22*, *23*). [U-$^{13}C_4$]malate and [U-$^{13}C_2$]acetyl-CoA could also be found when [U-$^{13}C_6$]citrate, CoA and NADH were incubated with commercially available CS and MDH (from porcine heart, Sigma) (**Figs. 1C, S3**), providing further evidence that the conversion of citrate in cell extracts is catalyzed by CS. The Michaelis constant (K_m) values of CS and MDH measured in *D. acetivorans* cell extracts were close to those for the porcine enzymes (**Table S4**). Apparently, the CS of *D. acetivorans* is not specifically adapted to citrate cleavage. This is also apparent from the high K_m value for citrate, thus requiring the observed high specific activity of the enzyme.

In addition to citrate cleavage, we were able to detect activity of another characteristic enzyme of the rTCA cycle, fumarate reductase, in *D. acetivorans* cell extracts. This activity was measured as fumarate-dependent succinyl-CoA formation in an assay coupled with endogenous succinyl-CoA synthetase (**Table 1**). The identity of the product, succinyl-CoA, was confirmed by LC-MS analysis (**Fig. S4**). The highest specific activity (9 nmol min^{-1} mg^{-1} protein) was observed with dithionite as the electron donor, lower activities could be detected when NADPH (reduced form of nicotinamide adenine dinucleotide phosphate) or NADH were used. No activity could be detected with reduced forms of benzyl viologen, methyl viologen, the menaquinone analogon 2,3-dimethyl-1,4-naphthoquinone, or flavin mononucleotide as electron donors. We assume that this reaction depends on a different, unidentified electron donor with low redox potential *in vivo*, possibly coupling fumarate reduction by H_2 with the build-up of a proton-motive force, as was discussed for deltaproteobacterium *Desulfuromonas acetoxidans* (*24*).

To test the function of the rTCA cycle in *D. acetivorans in vivo*, we grew autotrophic cultures in the presence of 0.2 mM [1-^{13}C]pyruvate, which was added in four 0.05 mM portions during the exponential growth phase. The cells were harvested and hydrolysed under acidic conditions. Four of the obtained amino acids Ala, Asp, Glu and Pro were then converted into tert-butyl-dimethylsilyl derivatives followed by gas chromatography-mass spectrometry analysis to determine ^{13}C-enrichments and positions in in the molecules (**Table S5**). Alanine, reflecting its precursor pyruvate, displayed about 6 % ^{13}C-excess. Incorporation into aspartate, reflecting its precursor oxaloacetate, and into glutamate and proline, reflecting the precursor 2-oxoglutarate, was lower (1-2 % ^{13}C-excess), but still significant. A more detailed MS-analysis of masses comprising all carbon atoms of the original amino acids (i.e. Ala, Asp, Glu and Pro at a mass/charge ratio of 260, 418, 432 and 286, respectively, with fragments having lost one or two carbon atoms from the respective precursor amino acids) revealed some positional assignment of the ^{13}C-label (**Fig. S5**). Thus, comparing of ^{13}C-excess in Ala-260 with Ala-232 (still carrying C-2 and C-3 of the original Ala molecule) immediately revealed that the ^{13}C-label in Ala must have been entirely located at C-1 which is lost in the fragment, as expected from its origin from the [1-

^{13}C]pyruvate precursor. The apparently identical ^{13}C-enrichments in Glu-432/Glu-404 and Pro-286/Pro-184 suggested that the ^{13}C-label is located in positions 2 – 5 in glutamate and proline. The lower ^{13}C-excess in Asp-390 (carrying C-2, C-3 and C-4 of Asp) in comparison with Asp-418 (comprising all carbon atoms of Asp) indicated that label must be present in C-1 of Asp. As shown in **Fig. S6**, these ^{13}C-distributions can be predicted by shuffling the [1-^{13}C]pyruvate tracer via phosphoenolpyruvate (PEP) carboxylation into [1-^{13}C]oxaloacetate, which enters the rTCA cycle and is converted into 2-oxoglutarate via the symmetric intermediates fumarate and succinate (**Fig. S6A**). On the other hand, pyruvate assimilation via [1-^{13}C]oxaloacetate followed by reactions of the oTCA cycle could not explain ^{13}C-incorporation into Glu and Pro, as the ^{13}C-label becomes lost during the conversion of isocitrate into 2-oxoglutarate (**Table S6, Figs. S5 and S6B**). Together, these results clearly proved the existence of a functional rTCA cycle under *in vivo* conditions.

The operation of the rTCA cycle was also confirmed by inhibitor analysis of autotrophically growing *D. acetivorans* cultures. Two inhibitors of the cycle, fluoroacetate (which is converted through the CS reaction to the aconitase inhibitor fluorocitrate in the cell, *25*) and glyoxylate (pyruvate:ferredoxin oxidoreductase inhibitor, *26*) suppressed growth of *D. acetivorans* (**Fig. S7**).

We designate this novel CS-dependent version of the rTCA cycle as "reversed oTCA cycle (roTCA)". The functioning of the roTCA cycle requires reduced ferredoxin, which is probably synthesized through electron bifurcation. Indeed, *D. acetivorans* genome contains genes for NAD-dependent ferredoxin:NADPH oxidoreductase NfnAB (*27*). Furthermore, the direct reduction of ferredoxin in a hydrogenase reaction is not implausible during growth at high H_2 concentration (80 % in our experiments).

The activities of the enzymes catalyzing the key reactions of the TCA cycle (**Table 1** and **Supplementary Text**) were nearly the same for *D. acetivorans* grown organoheterotrophically in medium with acetate or lithoautotrophically with hydrogen. However, the same set of the TCA cycle enzymes has to function in either the oxidative or reductive direction, depending on the growth conditions (**Fig. 3A, B**). The question then arises as to how the regulation of carbon flux can occur. Two obvious possibilities are that either the presence of H_2 shifts the flux towards the roTCA cycle, or exogenous acetate drives the TCA cycle in the oxidative direction. Isotopologue profiling of *Desulfurella* metabolism during growth with or without H_2 in the presence of CO_2 and [U-$^{13}C_2$]acetate revealed that acetate is mostly being oxidized under both conditions (**Tables S7, S8, Figs. S8, S9**). These data disprove the regulatory effect of H_2 and suggest that the presence of acetate itself leads to increase of intracellular acetyl-CoA concentration, triggering the direction of the cycle. The detected high activities of CS and MDH (**Table 1**) are not required for the growth under heterotrophic conditions. However, the high activities allow fast switching from heterotrophic to autotrophic growth and reflect the adaptation of *D. acetivorans* to fluctuating acetate concentrations characteristic for the *D. acetivorans* natural environment, where both active acetate formation and oxidation take place (*28*).

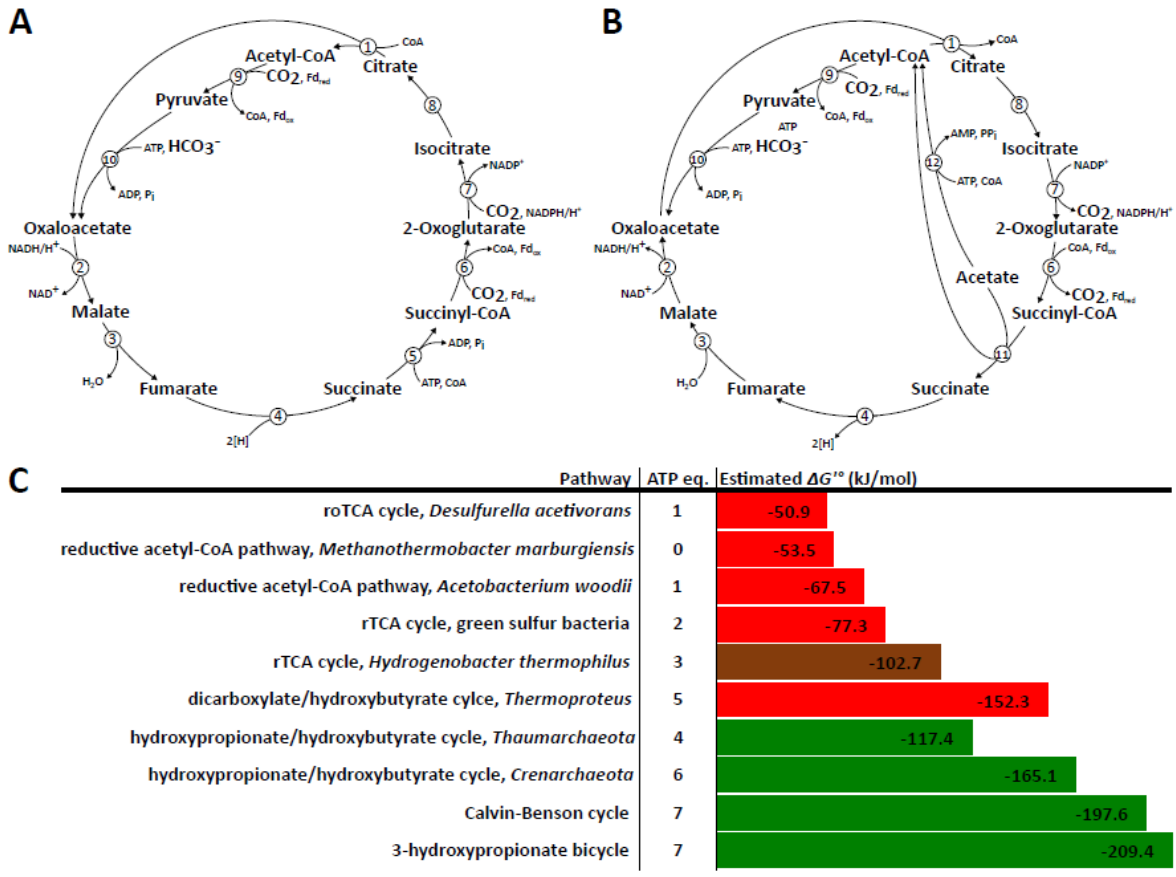

Fig. 3. A reversible TCA cycle in *D. acetivorans* and its efficiency in comparison with other autotrophic CO_2 fixation pathways. **A**: roTCA cycle during growth on CO_2, H_2 and elementary sulfur (S^0). **B**: oTCA cycle during growth on acetate and S^0. **C**: ATP costs and estimated $\Delta G'^{\circ}$ values for the synthesis of acetyl-CoA via the known autotrophic CO_2 fixation pathways (red, anaerobic; brown, microaerobic; green, aerobic; see **Table S10** for details). Note that comparison of the pathways by their ATP costs does not take into account the costs for ferredoxin reduction and thus overestimates the energetic efficiency of anaerobic pathways. Enzymes: **1**, citrate synthase; **2**, malate dehydrogenase; **3**, fumarase; **4**, fumarate reductase (roTCA cycle) or succinate dehydrogenase (oTCA cycle); **5**, succinyl-CoA synthetase; **6**, 2-oxoglutarate synthase; **7**, isocitrate dehydrogenase; **8**, aconitase; **9**, pyruvate synthase; **10**, pyruvate carboxylase; **11**, acetate:succinyl-CoA CoA-transferase; **12**, acetyl-CoA synthetase / acetate kinase + phosphate acetyltransferase.

What makes this newly discovered variant of the rTCA cycle so special? First, the roTCA cycle requires one less ATP molecule per synthesized acetyl-CoA compared with the classical ACL-dependent cycle (*1-3*). In bioenergetic terms the roTCA cycle seems to be the most efficient pathway of autotrophic CO_2 fixation known today (**Fig. 3C**). Still, the modified pathway is associated with an additional energy demand, as an organism using it must increase the amount of some catalysts to cope with their low substrate concentrations (note the very high activities of CS and MDH, **Table 1**). The high activities of the enzymes involved in thermodynamically unfavorable reactions ensure efficient coupling of the roTCA cycle to biosynthetic reactions. Anabolism is highly exergonic with a thermodynamic efficiency of about 40%, thus providing an additional driving force for the autotrophic pathway. Nevertheless, the

required low product to substrate ratio and high enzymatic activities may render this strategy infeasible for some organisms or under certain growth conditions. Second, the roTCA cycle can hardly be recognized bioinformatically. It makes (meta)genome-based bioinformatic predictions of the autotrophic potential of an anaerobic organism (or microbial community) difficult, if not impossible. Third, many bacteria using the rTCA cycle to fix CO_2 also possess CS genes (*29, 30*), and conversion of the ACL version of the rTCA cycle into the roTCA cycle appears to be quite easy. Notably, another *Desulfurella* species, *D. multipotens*, possesses an intact *acl* gene (**Fig. 1A**), but apparently uses the roTCA cycle, as can be judged from the ACL and CS activity measurements and ATP-independency of citrate cleavage (**Table S9**). The usage of the roTCA cycle could be a widespread trait of anaerobic autotrophic organisms. Considering a wide distribution of its enzymes in anaerobes, the cycle could have evolved convergently in different microbial groups. Fourth, CS is structurally simpler than ACL, which consists of several domains, with one of them being homologous to CS (*3*). Therefore, the roTCA cycle may even pre-date the modern ACL-rTCA, with an ancestral TCA cycle being fully reversible.

Our results show that unexpected discoveries are possible even when studying well-known metabolic pathways. If the highly endergonic citrate synthase reaction can be reversed *in vivo*, which other apparently unidirectional metabolic reactions may be reversed under certain conditions? Despite the many advances of the omics era, these features cannot be identified bioinformatically, but require classical biochemical studies for their discovery.

References and Notes

1. I. A. Berg, Ecological aspects of the distribution of different autotrophic CO_2 fixation pathways. *Appl. Environ. Microbiol.* **77**, 1925-1936 (2011).
2. G. Fuchs, Alternative pathways of carbon dioxide fixation: insights into the early evolution of life? *Annu. Rev. Microbiol.* **65**, 631-658 (2011).
3. M. Hügler, S. M. Sievert, Beyond the Calvin cycle: autotrophic carbon fixation in the ocean. *Ann. Rev. Mar. Sci.* **3**, 261-289 (2011).
4. G. Wächtershäuser, Evolution of the first metabolic cycles. *Proc. Natl. Acad. Sci. U.S.A.* **87**, 200-204 (1990).
5. E. Smith, H. J. Morowitz, Universality in intermediary metabolism. *Proc. Natl. Acad. Sci. U.S.A.* **101**, 13168-18173 (2004).
6. Keller, M. A., D. Kampjut, S. A. Harrison, M. Ralser, Sulfate radicals enable a non-enzymatic Krebs cycle precursor. *Nat. Ecol. Evol.* **1**, 0083 (2017).
7. R. K. Thauer, D. Möller-Zinkhan, A. M. Spormann, Biochemistry of acetate catabolism in anaerobic chemotrophic bacteria. *Annu. Rev. Microbiol.* **43**, 43-67 (1989).

8. R. N. Ivanovsky, N. V. Sintsov, E. N. Kondratieva, ATP-linked citrate lyase activity in the green sulfur bacterium *Chlorobium limicola* forma *thiosulfatophilum*. *Arch. Microbiol.* **128**, 239-241 (1980).
9. Möller, D., R. Schauder, G. Fuchs, R. K. Thauer, Acetate oxidation to CO_2 via a citric acid cycle involving an ATP-citrate lyase: a mechanism for the synthesis of ATP via substrate level phosphorylation in *Desulfobacter postgatei* growing on acetate and sulfate. *Arch. Microbiol.* **148**, 202-207 (1987).
10. M. Aoshima, M. Ishii, Y. Igarashi, A novel enzyme, citryl-CoA synthetase, catalysing the first step of the citrate cleavage reaction in *Hydrogenobacter thermophilus* TK-6. *Mol. Microbiol.* **52**, 751-761 (2004).
11. M. Aoshima, M. Ishii, Y. Igarashi, A novel enzyme, citryl-CoA lyase, catalyzing the second step of the citrate cleavage reaction in *Hydrogenobacter thermophilus* TK-6. *Mol. Microbiol.* **52**, 763-770 (2004).
12. ACL has been found only in *Bacteria* using the rTCA cycle for autotrophic CO_2 fixation and thus is regarded as its key enzyme. Two other characteristic enzymes of the cycle, 2-oxoglutarate:ferredoxin oxidoreductase and fumarate reductase, are present in many non-autotrophic anaerobes.
13. E. A. Bonch-Osmolovskaya, T. G. Sokolova, N. A. Kostrikina, G. A. Zavarzin, *Desulfurella acetivorans* gen. nov. and sp. nov. - a new thermophilic sulfur-reducing eubacterium. *Arch. Microbiol.* **153**, 151-155 (1990).
14. S. Pradella, H. Hippe, E. Stackebrandt, Macrorestriction analysis of *Desulfurella acetivorans* and *Desulfurella multipotens*. *FEMS Microbiol. Lett.* **159**, 137-144 (1998).
15. R. A. Schmitz, E. A. Bonch-Osmolovskaya, R. K. Thauer, Different mechanisms of acetate activation in *Desulfurella acetivorans* and *Desulfuromonas acetoxidans*. *Arch. Microbiol.* **154**, 274-279 (1990).
16. Materials and methods are available as supplementary materials at the Science website.
17. I. A. Berg, D. Kockelkorn, W. Buckel, G. Fuchs, A 3-hydroxypropionate/4-hydroxybutyrate autotrophic carbon dioxide assimilation pathway in Archaea. *Science* **318**, 1782-1786 (2007).
18. H. Huber, M. Gallenberger, U. Jahn, E. Eylert, I. A. Berg, D. Kockelkorn, W. Eisenreich, G. Fuchs, A dicarboxylate/4-hydroxybutyrate autotrophic carbon assimilation cycle in the hyperthermophilic Archaeum *Ignicoccus hospitalis*. *Proc Natl Acad Sci U.S.A.* **105**, 7851-7856 (2008).
19. M. Könneke, D. M. Schubert, P. C. Brown, M. Hügler, S. Standfest, T. Schwander, L. Schada von Borzyskowski, T. J. Erb, D. A. Stahl, I. A. Berg, Ammonia-oxidizing archaea use the most energy-efficient aerobic pathway for CO_2 fixation. *Proc Natl Acad Sci U.S.A.* **111**, 8239-8244 (2014).

20. R. W. Guynn, H. J. Gelberg, R. L. Veech, Equilibrium constants of the malate dehydrogenase, citrate synthase, citrate lyase, and acetyl coenzyme A hydrolysis reactions under physiological conditions. *J. Biol. Chem.* **248**, 6957-6965 (1973).
21. B. D. Bennett, E. H. Kimball, M. Gao, R. Osterhout, S. J. Van Dien, J. D. Rabinowitz, Absolute metabolite concentrations and implied enzyme active site occupancy in *Escherichia coli*. *Nat. Chem. Biol.* **5**, 593-599 (2009).
22. E. A. Siess, D. G. Brocks, O. H. Wieland, Distribution of metabolites between the cytosolic and mitochondrial compartments of hepatocytes isolated from fed rats. *Hoppe Seylers Z. Physiol. Chem.* **359**, 785-798 (1978).
23. E. A. Siess, R. I. Kientsch-Engel, O. H. Wieland, Concentration of free oxaloacetate in the mitochondrial compartment of isolated liver cells. *Biochem. J.* **218**, 171-176 (1984).
24. J. Paulsen, A. Kröger, R. K. Thauer, ATP-driven succinate oxidation in the catabolism of *Desulfuromonas acetoxidans*. *Arch. Microbiol.* **144**, 78-83 (1986).
25. A. T. Proudfoot, S. M. Bradberry, J. A.Vale, Sodium fluoroacetate poisoning. *Toxicol. Rev.* **25**, 213-219 (2006).
26. R. K. Thauer, E. Rupprecht, K. Jungermann, Glyoxylate inhibition of clostridial pyruvate synthase. *FEBS Lett.* **9**, 271-273 (1970).
27. A. P. Florentino, A. J. M. Stams, I. Sánchez-Andrea. Genome sequence of *Desulfurella amilsii* strain TR1 and comparative genomics of *Desulfurellaceae* family. *Front. Microbiol.* **8**, 222 (2017).
28. N. A. Chernyh, A. V. Mardanov, V. M. Gumerov, M. L. Miroshnichenko, A. V. Lebedinsky, A. Y. Merkel, D. Crowe, N. V. Pimenov, I. I. Rusanov, N. V. Ravin, M. A. Moran, E. A. Bonch-Osmolovskaya, Microbial life in Bourlyashchy, the hottest thermal pool of Uzon Caldera, Kamchatka. *Extremophiles* **19**, 1157-1171 (2015).
29. T. P. Turova, O. L. Kovaleva, V. M. Gorlenko, R. N. Ivanovskii, [Use of genes of carbon metabolism enzymes as molecular markers of *Chlorobi* Phylum representatives]. *Mikrobiologiia* **83**, 72-82 (2014).
30. K. H. Tang, R. E. Blankenship, Both forward and reverse TCA cycles operate in green sulfur bacteria. *J. Biol. Chem.* **285**, 35848-35854 (2010).

Acknowledgements:

We thank G. Fuchs, Albert-Ludwigs-Universität Freiburg, for his support, discussins, and the suggestions during this work and for critical reading of the manuscript. This work was supported by the Deutsche Forschungsgemeinschaft (BE 4822/5-1 and Heisenberg Fellowship BE 4822/1-2 to I.A.B.). We also thank the Hans-Fischer Gesellschaft (Munich) for financial support. All data to understand and assess the conclusions of this research are available in the main text, supplementary materials and the GenBank database (http://www.ncbi.nlm.nih.gov/Genbank/). The genome sequences of *Desulfurella acetivorans* and *Desulfurella multipotens* are deposited under GenBank accession numbers CP007051.1 and PRJNA262210, respectively. Amino acid sequences of candidate enzymes are available under their respective GenBank accesion numbers (see **Tables 1** and **S1**).

Supplementary Materials:

Materials and Methods

Supplementary Text

Tables S1 to S11

Figs. S1 to S9

References (*31-49*)

CHAPTER 4
OUTLOOK & DISCUSSION

In this work, we made considerable progress in the field of origin of life within the theory of a chemoautotrophic origin by combining the “Bottom-Up” and the “Top-Down” approach. One-step forward to the postulated chemoautotrophic theory of a pioneer organism was done by demonstrating a possible relevant pathway to primordial lipids. One-step forward to a postulated chemoautotrophic theory was advanced by disclosing the reversibility of the CS and thus a possible predated occurrence of the rTCA or roTCA, respectively. In the following chapter, the unpublished results of ongoing studies and their preliminary results are briefly discussed, but not disclosed.

4.1 A prebiotic Path to pre-cellular Aggregates

Methylthioacetat from acetylene – The presented work confirms our investigation on the prebiotic formation of lipids (Scheidler *et al*. 2016). Here, a mixture of monocarboxylic acids with the chain lengths of C3-C9 were obtained (Figure 23a). It is suggested that by the cooling of the earth within millions of years, the occurrence of acetylene would have decreased and the biosynthesis of lipids would have been replaced by enzymatic acetyl-CoA condensation (Figure 23c). This step-by-step transformation would have been mediated by the prebiotic synthesis of activated acetic acid as a possible precursor to acetyl-CoA (Figure 23b).

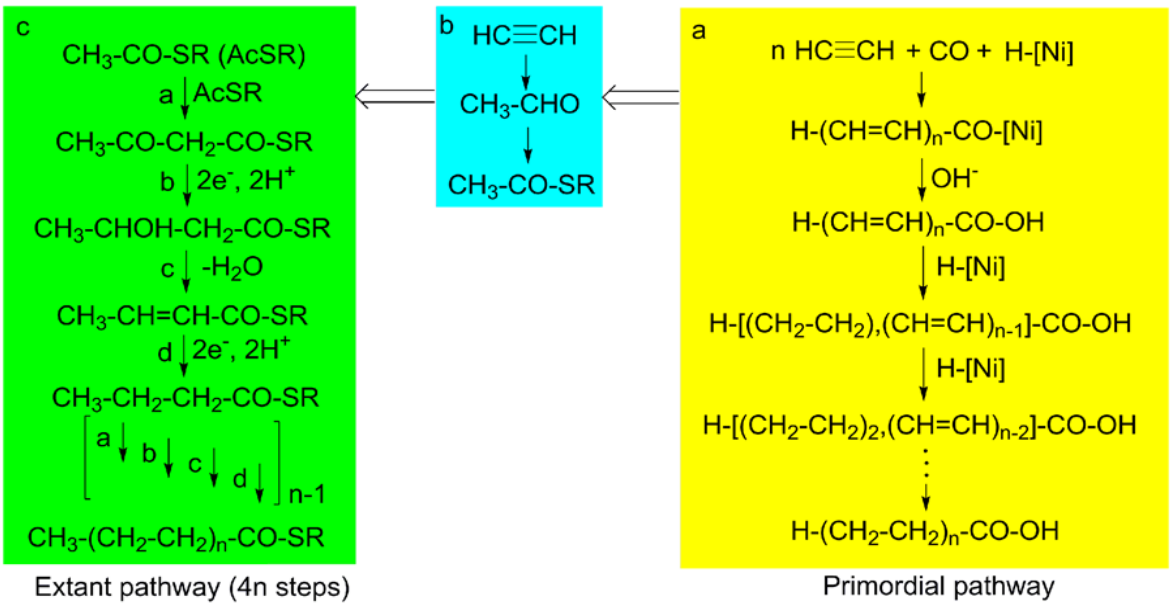

Figure 23: (a) Primordial one-pot pathway to the identified monocarboxylic acids. (b) Proposed conversion of acetylene to activated acetic acid. (c) Extant lipid pathway with activated acetic acid as precursor. (⟸) Evolutionary transformation steps (Scheidler *et al*. 2016).

Consequently, a further focus of this study was to proof the possibility of the thioester synthesis as suggested in Figure 23b. Indeed, we successfully observed the proposed formation of acetyl-thioester from acetylene and mercaptan and representing a further piece of evidence for the iron sulfur world (unpublished results) (Figure 23b).

Active sulfur chemistry - Besides the investigation on activated acetic acid, also the formation of sulfur-containing products in our reaction setting was analyzed. In all living organism, thioester formation is a common strategy to activate carboxylic acids, important intermediates that are used in plenty biological processes. Without the addition of mercaptan, acetyl-thioester could not be detected in experiments using NiS, acetylene and CO alone. Nonetheless, the Schmitt-Kopplin group (Helmholtz Zentrum Munich) found sulfur rich and active chemistry in the same reaction system by ultrahigh-resolution Fourier-transform ion cyclotron resonance mass spectrometry (FT-ICR-MS). The analysis revealed ~1200 molecules with the formula CHOS and ~400 compounds with CHO compositions (unpublished data), shown in Figure 24 as a van Krevelen diagram. A future cooperation with the Schmitt-Kopplin group will concentrate on the identification of new products and their formation in our reactions under hydrothermal vent conditions to support the iron sulfur theory.

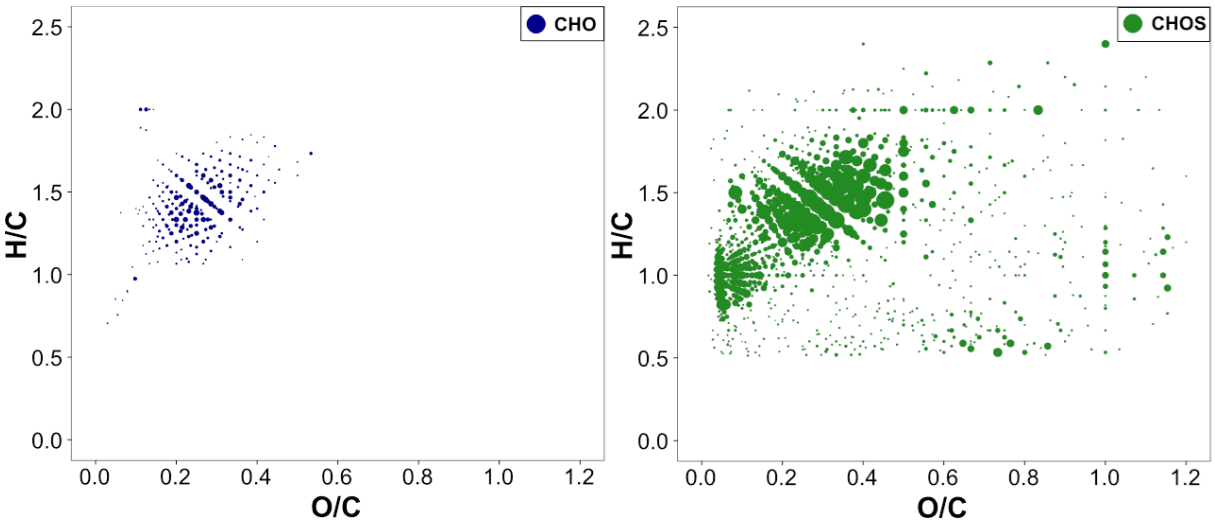

Figure 24: FT-ICR-MS data represented as van Krevelen diagram-type of CHO and CHOS space of C_2H_2, CO reaction catalyzed by NiS surface. Green dots represent compounds with the formula CHOS and blue dots compounds with CHO compositions (photo courtesy of Philippe Schmitt-Kopplin).

Prebiotic fatty acid addendum - Further analytical investigations *via* GC/MS on the aqueous solution in the reaction setting (NiS/CO/C_2H_2) revealed ~120 other recognizable products. Interestingly a further class of prebiotic fatty acids was identified, which resemble to membrane

spanning lipids containing carboxyl group at each end, namely 3,3'-thiobispropanoic acid as well as 4,4'-thiobisbutanoic acid (unpublished results). In addition, similar intermediates in the extant fatty acid biosynthesis of bacteria as well as intermediates used by archaea (unpublished results) could be detected, such as crotonic acid, 3-hydroxybutyric acid as well as hydroxymethylglutaric acid. These results strongly indicate a metabolism first theory. Other future experiments would focus on secondary products, which might be formed by adding these prebiotic intermediates in the catalytically active systems.

Micellar aggregates - In the experimental settings for short fatty acid formation, we recognized in some cases an increased viscosity of the obtained NiS solution. As amphiphilic compounds in an aqueous solution, fatty acids are able to self-assemble into micelles and further into bilayer structures such as vesicles. Micelle as well as vesicle formation depends on factors such as concentration, type of fatty acids, temperature and pH. At a high pH, the carboxylic groups are negatively charged and repel each other; if the pH is below a micelle specific threshold, the acidic heads of the fatty acids are protonated, resulting in coalescence and thus oil droplet formation. For fatty acid vesicles, the optimal formation pH value is considered be near the pKa of the associated fatty acid. The critical vesicle concentration (CVC) varies exponentially with chain length and is moreover dependent on type of fatty acid used. The shortest chain length fatty acid that is able to form vesicles is octanoic acid but this process requires very high concentration of the monomers of up to 250mM (Budin *et al*. 2014). The CVC can be lowered by admixture with fatty alcohols, hydrocarbons as well as with short monocarboxylic acids, those with C3 to C7 (Apel *et al*. 2002, Cape *et al*. 2011, Deamer 1985). Based on these insights, it was questionable if the increased viscosity found in the NiS solution is related to the issued unsaturated and saturated short fatty acids (C3, C5, C7, C9), which can be summed up in concentration to about 20mM (Scheidler *et al*. 2016). Therefore and as a proof-of-principle investigation, the formation of micellar and vesicular aggregate structures in outlined setup was studied in cooperation with the Friedrich Simmel group at TUM. Interestingly, using transmission electron microscopy (TEM), the formation of hydrophobic drop-like compartments could be visualized (Figure 25A) which were absent in control experiments (Figure 25B) (unpublished results).

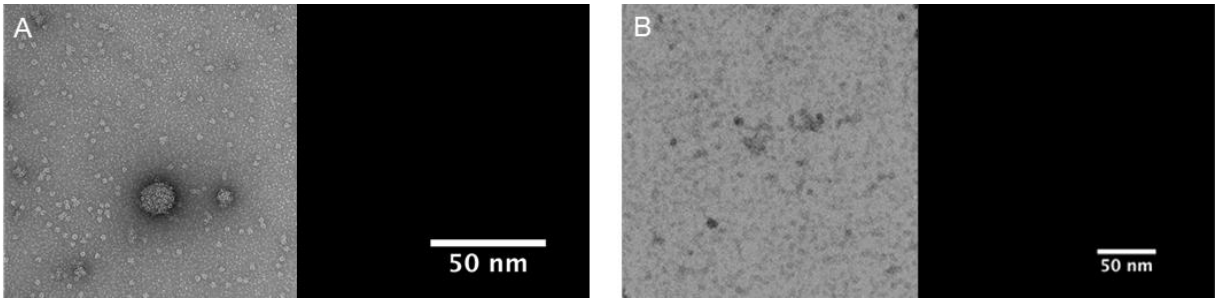

Figure 25: (A) TEM images of hydrophobic drops covered by alpha hemolysin, a hydrophobic protein pore, which helps in identifying vesicles. (B) TEM image of the control run whereby only protein pores can be visualized (B) (photo courtesy of Swati Krishnan and Friedrich Simmel).

Future collaborating work with Simmel's group will focus on providing evidence for an enclosed hydrated nanocrystalline NiS core shell structure with surrounding fatty acids according to the iron sulfur world theory (Figure 26). Aside the physico-chemical restriction of vesicle formation and the growth and reproduction of early vesicles, a certain permeability of the vesicles is needed to allow the uptake of nutrients. Therefore, the permeability should also be a point of interest. Permeability depends on membrane fluidity, which in turn depends on the chemical composition and also on temperature.

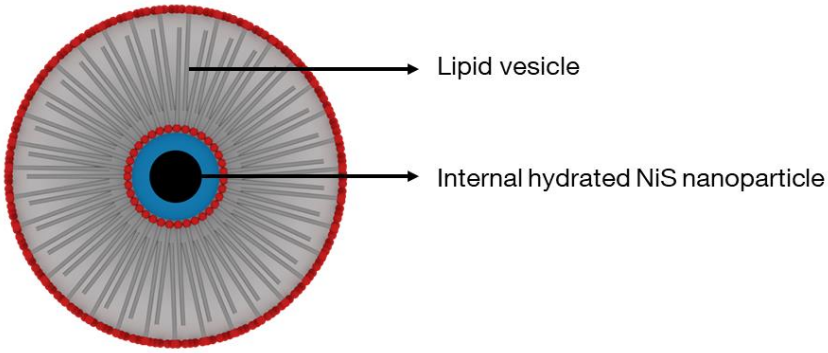

Figure 26: Enclosed hydrated nanocrystalline NiS-nanoparticle (with a core-shell structure) with detached lipid vesicle.

A membrane can change from permeable liquid state to a rigid crystalline or gel barrier at a characteristic temperature. The change of state is known as phase transition and the temperature at which it occurs can be lowered by shorter chain lengths, methyl branching or incorporation of *cis* double bonds. The latter two features prevent a close package of lipid layers and increase the fluidity (Koga 2012). Future experiments will consider the synthesis of the $C_{3,5,7,9}$-monocarboxylic acids, which are not commercially available, to test both their ability to form vesicles as well as their permeability. These polyunsaturated monocarboxylic acids can be obtained by related one-pot synthesis by straight chain C4-extension (Sobotta *et al*. 2017). There is the issue that it is not clear which amphiphilic compounds in the NiS suspension are responsible for vesicle formation and should be clarified. For the analysis of a broader product spectrum in these systems, the high mass accuracy of FT-ICR mass spectroscopy of the Schmitt-Kopplin group will be of great help.

4.2 Evolution of CO_2 Fixation Pathways

In this work, the physiological reversibility of CS in *Desulfurella acetivorans* was demonstrated (Mall *et al*. 2018). This novel insight opened the possibility of chemoautotrophic CO_2 fixation in form of roTCA in a wide range of ancient microorganisms (Mall *et al*. 2018). At the same time, T. Nunoura *et al*. also found citrate synthase activity in both directions in the thermophilic bacterium *Thermosulfidibacter takaii* (Nunoura *et al*. 2018). A phylogenetic analysis of *D. acetivorans* and *T. takaii* suggests that both, ACL and CCL originate from bidirectional CS (Nunoura *et al*. 2018). Although the conversion of citrate into acetyl-CoA and oxaloacetate is thermodynamically unfavorable, CS succeeded in overcoming this barrier with high efficiency. A simultaneously high activity of malate dehydrogenase was revealed that ensures a very low concentration of oxaloacetate, which is basically pulling the flux through the roTCA cycle. This strategy requires an additional energy source, such as reduced ferredoxin as a high potential iron-sulfur protein. A highlight of both publications (Mall *et al*. 2018, Nunoura *et al*. 2018) is the discovery that the direction of carbon flux *via* the roTCA cycle depends on the availability of organic *versus* inorganic carbon source. This bet-hedging strategy might be beneficial in the evolution and is probably a bio-signature of primordial microorganism.

Tracing primordial metabolism - A future work will be dedicated to further ancient microorganism from both domains, archaea and bacteria living at hydrothermal sites. For example, deeply branched chemolithoautotrophic microbes such as *Methanopyrus kandleri* or *Thermovibrio ammonificans* will be investigated in cooperation with William Orsi (LMU Munich). Both organisms encode the rTCA (in part or complete) and the Wood-Ljunghdal pathway. Future experiments will concentrate to provide constraints on the efficiency of these pathways under simulated early Earth environments. Additionally, these results will be compared to microbial communities isolated from hydrothermal environments conditions.

Dual carbon fixation pathways - Further, there are several chemoautotrophic organisms whose carbon fixation pathway have not yet been clarified including *Ammonifex degensii*, an anaerobic extremely thermophilic bacterium. This bacterium is isolated from hydrothermal environments and encodes two separate autotrophic pathways. On the one hand, the genes of the WL-pathway are present in *A. degensii* while on the other hand the genome contains the sequence for the archaic type III RuBisCo, known so far only from archaea. The aim of this work in cooperation with Ivan Berg (University of Münster) is to identify the used carbon fixation pathway under specific conditions (unpublished results).

Prebiotic CO_2 fixation intermediates.- Further analytical investigations *via* GC/MS of the aqueous solution in reaction setting (NiS/CO/C_2H_2) reflect ancestral metabolic traits under hydrothermal vent conditions. During the course of these experiments, a set of molecules closely related to the intermediates used in reductive CO_2 fixation pathways of extant microorganisms was identified for the first time under these conditions (unpublished results) including several intermediates of extant carbon fixation pathways. A follow up study is now focused on the discovery of non-enzymatic autocatalytic network reactions by adding these prebiotic intermediates into the catalytically active systems (unpublished results). Pilot experiments to establish a pioneer metabolism are still ongoing. These preliminary results have partly proven the theory that transition metal sulfides can catalyze reaction types such as hydration/dehydration, amination and methylation analogous to enzymatic-catalyzed reactions. A future aim will map further reactions to complete the metabolic network in our systems.

CHAPTER 5
REFERENCES

Allègre CJ, Poirier JP, Humler E, Hofmann AW (**1995**) The chemical composition of the Earth. *Earth Planet. Sci. Lett.* 134, 515-526.

Apel CL, Deamer DW, Mautner MN (**2002**) Self-assembled vesicles of monocarboxylic acids and alcohols: conditions for stability and for the encapsulation of biopolymers. *Biochim. Biophys. Acta* 1559, 1–9.

Auernik KS, Cooper CR, Kelly RM (**2008**) Life in hot acid: pathway analyses in extremely thermoacidophilic archaea. *Curr. Opin. Biotechnol.* 19, 445–453.

Bada JL, Fegley B, Miller SL, Lazcona A, Cleaves HJ, Hazen RM, Calmers J (**2007**) Debating Evidence for the Origin of Life on Earth. *Science* 315, 937-939 author reply 937-939.

Bada JL (**2013**) New insights into prebiotic chemistry from Stanley Miller's spark discharge experiments. *Chem. Soc. Rev.* 42, 2186-2196.

Barrault J, Boulinguiez M, Forquy C, Maurel R (**1987**) Synthesis of methyl mercaptan from carbon oxides and hydrogen sulfide with tungsten-alumina catalysts. *Appl. Catal.* 33, 309-330.

Bassham JA, Benson AA, Kay LD, Harris AZ, Wilson AT, Calvin M (**1954**) The path of carbon in photosynthesis. XXI. The cyclic regeneration of carbon dioxide acceptor. *J. Am. Chem. Soc.* 76, 1760–1770.

Beatty JT, Overmann J, Lince MT, Manske AK, Lang AS, Blankenship RE, Van Dover CL, Martinson TA, Plumley FG (**2005**) An obligately photosynthetic bacterial anaerobe from a deep-sea hydrothermal vent. *Proc. Natl. Acad. Sci. USA* 102, 9306–9310.

Becker S, Thoma I, Deutsch A, Gehrke T, Mayer P, Zipse H, Carell T (**2016**) A high-yielding, strictly regioselective prebiotic purine nucleoside formation pathway. *Science* 352, 833-836.

Bell EA, Boehnke P, Harrison TM, Mao WL (**2015**) Potentially biogenic carbon preserved in a 4.1 billion-year-old zircon. *Proc. Natl. Acad. Sci. USA* 112, 14518-14521.

Berg IA, Kockelkorn D, Buckel W, Fuchs G (**2007**) A 3-hydroxypropionate/4-hydroxybutyrate autotrophic carbon dioxide assimilation pathway in archaea. *Science* 318, 1782–1786.

Berg IA, Kockelkorn D, Ramos-Vera WH, Say RF, Zarzycki J, Hügler M, Alber BE, Fuchs G (**2010a**) Autotrophic carbon fixation in archaea. *Nat. Rev. Microbiol.* 8, 447–460.

Berg IA, Ramos-Vera WH, Petri A, Huber H, Fuchs G (**2010b**) Study of the distribution of autotrophic CO2 fixation cycles in *Crenarchaeota*. *Microbiology* 156, 256–269.

Berg IA (**2011**) Ecological aspects of the distribution of different autotrophic CO_2 fixation pathways. *Appl. Environ. Microbiol.* 77, 1925–1936.

Blöchl E, Keller M, Wächtershäuser G, Stetter KO (**1992**) Reactions depending on iron sulfide and linking geochemistry with biochemistry. *Proc. Natl. Acad. Sci. USA* 89, 8117-8120.

Boetius A (**2005**) Lost City Life. *Science* 307, 1420-1422.

Buchanan BB, Arnon DI (**1990**) A reverse KREBS cycle in photosynthesis: consensus at last. *Photosynth. Res.* 24, 47–53.

Budin I, Prwyes N, Zhang N, Szostak JW (**2014**) Chain-Length Heterogeneity Allows for the Assembly of Fatty Acid Vesicles in Dilute Solutions. *Biophys J*. 107, 1582–1590.

Bürstel I, Siebert E, Winter G, Hummel P, Zebger I, Friedrich B, Lenz O (**2012**) A Universal Scaffold for Synthesis of the $Fe(CN)_2(CO)$ Moiety of [NiFe] Hydrogenase. *J. Biol. Chem.* 287, 38845–3885.

Burton NP, Williams TD, Norris PR (**1999**) Carboxylase genes in Sulfolobus metallicus. *Arch. Microbiol.* 172, 349–353.

Bryant DA, Frigaard NU (**2006**) Prokaryotic photosynthesis and phototrophy illuminated. *Trends Microbiol*. 14, 488–496.

Cape JL, Monnard PA, Boncella JM (2011) Prebiotically relevant mixed fatty acid vesicles support anionic solute encapsulation and photochemically catalyzed trans-membrane charge transport. *Chem. Sci*. 2, 661–671.

Chen IA, Walde P (**2010**) From Self-Assembled Vesicles to Protocells. *Cold Spring Harb Perspect Biol.* 2.

Chuakrut, S, Arai H, Ishii M, Igarashi Y (**2003**) Characterization of a bifunctional archaeal acyl Coenzyme A carboxylase. *J. Bacteriol.* 185, 938–947.

Cockell CS (**2006**) The origin and emergence of life under impact bombardment. *Philos Trans R Soc Lond B Biol Sci.* 361, 1845–1856.

Cody GD, Boctor NZ, Filley TR, Hazen RM, Scott JH, Sharma A, Yoder HS (**2000**) Primoridal Carbonylated Iron-Sulfur Compounds and the Synthesis of Pyruvate. *Science* 289, 1337-1340.

Cody GD (**2004**) Transition metal sulfides and the origin of metabolism. *Annu. Rev. Earth Planet. Sci.* 32, 569–599.

Colín-García M, Heredia A, Cordero G, Camprubí A, Negrón-Mendoza A, Ortega-Gutiérrez F, Beraldi H, Ramos-Bernal S (**2016**) Hydrothermal vents and prebiotic chemistry: a review. *Bol. Soc. Geol. Mex.* 68, 599-620.

Corliss JB, Dymond J, Gordon LI, Edmond JM, von Herzen RP, Ballard RD, Green K, WilliamsD, Bainbridge A, Crane K, van Andel TH (**1979**) Submarine Thermal Springs on the Galápagos Rift. *Science* 203, 1073-1083.

Corliss JB, Baross JA, Hoffman SE (**1981**) An Hypothesis Concerning the Relationships Between Submarine Hot Springs and the Origin of Life on Earth. *Oceanol. Acta*, *Special issue* Open Access version 59-69.

Crick FHC (**1970**) Central Dogma of Molecular Biology. *Nature* 227, 561-563.

Darnault C, Volbeda A, Kim EJ, Legrand P, Vernède X, Lindahl PA, Fontecilla-Camps JC (**2003**) Ni-Zn-[Fe_4-S_4] and Ni-Ni-[Fe_4-S_4] clusters in closed and open subunits of acetyl-CoA synthase/carbon monoxide dehydrogenase. *Nat. Struct. Bio.* 10, 271–279.

Darwin CR (**1859**) On the Origin of Species. 1st Ed, London, *John Murray*.

De Rosa M, Gambacorta A, Gliozzi A (**1986**) Structure, biosynthesis and physico-chemical properties of archaebacterial lipids. *Microbiol. Rev.* 50, 70-80.

Deamer DW (**1985**) Boundary structures are formed by organic components of the Murchison carbonaceous meteorite. *Nature* 317, 792–794.

Dodd MS, Papineau D, Grenne T, Slack JF, Rittner M, Pirajno F, O'Neil J, Little CTS (**2017**) Evidence for early life in Earth's oldest hydrothermal vent precipitates. *Nature* 543, 60-64.

Doolittle WF (**2000**) Uprooting the tree of life. *SciAm* 282, 90-95.

Drobner E, Huber H, Wächtershäuser G, Rose D, Stetter KO (**1990**) Pyrite formation linked with hydrogen evolution under anaerobic conditions. *Nature* 346, 742–744.

Eckert H (**2017**) Synergy Effects in the Chemical Synthesis and Extensions of Multicomponent Reactions (MCRs)-The Low Energy Way to Ultra-Short Syntheses of Tailor-Made Molecules. *Molecules* 22, 349-381.

Eigen M (**1995**) What Will Endure of 20th Century Biology? In: Murphy MP, O'Neil LAJ, *What is life? The Next Fifty Years: Speculations on the Future of Biology* 5-23.

Eisenreich W, Huber C, Kutzner E, Knispel N, Schramek N (**2013**) Isotopologue Profiling – Toward a Better Understanding of Metabolic Pathways. In: Weckwerth W, Kahl G *The Handbook of plant metabolomics*, Wiley-Blackwell 22-56.

Eisenreich W, Dandekar T, Heesemann J, Goebel W (**2010**) Carbon metabolism of intracellular bacterial pathogens and possible links to virulence. *Nat. Rev. Microbiol.* 8, 401-412.

Elsner MP, Dittrich C, Agar DW (**2002**) Adsorptive reactors for enhancing equilibrium gas-phase reactions - two case studies. *Chem. Eng. Sci.* 57, 1607-1619.

Erb TJ, Zarzycki J (**2017**) A short history of RubisCO: the rise and fall (?) of Nature's predominant CO_2 fixing enzyme. *Curr. Opin. Biotechnol*. 49, 100-107.

Evans MCW, Buchanan BB, Arnon DI (**1966**) A new ferredoxin dependent carbon reduction cycle in a photosynthetic bacterium. *Proc. Natl. Acad. Sci. USA* 55, 928–934.

Feng X, Tang KH, Blankenship RE, Tang YJ (**2010**) Metabolic flux analysis of the mixotrophic metabolisms in the green sulfur bacterium *Chlorobaculum tepidum*. *J. Biol. Chem*. 285, 39544-39550.

Fontecilla-Camps JC, Amara P, Cavazza C, Nicolet Y, Volbeda A (**2009**) Structure–function relationships of anaerobic gas-processing metalloenzymes. *Nature* 460, 814-822.

Fuchs G (**2011**) Alternative pathways of carbon dioxide fixation: insights into the early evolution of life? *Annu. Rev. Microbiol*. 65, 631–658.

Fuson RC (**1935**) The Principle of Vinylogy. *Chem. Rev*. 16, 1-27.

Gamow G (**1954**) Possible Relation between Deoxyribonucleic Acid and Protein Structures. *Nature* 173, 318.

Gilbert W (**1986**) Origin of life: The RNA world. *Nature* 319, 618–618.

Guerrier-Takada C, Gardiner K, Marsh T, Pace N, Altman S (**1983**) The RNA moiety of ribonuclease P is the catalytic subunit of the enzyme. *Cell* 35, 849-857.

Hafenbrandl D, Keller M, Wächtershäuser G, Stetter KO (**1995**) Primordial amino Acids by Reductive Amination of α-Oxo Acids in Conjunction with the Oxidative Formation of Pyrite. *Tetrahedron Lett.* 36, 5179-5182.

Hagmann M (**2002**) Günter Wächtershäuser profile. Between a rock and a hard place. *Science* 295, 2006-2007.

Hao J, Giovenco E, Pedreira-Segade U, Montagnac G, Daniel I (**2018**) Compatibility of Amino Acids in Ice Ih: Implications for the Origin of Life. *Astrobiology* 18, 381-392.

Herter S, Fuchs G, Bacher A, Eisenreich W (**2002**) A bicyclic autotrophic CO_2 fixation pathway in *Chloroflexus aurantiacus*. *J. Biol. Chem.* 277, 20277–20283.

Hirata A, Murakami KS (**2009**) Archaeal RNA polymerase. *Curr Opin Struct Biol*. 19, 724-731.

Holo H (**1989**) *Chloroflexus aurantiacus* secretes 3-hydroxypropionate, a possible intermediate in the assimilation of CO_2 and acetate. *Arch. Microbiol.* 151, 252–256.

Huber C, Wächtershäuser G (**1997**) Activated Acetic Acid by Carbon Fixation on (Fe,Ni)S Under Primordial Conditions. *Science* 276, 245-247.

Huber C, Wächtershäuser G (**1998**) Peptides by Activation of Amino Acids with CO on (Ni,Fe)S Surfaces: Implications for the Origin of Life. *Science* 281, 670-672.

Huber C, Wächtershäuser G (**2003**) Primordial reductive amination revisited. *Tetrahedron Lett.* 44, 1695–1697.

Huber C, Eisenreich W, Hecht S, Wächtershäuser G (**2003b**) A Possible Primordial Peptide Cycle. *Science* 301, 938-940.

Huber C, Wächtershäuser G (**2006**) α-Hydroxy and α-Amino Acids Under Possible Hadean, Volcanic Origin-of-Life Conditions. *Science* 314, 630-632.

Huber C, Eisenreich W, Wächtershäuser G (**2010**) Synthesis of α-amino and α-hydroxy acids under volcanic conditions: implications for the origin of life. *Tetrahedron Lett.* 51,1069-1071.

Huber C, Kraus F, Hanzlik M, Eisenreich W, Wächtershäuser G (**2012**) Elements of Metabolic Evolution. *Chem. Euro. J.* 18, 2063-2080.

Huber C (**2013**) Die Chemie am Ursprung des Lebens. *BIOspectrum* 19, 363-365.

Huber H, Gallenberger M, Jahn U, Eylert E, Berg IA, Kockelkorn D, Eisenreich W, Fuchs G (**2008**) A dicarboxylate/4-hydroxybutyrate autotrophic carbon assimilation cycle in the hyperthermophilic Archaeum *Ignicoccus hospitalis*. *Proc. Natl. Acad. Sci. USA* 105, 7851–7856.

Hügler M, Krieger RS, Jahn M, Fuchs G (**2003**) Characterization of acetyl-CoA/propionyl-CoA carboxylase in Metallosphaera sedula. Carboxylating enzyme in the 3-hydroxypropionate cycle for autotrophic carbon fixation. *Eur. J. Biochem*. 270, 736–744.

Hügler M, Sievert SM (**2011**) Beyond the Calvin Cycle: Autotrophic Carbon Fixation in the Ocean. *Annu. Rev. Mar. Sci.* 3, 261–289.

Igari S, Maekawa T, Sakata S (**2000**) Light hydrocarbons in fumarolic gases: A case study in the Kakkonda geothermal area. *Chikyukagau* 34, 103–109.

Ivanovsky RN, Sintsov NV, Kondratieva EN (**1980**) ATP-linked citrate lyase activity in the green sulfur bacterium *Chlorobium limicola* forma *thiosulfatophilum*. *Arch. Microbiol.* 128, 239–241.

Ishii M, Miyake T, Satoh T, Sugiyama H, Oshima Y, Kodama T, Igarashi Y (**1997**) Autotrophic carbon dioxide fixation in *Acidianus brierleyi*. *Arch. Microbiol.* 166, 368–371.

Jones G (**1967**) The Knoevenagel Condensation. *Organic Reacti*ons 15, 204-599.

Jun SH, Reichlen MJ, Tajiri M, Murakami KS (**2012**) Archaeal RNA polymerase and transcription regulation. *Crit Rev Biochem Mol Biol*. 46, 27–40.

Keller MA, Kampjut D, Harrison SA, Ralser M (**2017**) Sulfate radicals enable a non enzymatic Krebs cycle precursor. *Nat. Ecol. Evol.* 1.

Kelley DS, Karson JA, Blackman DK, Früh-Green GL, Butterfield DA, Lilley MD, Olson EJ, Schrenk MO, Roe KK, Lebon GT, Rivizzigno P (**2001**) An off-axis hydrothermal vent field near the Mid-Atlantic Ridge at 30° N. *Nature* 412, 145-149.

Kelley DS, Karson JA, Früh-Green GL, Yoerger DR, Shank TM, Butterfield DA, Hayes JM, Schrenk MO, Olson EJ, Proskurowski G, Jakuba M, Bradley A, Larson B, Ludwig K, Glickson D, Buckman K, Bradley AS, Brazelton WJ, Roe K, Elend MJ, Delacour A, Bernasconi SM, Lilley MD, Baross JA, Summons RE, Sylva SP (**2005**) A Serpentinite-Hosted Ecosystem: The Lost City Hydrothermal Field. *Science* 307, 1428-1434.

Ljungdahl LG (**1986**) The autotrophic pathway of acetate synthesis in acetogenic bacteria. *Annu. Rev. Microbiol*. 40, 415–450.

Khare BN, Sagan C (**1971**) Synthesis of Cystine in Simulated Primitive Conditions. *Nature* 232, 577–579.

Koga Y (**2012**) Thermal Adaptation of the Archaeal and Bacterial Lipid Membranes. *Archaea.* 2012.

Kreysing M, Keil L, Lanzmich S, Braun D (**2015**) Heat flux across an open pore enables the continuous replication and selection of oligonucleotides towards increasing length. *Nat. Chem.* 7, 203–208.

Krishnamurthy SJ (**1982**) The Principle of Vinylogy. *J. Chem. Educ*. 59, 543-547.

Kruger K, Grabowski PJ, Zaug AJ, Sands J, Gottschling DE, Cech TR (**1982**) Self-splicing RNA: autoexcision and autocyclization of the ribosomal RNA intervening sequence of Tetrahymena. *Cell* 3, 147-157.

Lonsdale P. (**1977**) Clustering of suspension-feeding macrobenthos near abyssal hydrothermal vents at oceanic spreading centers. *Deep-Sea Res.* 24, 857–863.

Mall A, Sobotta J, Huber C, Tschirner C, Kowarschik S, Bačnik K, Mergelsberg M, Boll M, Hügler M, Eisenreich W, Berg IA (**2018**) Reversibility of citrate synthase allows autotrophic growth of a thermophilic bacterium. *Science* 359, 563-567.

Mast CB, Schink S, Gerland U, Braun D (**2013**) Escalation of polymerization in a thermal gradient. *Proc. Nat. Acad. Sci.* 110, 8030-8035.

McNichol J (**2008**) Primordial Soup, Fool's Gold, and Spontaneous Generation: A brief introduction to the theory, history, and philosophy of the search for the origin of life. *Biochem. Mol. Biol. Educ.* 36, 255-261.

Menendez C, Bauer Z, Huber H, Gad'on N, Stetter KO, Fuchs G (**1999**) Presence of acetyl coenzyme A (CoA) carboxylase and propionyl-CoA carboxylase in autotrophic *Crenarchaeota* and indication for operation of a 3-hydroxypropionate cycle in autotrophic carbon fixation. *J.Bacteriol.*181, 1088–1098.

Miller SL (**1953**) A Production of Amino Acids Under Possible Primitive Earth Conditions. *Science* 117, 528-529.

Mojzsis SJ, Arrhenius G, McKeegan KD, Harrison TM, Nutman AP, Friend CRL (**1996**) Evidence for life on Earth before 3,800 million years ago. *Nature* 384, 55-59.

Mojzsis SJ, Krishnamurthy R, Arrhenius G (**2005**) Before RNA and After: Geophysical and Geochemical Constraints on Molecular Evolution. In: Gesteland RF, Cech TR, Atkins JF 2nd Ed*, The RNA World: The N The Nature of Modern RNA Suggests a Prebiotic RNA World* 1-47.

Morasch M, Braun D, Mast CB (**2016**) Heat-Flow-Driven Oligonucleotide Gelation Separates Single-Base Differences. *Angew. Chem.* 55, 6676-6679.

Mukhin LM (**1976**) Volcanic processes and synthesis of simple organic compounds on primitive Earth. *Orig. Life* 7, 355–368.

Nelson KE, Levy M, Miller SL (**2000**) Peptide nucleic acids rather than RNA may have been the first genetic molecule. *Proc. Natl. Acad. Sci. USA* 97, 3868–3871.

Nirenberg MW, Matthaei JH (**1961**) The dependence of cell-free protein synthesis in *E. coli* upon naturally occurring or synthetic polyribonucleotides. *Proc. Natl. Acad. Sci. USA* 47, 1588-1602.

Nitschke W, Russell MJ (**2009**) Hydrothermal focusing of chemical and chemiosmotic energy, supported by delivery of catalytic Fe, Ni, Mo/W, Co, S and Se, forced life to emerge. *J Mol Evol* 69, 481-496.

Norris PR, Nixon A, Hart A (**1989**) Acidophilic, mineral-oxidizing bacteria: the utilization of carbon dioxide with particular reference to autotrophy in *Sulfolobus*. In: Da Costa MS, Duarte JC, Williams RAD. *Microbiology of extreme environments and its potential for biotechnology*. Elsevier, London 24–43.

Nunoura T, Chikaraishi Y, Izaki R, Suwa T, Sato T, Harada T, Mori K, Kato Y, Miyazaki M, Shimamura S, Yanagawa K, Shuto A, Ohkouchi N, Fujita N, Takaki Y, Atomi H, Takai K (**2018**) A primordial and reversible TCA cycle in a facultatively chemolithoautotrophic thermophile. *Science* 359, 559-563.

Nutman AP, Bennett VC, Friend CR, Van Kranendonk MJ, Chivas AR (**2016**) Rapid emergence of life shown by discovery of 3,700-million-year-old microbial structures. *Nature* 537, 535-538.

Oparin AI (**1924**) The Origin of Life. *Proiskhozhdenie zhizny, Moscow, Trad*.

Oremland RS, Voytek MA (**2008**) Acetylene as fast food: Implications for development of life on anoxic primordial Earth and in the outer Solar System. *Astrobiology* 8, 45–58.

Orgel LE (**2008**) The implausibility of metabolic cycles on the prebiotic Earth. *PLoS Biol*. 6.

Oró J (**1960**) Synthesis of adenine from ammonium cyanide. *Biochem. Biophys. Res. Commun.* 2, 407-412.

Oró J (**1961**) Mechanism of Synthesis of Adenine from Hydrogen Cyanide under Possible Primitive Earth Conditions. *Nature* 191, 1193-1194.

Oró J, Kimball AP (**1961**) Synthesis of purines under possible primitive earth conditions. I. Adenine from hydrogen cyanide. *Arch. Biochem. Biophys.* 94, 217-227.

Patel BH, Percivalle C, Ritson DJ, Colm D. Duffy & Sutherland JD (**2015**) Common origins of RNA, protein and lipid precursors in a cyanosulfidic protometabolism. *Nat. Chem.* 7, 301–307.

Peters JW, Williams LD (**2012**) The Origin of Life: Look Up and Look Down. *Astrobiology* 12, 1087-1092.

Powner MW, Gerland B, Sutherland JD (**2009**) Synthesis of activated pyrimidine ribonucleotides in prebiotically plausible conditions. *Nature* 459, 239–242.

Ragsdale SW (**2009**) Nickel-based Enzyme Systems. *J. Biol. Chem.* 284, 18571-18575.

Ramos-Vera WH, Berg IA, Fuchs G (**2009**) Autotrophic carbon dioxide assimilation in *Thermoproteales* revisited. *J. Bacteriol.* 191, 4286–4297.

Rauchfuss TB (**2010**) Unraveling the Biosynthesis of Nature's Fastest Hydrogenase. *Angew. Chem. Int. Ed.* 49, 4166 – 4168.

Ross DS (**2007**) The Viability of a Nonenzymatic Reductive Citric Acid Cycle – Kinetics and Thermochemistry. *Orig. Life Evol. Biosph.* 37, 61–65.

Russell MJ, Barge LM, Bhartia R, Bocanegra D, Bracher PJ, Branscomb E, Kidd R, McGlynn S, Meier DH, Nitschke W, Shibuya T, Vance S, White L, Kanik I (**2014**) The Drive to Life on Wet and Icy Worlds. *Astrobiology* 14, 308-343.

Salinas-de-León P, Phillips B, Ebert D, Shivji M, Cerutti-Pereyra F, Ruck C, Fisher CR, Marsh L (**2018**) Deep-sea hydrothermal vents as natural egg-case incubators at the Galapagos Rift. *Scientific Reports* 8.

Scheidler C, Sobotta J, Eisenreich W, Wächtershäuser G, Huber C (**2016**) Unsaturated $C_{3,5,7,9}$-Monocarboxylic Acids by Aqueous, One-Pot Carbon Fixation: Possible Relevance for the Origin of Life. *Sci. Rep.* 6.

Schleifer KH, Kandler O (**1972**) Peptidoglycan types of bacterial cell walls and their taxonomic implications. *Bacteriol.Rev.* 36, 407-477.

Schöning K, Scholz P, Guntha S, Wu X, Krishnamurthy R, Eschenmoser A (**2000**) Chemical etiology of nucleic acid structure: the alpha-threofuranosyl-(3'→2') oligonucleotide system. *Science* 290, 1347–1351.

Schreiber U, Mayer C, Schmitz OJ, Rosendahl P, Bronja A, Greule M, Keppler F, Mulder I, Sattler T, Schöler HF (**2017**) Organic compounds in fluid inclusions of Archean quartz-Analogues of prebiotic chemistry on early Earth. *PLoS ONE* 12.

Sobotta J, Schmalhofer M, Steiner TM, Eisenreich W, Wächtershäuser G, Huber C (**2017**) One-pot formation of 2,4-di- or 2,4,6-tri-olefinic monocarboxylic acids by straight chain C4-extension. *Heliyon* 3.

Span I, Wang K, Wang W, Zhang Y, Bacher A, Eisenreich W, Li K, Schulz C, Oldfield E, Groll M (**2012**) Discovery of acetylene hydratase activity of the iron-sulphur protein IspH. *Nat. Commun.* 3.

Smith E, Morowitz H (**2004**) Universality in intermediary metabolism. *Proc. Natl. Acad. Sci. USA* 101, 13168-13173.

Strauss G, Fuchs G (**1993**) Enzymes of a novel autotrophic CO_2 fixation pathway in the phototrophic bacterium *Chloroflexus aurantiacus*, the 3-hydroxypropionate cycle. *Eur. J. Biochem.* 215, 633–643.

Strecker A (**1850**) Ueber die künstliche Bildung der Milchsäure und einen neuen, dem Glycocoll homologen Körper. *Liebigs Ann. Chem.* 75, 27-45.

Tabita FR, Hanson TE, Li H, Satagopan S, Singh J, Chan S (**2007**) Function, structure, and evolution of the RubisCO-like proteins and their RubisCO homologs. *Microbiol. Mol. Biol. Rev*. 71, 576–599.

Trifonov EN (**2011**) Vocabulary of Definitions of Life Suggests a Definition. *J. Biomol. Struct. Dyn.* 29, 259-266.

Ueno Y, Yamada K, Yoshida N, Maruyama S, Isozaki Y (**2006**) Evidence from fluid inclusions for microbial methanogenesis in the early Archaean era. *Nature* 440, 516-519.

Van der Meer MT, Schouten S, de Leeuw JW, Ward DM (**2000**) Autotrophy of green non-sulphur bacteria in hot spring microbial mats: biological explanations for isotopically heavy organic carbon in the geological record. *Environ. Microbiol***.** 2, 428–435.

Volbeda A, Fontecilla-Camps JC (**2006**) Catalytic Nickel–Iron–Sulfur Clusters: From Minerals to Enzymes. In: Simonneaux G, *Bioorganometallic Chemistry. Topics in Organometallic Chemistry* 57-82.

Wächtershäuser G (**1988a**) Pyrite formation, the first energy source for life: a hypothesis. *System. Appl. Microbiol.* 10, 207–210.

Wächtershäuser G (**1988b**) Before Enzymes and Templates: Theory of Surface Metabolism. *Microbiol. Rev.* 52, 452-484.

Wächtershäuser G (**1990a**) The case for the chemoautotrophic origin of life in an iron-sulfur world. *Origins Life Evol. B.* 20, 173-176.

Wächtershäuser G (**1990b**) Evolution of the first metabolic cycles. *Proc. Natl. Acad. Sci. USA* 87, 200-204.

Wächtershäuser G (**1992**) Groundworks for an evolutionary biochemistry: The iron-sulphur world. *Prog. Biophys. molec. Biol*. 58, 85-201.

Wächtershäuser G (**2000**) Life as we don’t know it. *Science* 289, 1307-1308.

Wächtershäuser G (**2006**) From volcanic origins of chemoautotrophic life to Bacteria, Archaea and Eukarya. *Philos. Trans. R. Soc. Lond. B. Biol. Sci.* 361, 1787-1808.

Wächtershäuser G (**2007**) On the Chemistry and evolution of the Pioneer Organism. *Chem. Biodivers.* 4, 584-602.

Wächtershäuser G (**2014**) From Chemical Invariance to Genetic Variability. In: Weigand W, Schollhammer P 1st Ed, *Bioinspired Catalysis: Metal-Sulfur Complexes* 1-20.

Watson JD, Crick FHC (**1953**) Molecular structure of nucleic acids; a structure for deoxyribose nucleic acid. *Nature* 171, 737–8.

Wiberg N (**2007**) Chalkogenverbindungen der Erdalkalimetalle. In: 102th Eds *Hollemann-Wiberg, Lehrbuch der anorganischen Chemie* 1243–1247, Walter de Gruyter, Berlin.

Wochner A, Attwater J, Coulson A, Holliger P (**2011**) Ribozyme-catalyzed transcription of an active ribozyme. *Science* 332, 209–212.

Woese CR, Dugre DH, Saxinger WC, Dugre SA (**1966**) The molecular basis for the genetic code. *Proc. Natl. Acad. Sci. USA* 55, 966-974.

Woese CR (**1981**) Archaebaceria. *SciAm* 244, 98-122.

Woese CR, Kandler O, Wheelis ML (**1990)** Towards a natural system of organisms: Proposal for the domains archaea, bacteria, and eucarya. *Proc. Natl. Acad. Sci. USA* 87, 4576-4579.

Yilin H, Ribbe MW (**2016**) Maturation of nitrogenase cofactor—the role of a class E radical SAM methyltransferase NifB. *Curr. Opin. Chem. Biol.* 31, 188–194.

Zarzycki J, Brecht V, Müller M, Fuchs G (**2009**) Identifying the missing steps of the autotrophic 3-hydroxypropionate CO_2 fixation cycle in *Chloroflexus aurantiacus*. *Proc. Natl. Acad. Sci. USA* 106, 21317–21322.

Zhang L, Peritz A, Meggers E. (**2005**) A simple glycol nucleic acid. *J. Am. Chem. Soc*. 127, 4174–4175.

Zhang XV, Martin ST (**2006**) Driving Parts of Krebs Cycle in Reverse through Mineral Photochemistry. *J. Am. Chem. Soc.* 128, 16032-16033.

CHAPTER 6
REPRINT PERMISSIONS

6.1 Reprint Permission: Unsaturated $C_{3,5,7,9}$-Monocarboxylic Acids by aqueous, One-pot Carbon Fixation: Possible Relevance for the Origin of Life

Sobotta, Jessica

Allen antworten

Mo 30.04, 14:54

journalpermissions@springernature.com

Dear Sir or Madam,

in order to comply the criteria of my degree-granting institution (Technische Universitaet Muenchen) I need a written confirmation that I may reuse the following article, which is based on my PhD thesis.

Christopher Scheidler, Jessica Sobotta, Wolfgang Eisenreich, Günter Wächtershäuser, Claudia Huber
Unsaturated $C_{3,5,7,9}$-Monocarboxylic Acids by Aqueous, One-Pot Carbon Fixation: Possible Relevance for the Origin of Life.
Scientific Reports volume 6, Article number: 27595 (2016)
doi:10.1038/srep27595
Received:09 March 2016
Accepted:20 May 2016
Published:10 June 2016

As an author, I wish to include this full text article in the printed and electronic version of my dissertation, which I am required to deposit in the Technische Universität München's digital online archive, media TUM (https://mediatum.ub.tum.de/). MediaTUM is a non-commercial facility which is freely and open available for all.
I would be glad if you grant me confirmation.

Sincerely,
Jessica Sobotta

30.04.2018
TUM Department of Chemistry
PhD candidate
Chair of Biochemistry
Lichtenbergstraße 4
85748 Garching

Journalpermissions <journalpermissions@springernature.com>
Mo 30.04, 15:35

Dear Jessica,

Thank you for your email. This work is licensed under a Creative Commons Attribution 4.0 International License, which permits unrestricted use, distribution, and reproduction in any medium, provided you give appropriate credit to the original author(s) and the source, provide a link to the Creative Commons license, and indicate if changes were made. **You are not required to obtain permission to reuse this article.** The images or other third party material in this article are included in the article's Creative Commons license, unless indicated otherwise in the credit line; if the material is not included under the Creative Commons license, users will need to obtain permission from the license holder to reproduce the material. To view a copy of this license, visit http://creativecommons.org/licenses/by/4.0/.

Kind regards,
Oda

Oda Siqveland
Permissions Assistant

SpringerNature
The Campus, 4 Crinan Street, London N1 9XW,
United Kingdom
T +44 (0) 207 014 6851

http://www.nature.com
http://www.springer.com
http://www.palgrave.com

6.2 Reprint Permission: One-pot Formation of 2,4-di- or 2,4,6-tri-olefinic Monocarboxylic Acids by straight Chain C4-Extension

Sobotta, Jessica

Allen antworten

Mo 30.04, 15:11

permissionshelpdesk@elsevier.com

Dear Sir or Madam,

in order to comply the criteria of my degree-granting institution (Technische Universitaet Muenchen) I need a written confirmation that I may reuse the following article, which is based on my PhD thesis.

One-pot formationof 2,4-di- or 2,4,6-tri-olefinic monocarboxylic acids by straight chain C4-extension
Jessica Sobotta, Maximilian Schmalhofer, Thomas M. Steiner, Wolfgang Eisenreich, Günter Wächtershäuser, Claudia Huber
Received: 15 February2017
Revised: 19 July2017
Accepted: 19 July2017
Heliyon3(2017) e00368.
doi: 10.1016/j.heliyon.2017.e00368

As an author, I wish to include this full text article in the printed and electronic version of my dissertation, which I am required to deposit in the Technische Universität München's digital online archive, media TUM (https://mediatum.ub.tum.de/). MediaTUM is a non-commercial facility, which is freely and open available for all.
I would be glad if you grant me confirmation.

Sincerely,
Jessica Sobotta

30.04.2018
TUM Department of Chemistry
PhD candidate
Chair of Biochemistry
Lichtenbergstraße 4
85748 Garching

Permissions Helpdesk <permissionshelpdesk@elsevier.com>
Mo 30.04, 16:54

Dear Jessica,

As an Elsevier journal author, you retain the right to Include the article in a thesis or dissertation (provided that this is not to be published commercially) whether in full or in part, subject to proper acknowledgment; see https://www.elsevier.com/about/our-business/policies/copyright/personal-use for more information. As this is a retained right, no written permission from Elsevier is necessary.

As outlined in our permissions licenses, this extends to the posting to your university's digital repository of the thesis provided that if you include the published journal article (PJA) version, it is embedded in your thesis only and not separately downloadable:

19. Thesis/Dissertation: If your license is for use in a thesis/dissertation your thesis may be submitted to your institution in either print or electronic form. Should your thesis be published commercially, please reapply for permission. These requirements include permission for the Library and Archives of Canada to supply single copies, on demand, of the complete thesis and include permission for Proquest/UMI to supply single copies, on demand, of the complete thesis. Should your thesis be published commercially, please reapply for permission. Theses and dissertations which contain embedded PJAs as part of the formal submission can be posted publicly by the awarding institution with DOI links back to the formal publications on ScienceDirect.

Best of luck with your dissertation and best regards,

Laura

Laura Stingelin
Permissions Helpdesk Associate
ELSEVIER | Global E-Operations Books
+1 215-239-3867 office
l.stingelin@elsevier.com
Contact the Permissions Helpdesk
+1 800-523-4069 x3808 | permissionshelpdesk@elsevier.com

Copyright Clearance Center RightsLink®

SPRINGER NATURE

Title:	Unsaturated C3,5,7,9-Monocarboxylic Acids by Aqueous, One-Pot Carbon Fixation: Possible Relevance for the Origin of Life
Author:	Christopher Scheidler, Jessica Sobotta, Wolfgang Eisenreich, Günter Wächtershäuser, Claudia Huber
Publication:	Scientific Reports
Publisher:	Springer Nature
Date:	Jun 10, 2016

Creative Commons

6.3 Reprint Permission: Reversibility of Citrate Synthase allows autotrophic Growth of a thermophilic Bacterium

From: Sobotta, Jessica <jessica.sobotta@tum.de>
Sent: Monday, April 30, 2018 8:29 AM
To: permissions
Subject: AW: Reprint Permission

Dear Sir or Madam,

in order to comply the criteria of my degree-granting institution (Technische Universitaet Muenchen) I need a written confirmation that I may reuse the following article, which is based on my PhD thesis.

Reversibility of citrate synthase allows autotrophic growth of a thermophilic bacterium
Achim Mall, **Jessica Sobotta**, Claudia Huber, Carolin Tschirner, Stefanie Kowarschik, Katarina Bačnik, Mario Mergelsberg, Matthias Boll, Michael Hügler, Wolfgang Eisenreich, Ivan A. Berg
Science 02 Feb 2018:
Vol. 359, Issue 6375, pp. 563-567
DOI: 10.1126/science.aao2410

As an author, I wish to include this full text article in a printed version of my dissertation.
In my electronic version of dissertation, I wish to reuse the above stated work with appropriate citation.
I would be glad if you grant me confirmation.

Sincerely,

Jessica Sobotta

30.04.2018
TUM Department of Chemistry
PhD candidate
Chair of Biochemistry
Lichtenbergstraße 4
85748 Garching

permissions <permissions@aaas.org>
Mo 30.04, 15:09
Sobotta, Jessica

Allen antworten

Zur Nachverfolgung kennzeichnen. Beginnt am Montag, 30. April 2018. Fällig am Montag, 30. April 2018.

RE: Reversibility of citrate synthase allows autotrophic growth of a thermophilic bacterium
Achim Mall, **Jessica Sobotta**, Claudia Huber, Carolin Tschirner, Stefanie Kowarschik, Katarina Bačnik, Mario Mergelsberg, Matthias Boll, Michael Hügler, Wolfgang Eisenreich, Ivan A. Berg
Science 02 Feb 2018: Vol. 359, Issue 6375, pp. 563-567 DOI: 10.1126/science.aao2410

Dear Ms. Sobotta:

Thank you very much for getting in touch. This letter is to inform you of AAAS's policy on author use of his/her AAAS journal article(s) in a thesis or dissertation that he/she is writing.

1. After publication of a manuscript in an AAAS journal, the author may reprint his/her manuscript, in print format, in a thesis or dissertation written by the author as part of a course of study at an educational institution. Credit must be given to the first appearance of the material in the appropriate issue of the AAAS journal.

2. If the thesis or dissertation is to be published in electronic format, the accepted version of the work (the accepted version of the paper before Science's copy-editing and production) should be used and a link to the work on the AAAS journal website included.

3. Permission covers future revisions and editions of the thesis or dissertation by the author and author institution, provided the AAAS material covered by this permission remains in situ and is not distributed outside of the context of your thesis or dissertation.

4. Permission covers the distribution of your thesis or dissertation on demand by a third party distributor (e.g. ProQuest / UMI), provided the AAAS material covered by this permission remains in situ and is not distributed by that third party outside of the context of your thesis or dissertation.

5. The author may not permit others to reproduce the AAAS journal manuscript in a thesis or dissertation. In these cases, requesting parties should be instructed to contact AAAS directly for permission.

If you have any questions regarding this policy, please just let me know.

Kind regards,

Elizabeth Sandler
The American Association for the Advancement of Science (AAAS)
Rights & Permissions
1200 New York Ave., NW
Washington, DC 20005
+1-202-326-6765

CHAPTER 7
SUPPLEMENTARY MATERIAL

7.1 Supplementary Material: Unsaturated $C_{3,5,7,9}$-Monocarboxylic Acids by aqueous, One-Pot Carbon Fixation: Possible Relevance for the Origin of Life

Unsaturated $C_{3,5,7,9}$-Monocarboxylic Acids by Aqueous, One-Pot Carbon Fixation: Possible Relevance for the Origin of Life

Christopher Scheidler*, Jessica Sobotta*, Wolfgang Eisenreich, Günter Wächtershäuser, Claudia Huber

Supplementary Table S1: Monocarboxylic acid products of the nickel-catalyzed reaction of acetylene with carbon monoxide

Reactions were carried out in 125 ml serum bottles with 5 ml aqueous liquid phase containing 60ml CO and 60ml acetylene for 7 days at 105°C; Products were identified by GC-MS as *tert*-butyldimethylsilyl derivatives;
Acids are classified as follows: yellow: classes of monocarboxylic acids with identical chemical formulae; no colour: individual monocarboxylic acids within said classes; salmon: classes of monocarboxylic acids with identical numbers of C-atoms; red: total sum of identified monocarboxylic acids; blue: hydrogenation yields in % for successive hydrogenation steps, calculated according to the indicated formula (numerals in the formula identify the table rows where the yields for the computation are found).

	run	a	b	c	d	e	f	identification/	ordered characteristic fragment masses (silane fragments 73, 75, 115, 117 etc. not shown)			
	mmol NiS	1	1	0.5	0.5	0	0	quantification				
	mmol $Ni(OH)_2$ (α or β)	0	0	0.5(α)	0.5(β)	1(α)	1(β)	methods				
	end-pH	8.8	6.7	8.3	8.9	8.0	9.8	Notes	mass 1	mass 2	mass 3	mass 4
	C_3-acids (µM)											
1	C_2H_3-COOH	3884	5822	3318	6675	250	243	*, ‡, §, ☆	$129^{3\wedge}$	$55^{3\wedge}$	$85^{3\wedge}$	
2	C_2H_5-COOH	7132	1069	461	7391	510	171	*, ‡, §, ☆	$131^{1\bullet 5\wedge}$			
3	ΣC_3	11016	6891	3779	14066	760	414					
4	2*100/3	65	16	12	53	67	41	%1st hydrogenation				
	C_5-acids (µM)											
5	trCH$_2$=CH-CH=CH-COOH	369	1211	742	1212	53	0	*, ‡, §, ☆	$155^{1\bullet 5\wedge}$	$111^{5\wedge}$	$81^{1\bullet 5\wedge}$	$53^{5\wedge}$
6	cCH$_2$=CH-CH=CH-COOH	97	386	228	251	0	0	*, ‡, §, ††	$155^{1\bullet 5\wedge}$	$111^{5\wedge}$	$81^{1\bullet 5\wedge}$	$53^{5\wedge}$
7	ΣC_4H_5-COOH	466	1597	970	1463	53	0					
8	CH$_2$=CH-CH$_2$-CH$_2$-COOH	830	346	153	946	11	0	*, ‡, §, ll, #, ☆	$157^{1\bullet 7\wedge}$			
9	trCH$_3$-CH=CH-CH$_2$-COOH	3791	1565	839	3207	0	0	*, ‡, §, ll, #, ☆	$157^{1\bullet 7\wedge}$	$113^{7\wedge}$		
10	cCH$_3$-CH=CH-CH$_2$-COOH	2053	535	271	1550	0	0	*, ‡, §, ll, #, ††	$157^{1\bullet 7\wedge}$	$113^{7\wedge}$		
11	CH$_3$-CH=CH(CH$_3$)-COOH	578	60	45	1162	0	0	*, ‡, §, ll, #, ☆	$157^{1\bullet 7\wedge}$			
12	trC$_2$H$_5$-CH=CH-COOH	246	135	82	404	0	0	*, ‡, §, ll, #, ☆	$157^{1\bullet 7\wedge}$	$113^{7\wedge}$	$83^{1\bullet 7\wedge}$	$55^{7\wedge}$
13	ΣC_4H_7-COOH	7498	2641	1390	7269	11	0					
14	C_4H_9-COOH	309	32	11	363	0	0	*, ‡, §, ll, #, ☆	$159^{1\bullet 9\wedge}$			
15	ΣC_5	8273	4270	2371	9095	64	0					
16	(13+14)·100/15	94	63	59	84	17	—	%1st hydrogenation				
17	14·100/(13+14)	4	1	1	5	0	—	%2nd hydrogenation				
	C_7-acids (µM) (Note)											
18	trtrH(CH=CH)$_3$-COOH	26	5	0	24	0	0	†, §, ¶, #, **	181	77	79	59
19	C_6H_5-COOH	38	25	31	37	0	0	*, ‡, #, ☆	$179^{1\bullet 5\wedge}$	$105^{1\bullet 5\wedge}$	$77^{5\wedge}$	$135^{5\wedge}$
20	$\Sigma C_6H_{5\text{-}7}$-COOH	63	30	31	61	0	0					
21	C_6H_9-COOH (a)	19	4	0	42	0	0	‡, §, #, **	$183^{1\bullet 9\wedge}$			
22	C_6H_9-COOH (b)	29	14	8	32	0	0	‡, §, #, **	$183^{1\bullet 9\wedge}$			
23	C_6H_9-COOH (c)	237	92	41	100	0	0	‡, §, #, **	$183^{1\bullet 9\wedge}$			
24	C_6H_9-COOH (d)	35	38	20	72	0	0	‡, §, #, **	$183^{1\bullet 9\wedge}$			
25	ΣC_6H_9-COOH	320	148	69	246	0	0					
26	C_6H_{11}-COOH (a)	25	25	6	32	0	0	‡, §, #, **	$185^{1\bullet}$			
27	C_6H_{11}-COOH (b)	13	7	0	26	0	0	§, #, **	$185^{1\bullet}$	129		
28	C_6H_{11}-COOH (c)	14	10	0	38	0	0	§, #, **	$185^{11\wedge}$			
29	ΣC_6H_{11}-COOH	52	42	6	96	0	0					
30	ΣC_7	435	220	106	403	0	0					
31	(25+29)·100/30	86	86	71	85	—	—	%1st hydrogenation				
32	29·100/(25+29)	14	22	8	28	—	—	%2nd hydrogenation				
	C_9-acids (µM) (Note)											
33	C_6H_5-C_2H_4-COOH	0.6	3.01	1.5	0.5	0	0	*, ‡, #, ☆	$207^{1\bullet 9\wedge}$	$91^{7\wedge}$		
34	C_6H_5-C_2H_2-COOH	1.25	1.4	1.56	1.01	0	0	*, ‡, #, ☆	$205^{1\bullet 7\wedge}$	$131^{1\bullet 7\wedge}$	$103^{7\wedge}$	$161^{7\wedge}$
35	ΣC_6H_5-$C_2H_{2\text{-}4}$-COOH	1.85	4.41	3.06	1.51	0	0					
36	C_8H_{11}-COOH	0.61	0.79	0.09	0	0	0	‡, §, #, **	$209^{1\bullet 11\wedge}$	$91^{7\wedge}$		
37	C_8H_{13}-COOH (a)	3.76	0.33	2.47	5.44	0	0	§, #, **	$211^{13\wedge}$	167	109	183
38	C_8H_{13}-COOH (b)	0.80	0.99	1.09	0.48	0	0	§, #, **	211	167	109	137
39	ΣC_8H_{13}-COOH	4.56	1.32	3.56	5.92	0	0					
40	C_8H_{15}-COOH	3.86	0.39	0.37	3.72	0	0	‡, §, #, **	$213^{1\bullet}$	111		
41	ΣC_9	10.9	6.9	7.5	11.1	0	0					
42	(36+39+40)·100/41	83	36	54	87	—	—	%1st hydrogenation				
43	(39+40)·100/(36+39+40)	93	68	98	100	—	—	%2nd hydrogenation				
44	40·100/(39+40)	46	23	9	39	—	—	%3rd hydrogenation				
45	**ΣC_3-C_9**	19735	11388	6263	23575	824	414					

Note: The saturated monocarboxylic acids C_6H_{13}-COOH and C_8H_{17}-COOH were not detected.
* identified by mass spectrum and retention time of a purchased reference compound; † identified by mass spectrum and retention time of a synthesized compound; ‡ identified by D and/or ^{13}C labeling (n• signifies n ^{13}C-labels; n^ signifies n D-labels); § identified by mass spectrum analysis; ll identified by its formation from trans-C_4H_5-COOH; ¶ identified by inferred synthetic relationship to C_6H_5-COOH or C_6H_5-$C_2H_{2\text{-}4}$-COOH
# identified by relative retention times and ranges of retention times; ☆ quantified by calibration with authentic compound; ** quantified by calibration with closest saturated n-carboxylic acid; †† quantified by calibration with a regioisomer

Supplementary Table S2: Replicates (b′, b″, b‴) of run b. Single values of each detected C_{3-9} monocarboxylic acid as well as mean values and standard deviations are shown.

run	b´	b´´	b	b´´´		mean	std. dev.	std.dev [%]
end-pH	6.9	6.9	6.7	6.5				
C_3-acids (µM)								
C_2H_3-COOH	4238	3127	5822	5331		4629	1201	26
C_2H_5-COOH	865	586	1069	833		838	198	24
ΣC_3	5102	3714	6891	6164		5468	1381	25
C_5-acids (µM)								
trCH_2=CH-CH=CH-COOH	763	971	1090	1271		1024	213	21
cCH_2=CH-CH=CH-COOH	240	331	386	330		322	60	19
ΣC_4H_5-COOH	1003	1302	1476	1601		1345	259	19
CH_2=CH-CH_2-CH_2-COOH	244	200	346	225		253	64	25
trCH_3-CH=CH-CH_2-COOH	1089	1222	1565	1392		1317	207	16
cCH_3-CH=CH-CH_2-COOH	368	473	535	484		465	70	15
CH_3-CH=CH(CH_3)-COOH	85	108	121	141		114	23	21
trC_2H_5-CH=CH-COOH	43	44	60	51		50	8	16
ΣC_4H_7-COOH	1828	2047	2626	2293		2199	343	16
C_4H_9-COOH	27	22	32	27		27	4	15
ΣC_5	2858	3371	4270	3921		3605	620	17
C_7-acids (µM) (Note)								
trtrH($CH=CH)_3$-COOH	3	4	5	6		5	1	27
C_6H_5-COOH	18	24	25	16		20	4	22
ΣC_6H_{5-7}-COOH	21	28	30	22		25	4	17
C_6H_9-COOH (a)	3	6	4	2		4	2	43
C_6H_9-COOH (b)	14	12	14	20		15	3	21
C_6H_9-COOH (c)	60	64	92	91		77	17	22
C_6H_9-COOH (d)	19	20	38	34		28	9	34
ΣC_6H_9-COOH	97	102	148	146		123	28	23
C_6H_{11}-COOH (a)	8	20	25	27		20	8	42
C_6H_{11}-COOH (b)	7	1	7	8		6	3	55
C_6H_{11}-COOH (c)	5	7	10	13		9	4	42
ΣC_6H_{11}-COOH	16	28	42	48		34	15	43
ΣC_7	134	158	220	217		182	43	24
C_9-acids (µM) (Note)								
C_6H_5-C_2H_4-COOH	3.0	3.0	3.0	4.8		3.5	0.9	26
C_6H_5-C_2H_2-COOH	1.5	1.5	1.4	0.6		1.3	0.4	35
ΣC_6H_5-C_2H_{2-4}-COOH	4.6	4.5	4.4	5.4		4.7	0.5	10
C_8H_{11}-COOH	0.5	0.4	0.8	1.3		0.7	0.4	55
C_8H_{13}-COOH (a)	0.2	0.4	0.3	0.4		0.3	0.1	27
C_8H_{13}-COOH (b)	0.6	0.4	1.0	0.8		0.7	0.3	38
ΣC_8H_{13}-COOH	0.6	0.8	1.3	0.5		0.8	0.4	46
C_8H_{15}-COOH	0.2	0.3	0.4	0.3		0.3	0.1	22
ΣC_9	5.8	4.4	6.9	7.8		6.2	1.5	24
ΣC_{3-9}	**8100**	**7247**	**11388**	**10321**		**9261**	**1917**	**21**

Note: The saturated monocarboxylic acids C_6H_{13}-COOH and C_8H_{17}-COOH were not detected
Identification and quantification was performed as stated in Supplementary Table S1.

Supplementary Table S3: Mol% conversion of acetylene and mol% consumption of CO for production of monocarboxylic acids according to run d:

—The stoichiometric conversion of C_2H_2 into C_n-carboxylic acids (n = 3, 5, 7, 9) is determined as follows: The individual concentrations (µM) are multiplied by $5 \cdot 10^{-3}$ ml (to obtain µmol/5 ml) and by the factor 0.5(n-1) that accounts for the number of C_2H_2 molecules that entered the carbon chain.

—The stoichiometric consumption of CO for formation of C_n-carboxylic acids (n = 3, 5, 7, 9) is determined as follows: The individual concentrations (µM) are multiplied by $5 \cdot 10^{-3}$ ml and by the factor (1 + x), whereby x represents the number of hydrogenated double bonds.

			mol% conversion		mol% consumption		
	[µM]	µmol/5 ml	factor	acetylene	factor	CO	product name
C_2H_3-COOH	6675	33.38	1	1.38	1	1.38	Acrylic acid
C_2H_5-COOH	7391	36.96	1	1.53	2	3.05	Propionic acid
ΣC_3 acids	14066	70.33		2.91		4.43	
ΣC_4H_5-COOH	1463	7.315	2	0.60	1	0.3	Pentadienoic acid
ΣC_4H_7-COOH	7269	36.34	2	3.0	2	3.0	Pentenoic acid
C_4H_9-COOH	363	1.82	2	0.15	3	0.23	Pentanoic acid
ΣC_5 acids	9094	45.47		3.77		3.46	
trtrH$(CH=CH)_3$-COOH	24	0.12	3	0.015	1	0.005	Heptatrienoic acid
C_6H_5-COOH	37	0.19	3	0.024	1	0.008	Benzoic acid
ΣC_6H_9-COOH	246	1.23	3	0.15	2	0.102	Heptadienoic acid
ΣC_6H_{11}-COOH	96	0.48	3	0.06	3	0.06	Heptenoic acid
ΣC_7 acids	403	2.02		0.249		0.175	
C_6H_5-C_2H_4-COOH	0.5	0.0025	4	0.0004	2	0.0002	Hydrocinnamic acid
C_6H_5-C_2H_2-COOH	1.01	0.0051	4	0.0008	1	0.0002	Cinnamic acid
C_8H_{11}-COOH	0	0		0		0	Nonatrienoic acid
ΣC_8H_{13}-COOH	5.9	0.0295	4	0.0049	3	0.0037	Nonadienoic acid
C_8H_{15}-COOH	3.7	0.0185	4	0.0031	4	0.0031	Nonenoic acid
ΣC_9 acids	11.1	0.0555		0.0092		0.0072	
ΣC_3-C_9 acids	**23574**	**118**		**6.94**		**8.07**	

Supplementary Figure S4:
GC-MS chromatogram of run d in comparison to control runs without acetylene and/or without CO are shown; segments for C_3, C_5, C_7 and C_9 acids are shown separately.

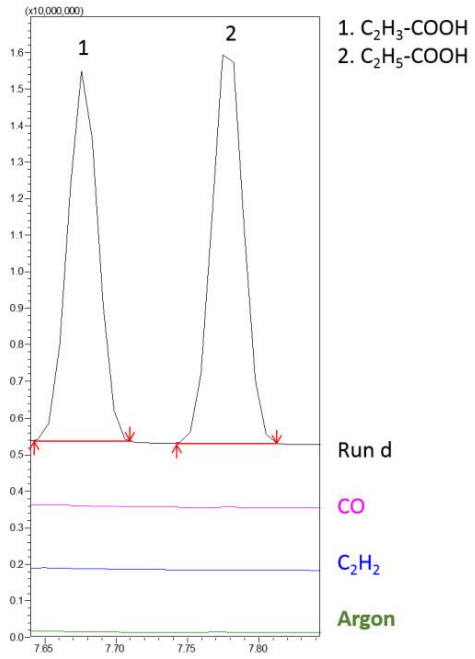

Figure S4a: GC-MS chromatogram of C_3 monocarboxylic acids of run d in comparison to three control runs.
Control runs were carried out identical to run d containing only 120 ml CO (pink) or 120 ml acetylene (blue) or only 120 ml argon (green). After 7 days at 105°C products were identified by GC-MS as *tert*-butyldimethylsilyl derivatives with GC-MS program 1 (0-6 min at 60 °C; 6-25 min at 60-280 °C, 10 °C/min; 25-28 min at 280 °C; injector temperature: 260 °C) .

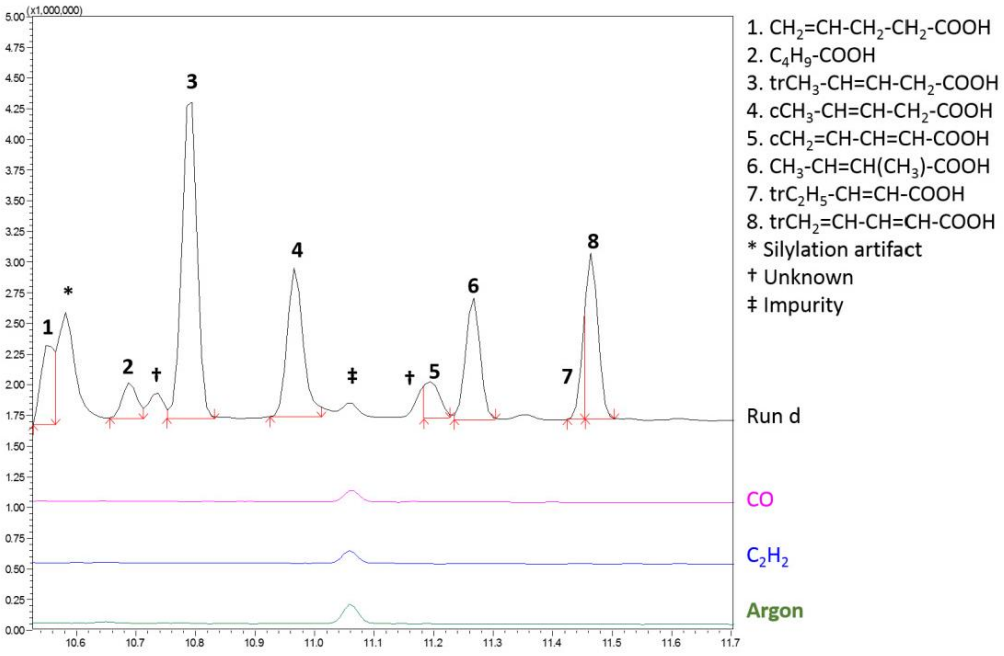

Figure S4 b: GC-MS chromatogram of C_5 monocarboxylic acids of run d in comparison to three control runs.
Control runs were carried out identical to run d containing only 120 ml CO (pink) or 120 ml acetylene (blue) or only 120 ml argon (green). After 7 days at 105°C products were identified by GC-MS as *tert*-butyldimethylsilyl derivatives with GC-MS program 1 (0-6 min at 60 °C; 6-25 min at 60-280 °C, 10 °C/min; 25-28 min at 280 °C; injector temperature: 260 °C) .

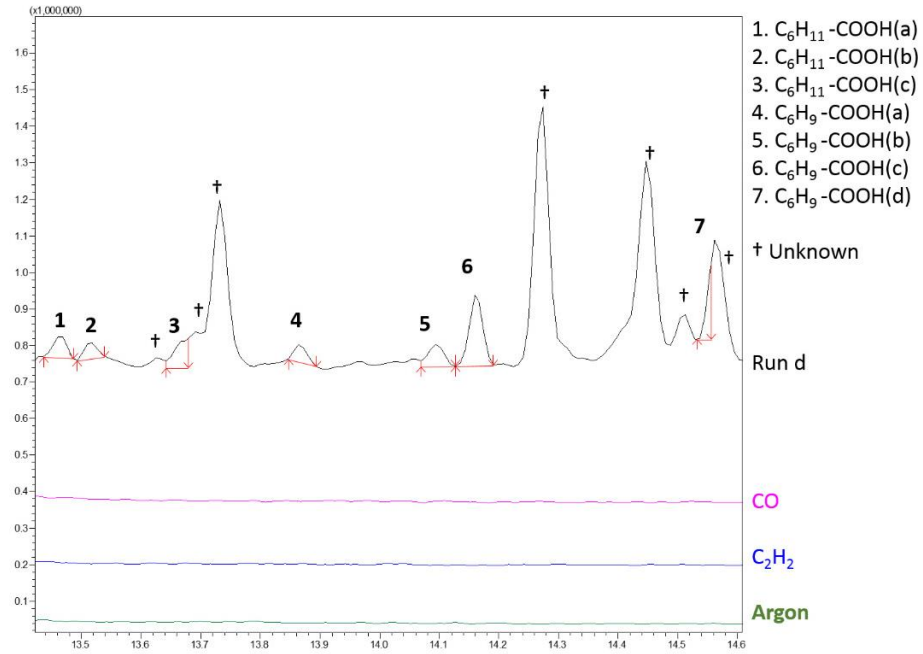

Figure S4 c: GC-MS chromatogram of C_7 monocarboxylic acids of run d in comparison to three control runs.
Control runs were carried out identical to run d containing only 120 ml CO (pink) or 120 ml acetylene (blue) or only 120 ml argon (green). After 7 days at 105°C products were identified by GC-MS as *tert*-butyldimethylsilyl derivatives with GC-MS program 1 (0-6 min at 60 °C; 6-25 min at 60-280 °C, 10 °C/min; 25-28 min at 280 °C; injector temperature: 260 °C).

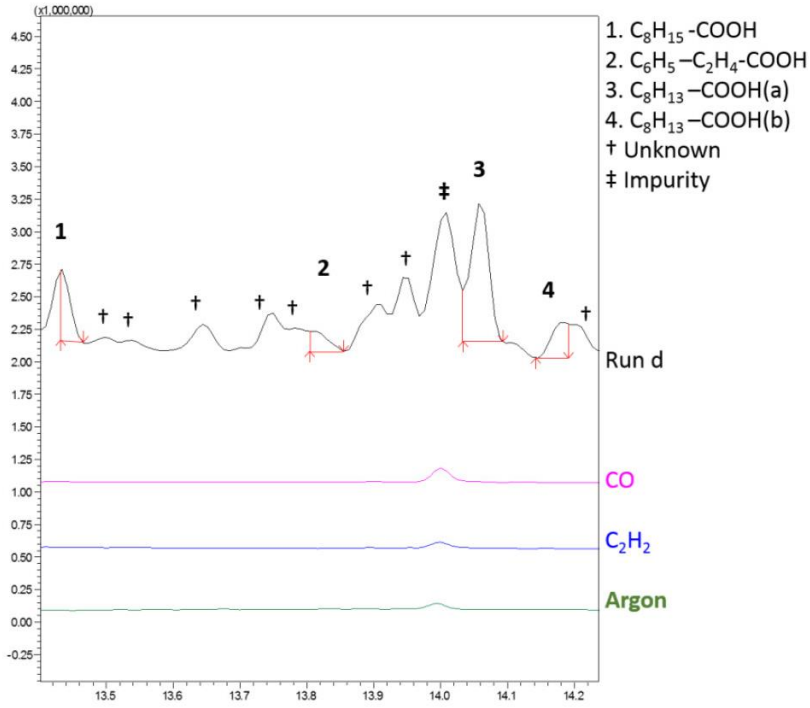

Figure S4 d: GC-MS chromatogram of C_9 monocarboxylic acids of run d in comparison to three control runs.
Control runs were carried out identical to run d containing only 120 ml CO (pink) or 120 ml acetylene (blue) or only 120 ml argon (green). After 7 days at 105°C products were identified by GC-MS as *tert*-butyldimethylsilyl derivatives with GC-MS program 2 (0-6 min at 90 °C; 6-25 min at 90-280 °C, 10 °C/min; 25-28 min at 280 °C).

7.2 Supplementary Material: One-pot Formation of 2,4-di- or 2,4,6-tri-olefinic Monocarboxylic Acids by straight Chain C4-Extension

Supplementary data

One-Pot Formation of 2,4-Di- or 2,4,6-Tri-olefinic Monocarboxylic Acids by Straight Chain C4-Extension

Jessica Sobotta[1], Maximilian Schmalhofer[1], Thomas M. Steiner[1], Wolfgang Eisenreich[1], Günter Wächtershäuser[2], Claudia Huber[1,*]

[1]Lehrstuhl für Biochemie, Technische Universität München, Lichtenbergstraße 4, D85747 Garching Germany.

[2]2209 Mill Race Drive, Chapel Hill, NC 27514, USA

Tables of Contents

1. MS and NMR Data of Compounds 3a-3f

1.1. (2*E*,4*E*)-Hepta-2,4,6-trienoic Acid (3a)

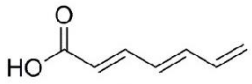

3a

MS (EI, 70 eV): m/z (%) = 181 (100) [(M-C_4H_9)$^+$], 137 (24) [(M-C_4H_9OSi)$^+$], 107 (27) [(M-$C_6H_{15}OSi$)$^+$], 79 (61) [(M-$C_7H_{15}O_2Si$)$^+$], 75 (100) [(TMS-OH)$^+$] ^{1}H NMR (500 MHz, DMSO-d_6) δ 7.19 (dd, *J* = 15.2, 11.3 Hz, 1H, H-3), 6.68 (dd, *J* = 15.0, 10.7 Hz, 1H, H-5), 6.57 – 6.41 (m, 2H, H-4, H-6), 5.92 (d, *J* = 15.3 Hz, 1H, H-2), 5.45 (d, *J* = 17.7 Hz, 1H, H-7Z), 5.33 (d, *J* = 9.9 Hz, 1H, H-7E). ^{13}C NMR (126 MHz, DMSO-d_6) δ 167.59 (C-1), 143.49 (C-3), 140.40 (C-5), 136.51 (C-4), 130.87 (C-6), 123.04 (C-2), 121.76 (C-7).

1.2. (2*E*,4*E*,6*E*)-Octa-2,4,6-trienoic Acid (3b)

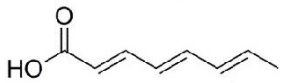

3b

MS (EI, 70 eV): m/z (%) = 195 (61) [(M-C_4H_9)$^+$], 151 (26) [(M-C_4H_9OSi)$^+$], 121 (76) [(M-$C_6H_{15}OSi$)$^+$], 93 (45) [(M-$C_7H_{15}O_2Si$)$^+$], 75 (100) [(TMS-OH)$^+$] ^{1}H NMR (500 MHz, Methanol-d_4) δ 7.30 (dd, *J* = 15.2, 11.3 Hz, 1H, H-3), 6.60 (dd, *J* = 14.9, 10.6 Hz, 1H, H-5), 6.30 – 6.12 (m, 2H, H-4, H-6), 6.06 – 5.96 (m, 1H, H-7), 5.84 (d, *J* = 15.2 Hz, 1H, H-2), 1.84 (dd, *J* = 7.0, 1.6 Hz, 3H, H-8). ^{13}C NMR (126 MHz, Methanol-d_4) δ 170.70 (C-1), 146.83 (C-5), 142.61 (C-7), 136.10 (C-6), 132.54 (C-3), 128.76 (C-4), 121.02 (C-2), 18.63 (C-8).

1.3.(2*E*,4*E*)-Octa-2,4-dienoic Acid (3c)

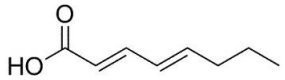

3c

MS (EI, 70 eV): m/z (%) = 197 (71) [(M-C_4H_9)$^+$], 153 (32) [(M-C_4H_9OSi)$^+$], 123 (20) [(M-$C_6H_{15}OSi$)$^+$], 95 (20) [(M-$C_7H_{15}O_2Si$)$^+$], 75 (100) [(TMS-OH)$^+$] ^{1}H NMR (500 MHz, Chloroform-*d*) δ 7.34 (dd, *J* = 15.3, 10.1 Hz, 1H, H-3), 6.22 – 6.16 (m, 2H, H-4, H-5), 5.78 (d, *J* = 15.4 Hz, 1H, H-2), 2.16 (td, *J* = 7.3, 5.5 Hz, 2H, H-6), 1.47 (h, *J* = 7.5 Hz, 2H, H-7), 0.92 (t, *J* = 7.4 Hz, 3H, H-8). ^{13}C NMR (126 MHz, Chloroform-*d*) δ 172.53 (C-1), 147.76 (C-3), 146.28 (C-5), 128.49 (C-4), 118.26 (C-2), 35.22 (C-6), 21.99 (C-7), 13.83 (C-8).

1.4. (2*E*,4*E*,8*Z*)-Undeca-2,4,8-trienoic acid (3d)

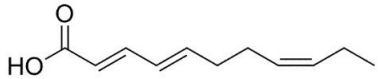

3d

MS (EI, 70 eV): m/z (%) = 237 (49) [(M-C_4H_9)$^+$], 193 (5) [(M-C_4H_9OSi)$^+$], 168 (58) [(M-C_4H_9-C_5H_9)$^+$], 109 (43) [(M-C_4H_9-$C_5H_8O_2Si$)$^+$], 75 (100) [(TMS-OH)$^+$] ^{1}H NMR (500 MHz, Methanol-d_4) δ 7.16 (dd, *J* = 15.3, 10.6 Hz, 1H, H-3), 6.19 (ddt, *J* = 15.2, 10.6, 1.0 Hz, 1H, H-4), 6.14 – 6.04 (m, 1H, H-5), 5.73 (d, *J* = 15.3 Hz, 1H, H-2), 5.38 – 5.31 (m, 1H, H-9), 5.28 (dddt, *J* = 10.7, 7.0, 5.5, 1.7 Hz, 1H, H-8), 2.21 – 2.10 (m, 4H, H-7, H-6), 2.04 – 1.96 (m, 2H, H-10), 0.90 (t, *J* = 7.5 Hz, 3H, H-11). ^{13}C NMR (126 MHz, Methanol-d_4) δ 170.99 (C-1), 146.57 (C-3), 144.94 (C-5), 133.40 (C-9), 129.98 (C-4), 128.78 (C-8), 120.93 (C-2), 34.09 (C-7), 27.36 (C-6), 21.47 (C-10), 14.67 (C-11).

1.5. (2*E*,4*E*,8*Z*)-Tetradeca-2,4,8-trienoic acid (3e)

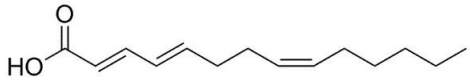

3e

MS (EI, 70 eV): m/z (%) = 279 (58) [(M-C_4H_9)$^+$], 168 (58) [(M-C_4H_9-C_8H_{15})$^+$], 129 (52) [(M-C_4H_9-$C_{11}H_{19}$)$^+$], 109 (42), 75 (100) [(TMS-OH)$^+$] ^{1}H NMR (500 MHz, Chloroform-*d*) δ 7.34 (dd, *J* = 15.2, 10.0 Hz, 1H, H-3), 6.28 – 6.10 (m, 2H, H-4, H-5), 5.79 (d, *J* = 15.4 Hz, 1H, H-2), 5.50 – 5.38 (m, 1H, H-9), 5.37 – 5.26 (m, 1H, H-8), 2.25 (q, *J* = 6.2 Hz, 2H, H-6), 2.21 – 2.14 (m, 2H, H-7), 2.07 – 1.96 (m, 2H, H-10), 1.38 – 1.31 (m, 2H, H-11), 1.31 – 1.23 (m, 4H, H-12, H-13), 0.89 (t, *J* = 7.0 Hz, 3H, H-14). ^{13}C NMR (126 MHz, Chloroform-*d*) δ 172.71 (C-

1), 147.67 (C-3), 145.71 (C-5), 131.36 (C-9), 128.64 (C-4), 128.09 (C-8), 118.48 (C-2), 33.27 (C-6), 31.66 (C-12), 29.46 (C-11), 27.39 (C-10), 26.45 (C-7), 22.72 (C-13), 14.23 (C-14).

1.6. (2*E*,4*E*,12*Z*)-Pentadeca-2,4,12-trienoic acid (3f)

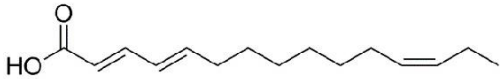

3f

MS (EI, 70 eV): m/z (%) = 293 (91) [(M-C_4H_9)$^+$], 181 (9) [(M-C_4H_9-C_8H_{15})$^+$], 155 (17) [(M-C_4H_9-$C_{10}H_{19}$)$^+$], 81 (62), 75 (100) [(TMS-OH)$^+$] ^{1}H NMR (500 MHz, Chloroform-*d*) δ 7.34 (dd, *J* = 15.3, 10.2 Hz, 1H, H-3), 6.22 – 6.17 (m, 2H, H-4, H-5), 5.78 (d, *J* = 15.3 Hz, 1H, H-2), 5.38 – 5.29 (m, 2H, H-13, H-12), 2.21 – 2.14 (m, 2H, H-6), 2.02 (ddd, *J* = 6.7, 2.5, 1.5 Hz, 4H, H-11, H-14), 1.46 – 1.40 (m, 1H, H-7), 1.36 – 1.28 (m, 6H, H-8, H-9, H-10), 0.95 (t, *J* = 7.5 Hz, 3H, H-15). ^{13}C NMR (126 MHz, Chloroform-*d*) δ 173.02 (C-1), 147.94 (C-3), 146.67 (C-5), 131.91 (C-13), 129.39 (C-4), 128.45 (C-12), 118.36 (C-2), 33.32 (C-6), 29.88 (C-10), 29.32 (C-9), 29.27 (C-8), 28.84 (C-7), 27.28 (C-11), 20.78 (C-14), 14.66 (C-15).

2. One and two-dimensional NMR-Spectra for Compounds 3a-3f

2.1. ^{1}H NMR of (2*E*,4*E*)-Hepta-2,4,6-trienoic Acid (3a)

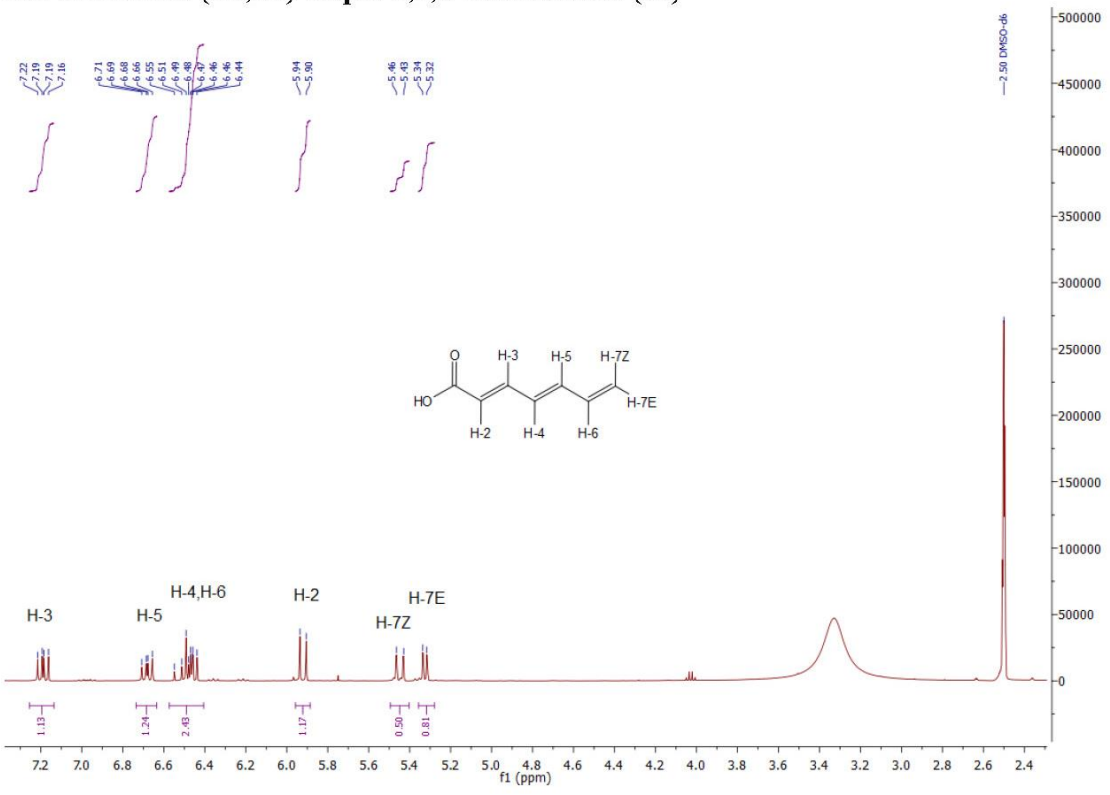

2.2.COSY of (2*E*,4*E*)-Hepta-2,4,6-trienoic Acid (3a)

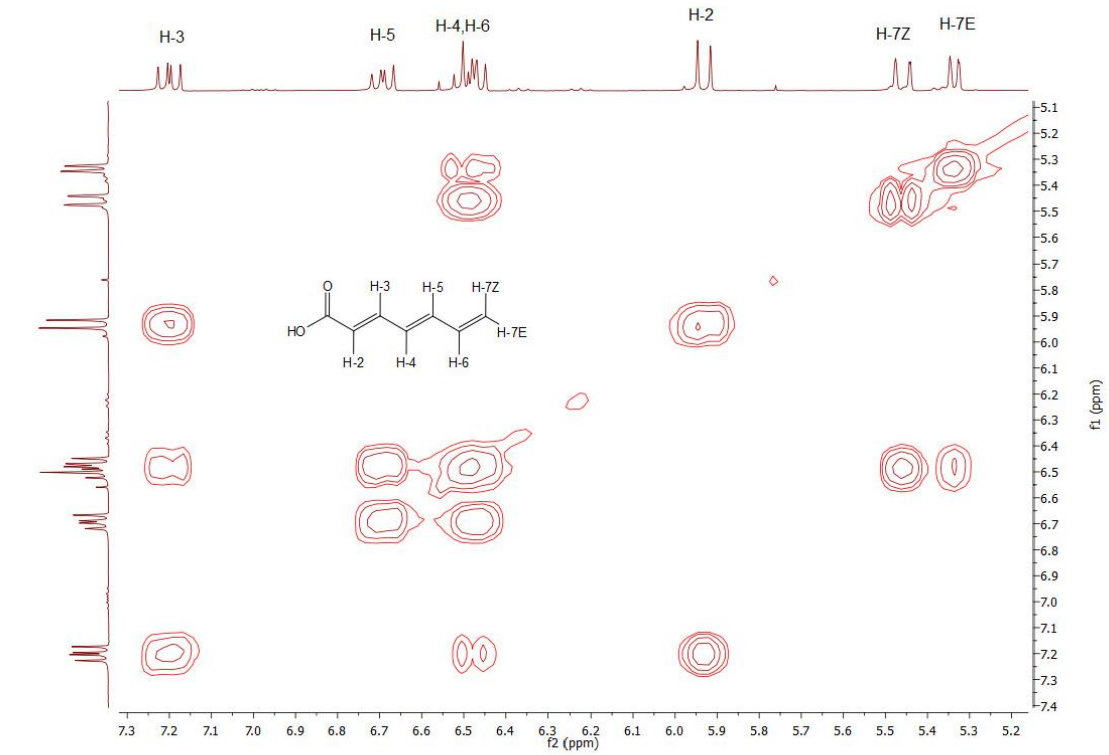

2.3.^{13}C NMR of (2*E*,4*E*)-Hepta-2,4,6-trienoic Acid (3a)

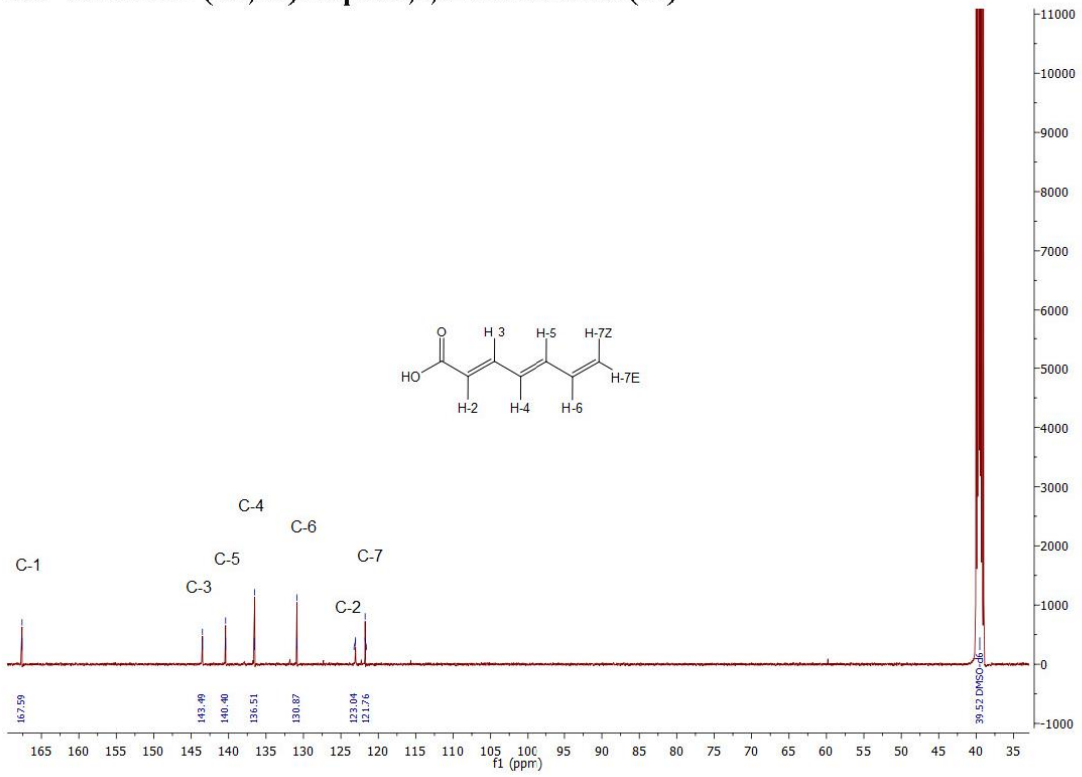

2.4.HSQCED of (2*E*,4*E*)-Hepta-2,4,6-trienoic Acid (3a)

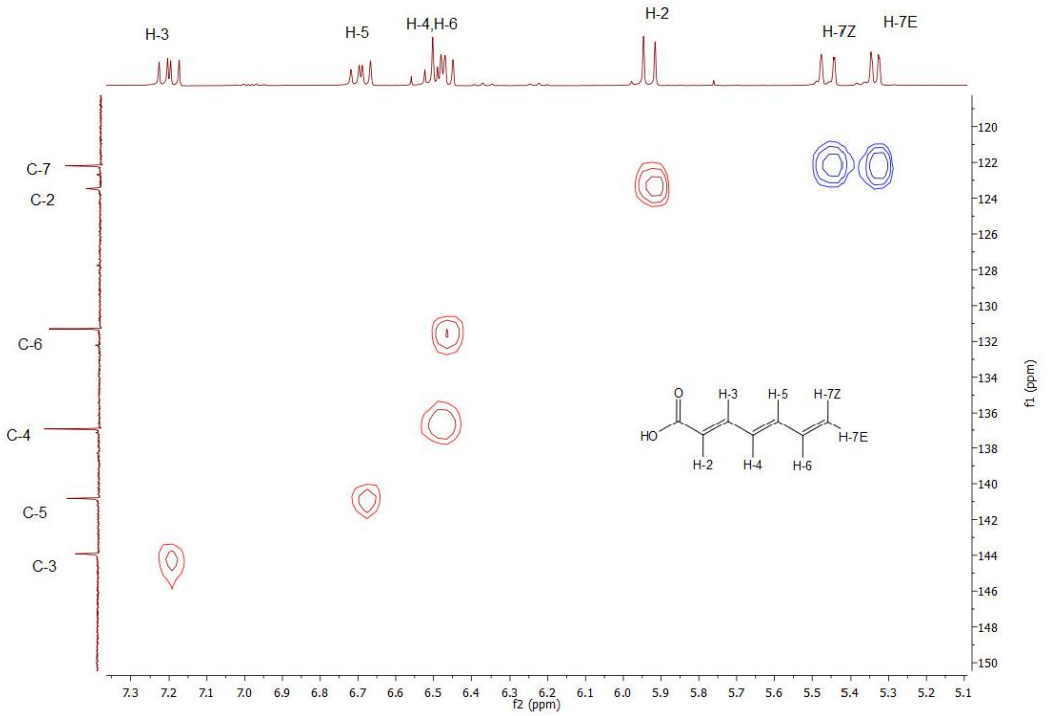

2.5.^{1}H NMR of (2*E*,4*E*,6*E*)-Octa-2,4,6-trienoic Acid (3b)

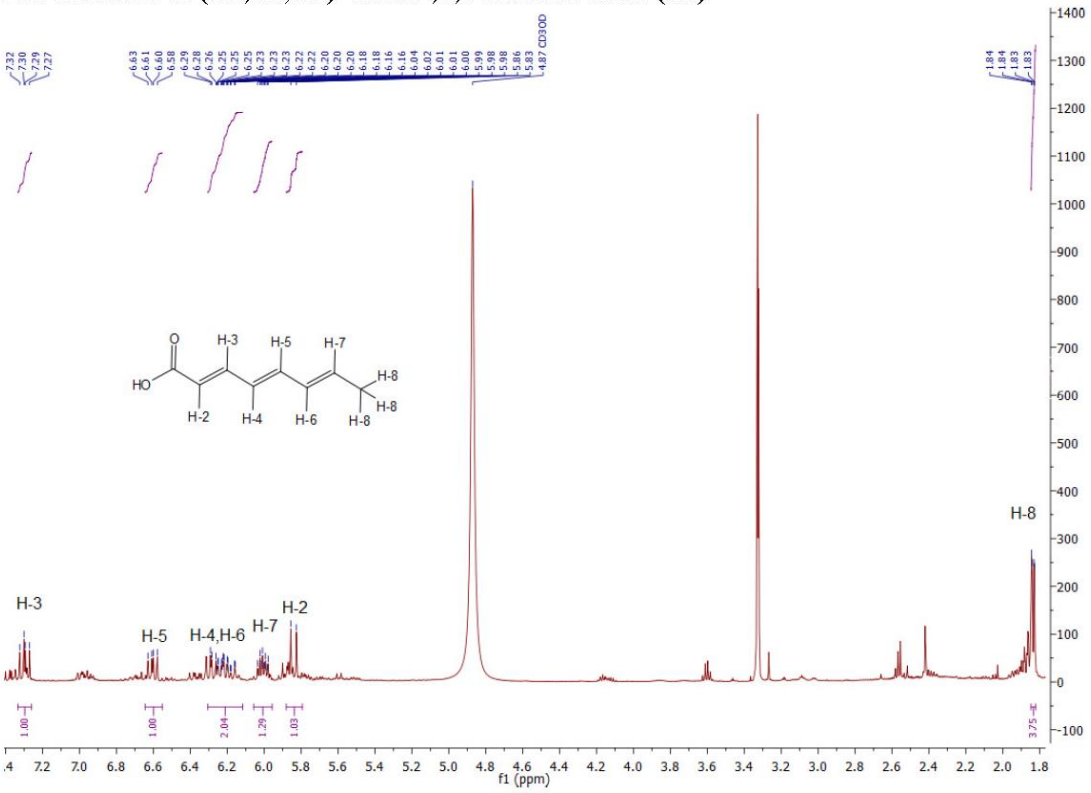

2.6. COSY of (2*E*,4*E*,6*E*)-Octa-2,4,6-trienoic Acid (3b)

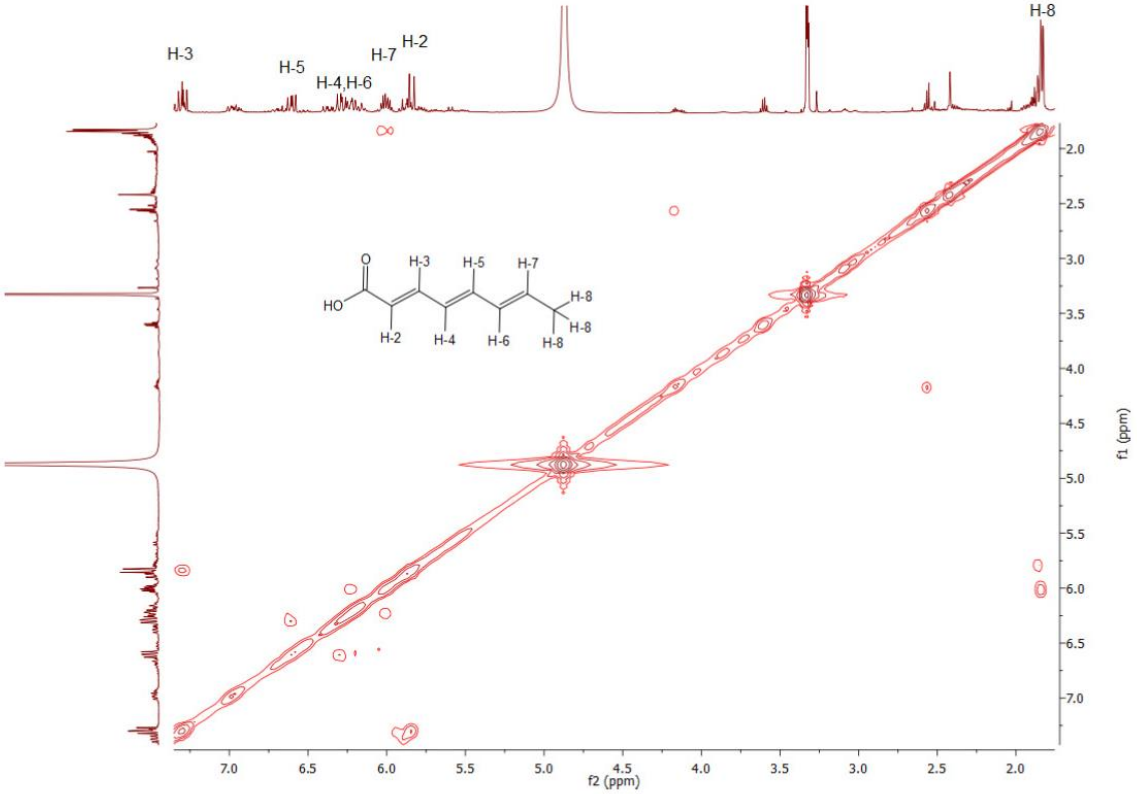

2.7. ^{13}C NMR of (2*E*,4*E*,6*E*)-Octa-2,4,6-trienoic Acid (3b)

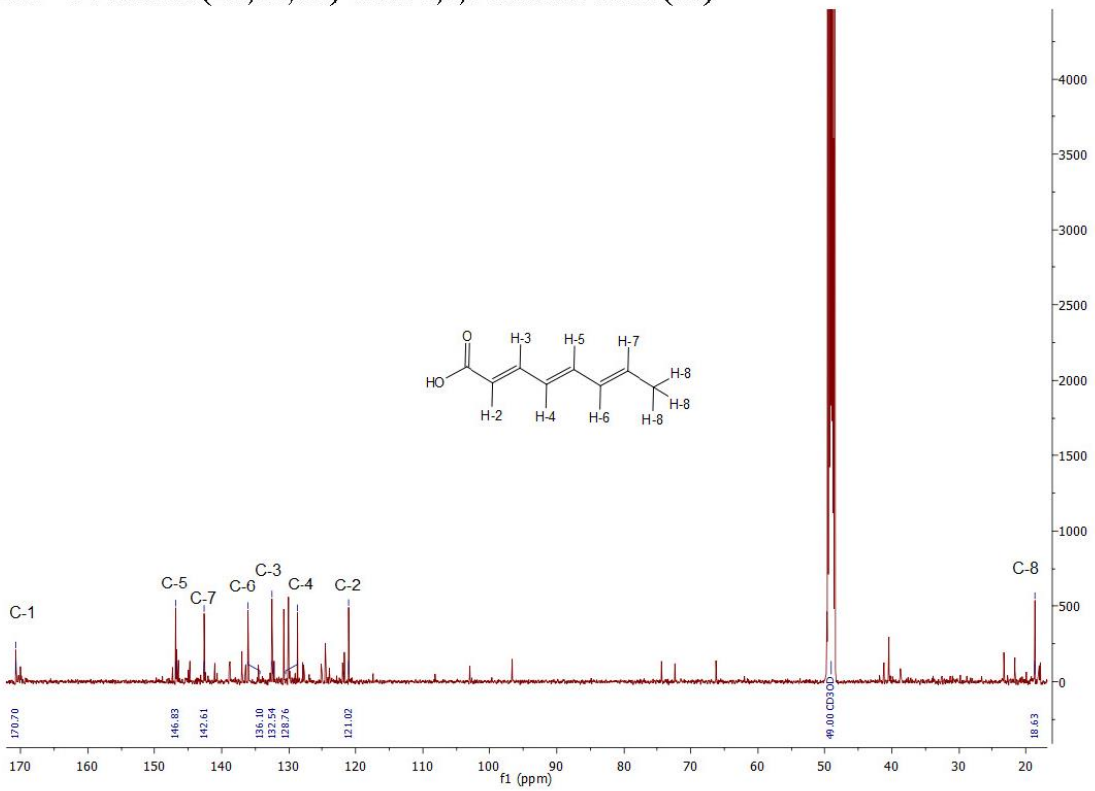

2.8. HSQCED of (2*E*,4*E*,6*E*)-Octa-2,4,6-trienoic Acid (3b)

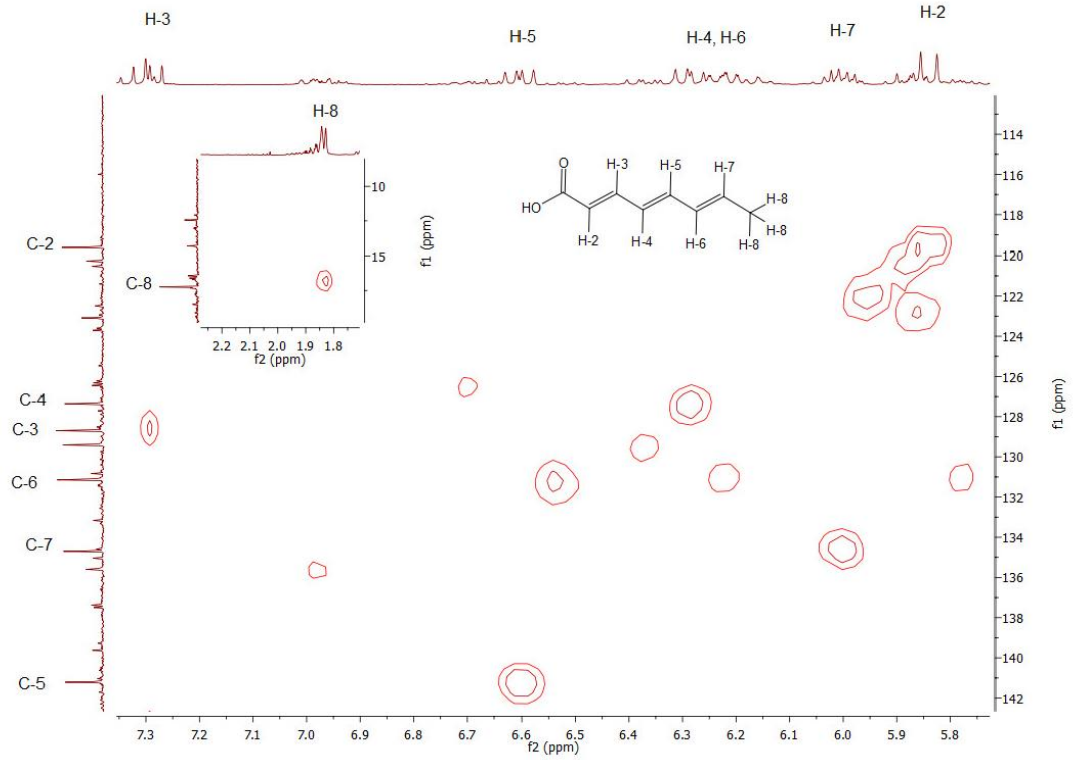

2.9. ^{1}H NMR of (2*E*,4*E*)-Octa-2,4-dienoic Acid (3c)

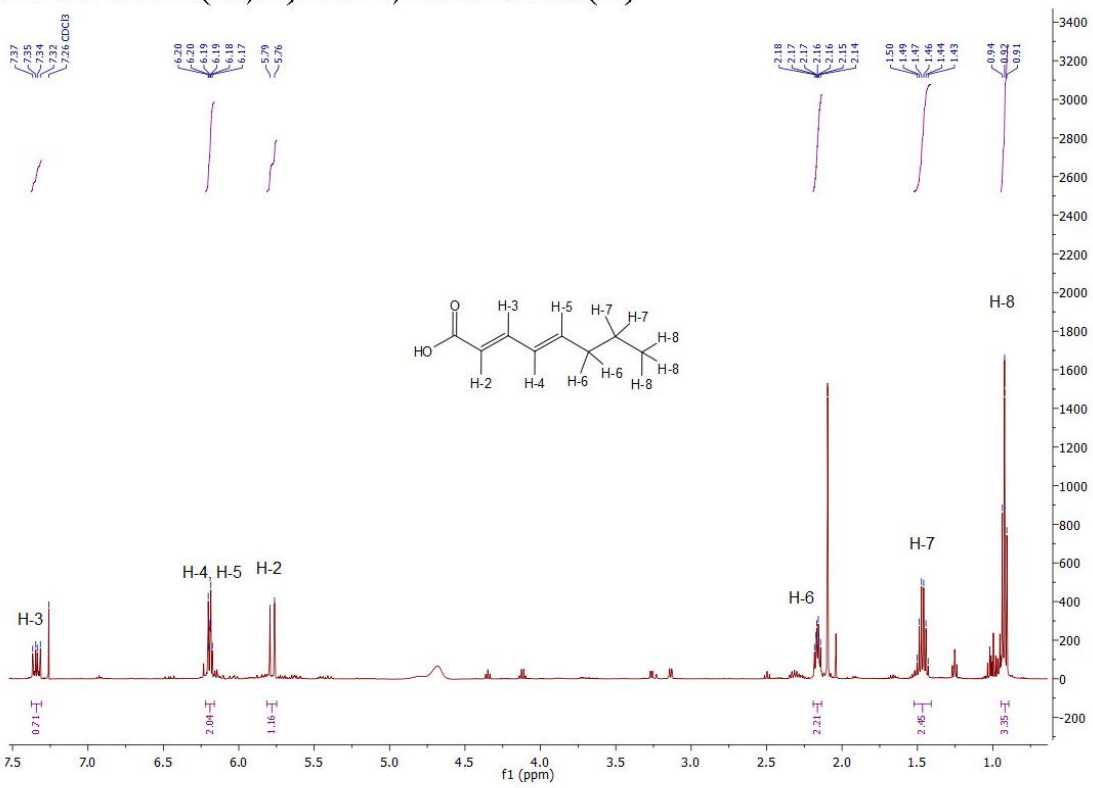

2.10. COSY of (2*E*,4*E*)-Octa-2,4-dienoic Acid (3c)

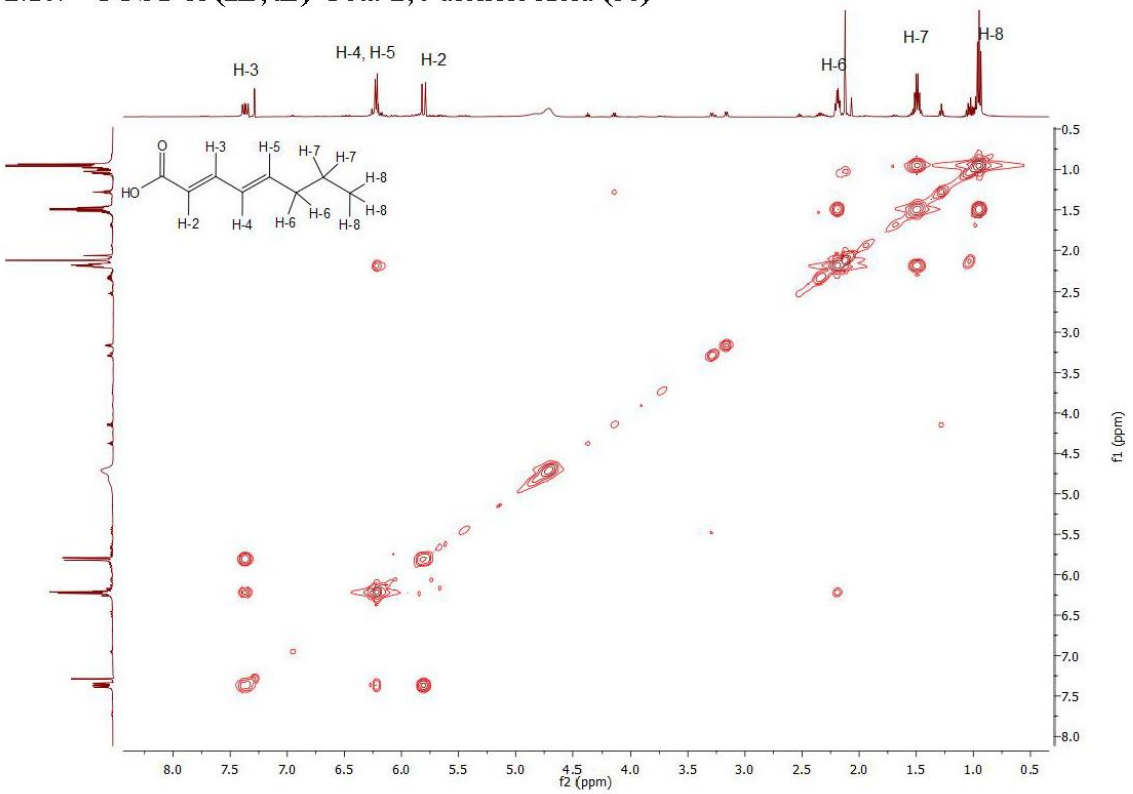

2.11. ^{13}C NMR of (2*E*,4*E*)-Octa-2,4-dienoic Acid (3c)

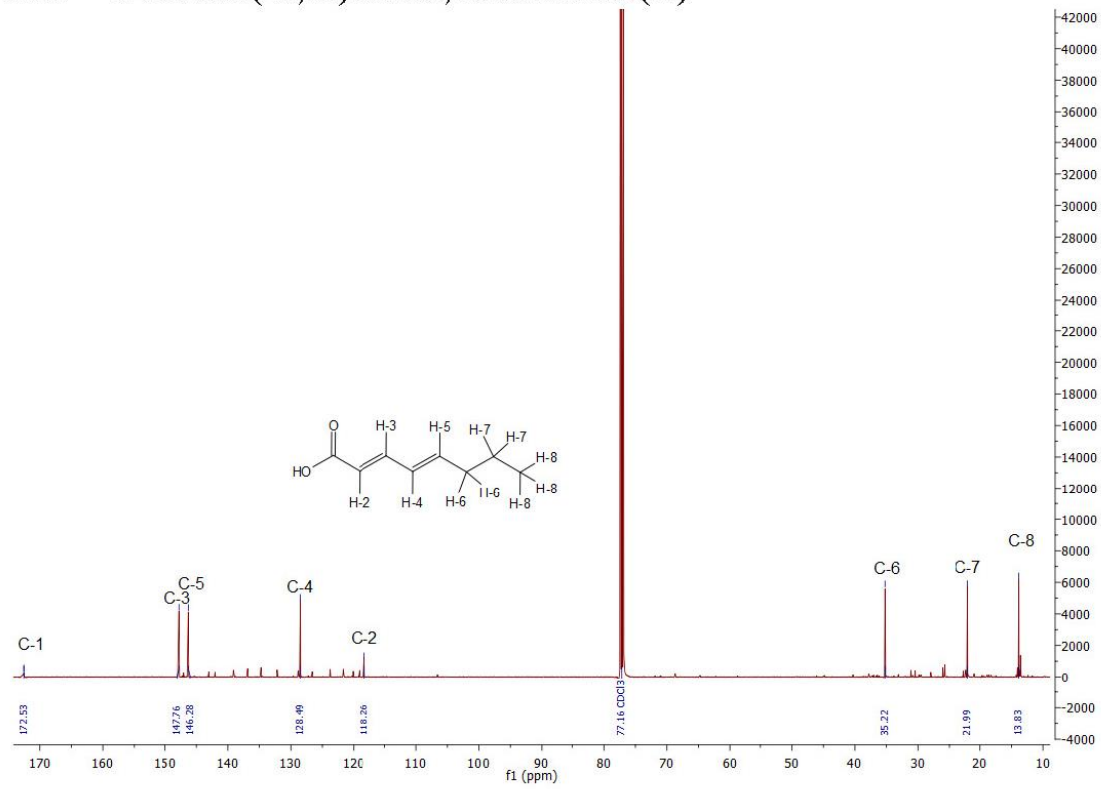

2.12. HSQCED of (2*E*,4*E*)-Octa-2,4-dienoic Acid (3c)

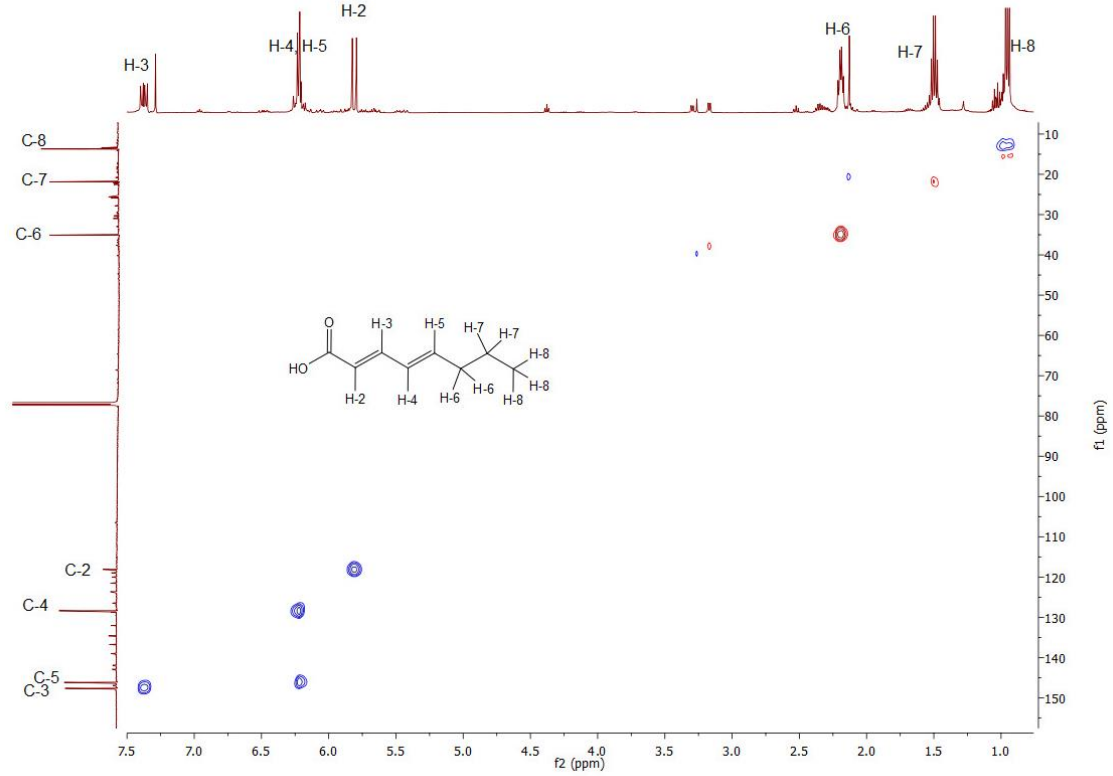

2.13. ^{1}H NMR of (2*E*,4*E*,8*Z*)-Undeca-2,4,8-trienoic acid (3d)

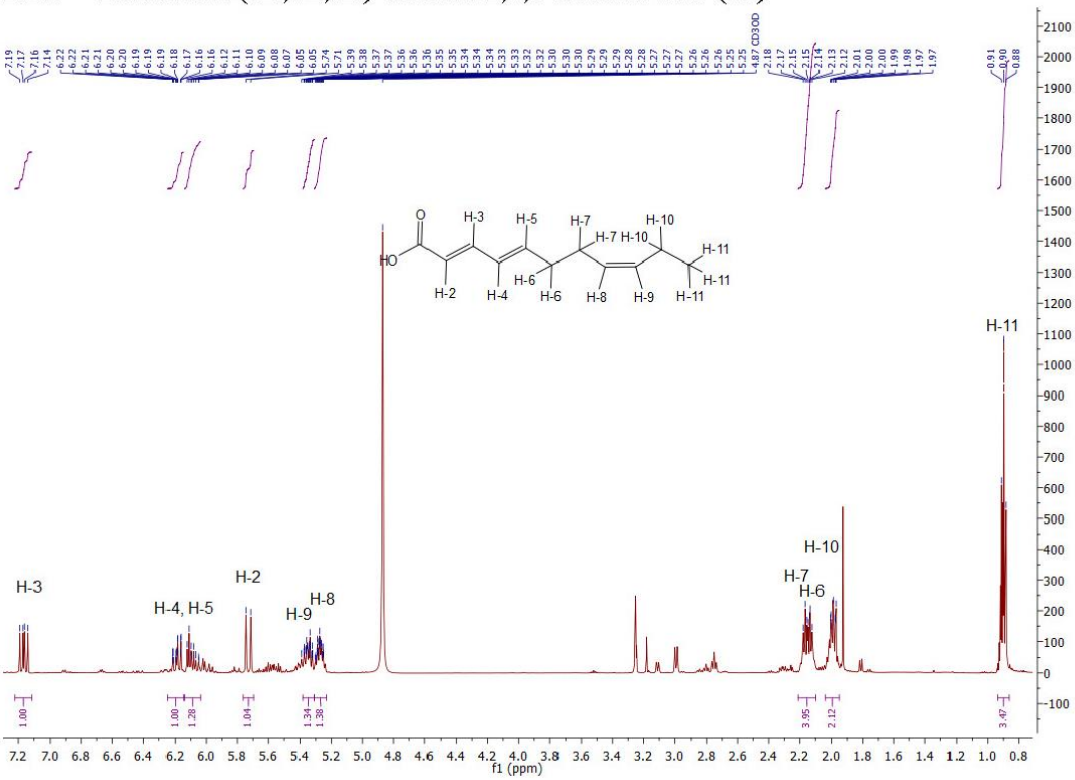

2.14. COSY of (2*E*,4*E*,8*Z*)-Undeca-2,4,8-trienoic acid (3d)

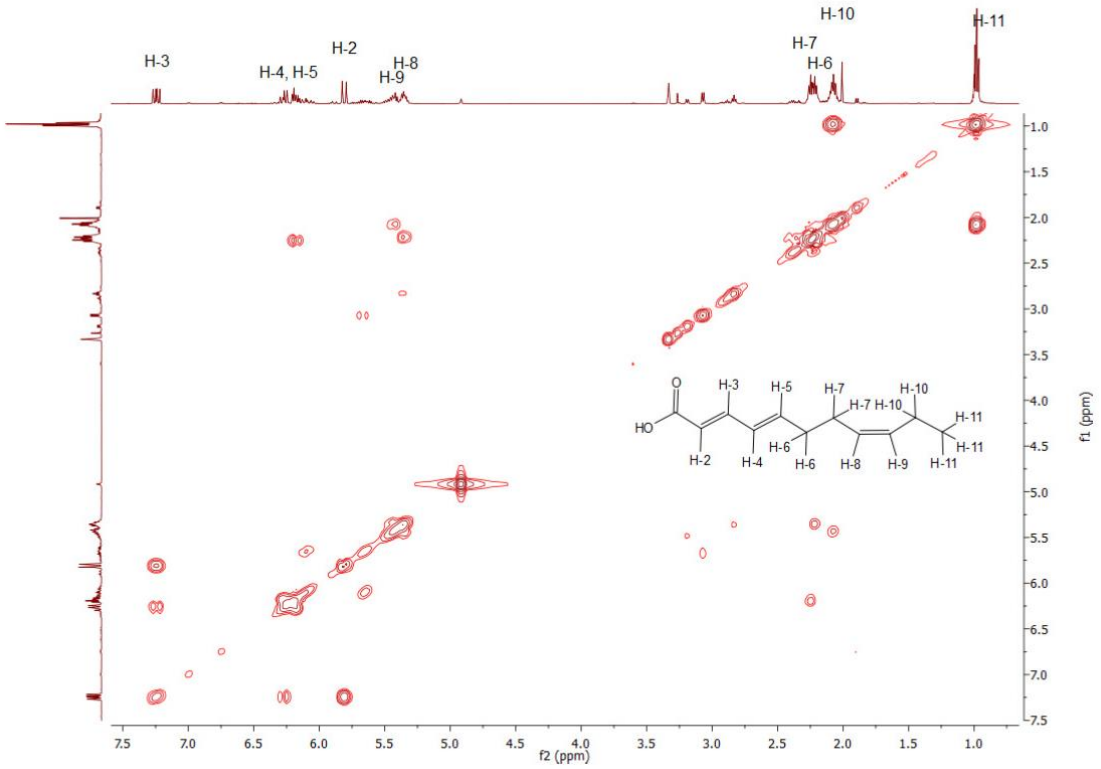

2.15. ^{13}C NMR of (2*E*,4*E*,8*Z*)-Undeca-2,4,8-trienoic acid (3d)

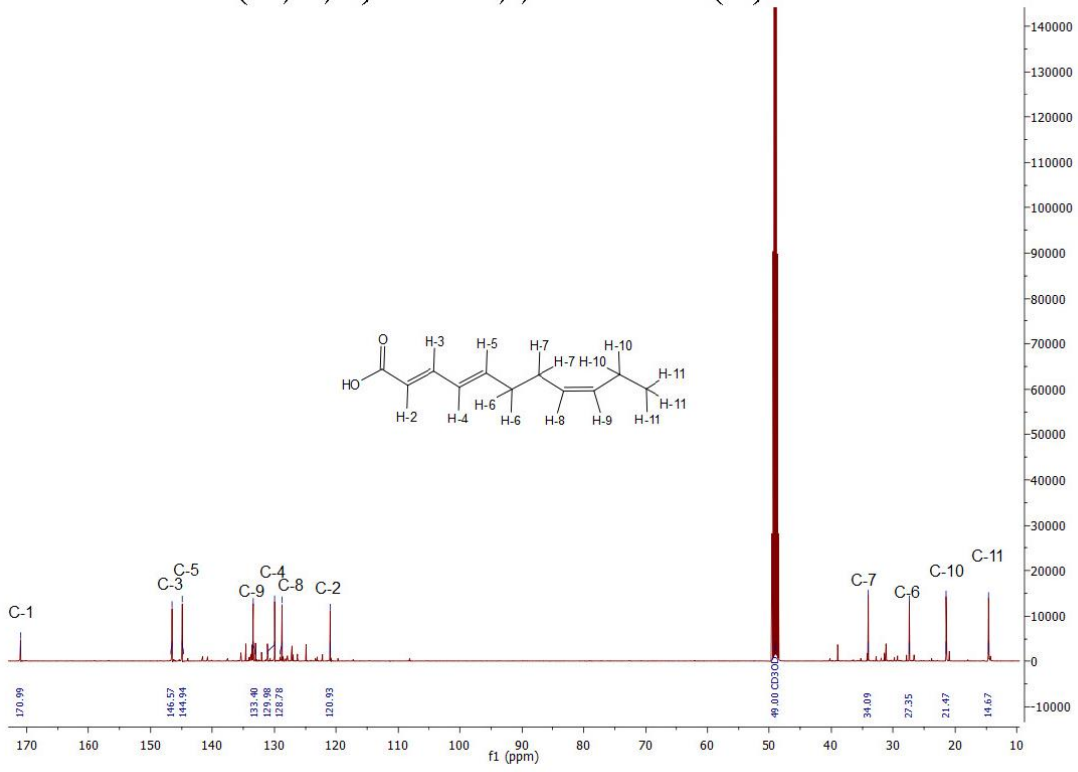

2.16. HSQCED of (2*E*,4*E*,8*Z*)-Undeca-2,4,8-trienoic acid (3d)

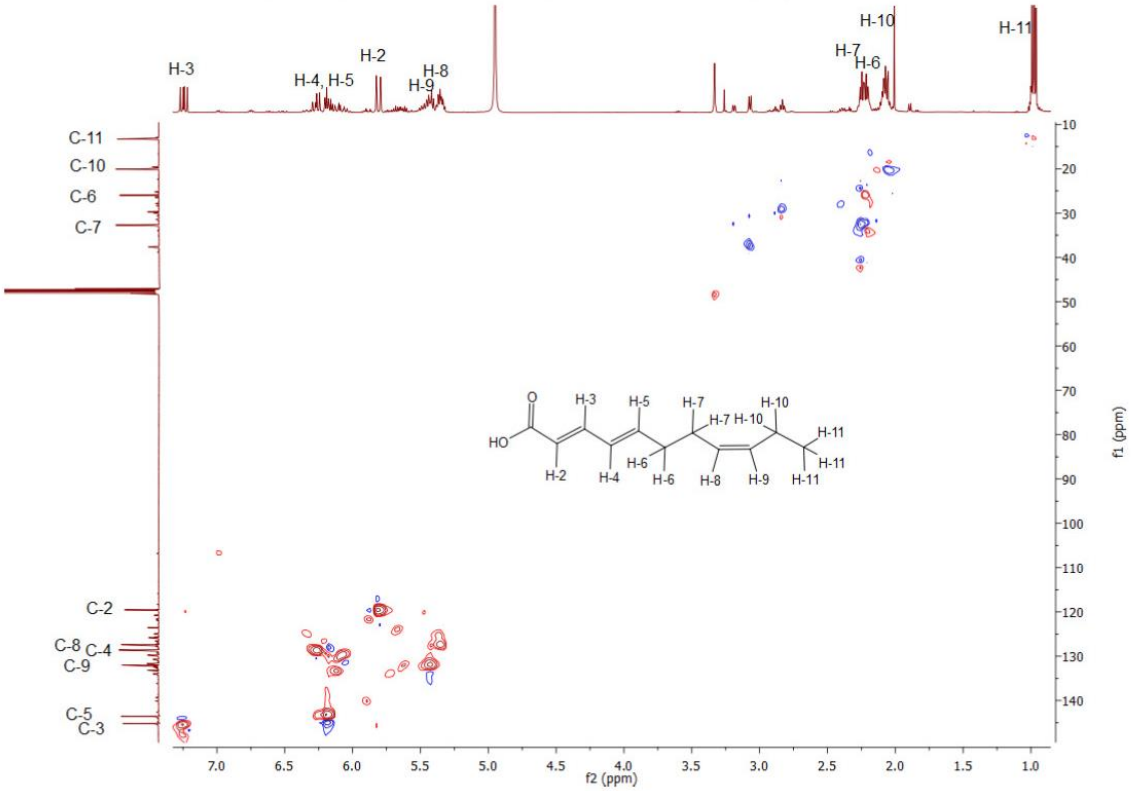

2.17. ^{1}H NMR of (2*E*,4*E*,8*Z*)-Tetradeca-2,4,8-trienoic acid (3e)

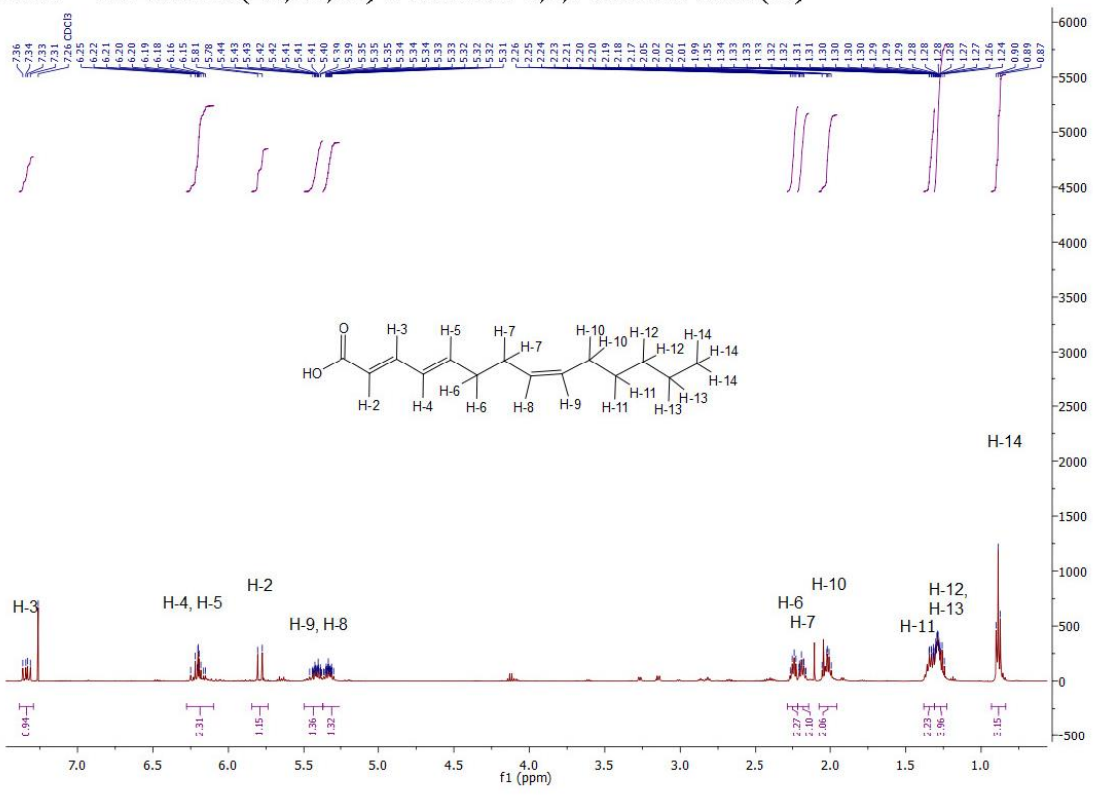

2.18. COSY of (2*E*,4*E*,8*Z*)-Tetradeca-2,4,8-trienoic acid (3e)

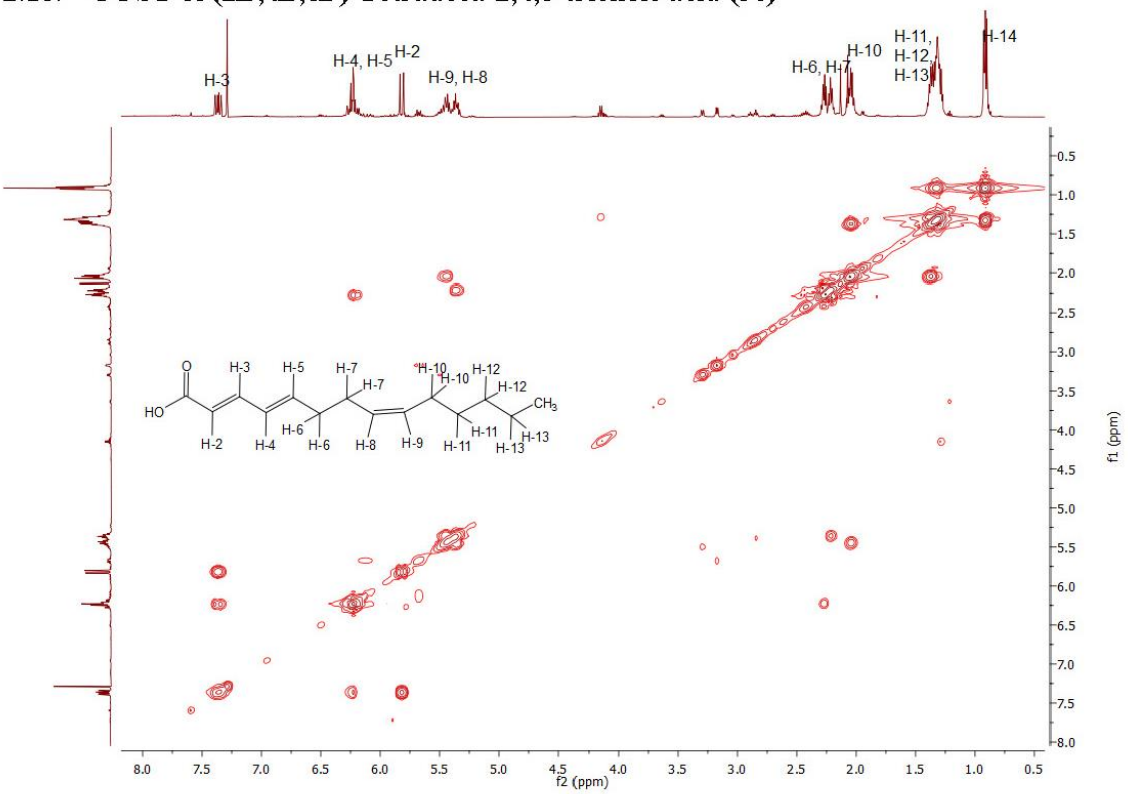

2.19. ^{13}C NMR of (2*E*,4*E*,8*Z*)-Tetradeca-2,4,8-trienoic acid (3e)

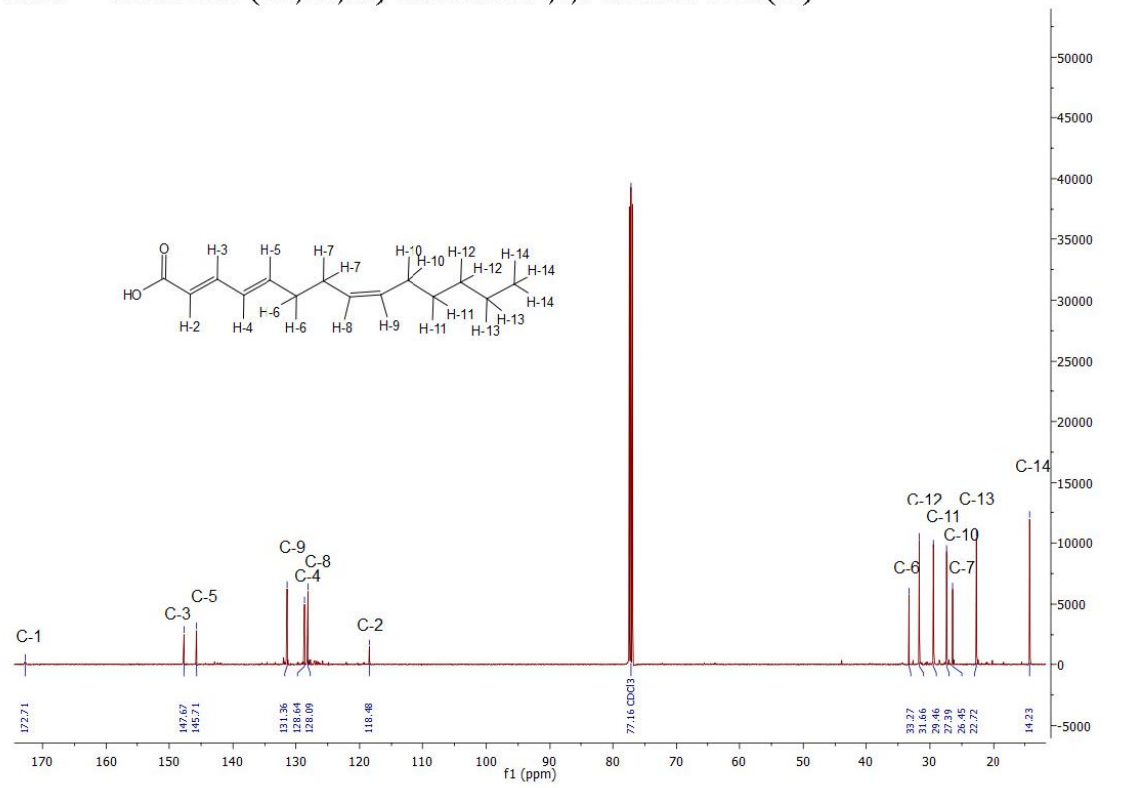

2.20. HSQCED of (2*E*,4*E*,8*Z*)-Tetradeca-2,4,8-trienoic acid (3e)

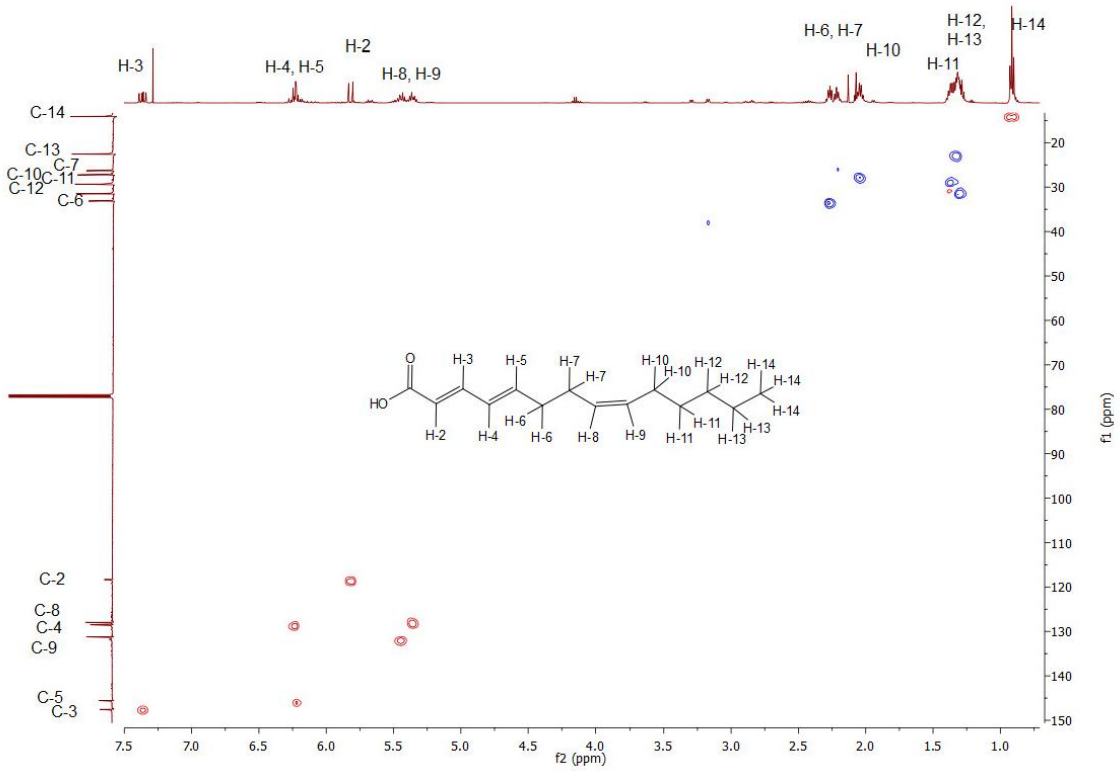

2.21. HMBC of (2*E*,4*E*,8*Z*)-Tetradeca-2,4,8-trienoic acid (3e)

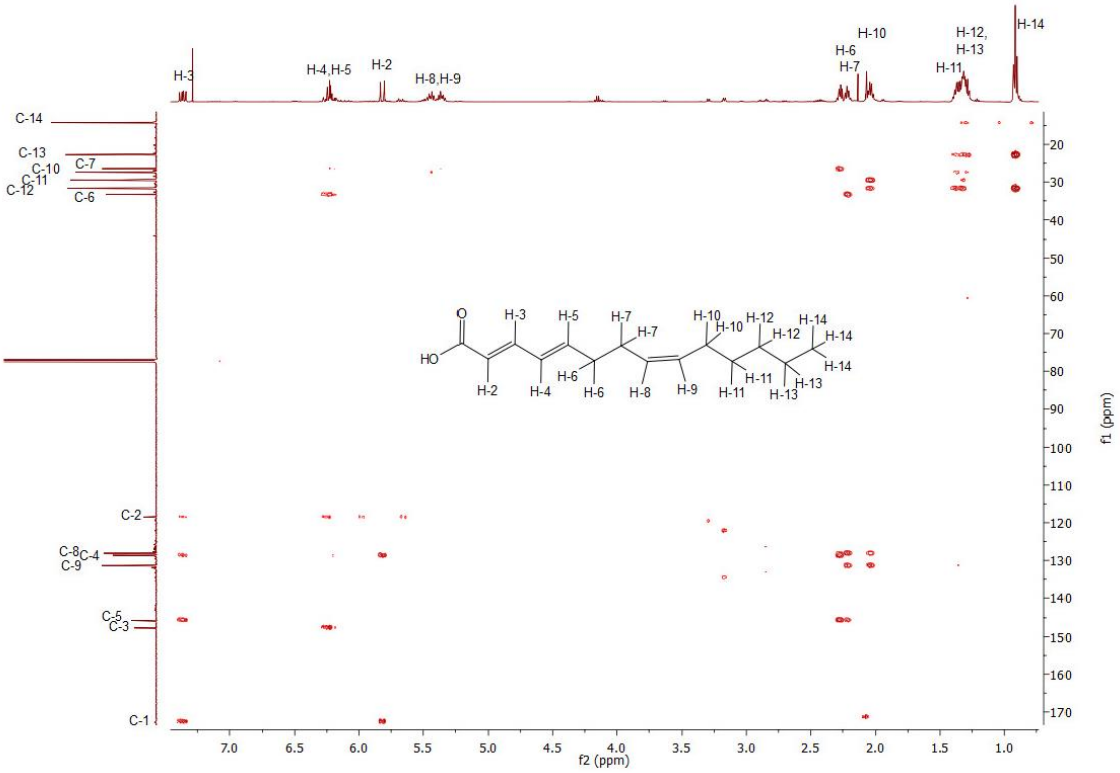

2.22. ^{1}H NMR of (2*E*,4*E*,12*Z*)-Pentadeca-2,4,12-trienoic acid (3f)

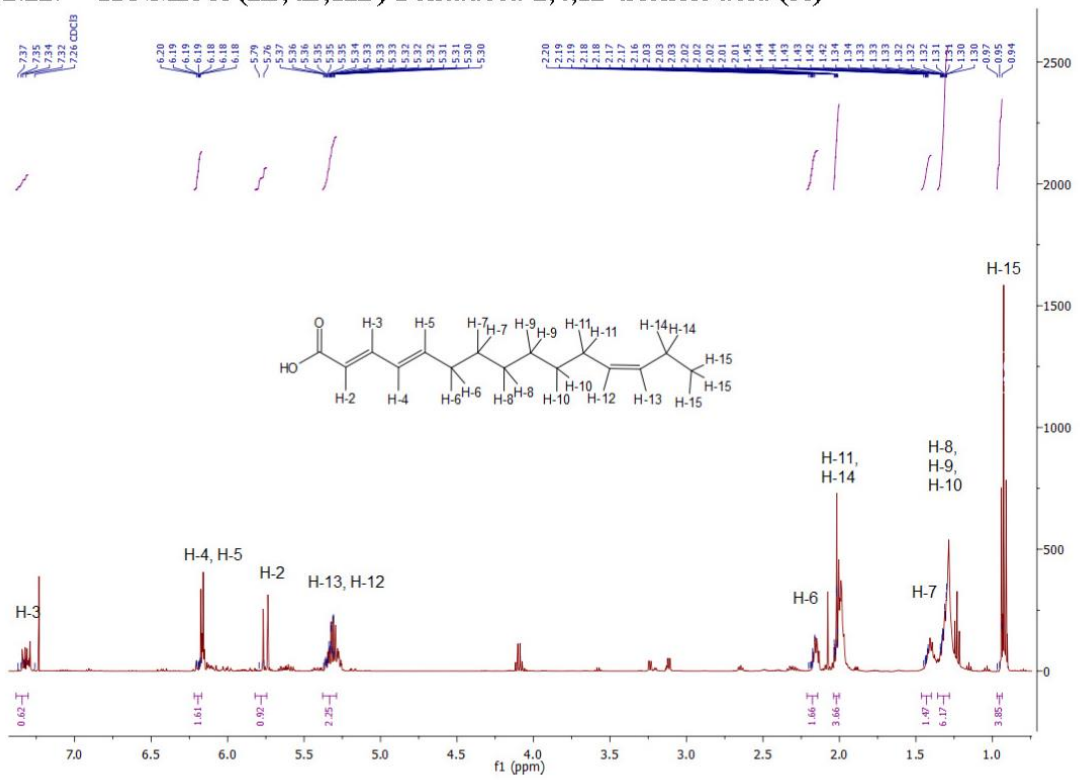

2.23. COSY of (2*E*,4*E*,12*Z*)-Pentadeca-2,4,12-trienoic acid (3f)

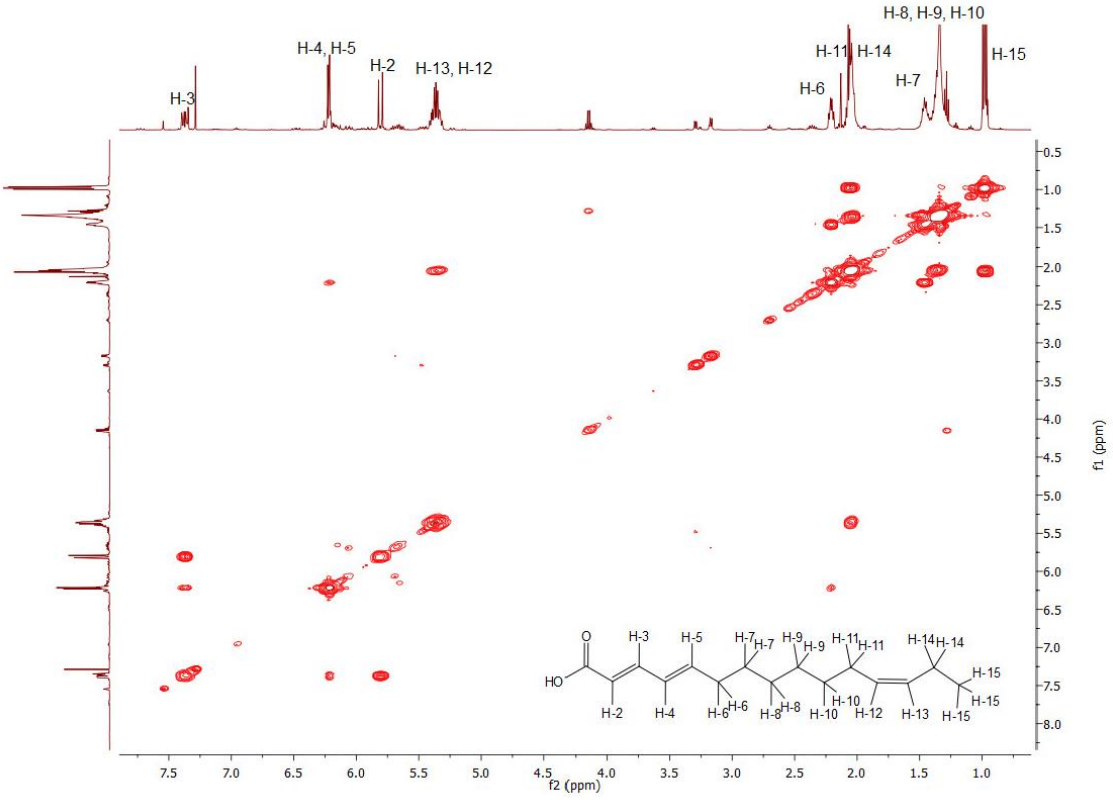

2.24. ^{13}C NMR of (2*E*,4*E*,12*Z*)-Pentadeca-2,4,12-trienoic acid (3f)

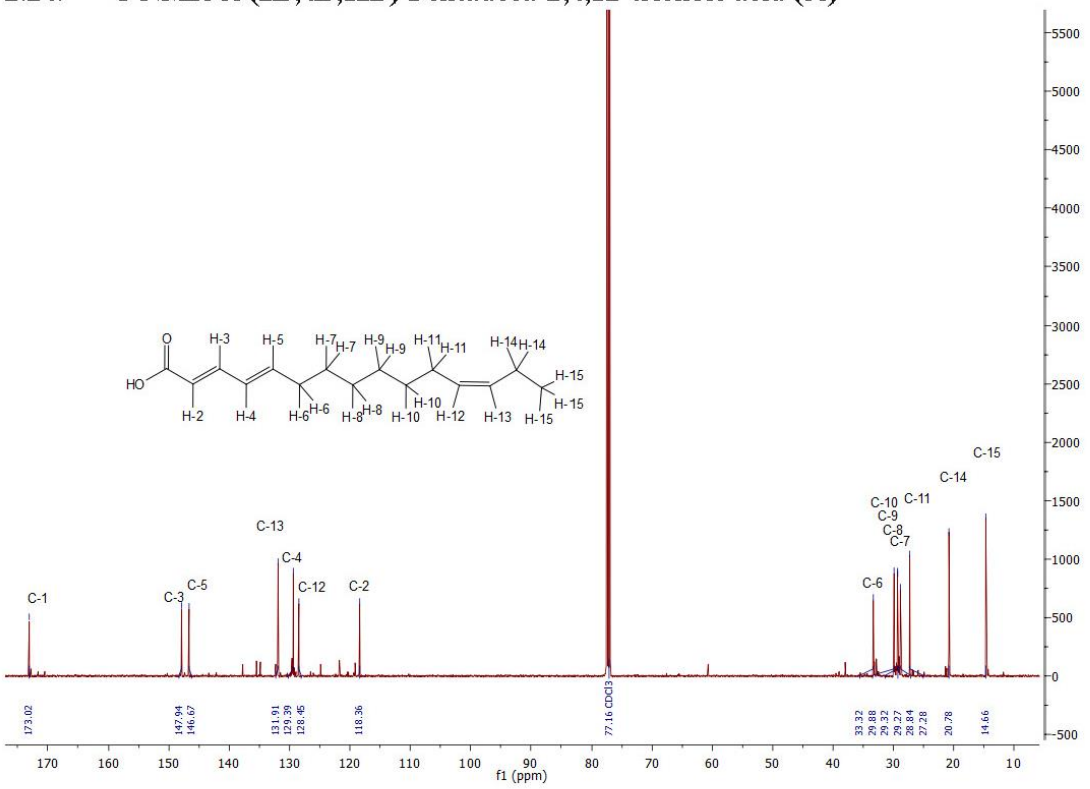

2.25. HSQCED of (2*E*,4*E*,12*Z*)-Pentadeca-2,4,12-trienoic acid (3f)

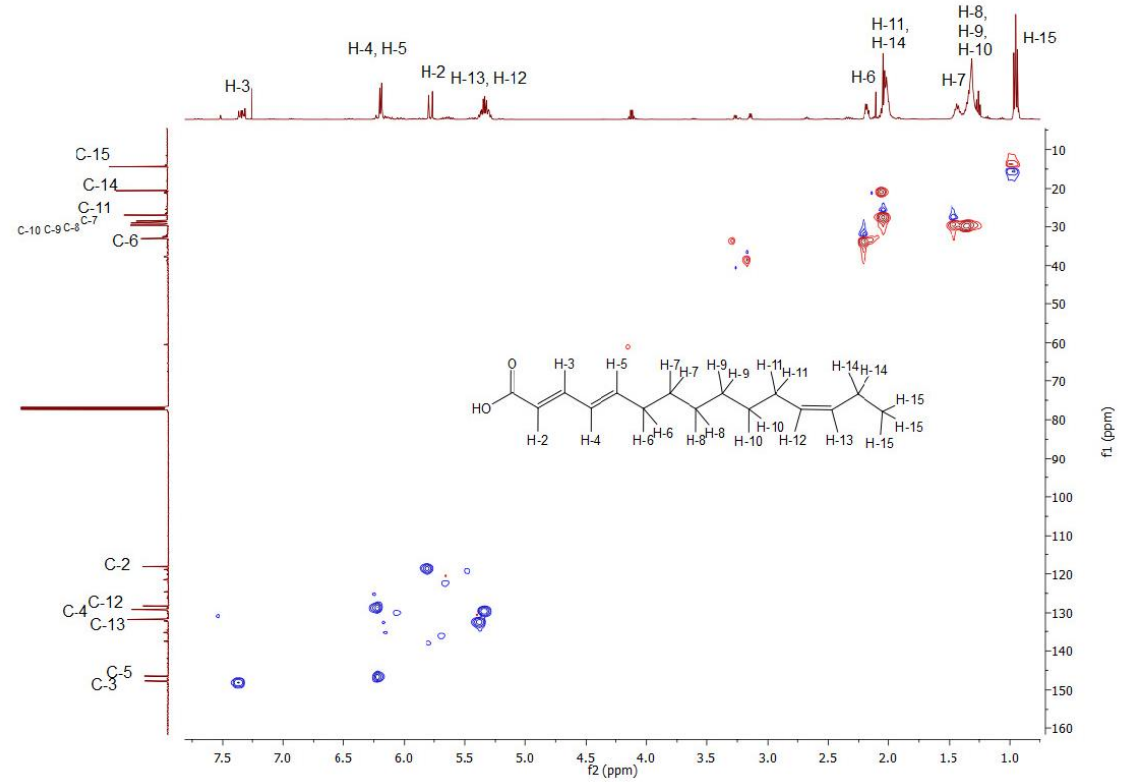

2.26. HMBC of (2*E*,4*E*,12*Z*)-Pentadeca-2,4,12-trienoic acid (3f)

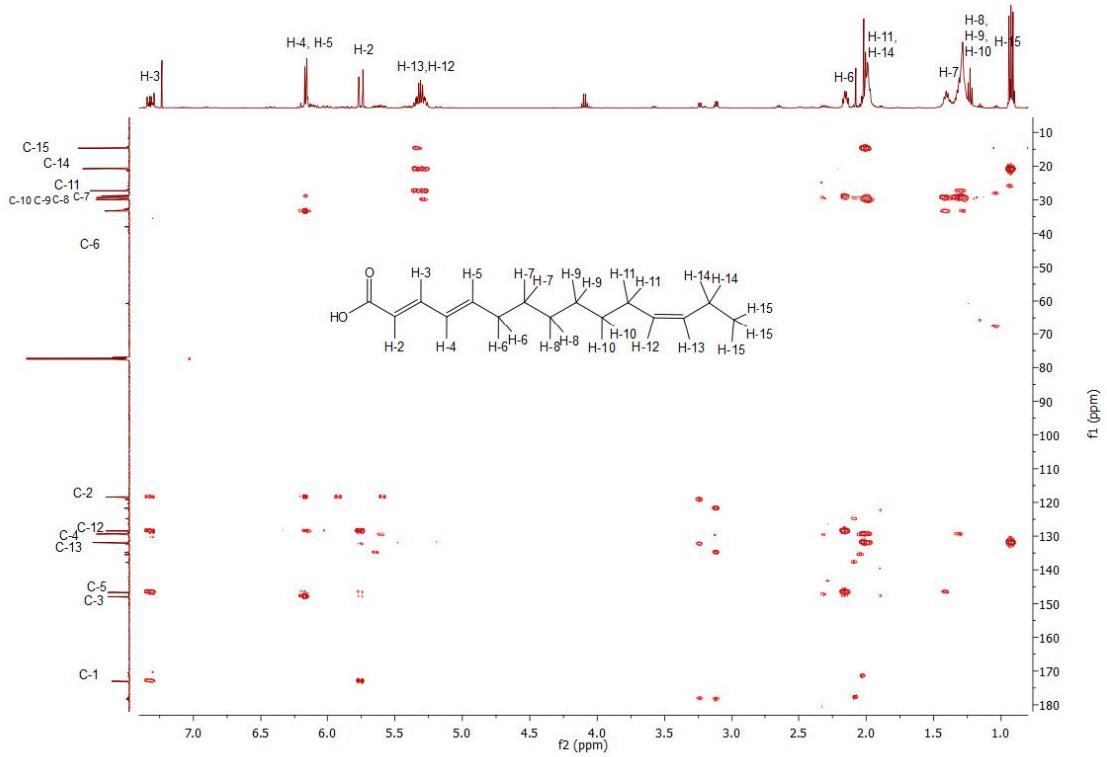

7.3 Supplementary Material: Reversibility of Citrate Synthase allows autotrophic Growth of a thermophilic Bacterium

www.sciencemag.org/content/359/6375/563/suppl/DC1

Supplementary Materials for

Reversibility of citrate synthase allows autotrophic growth of a thermophilic bacterium

Achim Mall, Jessica Sobotta, Claudia Huber, Carolin Tschirner, Stefanie Kowarschik, Katarina Bačnik, Mario Mergelsberg, Matthias Boll, Michael Hügler, Wolfgang Eisenreich,* Ivan A. Berg*

*Corresponding author. Email: ivan.berg@uni-muenster.de (I.A.B.); wolfgang.eisenreich@mytum.de (W.E.)

Published 2 February 2018, *Science* **359**, 563 (2018)
DOI: 10.1126/science.aao2410

Materials and Methods

Experimental design

Objective: Identification of the pathway of autotrophic CO_2 fixation in *Desulfurella acetivorans*. First, the capability to grow autotrophically was confirmed by growth experiments. Sequencing was done after PCR by standard methods. Subsequently, enzyme activities were determined. If the results of classical enzyme assays were dubious, products were analyzed by UPLC or by LC-MS. All products of the citrate cleavage reaction were also identified by NMR using [U-$^{13}C_6$]citrate. In order to prove that CS (together with MDH) can indeed catalyze citrate cleavage, the same assay was performed using CS/MDH from porcine heart (Sigma). To understand how flux through the TCA cycle is directed, metabolite concentrations were measured under autotrophic conditions using LC-MS. Additionally, the fate of [U-$^{13}C_2$]acetate and [1-^{13}C]pyruvate in the TCA cycle was determined by *in vivo* labeling experiments followed by GC-MS isotope analysis of amino acids that are synthesized from TCA cycle intermediates. Finally, growth experiments with rTCA cycle inhibitors were performed. For comparison, some assays were done with *D. multipotens*.

Materials

Chemicals were obtained from Fluka (Neu-Ulm, Germany), Sigma-Aldrich (Deisenhofen, Germany), Merck (Darmstadt, Germany), Serva (Heidelberg, Germany), or Roth (Karlsruhe, Germany). Biochemicals were from Roche Diagnostics (Mannheim, Germany), AppliChem (Darmstadt, Germany), 13C Molecular Inc. (Fayetteville, NC, USA). Materials for molecular biology were purchased from New England BioLabs (Frankfurt, Germany), MO BIO Laboratories (Carlsbad, CA, USA) and Qiagen (Hilden, Germany). Gases were obtained from Sauerstoffwerke Friedrichshafen (Germany). Primers were obtained from Sigma-Aldrich (Deisenhofen, Germany).

Strains and growth conditions

D. acetivorans A63 (DSM 5264) and *D. multipotens* (RH-8; DSM 8415) were obtained from Deutsche Sammlung von Mikroorganismen und Zellkulturen (DSMZ). The cells were grown autotrophically in medium containing 6.2 mM NH_4Cl, 2.2 mM $CaCl_2$, 1.6 mM $MgCl_2$, 4.4 mM KCl, 1.7 mM KH_2PO_4, 1.3 mM K_2HPO_4, 23.8 mM $NaHCO_3$, 20 g/l ground sulfur powder, 1 mg/l resazurin, 1 ml/l SL-10 trace element solution (3 g/l $FeCl_2 \cdot 4\ H_2O$, 70 mg/l $ZnCl_2$, 100 mg/l $MnCl_2 \cdot 4\ H_2O$, 4 mg/l $CuCl_2 \cdot 2\ H_2O$, 24 mg/l $NiCl_2 \cdot 6\ H_2O$, 36 mg/l $Na_2MoO_4 \cdot 2\ H_2O$, 30 mg/l H_3BO_3, 224 mg/l $CoCl_2 \cdot 6\ H_2O$) and 1 ml/l Wolfe's vitamin solution (20 mg/l biotin, 20 mg/l folic acid, 100 mg/l pyridoxamine dihydrochloride, 50 mg/l thiamine dihydrochloride, 50 mg/l riboflavin, 50 mg/l nicotinic acid, 50 mg/l DL-Ca-pantothenate, 1 mg/l cyanocobalamin, 50 mg/l 4-aminobenzoic acid, 50 mg/l lipoic acid). The medium was prepared without bicarbonate, sulfur and vitamins, made anaerobic by bubbling with N_2/CO_2 (80:20) and reduced by the addition of $Na_2S \cdot 9\ H_2O$ to a final concentration of 0.05%. The pH was adjusted to 5.9. The medium was dispensed anaerobically into serum bottles containing sulfur powder; the bottles were sealed with butyryl rubber stoppers and autoclaved for 20 min at 110°C. Prior to inoculation, the medium was supplemented with bicarbonate and vitamins, and the gas phase was replaced with H_2/CO_2 (80:20) at 1 bar overpressure. Cultures were incubated at 55°C while shaking at 80 rpm. Although cells were routinely grown in the presence of small amounts of vitamins and the redox dye resazurin, growth was also possible in strictly inorganic medium. For heterotrophic cultures, the medium was supplemented with 5 g/l sodium acetate before inoculation and the gas phase was N_2/CO_2 (80:20) at 1 bar overpressure. For labeling experiments, (1) 10 mM [U-$^{13}C_2$]acetic acid was added to the medium before inoculation, or (2) a total of 0.2 mM [1-^{13}C]pyruvic acid was added to an autotrophically

growing 20 ml-culture (4 x 50 µM at 57, 75, 91 and 98 h) during exponential growth phase. Cells were harvested during mid-exponential growth by centrifugation (4300 × g, 4°C, 20 min), frozen in liquid nitrogen and stored at -80°C.

Preparation of cell extracts

Cells were resuspended in 20 mM Tris-HCl pH 8, 5 mM DTE, lysed by sonication on ice (120 0.5-second-pulses with one-second pauses, 2 kJ total energy input). Insoluble material was removed by centrifugation (30,000 × g, 30 min, 4°C). For succinate dehydrogenase and fumarate reductase assays, centrifugation speed was reduced to 5000 × g in order to keep membranes in the supernatant. When anaerobic conditions were required, cell extracts were prepared inside of an anaerobic glove box. Protein concentration in cell extracts was determined with a Direct Detect spectrometer (Merck Millipore).

Enzyme assays

Spectrophotometric enzyme assays (0.5-ml assay mixture) were performed in a heated UV-Vis spectrometer in 0.5-ml quartz (for UV light) or glass (for visible light) cuvettes at 55°C for *D. acetivorans* and *D. multipotens* cell extracts or at 42°C for porcine citrate synthase. For anaerobic assays, cell extracts were prepared anaerobically, cuvettes were sealed with rubber plugs, made anaerobic by gassing with N_2, and anaerobic reaction mixture and substrates were added with Hamilton syringes. For UPLC analysis, reactions were stopped in an equal amount of ice-cold stop solution (1 M HCl, 10% acetonitrile (ACN)). Protein was removed by freeze-thawing the samples, followed by centrifugation (16,000 × g, 15', 4°C). Samples were analyzed on an Acquity UPLC system (Waters) using a Waters Acquity UPLC BEH C18 1.7 µm 2.1 × 100 mm column as described in (*31*).

Citrate synthase was measured spectrophotometrically at 412 nm as the oxaloacetate-dependent formation of free CoA from acetyl-CoA. The reaction mixture contained 100 mM Tris-HCl (pH 8), 5 mM oxaloacetate, 0.5 mM acetyl-CoA, 1 mM DTNB (ε_{412}=14.2 mM^{-1} cm^{-1}; *32*), and cell extract. The backward reaction was measured 1) spectrophotometrically at 365 nm in combination with MDH as the citrate- and CoA-dependent oxidation of NADH (ε_{365}=3.4 mM^{-1} cm^{-1}; *33*), 2) via UPLC as the citrate-, CoA- and NADH-dependent formation of acetyl-CoA, and 3) via NMR spectroscopy as the CoA-dependent formation of [U-$^{13}C_4$]malate and [U-$^{13}C_2$]acetyl-CoA from [U-$^{13}C_6$]citrate. For spectrophotometric assays, the assay mixture

contained 100 mM Tris-HCl (pH 8), 5 mM DTE, 5 mM $MgCl_2$, 0.5 mM CoA, 20 mM citrate, 0.5 mM NADH, and cell extract or porcine citrate synthase (Sigma C3260) and 20 U/ml porcine MDH (Sigma M1567). For UPLC assays, 1 mM CoA and 5 mM of NADH were used instead. For NMR assays, 1 ml of 50 mM Tris-HCl (pH 8), 5 mM $MgCl_2$, 2 mM DTE, 2 mM [U-$^{13}C_6$]citrate, 2 mM NADH, 2 mM CoA and cell extract or 8.4 U/ml porcine citrate synthase and 20 U/ml MDH were used. To stop the reaction, samples were mixed with an equal amount of ice-cold 6% (v/v) trifluoroacetic acid. Protein was removed by centrifugation (16,000 × g, 15 min, 4°C). Supernatants were frozen in liquid nitrogen and lyophilized. To test for an ATP-dependency of the citrate synthase backward reaction, 5 mM ATP was added to the assays. K_m values were determined spectrophotometrically by varying the concentration of one substrate while keeping the other substrates at saturating concentration.

Isocitrate dehydrogenase was measured spectrophotometrically at 365 nm as the isocitrate-dependent reduction of NADP (ε_{365}=3.5 mM^{-1} cm^{-1}; *33*). The assay mixture contained 100 mM Tris-HCl (pH 8), 5 mM DTE, 5 mM $MgCl_2$, 1 mM NADP, 10 mM DL-isocitrate, and cell extract.

Aconitase was measured spectrophotometrically at 365 nm under anaerobic conditions in combination with endogenous isocitrate dehydrogenase as the citrate-dependent reduction of NADP. The reaction mixture contained 100 mM Tris-HCl (pH 8), 5 mM DTE, 5 mM $MgCl_2$, 1 mM NADP, 5 mM citrate, and cell extract.

Malate dehydrogenase, succinyl-CoA reductase, malonyl-CoA reductase and *succinate semialdehyde reductase* were measured spectrophotometrically at 365 nm as the oxaloacetate-, succinyl-CoA-, malonyl-CoA- or succinate semialdehyde-dependent oxidation of NADH or NADPH. The assay mixtures contained 100 mM Tris-HCl (pH 8), 5 mM DTE, 5 mM $MgCl_2$, 0.5 mM NAD(P)H, 2.5 mM oxaloacetate or 0.2 mM succinyl-CoA/malonyl-CoA/succinate semialdehyde, and cell extract.

Succinyl-CoA synthetase and *acetyl-CoA synthetase / acetate kinase + phosphate acetyltransferase* were measured via UPLC as the ATP-dependent formation of succinyl-CoA and acetyl-CoA. The assay mixture contained 100 mM Tris-HCl (pH 8), 5 mM DTE, 5 mM $MgCl_2$, 10 mM succinate or acetate, 5 mM ATP, 1 mM CoA, and cell extract. Acetyl-CoA synthetase was alternatively measured photometrically at 365 nm and 42°C as the CoA- and

acetate-dependent oxidation of NADH in an assay containing 100 mM Tris-HCl (pH 8), 5 mM DTE, 5 mM $MgCl_2$, 10 mM acetate, 5 mM ATP, 0.5 mM CoA, 5 mM PEP, 5 U pyruvate kinase (rabbit muscle, Sigma P9136), 25 U lactate dehydrogenase (rabbit muscle, Sigma L2500), and cell extract.

Acetate:succinyl-CoA CoA-transferase was measured via UPLC as the acetate- and succinyl-CoA-dependent formation of acetyl-CoA. The assay mixture contained 100 mM Tris-HCl (pH 8), 5 mM DTE, 5 mM $MgCl_2$, 10 mM acetate, 1 mM succinyl-CoA, and cell extract.

Succinate dehydrogenase was measured spectrophotometrically at 600 nm as the succinate-dependent reduction of 2,6-dichlorophenolindophenol (DCPIP; ε_{600}=21 mM^{-1} cm^{-1}, *34*). The assay mixture contained 100 mM Tris-HCl (pH 8), 5 mM $MgCl_2$, 0.3 mM DCPIP, 1 mM phenazine methosulfate, 1 mM succinate, and cell extract.

Fumarate reductase was measured under anaerobic conditions via UPLC as the fumarate-dependent formation of succinyl-CoA in the reaction coupled with endogenous succinyl-CoA synthetase. The assay mixture contained 100 mM Tris-HCl (pH 8), 5 mM DTE, 5 mM $MgCl_2$, 5 mM fumarate, 5 mM ATP, 0.5 mM CoA, 1 mM dithionite and cell extract. In some experiments, 1 mM benzyl viologen, methyl viologen, 2,3-dimethyl-1,4-naphthoquinone, or flavin mononucleotide were added.

Fumarase was measured spectrophotometrically under anaerobic conditions at 240 nm as the cell extract-dependent formation of fumarate from L-malate (ε_{240}=2.4 mM^{-1} cm^{-1}; *35*). The assay mixture contained 100 mM Tris-HCl (pH 8), 5 mM $MgCl_2$, 0.4 mM fumarate or 5 mM L-malate, and cell extract.

Ribulose 1,5-bisphosphate (RuBP) carboxylase was measured as the RuBP-dependent fixation of $^{14}CO_2$ into an acid stable product. The assay mixture contained 100 mM Tris-HCl (pH 8), 5 mM DTE, 5 mM $MgCl_2$, 15 mM $NaHCO_3$, $NaH^{14}CO_3$ (50 kBq/ml), 1 mM RuBP, and cell extract. Samples were stopped in two volumes of 3% (v/v) trichloroacetic acid, chilled on ice, and protein was removed by centrifugation (16,000 × g, 15 min, 4°C). Supernatants were transferred into scintillation tubes and put on a shaker overnight to remove remaining carbonate from the solution. On the next day, 3 ml of scintillation cocktail (Rotiszint® eco plus, Roth,

Karlsruhe) was added to each sample and radioactivity was determined in a scintillation counter (Tri-Carb 2100TR, Packard, Meriden, USA).

Carbon monoxide dehydrogenase was measured spectrophotometrically at 578 nm by following the CO-dependent reduction of methyl viologen (ε_{578}=9.7 mM^{-1} cm^{-1}; *36*). The assay mixture contained 50 mM Tris-HCl (pH 8), 5 mM $MgCl_2$, 2.5 mM DTE, and 1 mM methyl viologen. Anaerobic cuvettes and reaction mixture were flushed with CO gas prior to the assay. The reaction was started by the addition of cell extract. Blank values were measured in a separate assay without CO. CO gas was synthesized by slightly heating an anaerobic mixture of 5 ml formic acid and 10 ml concentrated sulphuric acid in a 1 l Schott bottle while stirring. Gas was withdrawn with a syringe.

Formate dehydrogenase, pyruvate synthase and *2-oxoglutarate synthase* activities were measured in the same manner as described above for CO dehydrogenase, but the gas phase consisted of N_2 and the reactions were started by the addition of 10 mM formate, pyruvate or 2-oxoglutarate, respectively. Additionally, the pyruvate and 2-oxoglutarate synthase assays contained 0.5 mM CoA. In the case of 2-oxoglutarate synthase, benzyl viologen (ε_{578}=8.65 mM^{-1} cm^{-1}; *36*) was used instead of methyl viologen.

4-Hydroxybutyryl-CoA synthesis and *conversion* was measured via UPLC under anaerobic conditions as the 4-hydroxybutyrate-dependent formation of 4-hydroxybutyryl-CoA and subsequent formation of other CoA-esters. The reaction mixture contained 100 mM Tris-HCl (pH 8), 5 mM DTE, 5 mM $MgCl_2$, 1 mM CoA, 1 mM NAD, 10 mM 4-hydroxybutyrate, 2 mM ATP, and cell extract.

Phosphoenolpyruvate (PEP) carboxylase, PEP carboxykinase and *pyruvate carboxylase* were measured spectrophotometrically at 365 nm in combination with endogenous MDH as the PEP-dependent (PEP carboxylase), PEP- and ADP-dependent (PEP carboxykinase) or pyruvate- and ATP-dependent (pyruvate carboxylase) oxidation of NADH. The assay mixture for PEP carboxylase contained 100 mM 3-(N-morpholino)propanesulfonic acid (MOPS)-KOH (pH 7.2), 4 mM $MnCl_2$, 5 mM DTE, 40 mM $NaHCO_3$, 0.5 mM NADH, 5 mM PEP, and cell extract. For PEP carboxykinase assay, the reaction mixture was supplemented with ADP (5 mM). The assay mixture for pyruvate carboxylase contained 100 mM Tris-HCl (pH 8), 5 mM

DTE, 5 mM $MgCl_2$, 15 mM $NaHCO_3$, 0.5 mM NADH, 0.2 mM acetyl-CoA, 40 mM pyruvate, 5 mM ATP, and cell extract.

PEP synthase was measured using a discontinuous assay according to (*37*). The assay mixture contained 200 mM Tris-HCl (pH 8), 20 mM $MgCl_2$, 10 mM DTE, 50 mM NH_4Cl, 5 mM ATP, 0.8 mM pyruvate, and cell extract. The amounts of PEP formed in the reaction after 0, 5, and 10 min of incubation were determined by transferring the sample (0.1 ml) into an assay mixture (0.4 ml; 30°C) containing 200 mM Tris-HCl (pH 8), 20 mM $MgCl_2$, 1 mM ADP, and 0.5 mM NADH and measuring the decrease in absorption at 365 nm after the consecutive addition of lactate dehydrogenase (25 U) and pyruvate kinase (5 U).

Extraction and analysis of metabolites

Before harvesting mid-exponential cells, the incubator was stopped and cells were left standing at 55°C for 5 min to sediment insoluble sulfur. The supernatants were filtered through cellulose membrane filters (0.2 µm pore size) using a vacuum manifold. After filters were dry, they were immediately transferred into Schott bottles containing 8 ml ice-cold extraction solution (ACN:MeOH:H_2O, 40:40:20). To efficiently extract and stabilize CoA and CoA-esters, 0.1 M formic acid was added to the extraction solution (*38*). Metabolites were extracted for 30 min on ice, during this time the bottles were sonicated in an ultrasound bath thrice for 30 s to remove cell material from filters. The extraction solution was tranferred to 50 ml-polypropylene tubes and insoluble material was removed by centrifugation (6000 × g, 10 min, 4°C). Samples were frozen in liquid nitrogen, lyophilized and stored at -20°C. CoA esters and free acids were detected using an ESI/QTOF System (Synapt G2-S*i* HDMS, Waters) coupled to a UPLC (Acquity I-Class, Waters). For CoA esters, a gradient of 2 to 10% in 6 min and 10% to 70% ACN min in 10 mM ammonium acetate buffer (pH 6.8) at a flow rate of 0.3 ml min^{-1} was applied to a C18 HSS T3 column (Waters). For free acids, the gradient was from 2 to 90% ACN/0.1% formic acid (v/v) in H_2O/0.1 % formic acid (v/v) at a flow rate of 0.35 ml min^{-1}. For CoA esters, the ESI source was operated at 450°C desolvation temperature, 1000 l h^{-1} N_2 desolvation gas flow with the capillary voltage set to 3 kV in positive mode while for free acids the desolvation temperature was set to 400°C and the capillary voltage was set to 2 kV in negative mode. Ion chromatograms were extracted, and ion areas were calculated using QuanLynx integrated into MassLynx 4.1 (Waters).

Sequencing of the acl gene region in *D. acetivorans*

D. acetivorans genomic DNA was prepared using an UltraClean® Microbial DNA Isolation Kit (MO BIO Laboratories, Inc.). Five primer pairs were designed to amplify the gene region encoding the *acl* gene (**Table S11**). DNA was amplified using Q5 polymerase (New England Biolabs) according to the manufacturer's instructions. The amplified fragments were sequenced at GATC (Konstanz, Germany) and aligned with the published genome sequence (GenBank accession CP007051.1).

Determination of intracellular metabolite concentrations

To quantify metabolite concentrations, cultures were split and a defined concentration of the compounds of interest was added onto the filters after filtration of cells. Metabolite concentrations were extrapolated from these internal standards. The volume of one *D. acetivorans* cell was calculated to be 3.7×10^{-10} µl, assuming an average length of 1.5 µm, an average diameter of 0.6 µm (*13*) and a spherocylindrical shape. Cells were quantified directly by counting in a Neubauer chamber.

NMR analysis

NMR spectra were recorded at 27 °C using an Avance III 500 spectrometer (Bruker Instruments, Karlsruhe, Germany) equipped with a QNP cryo probehead. ^{1}H-decoupled ^{13}C-NMR spectra were measured in D_2O at 125.8 MHz typically using 1024 scans. Data analysis was done with TOPSPIN 3.2 (Bruker) or MestReNova 7.0.0 (Mestrelab Research, Santiago de Compostela, Spain). Prior to Fourier transformation, the spectra were zero-filled to 128k and multiplied with a mild Gaussian function.

Cell hydrolysis and GC-MS analysis

Approximately 10^9 bacterial cells (about 1 mg of freeze-dried pellet) were hydrolyzed in 0.5 ml of 6 M HCl for 24 h at 105°C, as described earlier (*39*). Samples were dried under a stream of nitrogen at 70°C. The residue was resolved in 200 µL of acetic acid and purified on a cation exchange column of Dowex 50Wx8 (H^+ form, 200-400 mesh, 5 × 10 mm), which was previously washed with 1 ml MeOH and 1 ml ddH_2O. Elution occurred after washing with 2 ml of ddH_2O with 1 ml of 4 M ammonium hydroxide. 200 µl of the eluate was dried at 70°C under a stream of nitrogen and dissolved in 50 µl dry ACN and 50 µl N-(tert-butyldimethyl-silyl)-N-methyl-trifluoroacetamide containing 1% tert-butyl-dimethyl-silylchlorid (Sigma). Derivatization occurred at 70°C for 30 min. The resulting tert-butyl-dimethylsilyl derivates

(TBDMS) of protein-derived amino acids, e.g. Ala, Asp, Glu and Pro, were used in GC/MS analysis. Acid hydrolyzation leads to conversion of glutamine and asparagine to glutamate and aspartate. Therefore, results for aspartate and glutamate correspond to asparagine/aspartate and glutamine/glutamate, respectively.

GC/MS-analysis was performed with a QP2010 Plus gas chromatograph/mass spectrometer (Shimadzu) equipped with a fused silica capillary column (Equity TM-5; 30 m × 0.25 mm, 0.25 μm film thickness; SUPELCO) and a quadrupole detector working with electron impact ionization at 70 eV. An aliquot (0.1 to 6 μl) of the derivatized samples were injected in 1:5 split mode at an interface temperature of 260°C and a helium inlet pressure of 70 kPa. After sample injection, the column was first kept at 150°C for 3 min and then developed with a temperature gradient of 7°C min^{-1} to a final temperature of 280°C. This temperature was held for further 3 min. TBDMS-derivatives of alanine (6.7 min), glycine (7.0 min), valine (8.5 min), leucine (9.1 min), isoleucine (9.5 min), proline (10.1 min), serine (13.2 min), phenylalanine (14.5 min), aspartate (15.4 min), glutamate (16.8 min), lysine (18.1 min), histidine (20.4 min), tyrosine (21.0 min) were detected and isotopologue calculations were performed with m/z [M-57]+ or m/z [M-85]+. Selected ion monitoring was used with a sampling rate of 0.5 s and LabSolution software (Shimadzu) was used for data collection and analysis. For technical replicates, samples were measured three times, respectively. Overall ^{13}C-excess values and isotopologue compositions were calculated as described earlier (*40*).

Statistical Analysis

Enzymatic activities were determined at least in two biological replicates, or more often when there was considerable variance. Values are given as the average ± standard deviation. NMR and UPLC analysis of the products of citrate cleavage in *D. acetivorans* was carried out in two biological replicates, representative results are shown. Isotopologue profiling experiments and metabolite measurements were performed at least in three biological replicates.

Supplementary Text

Regulation of enzymes involved in central carbon metabolism of *D. acetivorans* during autotrophic vs. heterotrophic growth

In *D. acetivorans* (*Deltaproteobacteria*, *Desulfurellales*), the most apparent regulation between autotrophic and heterotrophic growth modes can be observed in the activities of enzymes involved in the activation of acetate and succinate to their CoA-esters (**Table 1**). During heterotrophic growth, acetate is activated primarily by acetate:succinyl-CoA CoA-transferase, a strategy that has also been shown to operate in the closely related deltaproteobacteria *Desulfuromonas acetoxidans* (*Desulfuromonadales*) (*41*) and *Desulfobacter* spp. (*Desulfobacterales*) (*42*, *43*) (both containing menaquinones and cytochromes, *44-46*). During autotrophic growth, succinate activation proceeds via succinyl-CoA synthetase, which is highly upregulated under these conditions. In contrast, *Desulfobacter hydrogenophilus*, which is able to use an ACL version of the rTCA or oTCA cycle, depending on growth conditions, does not possess succinyl-CoA synthetase and activates succinate with acetyl-CoA during autotrophic growth. This means that acetyl-CoA has to be replenished by an anaplerotic reaction (*43*). The use of succinyl-CoA synthetase during autotrophic growth by *D. acetivorans* could help to conserve energy by avoiding the acetyl-CoA synthetase reaction that usually consumes two ATP equivalents. Note that our assays for acetate activation do not discriminate between acetyl-CoA synthetase (two putative AMP-forming enzymes are encoded in the genome, **Table 1**) and a two-enzyme system utilizing acetate kinase and phosphate-acetyltransferase that has been described for *D. acetivorans* (*15*). Furthermore, acetate:succinyl-CoA CoA-transferase, as well as the citrate cleavage, pyruvate carboxylase, PEP carboxykinase and PEP synthase reactions were reported to be absent in the aforementioned work. We could measure all of these activities in autotrophically as well as heterotrophically grown cells, albeit PEP synthase and pyruvate carboxylase, as well as pyruvate synthase activities were downregulated in the latter. This makes sense in light of the circumstance that during growth on acetate, most acetyl-CoA is directed to citrate synthesis and only small amounts need to be converted to oxaloacetate for anaplerosis, whereas during autotrophic growth, acetyl-CoA concentrations need to be kept to a minimum in order to facilitate ATP-independent citrate cleavage.

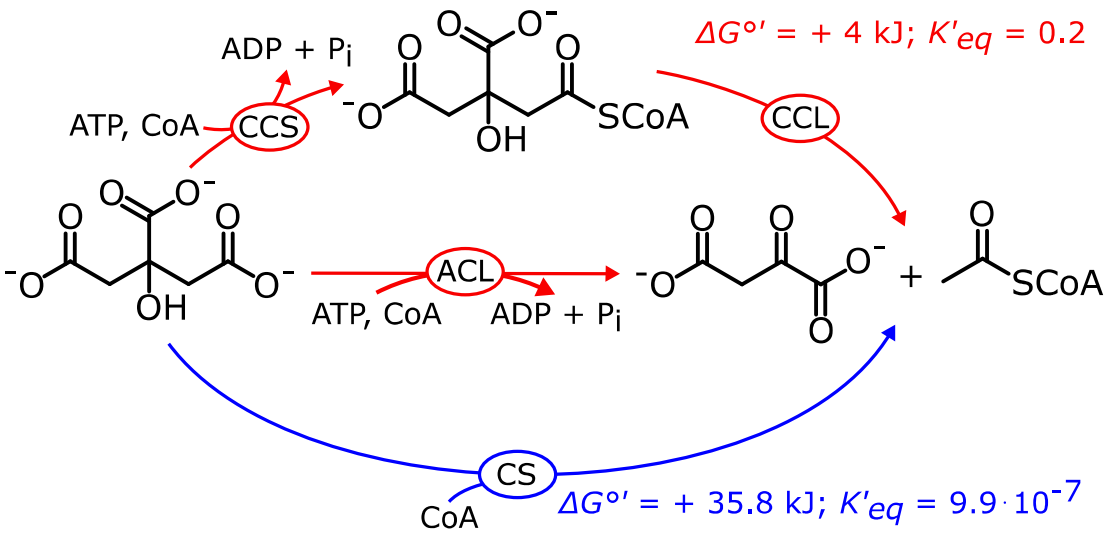

Fig. S1

Different variants of citrate cleavage in the rTCA cycle: ATP-citrate lyase reaction (*8*), citryl-CoA synthetase/citryl-CoA lyase reactions (*10, 11*), citrate synthase reaction (this work). CCS, citryl-CoA synthetase; CCL, citryl-CoA lyase; ACL: ATP:citrate lyase; CS: citrate synthase. Gibbs free energy and equilibrium constants for ATP-dependent citrate cleavage from (*2*), for ATP-independent citrate cleavage from (*20*). Please note that ACL functions in some bacteria for citrate synthesis in the oTCA cycle (*9*).

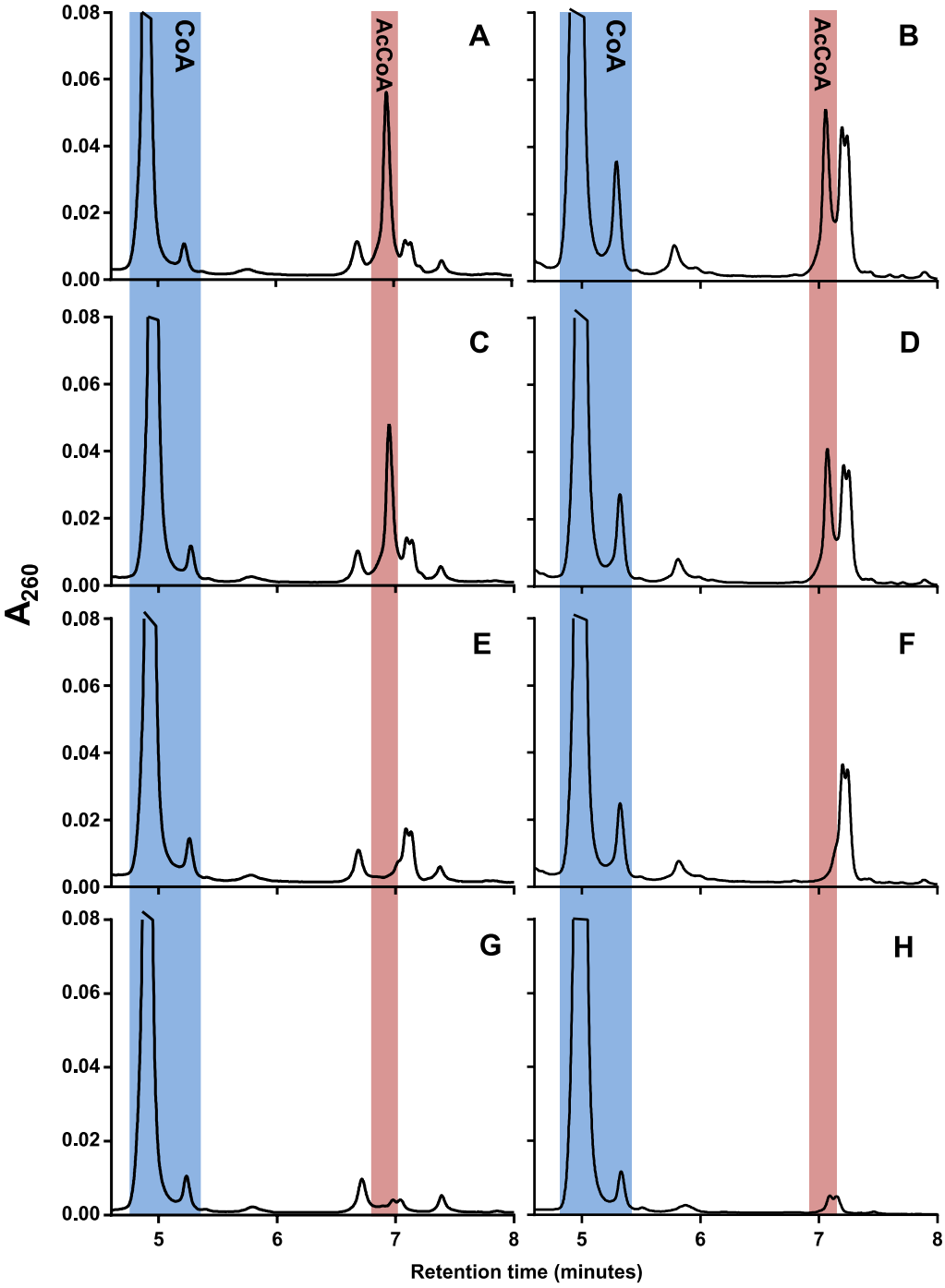

Fig. S2

UPLC analysis of products of the citrate cleavage catalyzed by *D. acetivorans* cell extracts (**A**, **C**, **E**, **G**) and by citrate synthase and malate dehydrogenase (**B**, **D**, **F**, **H**) from porcine heart (Sigma). The reaction mixture in (**A**) and (**B**) contained NADH, CoA, ATP and citrate. ATP was omitted from samples (**C**) and (**D**), citrate was omitted from samples (**E**) and (**F**), and NADH was omitted from samples (**G**) and (**H**).

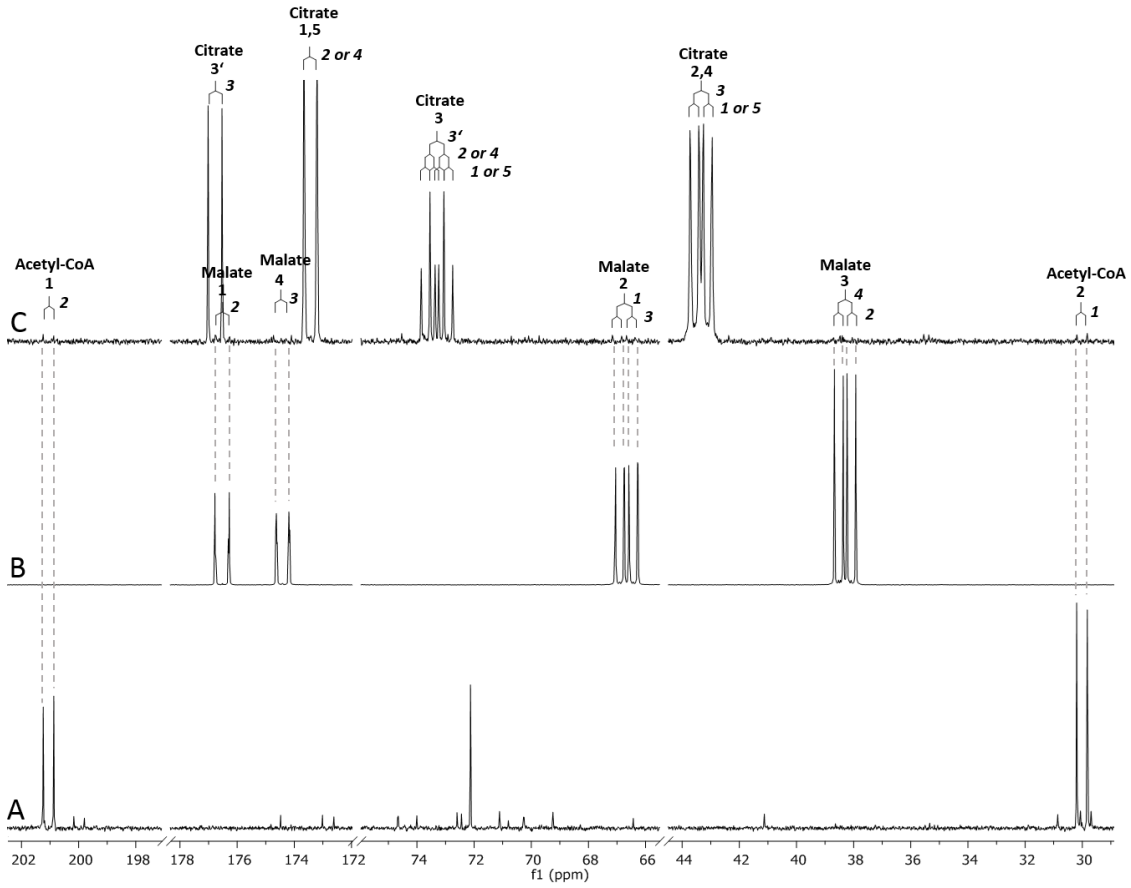

Fig. S3

^{13}C-NMR analysis of (**A**) [U-$^{13}C_2$]acetyl-CoA, (**B**) [U-$^{13}C_4$]malate, and (**C**) 2 mM [U-$^{13}C_6$]citrate, 2 mM NADH and 2 mM CoA incubated for 10 min in an assay containing 8.4 U/ml porcine citrate synthase (Sigma) and 20 U/ml porcine malate dehydrogenase (Sigma). Signals and couplings of [U-$^{13}C_6$]citrate, [U-$^{13}C_4$]malate and [U-$^{13}C_2$]acetyl-CoA are shown. The formation of [U-$^{13}C_2$]acetyl-CoA and [U-$^{13}C_4$]malate is indicated by dashed lines. For numerical values of chemical shifts and couplings, see **Table S2**.

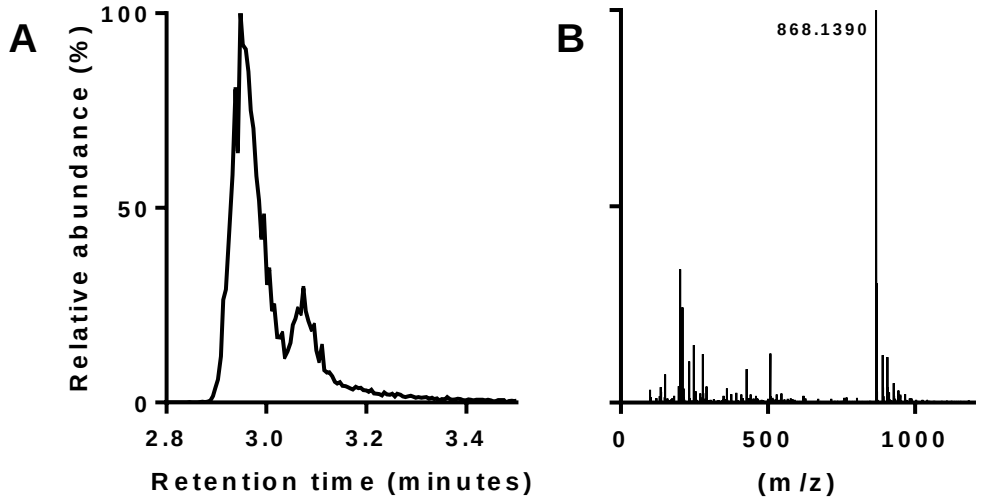

Fig. S4

LC-MS analysis of the fumarate-dependent succinyl-CoA formation catalyzed by cell extracts of *D. acetivorans*. **A**: Extracted ion chromatogram for succinyl-CoA (M+H: 868.1391 ± 0.02 Da), **B**: Mass spectrum of the succinyl-CoA peak (2.83 – 2.95 minutes), mass accuracy: < 0.2 ppm.

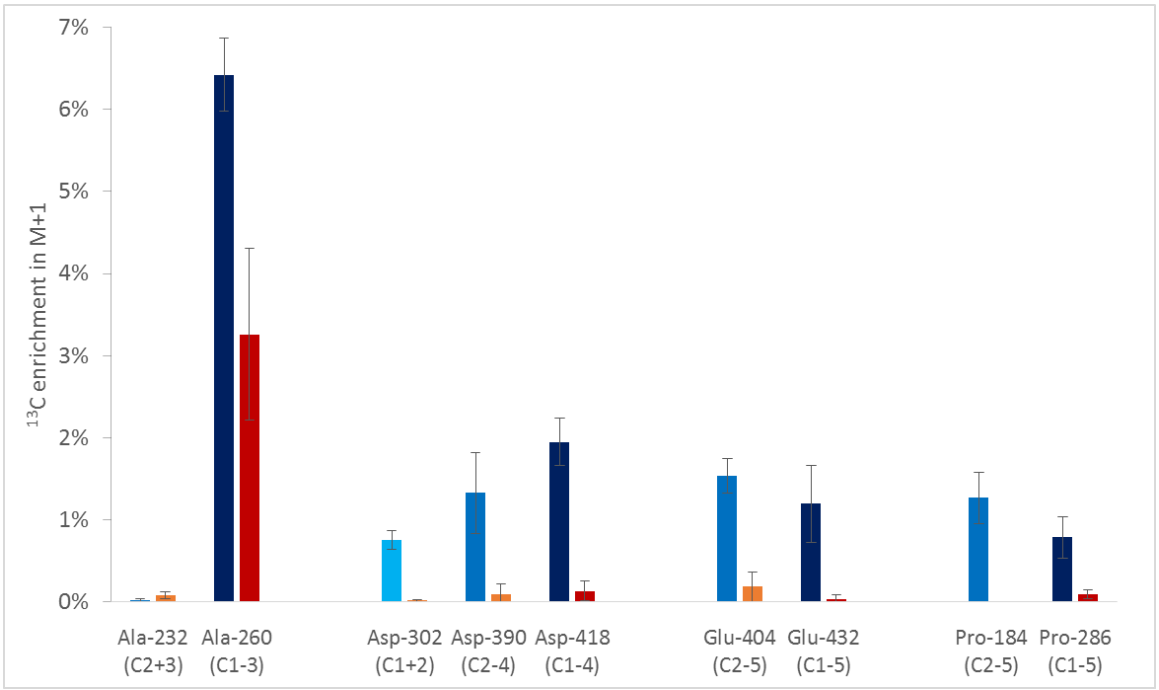

Fig. S5

^{13}C-Enrichments in mass fragments of alanine, aspartate, glutamate and proline from *D. acetivorans* A63 grown on [1-$^{13}C_1$]pyruvate (autotrophic growth in blue bars vs. heterotrophic growth in red/orange bars). Prior to MS analysis, the amino acids were converted into TBDMS derivatives. The m/z values of the fragments under study and the corresponding number of C atoms are indicated. Fragments containing all C atoms of the amino acids are shown in dark blue or red, fragments missing C_1 of the amino acids are shown in blue or orange and the fragment containing C-1 and C-2 of Asp is shown in light blue. Error bars represent the standard error of the mean of three independent biological replicates.

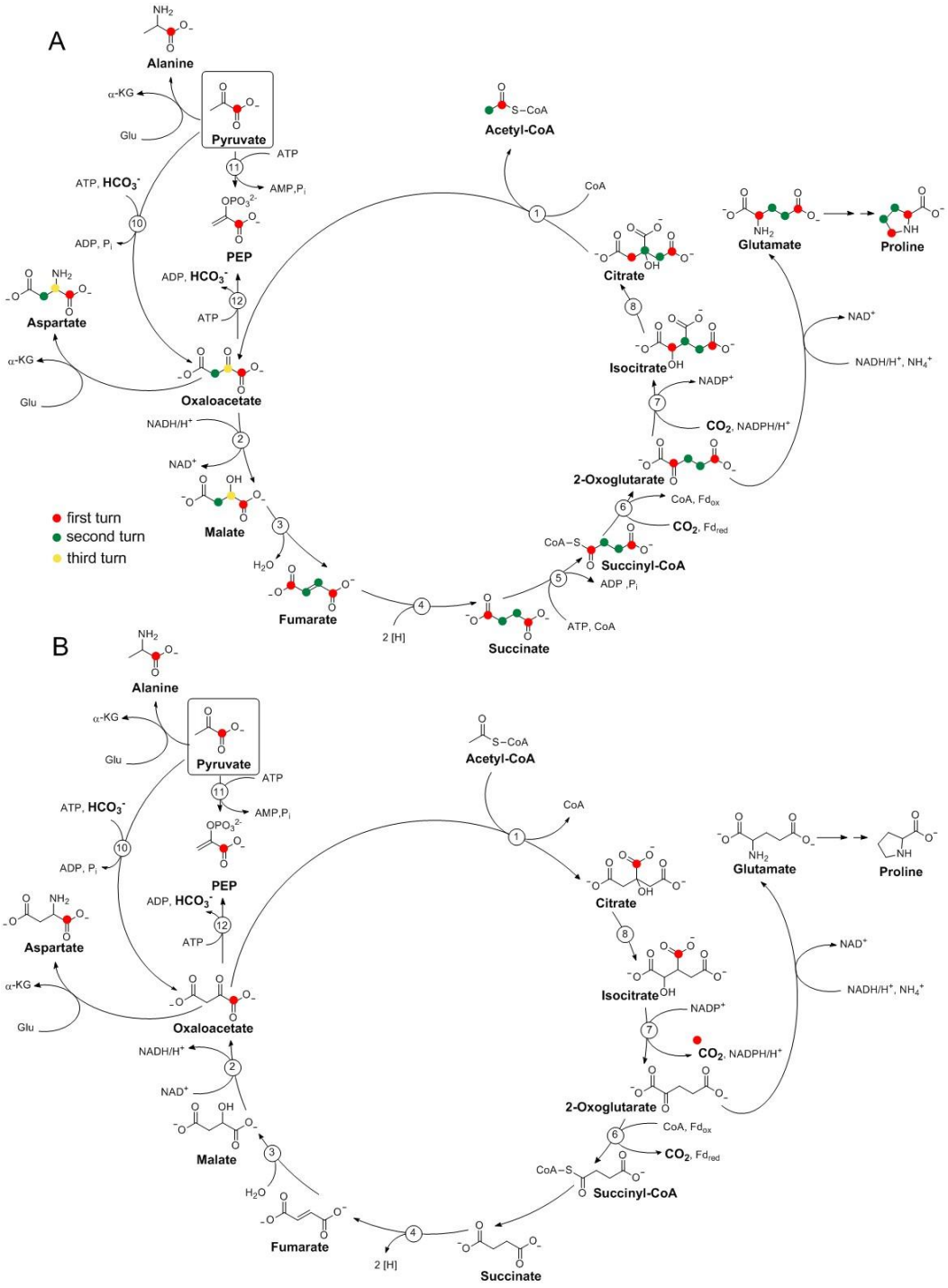

Fig. S6

^{13}C-Incorporation into alanine, aspartate, glutamate and proline from *D. acetivorans* A63 grown with H_2, CO_2 and S^0 in the presence of 0.2 mM [1-$^{13}C_1$]pyruvate (in box; added 4 x 50 µM at 57, 75, 91 and 98 h) following (**A**) the rTCA cycle with *Si*-specific CS or (**B**) the oTCA cycle with *Si*-specific CS. The labeled C atoms are indicated by red dots (first turn), green dots (second turn), and yellow dots (third turn). For the enzyme names, see **Fig. 3**.

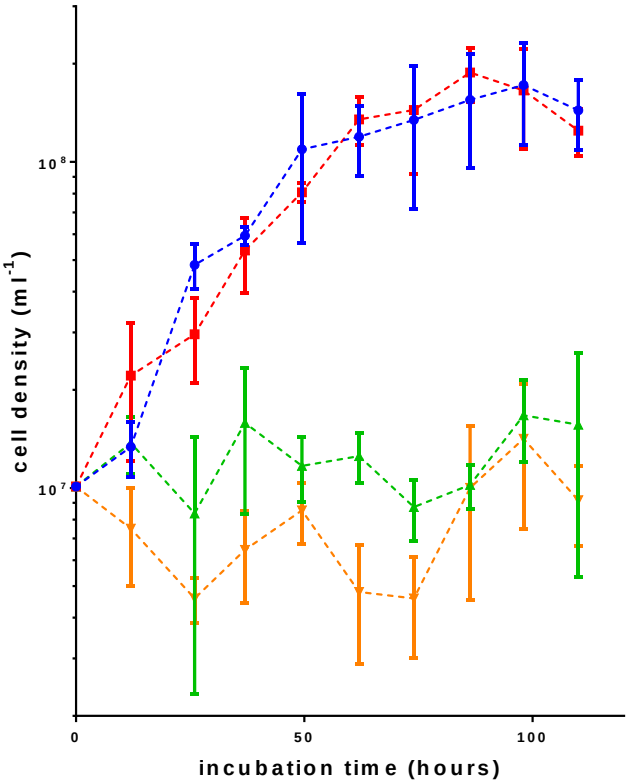

Fig. S7

Growth of *D. acetivorans* on H_2 +CO_2 +S^0 (blue circles), acetate + CO_2 + S^0 (red squares), H_2 + CO_2 + S^0 + 1 mM fluoroacetate (green pyramids), H_2 + CO_2 + S^0 + 1 mM glyoxylate (orange inverted pyramids). The means of three replicate cultures are shown; error bars represent the standard deviation.

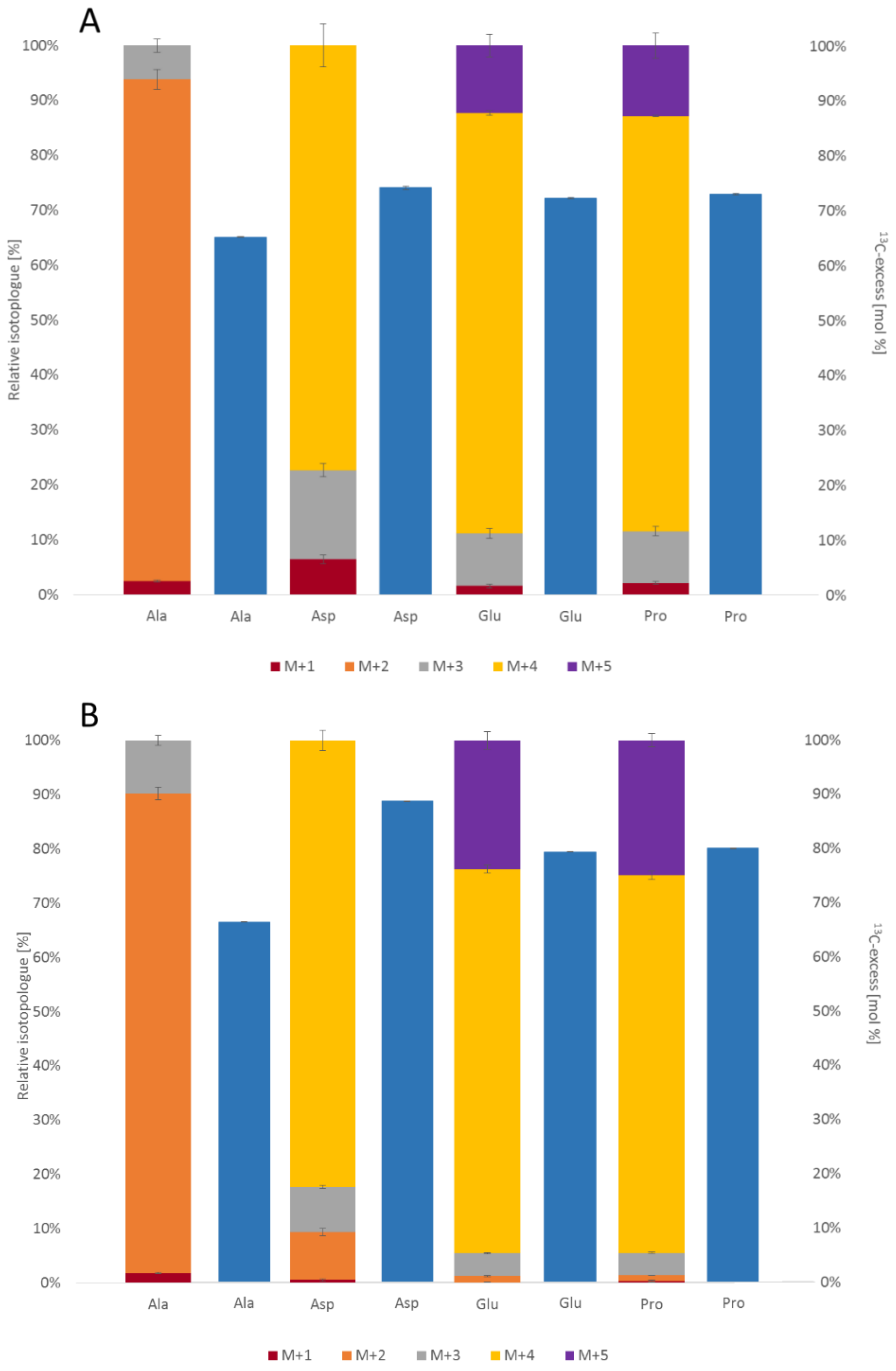

Fig. S8

^{13}C enrichment and isotopologue fractions in alanine, aspartate, glutamate and proline from *D. acetivorans* A63 grown on [1,2-^{13}C]acetate in (**A**) the presence of H_2 or (**B**) the presence of N_2. The blue bars represent ^{13}C enrichment and colored bars represent the isotopologue fractions (normalized to 100). The error bars indicate the standard error of the mean (n=3).

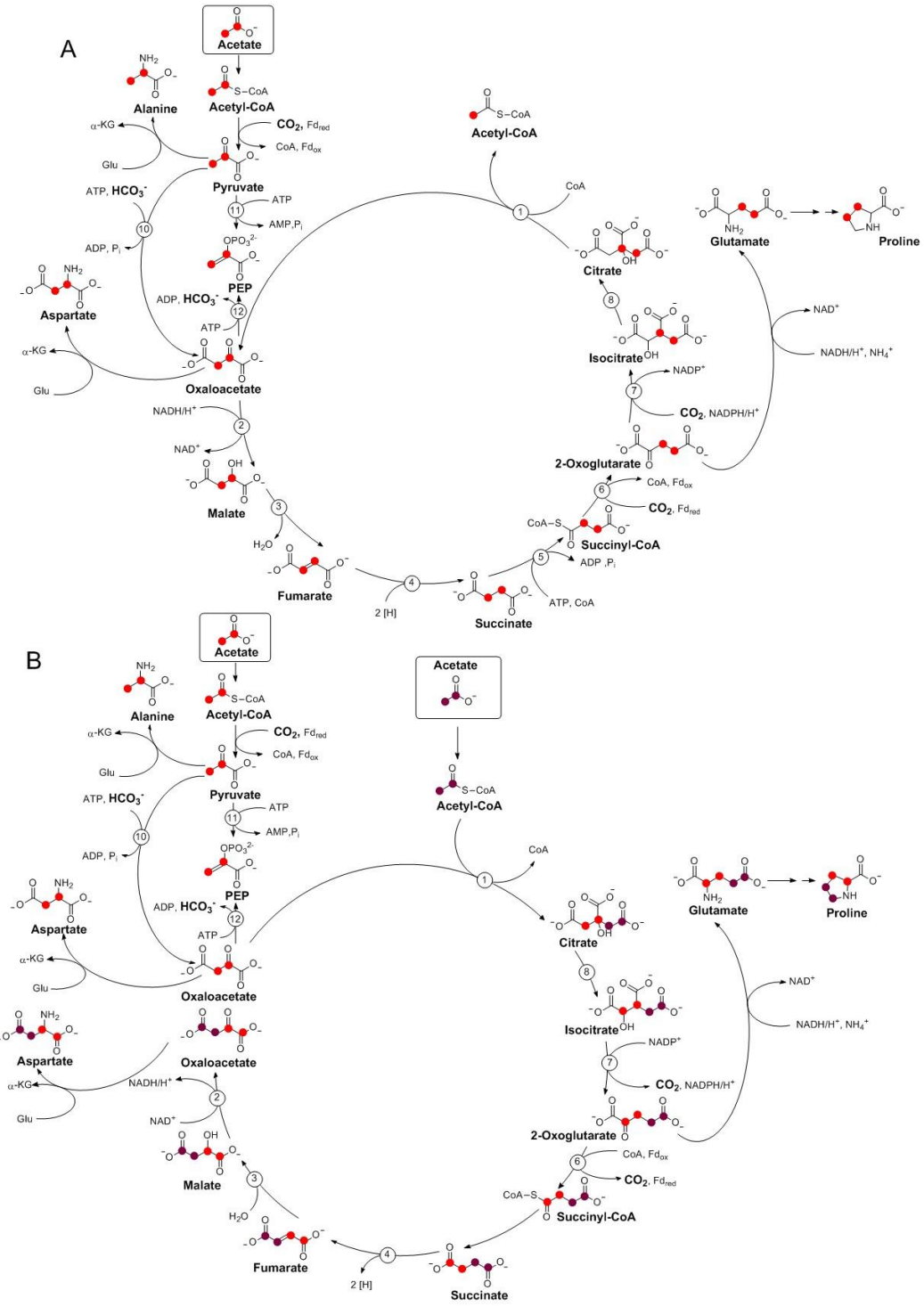

Fig. S9

^{13}C-Incorporation into alanine, aspartate, glutamate and proline from *D. acetivorans* A63 grown in the presence of 10 mM [1,2-$^{13}C_2$]acetate (in box) following (**A**) the rTCA cycle with *Si*-specific CS or (**B**) the oTCA cycle with *Si*-specific CS. The labeled C atoms are indicated by red and purple dots. For the enzyme names, see **Fig. 3**.

Table S1

Activities of enzymes involved in autotrophic CO_2 fixation in *D. acetivorans*. Activities were measured at 55°C. The number of biological repetitions (n) is shown.

Pathway/Enzyme	Specific activity [µmol min^{-1} mg^{-1} protein] ± standard deviation for cells grown on CO_2	Candidate gene(s) Genbank Accn.:
rTCA cycle		
ATP-citrate lyase[1]	< 0.01 (n=2)	CP007051, Region: 484760-487933 [2]
Calvin-Benson cycle		
Ribulose 1,5-bisphosphate carboxylase	< 0.005 (n=2)	-
Reductive acetyl-CoA pathway		
Carbon monoxide dehydrogenase	0.017 ± 0.013 (n=2)	-
Formate dehydrogenase	0.033 ± 0.007 (n=2)	AHF97383, AHF97384, AHF97385
4-Hydroxybutyrate cycles		
Succinyl-CoA reductase[3]	< 0.01 (n=3)	-
4-Hydroxybutyryl-CoA conversion[4]	< 0.0001	AHF97293[5]
Succinate semialdehyde reductase[3]	< 0.01 (n=3)	-
3-Hydroxypropionate cycle		
Malonyl-CoA reductase[3]	< 0.01 (n=2)	-

1 Measured as the ATP-dependent oxaloacetate formation from citrate and CoA (coupled to MDH)

2 Pseudogene

3 The enzymes were measured with both NADH and NADPH.

4 Low amounts of 4-hyroxybutyryl-CoA (<1 nmol min^{-1} mg^{-1} protein) were formed from CoA, ATP and 4-hydroxybutyrate, but no further conversion could be detected by UPLC.

5 4-Hydroxybutyryl-CoA dehydratase.

Table S2

NMR data of [U-$^{13}C_6$]citrate conversion using *D. acetivorans* cell extracts.

Position	Chemical shift ^{13}C, ppm	Coupling constants J_{cc}, Hz
Acetyl-CoA		
1	201.2(d)	46.4
2	30.2(d)	46.4
Malate		
1	176.6(d)	59.5
2	66.7(dd)	60.2, 38.6
3	38.3(dd)	55.5, 38.7
4	174.4(d)	55.8
Citrate		
3’	176.3(d)	60.5
1, 5	173.3(d)	56.9
3	73.2(dt)	60.8, 38.7
2, 4	43.2(dd)	59.6, 38.7

Table S3

Intracellular concentration (± SD) of metabolites involved in the rTCA cycle in autotrophically grown *D. acetivorans*. None of the following CoA esters could be detected in cell extracts of *D. acetivorans* grown on CO_2 (< 0.5 µM): citryl-CoA, malonyl-CoA, propionyl-CoA, malyl-CoA, citramalyl-CoA, mesaconyl-CoA, 4-hydroxybutyryl-CoA, crotonyl-CoA, acetoacetyl-CoA, acryloyl-CoA, 3-hydroxypropionyl-CoA, thus disproving the functioning of 3-hydroxypropionate bi-cycle and 4-hydroxybutyrate cycles of autotrophic CO_2 fixation (*1-3*).

Metabolite	**Concentration, µM**
Acetyl-CoA	12 ± 8
CoA	1070 ± 420
Citrate	1430 ± 600
Succinate	2910 ± 180
Malate	300 ± 40

Table S4

K_M values (μM) for citrate synthase and malate dehydrogenase in extracts of autotrophically grown *D. acetivorans* cells and for porcine citrate synthase. ND, not determined.

	D. acetivorans **cell extract**	**porcine enzyme**
Citrate synthase		**porcine citrate synthase (Sigma C3260)**
Citrate	4960 ± 480	8190 ± 1060
CoA	200 ± 40	340 ± 60
Oxaloacetate	36 ± 15	ND
Acetyl-CoA	71 ± 20	ND
Malate dehydrogenase (NADH)		**porcine MDH (mitochondrial)**
Oxaloacetate	43 ± 9	40 (*47*)

Table S5

^{13}C-Enrichments in protein derived alanine, aspartate, glutamate and proline from *D. acetivorans* A63 grown on [1-$^{13}C_1$]pyruvate analyzed as tert-butyl-dimethylderivatives. The m/z values of the fragments under study and the corresponding number of C atoms are indicated. Values for three independent biological replicates (measured in triplicate) are given, as well as mean values and standard error of the mean (SEM). In the second column, the isotopologue status of the fragment is given, where 0 means ^{12}C, 1 means ^{13}C, Y represents an unknown state and X represents a missing C atom. The numbers outside the brackets indicate the total amount of ^{13}C atoms in the fragment.

		Replicate 1	Replicate 2	Replicate3	MEAN	SEM
Ala-232 (C2+3)	{X00}	99.89 % ± 0.02 %	99.92% ± 0.07 %	99.95 % ± 0.07 %	**99.92 %**	0.02%
	{XYY}1	0.00 % ± 0.00 %	0.04% ± 0.08 %	0.00 % ± 0.00 %	**0.01 %**	0.02%
	{X11}	0.11 % ± 0.02 %	0.03% ± 0.05 %	0.05 % ± 0.07 %	**0.06 %**	0.03%
Ala-260 (C1-3)	{000}	92.88 % ± 0.32 %	93.86% ± 0.51 %	93.73 % ± 0.68 %	**93.49 %**	0.44%
	{YYY}1	7.05 % ± 0.33 %	6.03% ± 0.53 %	6.20 % ± 0.71 %	**6.42 %**	0.44%
	{YYY}2	0.02 % ± 0.03 %	0.03% ± 0.05 %	0.01 % ± 0.02 %	**0.02 %**	0.01%
	{111}	0.06 % ± 0.02 %	0.08% ± 0.03 %	0.06 % ± 0.02 %	**0.06 %**	0.01%
Asp-302 (C1+2)	{00XX}	99.40 % ± 0.20 %	99.21% ± 0.29 %	99.13 % ± 0.20 %	**99.25 %**	0.11%
	{YYXX}1	0.60 % ± 0.20 %	0.79% ± 0.29 %	0.87 % ± 0.20 %	**0.75 %**	0.11%
	{11XX}	0.00 % ± 0.00 %	0.00% ± 0.00 %	0.00 % ± 0.00 %	**0.00 %**	0.00%
Asp-390 (C2-4)	{X000}	97.94 % ± 0.32 %	99.08% ± 0.62 %	98.68 % ± 0.03 %	**98.56 %**	0.47%
	{XYYY}1	1.99 % ± 0.29 %	0.82% ± 0.64 %	1.17 % ± 0.12 %	**1.33 %**	0.49%
	{XYYY}2	0.04 % ± 0.06 %	0.00% ± 0.00 %	0.05 % ± 0.09 %	**0.03 %**	0.02%
	{X111}	0.04 % ± 0.03 %	0.10% ± 0.03 %	0.10 % ± 0.04 %	**0.08 %**	0.03%
Asp-418 (C1-4)	{0000}	97.65 % ± 0.10 %	98.15% ± 0.32 %	98.33 % ± 0.10 %	**98.05 %**	0.29%
	{YYYY}1	2.35 % ± 0.10 %	1.83% ± 0.34 %	1.67 % ± 0.10 %	**1.95 %**	0.29%
	{YYYY}2	0.00 % ± 0.00 %	0.00% ± 0.00 %	0.00 % ± 0.00 %	**0.00 %**	0.00%
	{YYYY}3	0.00 % ± 0.00 %	0.02% ± 0.03 %	0.00 % ± 0.00 %	**0.01 %**	0.01%
	{1111}	0.00 % ± 0.00 %	0.00% ± 0.00 %	0.00 % ± 0.00 %	**0.00 %**	0.00%
Glu-404 (C2-5)	{X0000}	97.83 % ± 0.31 %	98.46% ± 0.21 %	98.03 % ± 0.46 %	**98.11 %**	0.26%
	{XYYYY}1	1.77 % ± 0.22 %	1.26% ± 0.36 %	1.56 % ± 0.28 %	**1.53 %**	0.21%
	{XYYYY}2	0.39 % ± 0.13 %	0.28% ± 0.14 %	0.41 % ± 0.17 %	**0.36 %**	0.06%
	{XYYYY}3	0.00 % ± 0.00 %	0.00% ± 0.00 %	0.00 % ± 0.00 %	**0.00 %**	0.00%
	{X1111}	0.00 % ± 0.00 %	0.00% ± 0.00 %	0.00 % ± 0.00 %	**0.00 %**	0.00%
Glu-432 (C1-5)	{00000}	98.03 % ± 0.24 %	99.02% ± 0.15 %	98.85 % ± 0.09 %	**98.63 %**	0.43%
	{YYYYY}1	1.86 % ± 0.29 %	0.83% ± 0.15 %	0.90 % ± 0.14 %	**1.19 %**	0.47%
	{YYYYY}2	0.09 % ± 0.11 %	0.15% ± 0.16 %	0.24 % ± 0.22 %	**0.16 %**	0.06%
	{YYYYY}3	0.02 % ± 0.04 %	0.00% ± 0.00 %	0.01 % ± 0.02 %	**0.01 %**	0.01%
	{YYYYY}4	0.00 % ± 0.00 %	0.00% ± 0.00 %	0.00 % ± 0.00 %	**0.00 %**	0.00%
	{11111}	0.00 % ± 0.00 %	0.00% ± 0.00 %	0.00 % ± 0.00 %	**0.00 %**	0.00%
Pro-184 (C2-5)	{X0000}	98.25 % ± 0.01 %	98.84 % ± 0.05 %	98.95 % ± 0.12 %	**98.68 %**	0.31%
	{XYYYY}1	1.70 % ± 0.03 %	1.11 % ± 0.06 %	0.99 % ± 0.09 %	**1.27 %**	0.31%
	{XYYYY}2	0.03 % ± 0.01 %	0.03 % ± 0.02 %	0.03 % ± 0.03 %	**0.03 %**	0.00%
	{XYYYY}3	0.01 % ± 0.01 %	0.01 % ± 0.01 %	0.02 % ± 0.01 %	**0.01 %**	0.00%
	{X1111}	0.00 % ± 0.00 %	0.01 % ± 0.01 %	0.02 % ± 0.03 %	**0.01 %**	0.01%
Pro-286 (C1-5)	{00000}	98.65 % ± 0.17 %	99.26 % ± 0.23 %	98.90 % ± 0.42 %	**98.94 %**	0.25%
	{YYYYY}1	1.14 % ± 0.13 %	0.54 % ± 0.23 %	0.67 % ± 0.16 %	**0.78 %**	0.26%
	{YYYYY}2	0.00 % ± 0.00 %	0.00 % ± 0.00 %	0.00 % ± 0.00 %	**0.00 %**	0.00%
	{YYYYY}3	0.16 % ± 0.05 %	0.11 % ± 0.02 %	0.20 % ± 0.08 %	**0.16 %**	0.03%
	{YYYYY}4	0.06 % ± 0.07 %	0.08 % ± 0.04 %	0.23 % ± 0.26 %	**0.12 %**	0.08%
	{11111}	0.00 % ± 0.00 %	0.00 % ± 0.00 %	0.00 % ± 0.00 %	**0.00 %**	0.00%

Table S6.

^{13}C-Enrichments in protein derived alanine, aspartate, glutamate and proline from heterotrophically grown *D. acetivorans* A63 in the presence of [1-$^{13}C_1$]pyruvate. For more details, see title of **Table S5**.

		Replicate 1			Replicate 2			Replicate3			MEAN	SEM
Ala-232 (C2+3)	{X00}	99.83 %	±	0.02 %	99.57%	±	0.13 %	99.68 %	±	0.10 %	**99.69 %**	0.10%
	{XYY}1	0.03 %	±	0.05 %	0.11%	±	0.15 %	0.09 %	±	0.08 %	**0.08 %**	0.04%
	{X11}	0.15 %	±	0.07 %	0.31%	±	0.06 %	0.23 %	±	0.05 %	**0.23 %**	0.07%
Ala-260 (C1-3)	{000}	95.45 %	±	0.23 %	95.92%	±	0.32 %	97.84 %	±	0.17 %	**96.41 %**	1.03%
	{YYY}1	4.31 %	±	0.17 %	3.64%	±	0.33 %	1.83 %	±	0.13 %	**3.26 %**	1.05%
	{YYY}2	0.05 %	±	0.08 %	0.11%	±	0.04 %	0.07 %	±	0.08 %	**0.08 %**	0.03%
	{111}	0.19 %	±	0.02 %	0.32%	±	0.04 %	0.26 %	±	0.02 %	**0.26 %**	0.05%
Asp-302 (C1+2)	{00XX}	99.97 %	±	0.04 %	99.88%	±	0.08 %	100.0%	±	0.00 %	**99.95 %**	0.05%
	{YYXX}1	0.03 %	±	0.05 %	0.00%	±	0.00 %	0.00 %	±	0.00 %	**0.01 %**	0.01%
	{11XX}	0.00 %	±	0.01 %	0.12%	±	0.08 %	0.00 %	±	0.00 %	**0.04 %**	0.05%
Asp-390 (C2-4)	{X000}	99.81 %	±	0.05 %	99.44%	±	0.47 %	99.84 %	±	0.09 %	**99.70 %**	0.18%
	{XYYY}1	0.00 %	±	0.00 %	0.27%	±	0.47 %	0.00 %	±	0.00 %	**0.09 %**	0.13%
	{XYYY}2	0.00 %	±	0.00 %	0.00%	±	0.00 %	0.00 %	±	0.00 %	**0.00 %**	0.00%
	{X111}	0.19 %	±	0.05 %	0.29%	±	0.02 %	0.16 %	±	0.09 %	**0.21 %**	0.06%
Asp-418 (C1-4)	{0000}	99.71 %	±	0.51 %	99.75%	±	0.15 %	99.98 %	±	0.01 %	**99.81 %**	0.12%
	{YYYY}1	0.28 %	±	0.49 %	0.10%	±	0.16 %	0.00 %	±	0.00 %	**0.13 %**	0.12%
	{YYYY}2	0.00 %	±	0.00 %	0.00%	±	0.00 %	0.00 %	±	0.00 %	**0.00 %**	0.00%
	{YYYY}3	0.01 %	±	0.02 %	0.00%	±	0.00 %	0.00 %	±	0.00 %	**0.00 %**	0.00%
	{1111}	0.00 %	±	0.00 %	0.16%	±	0.02 %	0.02 %	±	0.01 %	**0.06 %**	0.07%
Glu-404 (C2-5)	{X0000}	99.42 %	±	0.37 %	98.91%	±	0.55 %	99.57 %	±	0.10 %	**99.30 %**	0.28%
	{XYYYY}1	0.00 %	±	0.00 %	0.43%	±	0.67 %	0.12 %	±	0.11 %	**0.18 %**	0.18%
	{XYYYY}2	0.58 %	±	0.37 %	0.59%	±	0.25 %	0.31 %	±	0.07 %	**0.49 %**	0.13%
	{XYYYY}3	0.00 %	±	0.00 %	0.00%	±	0.00 %	0.00 %	±	0.00 %	**0.00 %**	0.00%
	{X1111}	0.00 %	±	0.00 %	0.06%	±	0.03 %	0.00 %	±	0.00 %	**0.02 %**	0.03%
Glu-432 (C1-5)	{00000}	99.49 %	±	0.22 %	98.80%	±	0.23 %	99.41 %	±	0.12 %	**99.24 %**	0.31%
	{YYYYY}1	0.00 %	±	0.00 %	0.00%	±	0.00 %	0.10 %	±	0.09 %	**0.03 %**	0.05%
	{YYYYY}2	0.29 %	±	0.26 %	0.48%	±	0.34 %	0.21 %	±	0.15 %	**0.33 %**	0.11%
	{YYYYY}3	0.01 %	±	0.02 %	0.18%	±	0.12 %	0.02 %	±	0.02 %	**0.07 %**	0.08%
	{YYYYY}4	0.01 %	±	0.01 %	0.00%	±	0.00 %	0.00 %	±	0.00 %	**0.00 %**	0.00%
	{11111}	0.19 %	±	0.01 %	0.54%	±	0.00 %	0.26 %	±	0.01 %	**0.33 %**	0.15%
Pro-184 (C2-5)	{X0000}	99.72 %	±	0.02 %	99.37 %	±	0.02 %	99.61 %	±	0.03 %	**99.57 %**	0.15%
	{XYYYY}1	0.00 %	±	0.00 %	0.00 %	±	0.00 %	0.00 %	±	0.00 %	**0.00 %**	0.00%
	{XYYYY}2	0.07 %	±	0.03 %	0.24 %	±	0.01 %	0.10 %	±	0.02 %	**0.14 %**	0.07%
	{XYYYY}3	0.04 %	±	0.01 %	0.05 %	±	0.01 %	0.03 %	±	0.01 %	**0.04 %**	0.01%
	{X1111}	0.16 %	±	0.00 %	0.34 %	±	0.00 %	0.26 %	±	0.01 %	**0.26 %**	0.08%
Pro-286 (C1-5)	{00000}	99.51 %	±	0.17 %	99.32 %	±	0.05 %	99.33 %	±	0.11 %	**99.39 %**	0.08%
	{YYYYY}1	0.11 %	±	0.18 %	0.02 %	±	0.04 %	0.15 %	±	0.13 %	**0.09 %**	0.05%
	{YYYYY}2	0.00 %	±	0.00 %	0.00 %	±	0.00 %	0.00 %	±	0.00 %	**0.00 %**	0.00%
	{YYYYY}3	0.17 %	±	0.03 %	0.28 %	±	0.04 %	0.17 %	±	0.02 %	**0.20 %**	0.05%
	{YYYYY}4	0.21 %	±	0.01 %	0.18 %	±	0.01 %	0.20 %	±	0.00 %	**0.19 %**	0.01%
	{11111}	0.01 %	±	0.01 %	0.20 %	±	0.01 %	0.15 %	±	0.00 %	**0.12 %**	0.08%

Table S7

^{13}C-Enrichments in protein derived alanine, aspartate, glutamate and proline from *D. acetivorans* A63 grown on [U-$^{13}C_2$]acetate under H_2/CO_2. For more details, see title of **Table S5**.

		Replicate 1			Replicate 2			Replicate3			MEAN	SEM
Ala-232 (C2+3)	{X00}	4.03 %	±	0.09 %	5.21%	±	0.05 %	5.39 %	±	0.05 %	**4.88 %**	0.60%
	{XYY}1	1.75 %	±	0.03 %	1.82%	±	0.09 %	1.51 %	±	0.09 %	**1.69 %**	0.13%
	{X11}	94.22 %	±	0.11 %	92.97%	±	0.04 %	93.09 %	±	0.04 %	**93.43 %**	0.56%
Ala-260 (C1-3)	{000}	4.24 %	±	0.10 %	5.45%	±	0.09 %	5.59 %	±	0.19 %	**5.09 %**	0.60%
	{YYY}1	2.39 %	±	0.03 %	2.45%	±	0.10 %	2.12 %	±	0.06 %	**2.32 %**	0.14%
	{YYY}2	89.18 %	±	0.40 %	85.59%	±	0.88 %	85.49 %	±	0.53 %	**86.75 %**	1.71%
	{111}	4.19 %	±	0.45 %	6.51%	±	0.86 %	6.79 %	±	0.62 %	**5.83 %**	1.17%
Asp-302 (C1+2)	{00XX}	7.73 %	±	0.24 %	8.33%	±	0.23 %	7.94 %	±	0.36 %	**8.00 %**	0.25%
	{YYXX}1	36.59 %	±	0.62 %	30.74%	±	0.66 %	29.88 %	±	0.79 %	**32.40 %**	2.98%
	{11XX}	55.68 %	±	0.78 %	60.93%	±	0.50 %	62.18 %	±	1.03 %	**59.60 %**	2.82%
Asp-390 (C2-4)	{X000}	5.52 %	±	0.24 %	6.39%	±	0.34 %	6.16 %	±	0.33 %	**6.03 %**	0.37%
	{XYYY}1	5.21 %	±	0.31 %	4.59%	±	0.15 %	3.76 %	±	0.09 %	**4.52 %**	0.59%
	{XYYY}2	35.62 %	±	1.46 %	30.42%	±	0.88 %	28.68 %	±	1.28 %	**31.57 %**	2.95%
	{X111}	53.65 %	±	1.97 %	58.60%	±	1.01 %	61.39 %	±	1.68 %	**57.88 %**	3.20%
Asp-418 (C1-4)	{0000}	5.76 %	±	0.13 %	6.80%	±	0.37 %	7.14 %	±	0.36 %	**6.57 %**	0.59%
	{YYYY}1	4.91 %	±	0.28 %	3.85%	±	0.16 %	3.78 %	±	0.22 %	**4.18 %**	0.52%
	{YYYY}2	32.90 %	±	1.34 %	26.57%	±	0.87 %	26.64 %	±	1.56 %	**28.70 %**	2.97%
	{YYYY}3	9.86 %	±	0.87 %	11.57%	±	0.56 %	10.01 %	±	0.17 %	**10.48 %**	0.77%
	{1111}	46.57 %	±	1.24 %	51.21%	±	0.90 %	52.43 %	±	1.65 %	**50.07 %**	2.52%
Glu-404 (C2-5)	{X0000}	4.74 %	±	0.04 %	5.82%	±	0.03 %	5.89 %	±	0.22 %	**5.48 %**	0.53%
	{XYYYY}1	2.08 %	±	0.09 %	1.45%	±	0.12 %	1.34 %	±	0.11 %	**1.62 %**	0.33%
	{XYYYY}2	9.99 %	±	0.04 %	6.50%	±	0.29 %	6.06 %	±	0.15 %	**7.52 %**	1.76%
	{XYYYY}3	11.63 %	±	0.23 %	12.44%	±	0.13 %	10.35 %	±	0.28 %	**11.48 %**	0.86%
	{X1111}	71.55 %	±	0.21 %	73.79%	±	0.41 %	76.36 %	±	0.51 %	**73.90 %**	1.97%
Glu-432 (C1-5)	{00000}	5.32 %	±	0.06 %	6.94%	±	0.10 %	7.10 %	±	0.28 %	**6.45 %**	0.80%
	{YYYYY}1	1.80 %	±	0.06 %	1.20%	±	0.08 %	1.05 %	±	0.08 %	**1.35 %**	0.32%
	{YYYYY}2	10.09 %	±	0.08 %	6.60%	±	0.06 %	5.93 %	±	0.15 %	**7.54 %**	1.82%
	{YYYYY}3	9.27 %	±	0.23 %	8.20%	±	0.12 %	7.26 %	±	0.14 %	**8.24 %**	0.82%
	{YYYYY}4	65.35 %	±	0.09 %	65.97%	±	0.43 %	66.21 %	±	0.61 %	**65.84 %**	0.36%
	{11111}	8.17 %	±	0.13 %	11.10%	±	0.14 %	12.44 %	±	0.11 %	**10.57 %**	1.78%
Pro-184 (C2-5)	{X0000}	4.31 %	±	0.18 %	4.85 %	±	0.17 %	5.05 %	±	0.05 %	**4.74 %**	0.32%
	{XYYYY}1	1.90 %	±	0.04 %	1.39 %	±	0.01 %	1.24 %	±	0.03 %	**1.51 %**	0.28%
	{XYYYY}2	9.96 %	±	0.17 %	6.54 %	±	0.17 %	6.13 %	±	0.07 %	**7.54 %**	1.72%
	{XYYYY}3	9.06 %	±	0.09 %	8.36 %	±	0.11 %	7.60 %	±	0.05 %	**8.34 %**	0.60%
	{X1111}	74.78 %	±	0.46 %	78.86 %	±	0.44 %	79.99 %	±	0.19 %	**77.88 %**	2.24%
Pro-286 (C1-5)	{00000}	4.91 %	±	0.11 %	6.29 %	±	0.13 %	6.22 %	±	0.05 %	**5.81 %**	0.63%
	{YYYYY}1	2.10 %	±	0.09 %	1.86 %	±	0.10 %	1.63 %	±	0.04 %	**1.86 %**	0.19%
	{YYYYY}2	9.13 %	±	0.39 %	5.55 %	±	0.11 %	5.24 %	±	0.26 %	**6.64 %**	1.76%
	{YYYYY}3	9.14 %	±	0.39 %	8.32 %	±	0.31 %	7.28 %	±	0.18 %	**8.25 %**	0.76%
	{YYYYY}4	66.08 %	±	0.25 %	66.30 %	±	0.27 %	66.15 %	±	0.60 %	**66.17 %**	0.09%
	{11111}	8.65 %	±	0.85 %	11.68 %	±	0.30 %	13.49 %	±	0.78 %	**11.27 %**	2.00%

Table S8

^{13}C-Enrichments in protein derived alanine, aspartate, glutamate and proline from *D. acetivorans* A63 grown on [U-$^{13}C_2$]acetate under N_2/CO_2 (i.e. without H_2). For more details, see title of **Table S5**.

		Replicate 1			Replicate 2			Replicate3			MEAN	SEM
Ala-232 (C2+3)	{X00}	5.51 %	±	0.08 %	4.09 %	±	0.06 %	6.12 %	±	0.06 %	**5.24 %**	0.85%
	{XYY}1	1.24 %	±	0.07 %	1.04 %	±	0.02 %	1.09 %	±	0.05 %	**1.13 %**	0.08%
	{X11}	93.25 %	±	0.14 %	94.87 %	±	0.07 %	92.79 %	±	0.10 %	**93.64 %**	0.89%
Ala-260 (C1-3)	{000}	5.60 %	±	0.11 %	4.21 %	±	0.02 %	6.35 %	±	0.06 %	**5.39 %**	0.89%
	{YYY}1	1.89 %	±	0.05 %	1.59 %	±	0.01 %	1.62 %	±	0.08 %	**1.70 %**	0.13%
	{YYY}2	84.38 %	±	0.52 %	84.34 %	±	0.25 %	82.07 %	±	0.57 %	**83.60 %**	1.08%
	{111}	8.13 %	±	0.54 %	9.86 %	±	0.26 %	9.96 %	±	0.45 %	**9.32 %**	0.84%
Asp-302 (C1+2)	{00XX}	5.75 %	±	0.17 %	4.43 %	±	0.10 %	6.58 %	±	0.14 %	**5.58 %**	0.89%
	{YYXX}1	11.46 %	±	0.15 %	10.47 %	±	0.11 %	11.34 %	±	0.30 %	**11.09 %**	0.44%
	{11XX}	82.79 %	±	0.30 %	85.10 %	±	0.15 %	82.08 %	±	0.44 %	**83.33 %**	1.29%
Asp-390 (C2-4)	{X000}	5.51 %	±	0.17 %	3.98 %	±	0.08 %	6.20 %	±	0.13 %	**5.23 %**	0.92%
	{XYYY}1	0.84 %	±	0.01 %	0.64 %	±	0.07 %	0.77 %	±	0.05 %	**0.75 %**	0.08%
	{XYYY}2	11.36 %	±	0.22 %	10.86 %	±	0.11 %	11.64 %	±	0.47 %	**11.29 %**	0.32%
	{X111}	82.29 %	±	0.38 %	84.52 %	±	0.16 %	81.40 %	±	0.52 %	**82.73 %**	1.31%
Asp-418 (C1-4)	{0000}	6.04 %	±	0.19 %	4.53 %	±	0.13 %	6.98 %	±	0.35 %	**5.85 %**	1.01%
	{YYYY}1	0.80 %	±	0.04 %	0.27 %	±	0.05 %	0.37 %	±	0.24 %	**0.48 %**	0.23%
	{YYYY}2	9.10 %	±	0.12 %	7.51 %	±	0.08 %	8.49 %	±	0.35 %	**8.37 %**	0.65%
	{YYYY}3	7.58 %	±	0.18 %	7.73 %	±	0.22 %	8.15 %	±	0.31 %	**7.82 %**	0.24%
	{1111}	76.48 %	±	0.44 %	79.96 %	±	0.27 %	76.02 %	±	0.33 %	**77.49 %**	1.76%
Glu-404 (C2-5)	{X0000}	5.69 %	±	0.21 %	4.11 %	±	0.10 %	6.51 %	±	0.13 %	**5.44 %**	1.00%
	{XYYYY}1	0.38 %	±	0.09 %	0.12 %	±	0.05 %	0.04 %	±	0.06 %	**0.18 %**	0.14%
	{XYYYY}2	1.47 %	±	0.04 %	1.24 %	±	0.07 %	1.42 %	±	0.09 %	**1.38 %**	0.10%
	{XYYYY}3	5.89 %	±	0.10 %	5.88 %	±	0.10 %	5.97 %	±	0.21 %	**5.91 %**	0.04%
	{X1111}	86.56 %	±	0.14 %	88.64 %	±	0.06 %	86.05 %	±	0.28 %	**87.09 %**	1.12%
Glu-432 (C1-5)	{00000}	6.27 %	±	0.13 %	4.64 %	±	0.03 %	7.00 %	±	0.12 %	**5.97 %**	0.99%
	{YYYYY}1	0.23 %	±	0.05 %	0.00 %	±	0.00 %	0.00 %	±	0.00 %	**0.08 %**	0.11%
	{YYYYY}2	1.21 %	±	0.04 %	0.99 %	±	0.03 %	1.12 %	±	0.05 %	**1.11 %**	0.09%
	{YYYYY}3	4.04 %	±	0.02 %	3.84 %	±	0.06 %	4.10 %	±	0.08 %	**3.99 %**	0.11%
	{YYYYY}4	67.47 %	±	0.12 %	66.16 %	±	0.51 %	65.96 %	±	0.24 %	**66.53 %**	0.67%
	{11111}	20.77 %	±	0.24 %	24.37 %	±	0.41 %	21.82 %	±	0.32 %	**22.32 %**	1.51%
Pro-184 (C2-5)	{X0000}	5.14 %	±	0.12 %	3.38 %	±	0.05 %	5.22 %	±	0.07 %	**4.58 %**	0.85%
	{XYYYY}1	0.34 %	±	0.01 %	0.07 %	±	0.01 %	0.09 %	±	0.02 %	**0.17 %**	0.12%
	{XYYYY}2	1.44 %	±	0.04 %	1.33 %	±	0.01 %	1.49 %	±	0.01 %	**1.42 %**	0.07%
	{XYYYY}3	4.64 %	±	0.05 %	4.63 %	±	0.03 %	4.89 %	±	0.05 %	**4.72 %**	0.12%
	{X1111}	88.44 %	±	0.17 %	90.58 %	±	0.06 %	88.30 %	±	0.09 %	**89.11 %**	1.04%
Pro-286 (C1-5)	{00000}	5.90 %	±	0.17 %	4.17 %	±	0.08 %	6.07 %	±	0.18 %	**5.38 %**	0.86%
	{YYYYY}1	0.50 %	±	0.03 %	0.26 %	±	0.07 %	0.15 %	±	0.05 %	**0.30 %**	0.15%
	{YYYYY}2	1.03 %	±	0.05 %	0.92 %	±	0.02 %	1.00 %	±	0.09 %	**0.98 %**	0.04%
	{YYYYY}3	4.04 %	±	0.10 %	3.79 %	±	0.07 %	4.11 %	±	0.07 %	**3.98 %**	0.14%
	{YYYYY}4	66.55 %	±	0.57 %	66.18 %	±	0.26 %	64.72 %	±	0.52 %	**65.82 %**	0.79%
	{11111}	21.98 %	±	0.70 %	24.68 %	±	0.24 %	23.96 %	±	0.68 %	**23.54 %**	1.14%

Table S9.

Enzyme activities in cell extracts of autotrophically grown *D. multipotens* (in µmol min^{-1} mg^{-1} protein). The number of biological repetitions (n) is shown.

Enzyme	Specific activity ± standard deviation
ATP-citrate lyase[1]	< 0.02 (n=2)
Citrate synthase backward (NADH oxidation)	0.23 ± 0.04 (n=8)
Citrate synthase	32.5 ± 0.5 (n=5)
Malate dehydrogenase	22.8 ± 0.6 (n=2)

[1] Measured as the ATP-dependent oxaloacetate formation from citrate and CoA (coupled to MDH)

Table S10

Energetic efficiencies of different autotrophic CO_2 fixation pathways. The calculatons were done using eQuilibrator (*48*). Ferredoxin (Fd) is shown here as one electron carrier with E°' -414 mV corresponding to that of the hydrogen/proton couple. Please note that we did not take into account that E°' of Fd is much lower in methanogens (~-500 mV, which is the $E^{0'}$ of the CO_2/CHO-methanofuran couple; *49*), thus overestimating the energetic efficiency of the reductive acetyl-CoA pathway in *Methanothermobacter marburgiensis*. Temperature is assumed 25 °C, pressure 1 bar. CO_2(total) is the sum of CO_2(aq) and its three hydrated forms (H_2CO_3, HCO_3^- and CO_3^{2-}).

Pathway	Assumptions	Net reaction	Estimated $\Delta G'°$ (kJ/mol)
Anaerobic pathways			
roTCA cycle (*D. acetivorans*)	NADH-dependent fumarate reductase[1]	2 CO_2(total) + NADPH + 2 NADH + 2 Fd_{red} + CoA + ATP <=> acetyl-CoA + $NADP^+$ + 2 NAD^+ + 2 Fd_{ox} + ADP + P_i + 4 H_2O	**-50.9** ± 12.7
Reductive acetyl-CoA pathway (*Methanothermobacter marburgiensis*)		2 CO_2(total) + 4 Fd_{red} + CoA + 2 $F_{420}H_2$ <=> acetyl-CoA + 4 Fd_{ox} + 2 F_{420} + 5 H_2O	**-53.5** ± 26.6
Reductive acetyl-CoA pathway (*Acetobacterium woodii*)		2 CO_2(total) + NADPH + NADH + 4 Fd_{red} + CoA + ATP <=> acetyl-CoA + $NADP^+$ + NAD^+ + 4 Fd_{ox} + ADP + P_i + 4 H_2O	**-67.5** ± 23.8
rTCA cycle (green sulfur bacteria)	NADH-dependent fumarate reductase[1]	2 CO_2(total) + NADPH + 2 NADH + 2 Fd_{red} + CoA + 2 ATP <=> acetyl-CoA + $NADP^+$ + 2 NAD^+ + 2 Fd_{ox} + 2 ADP + 2 P_i + 3 H_2O	**-77.3** ± 12.7
rTCA cycle (*Hydrogenobacter thermophilus*)	NADH-dependent fumarate reductase	2 CO_2(total) + 3 NADH + 2 Fd_{red} + CoA + 3 ATP <=> acetyl-CoA + 3 NAD^+ + 2 Fd_{ox} + 3 ADP + 3 P_i + 2 H_2O	**-102.7** ± 12.8
Dicarboxylate/ hydroxybutyrate cycle (*Thermoproteus*)	NADH-dependent fumarate reductase	2 CO_2(total) + 3 ATP + 2 NADPH + NADH + CoA + 2 Fd_{red} <=> 5 P_i + ADP + 2 AMP + 2 $NADP^+$ + NAD^+ + 2 Fd_{ox} + acetyl-CoA	**-152.3** ± 12.9
Aerobic pathways			
Hydroxypropionate/ hydroxybutyrate cycle (*Thaumarchaeota*)		2 CO_2(total) + 4 ATP + 5 NADPH + NAD^+ + CoA <=> 4 P_i + 4 ADP + 5 $NADP^+$ + NADH + acetyl-CoA + H_2O	**-117.4** ± 5.8
Hydroxypropionate/ hydroxybutyrate cycle (*Crenarchaeota*)		2 CO_2(total) + 4 ATP + 5 NADPH + NAD^+ + CoA + H_2O <=> 6 P_i + 2 ADP + 2 AMP + 5 $NADP^+$ + NADH + acetyl-CoA	**-165.1** ± 6.2
Calvin-Benson cycle, glycolysis, pyruvate synthase		2 CO_2(total) + 7 ATP + 6 NADPH + NAD^+ + 2 Fd_{ox} + CoA + 2 H_2O <=> 7 ADP + 6 $NADP^+$ + NADH + 2 Fd_{red} + acetyl-CoA + 7 P_i	**-181.0** ± 13.5
3-Hydroxypropionate bi-cycle, pyruvate synthase	FAD-dependent succinate dehydrogenase	2 CO_2(total) + 5 ATP + 6 NADPH + 2 Fd_{ox} + CoA + FAD + 2 H_2O <=> 3 ADP + 2 AMP + 6 $NADP^+$ + 2 Fd_{red} + acetyl-CoA + 7 P_i + $FADH_2$	**-192.8** ± 14.9
Calvin-Benson cycle, glycolysis, pyruvate dehydrogenase		2 CO_2(total) + 7 ATP + 6 NADPH + 2 NAD^+ + CoA + 2 H_2O <=> 7 ADP + 6 $NADP^+$ + 2 NADH + acetyl-CoA + 7 P_i	**-197.6** ± 6.8
3-Hydroxypropionate bi-cycle, pyruvate dehydrogenase	FAD-dependent succinate dehydrogenase	2 CO_2(total) + 5 ATP + 6 NADPH + NAD^+ + CoA + FAD + 2 H_2O <=> 3 ADP + 2 AMP + 6 $NADP^+$ + NADH + acetyl-CoA + 7 P_i + $FADH_2$	**-209.4** ± 9.0

[1] With menaquinol-dependent fumarate reductase, the estimated $\Delta G'°$ values for the rTCA and roTCA cycles are -28.6 ± 14.0 and -2.2 ± 14.0 kJ/mol, respectively. Please note that *D. acetivorans* possesses menaquinones and cytochromes (*27*).

Table S11

Primer sequences used for the sequencing of the *acl* gene in *D. acetivorans*.

Primer	Sequence
Primer 1 Fwd	TGCATGCGATTTGGCTGTA
Primer 1 Rev	TGGTAGGCGTTTGCAACAA
Primer 2 Fwd	AGGAGGGGGTAATGGCTGA
Primer 2 Rev	TGGCCCTCCCCTTCTAACA
Primer 3 Fwd	GCTGGAGGTGGAGCTTCTG
Primer 3 Rev	GCGCCTGCATGTCCAAAC
Primer 4 Fwd	AACTCGCTCTGGTGGCCT
Primer 4 Rev	GCGAAACGCCAATTGCACC
Primer 5 Fwd	CCTAGGTTTGGTGGCGCA
Primer 5 Rev	TTGAGCGCCTTTTGCAACT

References and Notes

31. J. Sasikaran, M. Ziemski, P. K. Zadora, A. Fleig, I. A. Berg, Bacterial itaconate degradation promotes pathogenicity. *Nat. Chem. Biol.* **10**, 371–377 (2014).
32. P. W. Riddles, R. L. Blakeley, B. Zerner, Ellman's reagent: 5,5′-dithiobis(2-nitrobenzoic acid) - a reexamination. *Anal. Biochem.* **94** 75–81 (1979).
33. H. Bergmeyer, Neue Werte für die molaren Extinktions-Koeffizienten von NADH und NADPH zum Gebrauch im Routine-Laboratorium. *Z. Klin. Chem. Klin. Biochem.*, **13** 507–510 (1975).
34. J. Armstrong, The molar extinction coefficient of 2,6-dichlorophenol indophenol. *Biochim. Biophys. Acta* **86**, 194–197 (1964).
35. D. H. Flint, Initial kinetic and mechanistic characterization of *Escherichia coli* fumarase A. *Arch. Biochem. Biophys.* **311**, 509–516 (1994).
36. R. M. C. Dawson, D. C. Elliott, W. H. Elliott, K. M. Jones, *Data for biochemical research, 3rd edition* p. 424 (Clarendon Press, Oxford, 1986).
37. J. Eyzaguirre, K. Jansen, G. Fuchs, Phosphoenolpyruvate synthetase in *Methanobacterium thermoautotrophicum*. *Arch. Microbiol.* **132**, 67–74 (1982).
38. J. D. Rabinowitz, E. Kimball, Acidic acetonitrile for cellular metabolome extraction from *Escherichia coli*. *Anal. Chem.* **79**, 6167–6173 (2007).

39. E. Eylert *et al.*, Isotopologue Profiling of *Legionella pneumophila*: Role of serine and glucose as carbon substrates. *J. Biol. Chem.* **285**, 22232–22243 (2010).

40. E. Eylert *et al.*, Carbon metabolism of *Listeria* monocytogenes growing inside macrophages. *Mol. Microbiol.* **69**, 1008–1017 (2008).

41. N. A. Gebhardt, R. K. Thauer, D. Linder, P. M. Kaulfers, N. Pfennig, Mechanism of acetate oxidation to CO_2 with elemental sulfur in *Desulfuromonas acetoxidans*. *Arch. Microbiol.* **141**, 392–398 (1985).

42. A. Brandis-Heep, N. A. Gebhardt, R. K. Thauer, F. Widdel, N. Pfennig, Anaerobic acetate oxidation to CO_2 by *Desulfobacter postgatei*. *Arch. Microbiol.* **136**, 222–229 (1983).

43. R. Schauder, F. Widdel, G. Fuchs, Carbon assimilation pathways in sulfate-reducing bacteria II. Enzymes of a reductive citric acid cycle in the autotrophic *Desulfobacter hydrogenophilus*. *Arch. Microbiol.* **148**, 218–225 (1987)

44. M. D. Collins, F. Widdel, Respiratory quinons of sulphate-reducing and sulphur-reducing bacteria: a systematic investigation. *Syst. Appl. Microbiol.* **8**, 8-18 (1986).

45. F. Widdel, N. Pfennig, Studies on dissimilatory sulfate-reducing bacteria that decompose fatty acids. I. Isolation of new sulfate-reducing bacteria enriched with acetate from saline environments. Description of *Desulfobacter postgatei* gen. nov., sp. nov. *Arch. Microbiol.* **129**, 395-400 (1981).

46. I. Probst, M. Bruschi, N. Pfennig, J. LeGall, Cytochrome $c_{551.5}$ (c_7) from *Desulfuromonas acetoxidans*. *Biochim. Biophys. Acta* **460**, 58-64 (1977).

47. L. H. Bernstein, M. B. Grisham, K. D. Cole, J. Everse, Substrate inhibition of the mitochondrial and cytoplasmic malate dehydrogenases. *J. Biol. Chem.* **253**, 8697-8701 (1978)

48. A. Flamholz, E. Noor, A. Bar-Even, R. Milo, eQuilibrator--the biochemical thermodynamics calculator. *Nucleic Acids Res.* **40**, D770-D775 (2012)

49. R. K. Thauer, A. K. Kaster, H. Seedorf, W. Buckel, R. Hedderich, Methanogenic archaea: ecologically relevant differences in energy conservation. *Nat. Rev. Microbiol.* **6**, 579-591 (2008)

CHAPTER 8
PUBLICATIONS & CONFERENCE CONTRIBUTIONS

8.1 Journal Articles

Christopher Scheidler, **Jessica Sobotta**, Wolfgang Eisenreich, Günter Wächtershäuser and Claudia Huber, "Unsaturated $C_{3,5,7,9}$-Monocarboxylic Acids by Aqueous, One-Pot Carbon Fixation: Possible Relevance for the Origin of Life", *Scientific Reports* **2016** (6).

DOI: 10.1038/srep27595.

Jessica Sobotta, Maximilian Schmalhofer, Thomas M. Steiner, Wolfgang Eisenreich, Günter Wächtershäuser, Claudia Huber, "One-pot formationof 2,4-di- or 2,4,6-tri-olefinic monocarboxylic acids by straight chain C4-extension" *Heliyon* **2017**, (3).

DOI: 10.1016/j.heliyon.2017.e00368.

Achim Mall, **Jessica Sobotta**, Claudia Huber, Carolin Tschirner, Stefanie Kowarschik, Katarina Bačnik, Mario Mergelsberg, Matthias Boll, Michael Hügler, Wolfgang Eisenreich, Ivan A. Berg, "Reversibility of citrate synthase allows autotrophic growth of a thermophilic bacterium" *Science* **2018**, (6375), 563-567.

DOI: 10.1126/science.aao2410.

8.2 Talks and Posters

10/2015 Hans Fischer members' meeting, Munich, Germany– Talk on "Transition metal catalysed formation of biomolecules"

04/2016 OLIM Workshop, Munich, Germany-Talk on "Surface catalysed formation of biomolecules under hydrothermal vent conditions and ^{13}C based metabolic studies with archaebacteria."

09/2016 NIM conference: Molecular origins of life, Munich, Germany – Poster on „From extroverted catalytic nanostructures to introverted lipid vesicles"

09/2016 NIM conference: Molecular origins of life, Munich, Germany – Poster on „Tracing primordial metabolism reflected by microorganisms under serpentinization conditions"

10/2016 Hans Fischer members' meeting, Munich, Germany – Talk on "Transition metal catalysed formation of biomolecules"

03/2017 DPG Spring Meeting: Physics of the Genesis of Life, Dresden, Germany – Poster on „High-resolving chemical analysis of products formed under hydrothermal vent conditions"

10/2017 Hans Fischer members' meeting, Munich, Germany – Talk on "Transition metal catalysed formation of biomolecules"